Computer simulation of the sprint start

COMPUTER SIMULATION OF THE SPRINT START

by

David Jessop

A Doctoral Thesis

Submitted in partial fulfillment of the requirements for the award of
Doctor of Philosophy of Loughborough University

April 2011

Abstract

Computer Simulation of the Sprint Start

David Jessop, Loughborough University, 2011

The aim of this project was to investigate the mechanics of the sprint start through the use of computer simulation. Experimental data was collected on one male athlete in accordance with a procedure agreed by Loughborough University Ethical Advisory Committee. The data provided subject specific data for the creation of a four and fourteen segment, angle and torque driven models of the sprint start. The models simulated the start from the moment of onset of force production until takeoff from the starting block. The four segment model comprised a head and trunk, thigh, shank and foot whilst the fourteen segment model also included a lower spine and pelvis, upper arms, forearms and hands, as well as the other leg including two segment feet. Subject specific torque data was combined with EMG data to provide input to the torque models

Results from the four segment angle driven model demonstrated that the participant will benefit from using smaller joint angles than usual in the set position as this resulted in increased velocity on takeoff with minimal increase in movement time. The model also showed large joint torques during such starts and so suggested that this is likely to limit start performance. The four segment torque driven model also revealed that optimal joint angles exist for the hip and knee but such a result was not clear for the ankle. For this model the optimum angle at the hip was 73° (the smallest tested) and 108° at the knee which was the athlete's usual angle. Increasing the athlete's strength parameters resulted in a small increase in horizontal velocity on takeoff for some simulations and all simulations had enhanced acceleration. Increasing initial muscle activations didn't increase horizontal takeoff velocity but did also increase horizontal acceleration. The fourteen segment angle driven model was used to optimise spring parameters for input into a torque driven model. The fourteen segment torque driven model simulated movements and forces realistically but an adequate match was not found to the sprint start performance of the participant due to long simulation times and lack of computing power.

Key words: computer simulation, sprint start, velocity, acceleration, impulse.

Presentations

Jessop, D. M. and Pain M. T. G. (2009), Mechanical and biomechanical limitations of the sprint start. Journal of Sport Sciences. 27 (S2) S104.

Jessop, D. M. and Pain, M. T. G. (2007), An angle driven model of the sprint start. *Journal of Biomechanics, Program and Abstracts of the XXI Congress, International Society of Biomechanics*. Taipei, Taiwan, 1-5 July*, 2007*. 40, S2, p. S782.

Jessop, D. M. and Pain, M.T.G. (2007), Effect of number of foot segments and viscoelastic properties of the foot in an angle driven model of the sprint start. In *Proceedings of the British Association of Sport and Exercise Science Biomechanics Interest Group Meeting*. Liverpool John Moores University, March 2007.

Jessop, D. M. (2006), Marker position and model creation using VICON. In *Proceedings of the British Association of Sport and Exercise Science Biomechanics Interest Group Meeting,* March 2006.

Pain, M. T. G., Mills, C and Jessop, D. M. (2005), Determining subject specific torque-velocity relationships with the inclusion of high velocity torque data. *In: Proceedings of the International Society of Biomechanics Conference,* 2005.

Jessop, D. M. and Pain, M. T. G. (2004), Strategies for Maximum Velocity Movements in Relation to Reaction Time and Performance Outcome. *In Proceedings of the Annual Conference of The British Association of Sport and Exercise Sciences.* Liverpool John Moores University, 7th-9th September 2004. pp. 17 – 18.

Jessop, D. M. and Pain, M. T. G. (2004), Maximum Velocity Movements. *In Proceedings of The British Association of Sport and Exercise Sciences Student Conference*. Lilleshall Sports Injury and Human Performance Centre, 27th-28th April 2004.

Acknowledgements

Dedication

To Caz

Contents

List of Figures

linear spring damper.

Chapter 1

Introduction

A good sprint start provides an athlete with a physical and psychological advantage over his slower starting competitors (Martin and Buoncristiani, 1995) so many have considered that a good start is an essential component to winning races (e.g. Henson et al., 2002; Stevenson, 1997; Tellez and Doolittle, 1984; Sigerseth and Grinaker, 1962; Hayden and Walker, 1933). Because of this, the sprint start has been the focus of much research over the last century but a consensus has not been reached with regards to the best starting technique to use.

An athlete's positioning for the start is usually found though trial and error or is something that they have become used to since early on in their career. However, it is something which is difficult to quantify in a practical setting and so is likely to be decided upon by how it feels to the athlete and looks to the coach. As will be discussed, in the past coaches and scientists have adopted a 'one size fits all' approach, assuming that what works for one elite athlete will be suitable for everyone. A sound reasoning for the positions adopted and movements that an athlete performs is often neglected which may lead to problems which are not identified until much later on in an athlete's career. For example Christie (1995) noted that large faults with his start were not noted until reaching an elite level.

1.1 Description

In the modern day sprint race, athletes have to use a crouched start from starting blocks (Rule 161, IAAF rules for competition, 2010 - 2011). One leg is placed in front of the other, pushing back against starting blocks whilst their hands are positioned directly behind the start line. The hips are held just above shoulder height with the head held in alignment with the back. On the sound of the gun, a vigorous arm action and powerful drive from the legs propel the athlete out of the blocks (Williams, 1980).

The first step a sprinter takes out of the block is the shortest step they will take in the whole race (Moore, 1980). The foot should land behind the knee helping the leg to drive back again, limiting deceleration on landing. A low body angle to the track enhances the athlete's horizontal velocity and hence he runs faster out of the block (Pender, 1983).

Ideally, athletes should have a controlled method of finding their most efficient method of starting. One which would allow them to leave the starting blocks with the highest velocity, in the shortest time. And also one which accounts for the athlete's individual characteristics such as body type, limb lengths etc. This study will use a biomechanical approach in an attempt to develop such a method.

The area of biomechanics itself uses mechanics to explore and explain the movements of living organisms (Enoka, 1988). Therefore, a biomechanical examination of the sprint start should examine an athlete's movements during the start, examine their contact with the starting block and apply mechanical theory in order to understand the processes involved.

1.2 Scientific Method

The study will use the scientific method in order to find justified answers to questions which will be set out at the end of this section. The scientific method, shown in Figure 1.0, seeks to explain the complexities of nature in a replicable way by a logical process of developing and testing hypotheses. Results may then be used to explain occurrences and to make useful predictions (e.g. Thomas and Nelson, 2001; Clarke and Clarke, 1984). Importantly Yeadon (2005) made the distinction between two approaches to research which use the scientific method; experimental and theoretical research.

Figure 1.0 The scientific method (Yeadon, 2005).

In experimental research, after some initial exploration, the investigator tests hypotheses through testing using controlled experiments in order to reach a conclusion. In theoretical research the investigator proposes a theory which "may lead to conclusions only after much development and analysis" and depends upon "how much hitherto unexplained phenomena can be accounted for" (Yeadon, 2005).

1.2.1 Experimental Studies

To date almost all research into the biomechanics of the sprint start has been experimentally based. A problem that often exists in experimental research is linking the events examined to a definite cause, particularly if the study is not a 'true' experiment; for example Mero et al. (1983) used correlations to link variables such as force production, joint angles and step duration to block velocity and velocity in acceleration.

Sprint start research has presented optimum angles for starting block positioning and body configuration (e.g. Mero et al., 1983; Atwater, 1982). Much of this research is dated and there is a need for greater depth of quantitative research into the sprint start, particularly the positioning of the blocks themselves (Harland and Steele, 1997).

Indeed Beaumont (1980) noted that, at the time of writing, athletes were able to reach world class performance levels without the use of blocks at all.

1.2.2 Theoretical Studies

Theoretical research, by nature, is more conducive to providing reasons behind cause and effect relationships (Yeadon and Challis, 1994). Through the creation of computer simulation models which replicate a performer's movements (or other areas of interest), the performance may be optimised in order to improve existing, or find new techniques. Alternatively a single component may be changed in order to examine its effects without inadvertently changing others or having to spend time learning the movement. For example, Gutiérrez-Dávilla et al. (2006) examined levels of pre-activation during the sprint start. Because real subjects were used, it was difficult to account for changes that the level of pre-activation caused in the position of the CoM (centre of mass). This could be kept constant in a simulation model to examine each variable individually. Computer simulation also has the advantage that the performer's actions can be investigated without them tiring or putting them at risk from injury. For example a new move in gymnasts or aerial skiing can be tested to see if it is possible without finding it isn't at the expense of the athlete (Yeadon and Challis, 1994).

The use of computer simulation models also has limitations; mainly it is always less than a full representation of the chosen system. Whilst mechanical principles may be applied, the nature of computer simulation models means that subject numbers are typically very small and therefore conclusions are based around very small sample sizes. Until a model has been evaluated to check its closeness to reality, no conclusions may be drawn from it, as there is no guarantee of its accuracy. Even after this, it is still not certain the model will accurately predict behaviour in new conditions (Panjab, 1979).

Concluding a comprehensive review on sprint start research, Helmick (2003) summarised that future work in the area of sprint starts should examine; the use of computer simulation models, how an athletes' start may be adapted to make the best

use of their individual strengths and finally how reaction time is affected by the starting configuration used. Schot and Knutzen (1992) recommended that future sprint start studies should examine "individual lower extremity kinematics to better explain the CoM (centre of mass) motion and subsequent movement/ performance effects. An accompanying simultaneous examination of the kinetics of the athlete block interaction would provide a more comprehensive assessment of sprint start performance". These too are areas which could be examined through computer simulation research.

1.3 Approach

In order to replicate the sprint start and explain its complexities, a computer simulation model will be developed. The process of constructing a simulation model is a design process where the designer must decide which are the important factors to include in the model and which can be discarded (Hubbard, 1993). Hubbard (1993) went on to recommend starting with "the simplest possible model which captures the essence of the task being studied" and that if a model is too complex, misinterpretations are likely to occur. A key part of the modelling process is therefore to decide which variables to include in the model and which to leave out.

When examining how a performance may be improved through the use of theoretical methods, Bobbert and Van Soest (1994) suggested that "three questions must be answered: 1) Which factors determine (limit) performance? 2) Which of these factors can be changed? 3) On which of the changeable factors should we focus training"? Computer simulation models may be used to answer these questions and in turn enhance understanding of the activity (Hubbard, 1993).

Taking the above into consideration, this study will begin by investigating existing research in sprint starts. This will allow the determination of important variables and enhance knowledge of the techniques involved. A series of computer simulation models will then be created, matched as closely as possible to the start of an athlete, and then utilised in order to identify key parameters.

Q1. Does the optimum start depend upon the methods used to evaluate it?

Different studies which have examined the sprint start have used different methods to determine the best start. For example, time to clear the starting block (Hayden and Walker, 1933), velocity on clearing the starting block (Henry, 1952), impulse (Coh et al 1998; Guissard and Duchateau, 1990), time to 10 m and 30 m (Henson et al., 2002) and time to 50 yds (Sigerseth and Grinaker, 1962; Stock, 1962) have all be used to determine the most appropriate start. Optimisation of a computer model using different criteria will reveal if different definitions result in the same initial position and movements.

Q2. How do joint angles in the 'set' position influence the start?

Over the years there has been much experimental research into finding optimal positions for starting blocks (e.g. Mero et al., 1997; Payne and Bladder, 1971; Menely and Rosemier, 1969; Stock, 1962, Dickinson, 1934) as well as joint angles in the 'set' position (e.g. Coh et al., 1998; Merni et al., 1992; Mero and Komi, 1990). However, nearly one hundred years after the introduction of the crouched start using starting blocks, a consensus has not been found. Indeed, recent studies are still considering if a crouched start is any better than one from standing (Salo and Bezodis, 2004).

Q3. How does increasing muscle tension in the 'set' position affect the start?

Experimental studies have examined the effects of increased muscle activation levels whilst in the 'set' position. Pain and Hibbs (2007) noted that some athlete's may benefit from this whilst Gutiérrez-Dávilla et al. (2006) found that changes in the level of pre-activation also changed the position of the centre of mass and so made comparisons between the conditions difficult. A theoretical approach allows variables such as this to be changed whilst everything else is kept constant. This could therefore be analysed is greater depth.

Q4. Does increased strength alter the best starting technique?

If an athlete became stronger could this result in a different starting position that in turn would be more effective? Vertical jumping research (e.g. Domire and Challis, 2007) suggests that athletes should be able to jump higher when using a deeper squat. It is likely that parallels exist to the sprint start and that increases in strength could facilitate a more compact 'set' position.

By answering these questions it will be possible to begin to provide theoretical underpinnings to sprint start research. These findings may then be considered in terms of their practical applications and their implications for coaches and athletes. This may be for example through changes to the starting block position, starting technique or areas to focus on in training such as strength or flexibility.

1.4 Outline of Chapters

Chapter 2 examines previous published sprint start research, methods used to investigate sprint starts and key findings. Important kinetic and kinematic variables are identified as well as their effect on the start. Methods used for creating and optimising computer simulation models are also considered.

Chapter 3 reports the procedures used to collect subject specific data. The development of instrumented starting blocks and an anatomic model with accompanying marker set are also presented.

Chapter 4 discusses how ground contact may be modelled and presents a four segment computer simulation models of the sprint start. These are used to investigate the result of changes to initial joint configurations and joint angle time histories.

Chapter 5 describes fourteen segment angle, and torque driven models of the sprint start, and evaluates their ability to represent measured data. Investigation in to the effect of alterations to the initial start position concludes this section.

Chapter 6 is a discussion of the computer simulation models, methods used and results gained in relation to the previous research discussed in Chapter 2. Responses to the research questions set out in Chapter 1 are presented, limitations are considered as well as pathways for future research.

Chapter 2

Review of Literature

The following review will consider variables that affect the sprint start and how existing research has attempted to explore them. In addition, the composition of, and data needed to create computer simulation models will be discussed.

2.1 History

Even in the ancient Olympics a primitive type of starting block was used. This took the form of a stone sill across the start line over which athletes curled their toes in order to push off more forcefully. At this time athletes started from an upright position and it wasn't until 1888 that the crouch start was used in competition (Watkin, 1997).

At the turn of the twentieth century, athletes began to dig holes in the track (Henson et al., 2002) and this method was used until the IAAF (International Association of Athletics Federations) sanctioned the use of starting blocks in 1937 (IAAF, 2009). At this time much scepticism existed as to whether they were of any greater benefit than holes dug in the track. Hayden and Walker (1933) conducted a study to compare the two methods. It was concluded that blocks gave the faster start as the block clearance time was on average 0.0337 ± 0.0021 s quicker for the test group. This is perhaps a poor indicator of performance as it does not indicate the velocity with which the athlete cleared the starting block, indeed any position in which the lower limbs are more extended could conceivably result in less time spent in the starting block.

The introduction of starting blocks was considered "instrumental in providing a basis for improved technique and resultant lower elapsed times" (Menely and Rosemier, 1969) and since, there have been many studies examining optimal body configuration to use in the 'set' position. Currently the rules stipulate that starting blocks must be used for all sprint races (see below) however debate remains as to whether they really

do provide an advantage over standing methods (Salo and Bezodis, 2004; Gagnon, 1978; Desipres, 1972).

2.2 Summary of Rules

The following is a summary of the principal IAAF rules for starting blocks and starting sprint races (2010-2011, rules 161 and 162).

Starting blocks should be used for all races 400 m or less. Blocks should be rigid, fixed to the track using spikes and provide no unfair advantage. They should consist of two foot plates mounted on a frame for the feet to press against. The angle of the foot plates may be adjustable and can be straight or concaved (Rule 161).

Rule 161.2 states that when the starting blocks are linked to an IAAF approved false start apparatus, "the Starter and/or assigned Recaller shall wear head phones in order to clearly hear the acoustic signal emitted when the apparatus detects a false start (i.e. when the reaction time is less than 100/1000^{ths} of a second)".

Races are initiated by the Starter who calls the commands "On your marks", "Set" and then fires the gun. The athletes should not contact the ground on, or in front of the start line when in the 'on your marks' and 'set' positions (Rule 162.3).

Since January 1st this year (2010), any athlete who is deemed to be responsible for a false start will be disqualified. A false start is given for moving within 0.1s of the gun firing but warnings may also be given for; failing to comply with the Starter's commands, disturbing other competitors in the block or aborting the start without a valid reason (Rule 162.5).

It therefore appears that the rules allow for little radical variation in the design of the block. Any adaptations that an athlete makes to his start are likely to come from changes within the accepted crouched position.

2.3 Kinematics

A large number of studies have examined sprint start kinematics. This section will begin by considering the more general 'set' position and starting movements before examining the influences made by utilising a starting block.

A comparison of elite and sub-elite athletes found four key factors that separated elite sprinters from sub-elite sprinters during the start (Favérial et al., 2000). Three of these were kinematic variables: delay between end of rear and front push off, total block time and mean rear ankle velocity for the first step (the only kinetic variable was peak force exerted by the rear foot). Interestingly elite sprinters spent less time in the block and had less delay between the rear foot and the front foot leaving the blocks. However, Baumann (1976) noted the amount of time athletes spend in the blocks has little association to 100m performance. Table 1 reveals the timing of events during the sprint start based on 23 male sprinters with a 100 m personal best 10.35 ± 0.12s.

Table 1. Timing and order of events during the sprint start of elite athletes (adapted from Baumann, 1976).

Event	Time from gun to event (s)	
	Mean	S.D.
Reaction of rear leg	0.101	0.018
Reaction of front leg	0.117	0.024
Hands off	0.214	0.040
Rear leg off	0.302	0.027
Front leg off	0.470	0.036
5m distance	1.334	0.048
20m distance	3.118	0.046

Forward lean in the 'set' position, is necessary to help the athletes accelerate forwards out of the blocks (e.g. Bauman, 1976; Pender, 1983; McInnis, 1980). Nevertheless, if an athlete leans too far forward he won't feel any force against the blocks, will have too large an angle at the ankle, will be hindered by the shoulders, as well as feel uncomfortable due to there being too much pressure on his hands (Tellez and

Doolittle, 1984). It may also delay reaction time by 0.05 – 0.15 s (Hoster and May, 1979). For elite athlete's, greater upper body strength permits larger forward lean in the set position than sub-elite athletes. Bauman (1976) compared athletes with 100m personal best times of 10.2-10.6 s, 10.9-11.4 s and 11.6-12.4 s. The proportion of the athlete's weight on his hands was 82-73%, 75-62% and 67-52% respectively. More recent research considered that the increase in weight over the hands increases the vertical velocity component, however, having the shoulders perpendicular to the line allowed greater anterior-posterior forces and velocities at 2 m (Schot and Knutzen 1992)

Athletes drive out of the starting block at an angle of $49.54 \pm 2.91°$ (Čoh et al., 1998). Tellez and Doolittle (1984) stated a slightly lower angle of 45° although no evidence was given in justification, Figure 2.1. This amount of lean does not last long into the race as Mero et al. (1983) observed that by the third stride the CoM is behind the point of first ground contact. It seems that, to a point, the lower the angle of lean, the faster the athlete's start will be. Payne and Bladder (1971) noted that when an athlete's forward lean became too great the athlete appeared to stumble out of the blocks. Despite this it was during these starts that the athletes achieved their best times to 20' perhaps revealing how important the forward lean is in creating horizontal velocity.

Figure 2.1. Sprinter coming out of the blocks (Tellez and Doolittle, 1984).

Data collected by Merni et al. (1992) reveals linear and angular displacements and velocities during the start and first step (Tables 2 and 3). The 3 subjects involved in this study had personal best 100 m times of 10.68 ± 0.25 s and were 1.77 ± 0.4 m in stature. Whilst this represents a small sample population, it does provide a useful account of many variables involved in the sprint start.

Table 2. Kinematics of the sprint start (adapted from Merni et al., 1992).

Variable Name	Mean
Horizontal distances (m)	
Toe-to-toe in 'set' position	0.26 ± 0.041
Hand to front foot in 'set' position	0.53 ± 0.076
First step length	1.38 ± 0.086
Horizontal displacements (m)	
Hip displacement between rear leg takeoff and front leg takeoff	0.40 ± 0.073
Hip displacement between front leg takeoff and touchdown	0.37 ± 0.10
Vertical Displacements (m)	
Shoulder displacement between rear and front foot take off	0.30 ± 0.031
Shoulder displacement between front leg take off and touch down	0.03 ± 0.043
Shoulder displacement between impact and takeoff off on first step	0.07 ± 0.047
Hip displacement between rear leg takeoff to front leg takeoff	0.02 ± 0.024
Hip displacement between front leg takeoff and ground contact	0.04 ± 0.015
Transversal displacements (m)	
Hip displacement between front leg take off and ground contact	0.02 ± 0.038
Toe displacement between front leg take off and ground impact	0.08 ± 0.055
Rear leg angles (°)	
Ankle in 'set' position	116 ± 15.6
Knee in 'set' position	139 ± 3.2
Hip in 'set' position	129 ± 16.6
Rear leg takeoff: ankle	134 ± 14.0
Rear leg takeoff: knee	144 ± 6.8
Rear leg takeoff: hip	144 ± 11.6
Front leg takeoff: ankle	111 ± 6.3
Front leg takeoff: knee	110 ± 4.7
Take off from first step: ankle	135 ± 12.6
Take off from first step: knee	168 ± 12.1
Take off from first step: hip	196 ± 20.4
Front leg angles (°)	
Knee in 'set' position	108 ± 8.8
Hip in 'set' position	95 ± 18.9
Ankle on rear leg takeoff	111 ± 2.7
Knee on rear leg takeoff	115 ± 6.4
Hip on rear leg takeoff	119 ± 14.6
Knee on front leg takeoff	170 ± 4.3
Knee on takeoff from first step	87 ± 7.9

Table 3. Linear and angular velocities recorded during the sprint start (adapted from Merni et al. 1992).

Variable Name	Mean
Horizontal velocity (m.s^{-1})	
Hip: rear leg take off	1.70 ± 0.14
Hip: Front leg take off (Block velocity)	3.08 ± 0.3
Hip: toe touch down	3.23 ± 0.26
Hip: takeoff from first stride	4.36 ± 0.49
Front Toe: peak velocity	9.30 ± 0.80
Back Toe: peak velocity	7.60 ± 0.40
Vertical Velocity (m.s^{-1})	
Hip: Front leg take off	0.17 ± 0.32
Hip: take off from first stride	0.88 ± 0.61
Hip peak joint angular velocity ($^\circ$.s^{-1})	
Front hip extension before take off	369 ± 113
Front hip flexion after take off	648 ± 252
Rear leg flexion after rear leg take off	565 ± 122
Rear leg extension before take off from first stride	694 ± 195
Knee peak joint angular velocity ($^\circ$.s^{-1})	
Front leg knee extension before take off	623 ± 38
Front leg knee flexion after take off	827 ± 94
Rear leg extension before touchdown	570 ± 89

As can be seen in the analysis above, and will be seen throughout, research has tended to focus on the lower limb with relatively little consideration to the arms. The initial movement of the arms is the highest velocity movement during the entire sprint event (Pender, 1983) but it has been noted that the arms do not directly contribute to the horizontal velocity of the accelerating athlete. Bhommick and Bhattacharyya (1988) considered that the arms aid a forceful leg drive and help regulate leg actions as well as increasing stride length. Angular momentum produced by the arms helps to counter that which is produced by the legs swinging around each hip joint, therefore helping the athlete to maintain a straight path.

2.4 Starting Blocks

As stated in section 2.2, rules set by the IAAF limit the ways in which a starting block can be adjusted to allow an athlete to customise their start. Figure 2.2 depicts how starting blocks may be adjusted in three ways: (a) the distance of each block from the

start line, known as block distance or spacing, (b) the angle of each block from the track /horizontal, known as block angles and, (c) the width of spacing between the feet, known as block width. Adjustments to any of these will cause changes in the athlete's starting posture and in turn the mechanics of their start.
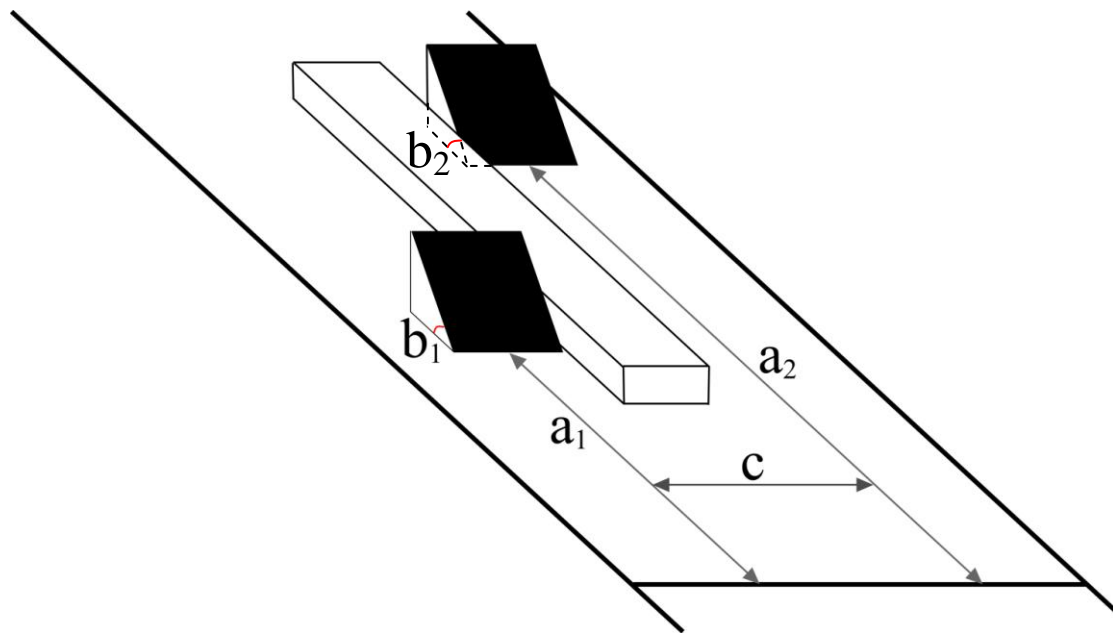
Figure 2.2. Starting blocks (a = block distance, b = block angle, c = block width, 1 = front foot side, 2 = rear foot side).

2.4.1 Block Spacing

The distance that an athlete positions each starting block back from the start line is referred to as block or foot spacing or distance. Since the crouched start was first introduced the optimum distance to have between the toes and the start line has been the focus of much research. Starting positions are often referred to as bunched, medium and elongated, or variations thereof.

Table 4 compares interpretations of each type of start and which starts were considered the fastest in each case. It can be seen that in each case the medium type start gave the fastest times, however, these starting positions are all different. For

example there is up to 34" (86.4cm) difference in front foot distance from the start line. Interestingly Sigerseth and Grinaker (1962) increased the distance from the front foot to the start line with block spacing but Menely and Rosemier (1969) decreased the gap. No justification for this was given in either case.

Table 4. Comparison of different types of sprint start.

Study	Start type				Result
	Bunched	Medium	Other	Elongated	
Sigerseth and Grinaker (1962)					
Toe to toe distance	10"	19"	N/A	28"	Medium resulted in fastest times over every 10yds to 50yd*
Distance from start line	29"	34"	N/A	41"	
Stock (1962)					
Toe to toe distance	11"	16" (back knee <130°)	Medium, high hip (back knee >165°) 16"	24"	Medium, high hip fastest times up to 50yd*
Distance from start line	NG	NG	NG	NG	
Menely and Rosemier (1969)					
Toe to toe distance	Toe of back foot placed opposite heel of front foot when standing	Knee of back leg is placed opposite front arch of front foot when kneeling	Hyper – extended. As for medium	Subject places back knee opposite front foot heel when kneeling	Hyperextended start gave fastest times to 10 and 30 yd (the only two times taken)
Distance from start line	19"	15"	As close to the line as possible	13"	
Henry (1952)					
Toe to toe distance	11"	16"	21"	26"	26" fastest block velocity, 21" gave fastest time to 10 yd, 16" gave fastest to 50 yd.
Distance from start line	NG	NG	NG	NG	

*Study only measured times up to 50 yd.

NG- Not given.

Although Stock (1962) found medium starts to give the fastest times to 50 yds, the bunched start was found to be fastest up to 20 yds and still faster than the elongated starts at 50 yds. It was thought that this was due (in the elongated start) to the greater range of movement the legs had to travel through in order to complete the first step as well as the CoM being positioned too far behind the start line. Henry (1952) noted that an elongated block spacing allow a higher block velocity, when compared to a medium spacing. However, this advantage was lost within 10 yds revealing that it is not the only factor involved in the process (Henry, 1952).

In one of the first studies to examine the effects of block spacing, Dickinson (1934) considered that a bunched spacing (defined as when the toe of the back foot is opposite the heel of the front foot when standing) allowed athletes a faster clearance time from the block as well as a faster time to 7½ ft (2.25 m). Henry (1952) agreed that a more bunched spacing allowed a faster block clearance time. This is perhaps not surprising as it seems that the rear block position remained constant (rear block contact times had a range of 0.007 s) whilst the front block was moved backwards in order to reduce the spacing. The effect was that the legs became extended in the 'set' position and had less range to extend through before they had to take off. It can therefore be considered that this would also reduce the impulse and hence block velocity. Menely and Rosemier (1969) moved the front block closer to the start line when adjusting their spacings. Interestingly the condition which placed the front leg directly behind the line gave the fastest times to each interval.

As can be seen, there have been many recommendations from published works in this area (others also include Schmolinski cited in Hoster and May, 1979; Bandejkina, 1962, cited in Hoster and May, 1979; Williams 1980, Pender, 1983), however, supporting evidence has often been lacking. Despite some research suggesting that athletes are unlikely to gain by using different starting positions (eg Henry, 1952; Blader, 1967 and Borsov, 1980) a limitation concerning the majority of the studies discussed so far is that differences in stature were not taken into account. Therefore, athletes of varying sizes would have their feet positioned the same distance apart meaning that the athletes' joint angles and in turn whole body position were different. More recently studies have attempted to overcome this by investigating angles at the hips and knees (Table 5).

Table 5. Cited and suggested lower limb angles in the 'set' position.

Study	Level of subjects	Front leg knee angle (°)	Rear leg knee angle (°)	Front leg hip angle (°)	Rear leg hip angle (°)	Trunk angle to horizontal (°)
Borzov (1980)	Elite	92-105	115-132	19-23	8-17	-8 to-22
Atwater (1982)		89 (56-112)	118 (90-154)			-23 (-9 to –34)
Mero et al. (1983)	10.2-11.8s	111	134	41	80	-29
Tellez and Doolittle (1984)	N/A	90	135			
Mero (1988)	10.79 ± 0.21	96	126			-21
Mero and Komi (1990)	10.76 ± 0.19	99	136	43 ± 5	80 ± 11	-21
Walker, (1980)	N/A	90	120			
Moore (1980)	N/A	90	120			Hips 4" above shoulders
Čoh et al. (1998)	Ave PB 10.73s	93.75 ± 8.26	112.72 ± 13.31	44.78 ± 6.15	24.91 ± 4.27	20.05 ± 8.60

N/A, angles were recommended

2.4.2 Block angle

Research to find optimum angles of starting blocks has been less extensive with just a few studies considering how the angle of the starting block to the floor may affect the athlete's start.

A lower angle of the front block to the horizontal allows a greater acceleration, horizontal velocity ($p<0.05$), and first two step lengths (not significant) (Guissard et al., 1992). When the angle of the front block was 30°, subjects took off from the block with an average velocity of 2.94 ± 0.20 m.s^{-1}. This compared to 2.80 ± 0.23 m.s^{-1} and 2.37 ± 0.31 m.s^{-1} for front block angles of 50° and 70° respectively. This is closely related to the angle at the front and rear ankle where a negative correlation has been identified (Čoh et al., 1998), the smaller the ankle angle, the greater the horizontal velocity.

Mero et al. (1997) examined two different angles of the front block, 40 and 65°, whilst the rear block was kept at a constant angle. Findings were consistent with the results above. A lower block angle resulted in a greater block velocity, duration of force production, horizontal impulse on the rear block and therefore total block impulse. However, Mero et al. identified a shorter first stride but with a higher stride frequency.

As may be expected, adjustment of a block to a lower angle increased the initial length of the Medial Gastrocnemius and Soleus. It was thought that this "may place the muscle in a more effective part of its length tension relationship" (Guissard et al. 1992). Furthermore, Guissard et al. (1992) considered that decreasing block obliquity shortened the time between the two phases of the stretch shortening cycle and increases the potential energy stored in the series elastic components. It may be because of this that Borzov (1980) considered that placing the front part of the foot flat on the ground, prolonged the thrust duration and put muscles into a greater stretch.

The pattern of extension and contraction for the Medial Gastrocnemius and Soleus can be seen in figure 2.3 (Guissard et al., 1992). It can be seen that with the front block positioned at 30° the Medial Gastrocnemius and Soleus both rapidly lengthen (for 40-50ms) and then quickly contract with a stretch shortening cycle. The pattern is similar with the block at 50° only with a greater delay between the stretch and shorten phases. However, with the block at 70° the Gastrocnemius never concentrically contracts as its overall length is increased due to extension of the knee.

Figure 2.3. Change in Gastrocnemius and Soleus muscle length during starts with different front block obliquities (Guissard et al., 1992).

Thirty degrees was the lowest block angle studied in any of these investigations. It could be that the optimum angle may be lower however the current design of starting blocks may not allow such obliquities. An examination of a selection of starting blocks revealed that the lowest angle which could be selected was 45°. These starting blocks only allowed 5 adjustments of 5°. The blocks which allowed the most adjustment allowed 7 increments at approximately 4° intervals but here the lowest angle was approximately 51°. This may therefore not allow athletes to select a position that would allow their optimum start.

2.4.3 Block Width

Spacing between the blocks i.e. how far the athlete spaces their feet apart laterally in the block, has also received little attention. Traditionally this has been something that was determined by the design of the block and was not adjustable. At the 1996 Olympic Games in Atlanta athletes complained of the blocks being too narrow (Henson et al., 2002), hence some investigation was carried out into the effect of varying the width between foot positions. Three widths were tested, 'conventional'- 24 cm, 'intermediate'- 38 cm and 'lateral'- 52 cm. Reaction time was found to be fastest under conventional settings and it was thought that this was due to the skill being highly practised from this position. Times to 5, 10 and 30 m were all fastest under the intermediate condition. Biancani (1975) observed that a 'wider' block spacing (similar to Henson et al.'s intermediate spacing) gave an average 0.25 s faster time to 5, 10, 20, and 30 yds. Both studies considered that this condition placed the athlete's legs in such a way that they travel with minimum deviation from a straight path towards the finish, as opposed to the legs flailing out to the side which is often seen during a sprinter's first few strides. Henson et al. (2002) suggested that manufacturers should account for this and links may be found to relate ideal spacings to anthropometric measurements such as hip width.

2.6 Kinetics

As the race starts, sprinters attempt to maximise their horizontal velocity by keeping their centre of gravity low to the ground through a forward lean (McInnis, 1980). Newton's third law of motion means that for the force with which an athlete pushes back against the blocks, an equal and opposite force will thrust the athlete forwards. Because of this it is thought that kinetic factors primarily determine the success of an athlete's sprint start (Faverial et al., 2000; Bauman, 1976), this means the creation of large horizontal forces and indeed a relationship has been observed between knee extensor strength and propelling force when sprinting (Ikai, 1967).

For convenience it is sometimes assumed that the resultant force vector passes through the athletes' centre of gravity (e.g. Bartlett, 1980). This however is an

oversimplification, during the initial push out of the block the force vector passes below the centre of gravity, rotating the athlete upwards. Then as the rear leg drives through, the vector passes above the athlete's CoM causing a downwards rotation. As the athlete then gets into their running the force vector must then pass below the athlete's CoM to bring them into a more upright position for sprinting (Payne and Bladder, 1971). Despite this, it is also suggested that better sprinters reduce their whole body angular momentum due to the force vector acting closer to the CoM (Gagnon, 1978).

Figure 2.4 displays a typical force trace for the sprint start. Two peaks are shown, the initial peak, created by the rear foot is sharp. The total force then falls as the rear foot leaves the block before a steady rise as the force exerted by the front foot increases. Finally the force falls as the front foot also leaves the starting block.

Figure 2.4. Force-time graph of the sprint start (Blader, 1967).

When comparing elite and non-elite sprinters, Favérial et al. (2000) noted that the key kinetic factor that distinguished the elite sprinters was a greater peak force on the rear block (group mean 1436.09 N compared to 949.41 N). Time to maximum force on the front block was also an average of 43.89 ms lower for elite sprinters. Whilst it was acknowledged that a short time to peak force is important for efficient sprint starting, it was not noted as one of the differentiating factors between elite and sub-elite sprinters.

Despite all that has been written concerning the forces involved in the sprint start, little research has examined the joint torques involved. This may be a reflection of the fact that there has also been little investigation into the angular velocities and displacements.

2.6.1 Impulse

One of the first quantitative studies into the start examined the difference between holes dug in the track and starting blocks (Hayden and Walker, 1933). It was considered that starting blocks offered the best start because the block clearance time was shorter. Therefore, spending less time in the blocks would mean reaching the end of the race sooner and hence the athlete would be faster. This is not necessarily true as it reduces the impulse (equation 2.1) that may be applied against the blocks and hence the velocity that can be created on push off (Schot and Knutzen, 1992). Shown by equation 2.2 (impulse is equal to change in linear momentum)

$$I = \int F dt \tag{2.1}$$

$$F dt = m \Delta v \tag{2.2}$$

A large impulse is important when examining the sprint start, not purely peak force (Favérial at al., 2000; Beaumont, 1980; Ludwig, 1978; Henry, 1952). "The best sprinters are characterized by a very regular impulse. They apply the maximum front foot force early and maintain it throughout the whole period on the blocks. They also exert more force with each leg" (Henry, 1952). Ludwig (1978) found a negative correlation between time spent in the starting block and 10 yd time. The effect of this was surprisingly large as on their fastest run, athlete's spent ¼ of the total time in the blocks. 10 yd time for this was 0.03 s faster than for a trial in which the athlete spent 1/7 of their time in the blocks. The data in Table 6 displays that elite athletes exert higher impulses, peak forces and have higher block velocities but often achieve this through a shorter contact period.

Table 6. Summary of studies that have examined the forces applied in starting blocks and the velocity on takeoff

Study	Level of subject (times denote 100m best)	Front leg			Rear leg			Block velocity (m.s^{-1})
		Time of front leg in block (s)	Peak force (N)	Impulse (Ns)	Time of rear leg in block (s)	Peak force (N)	Impulse (Ns)	
Payne and Blader (1971)	Elite	0.327-0.370			0.123-0.182			
Favérial et al. (2000)	Elite	0.3705	1687.61		0.25389	1436.09		
Favérial et al. (2000)	Sub-Elite	0.40511	1743.43		0.26822	949.41		
Čoh et al. (1998)	10.73s Average	0.3	936.2	201.4	0.2	1002.6	97.6	
Mero et al. (1983)	10.80 ± 0.3	0.361± 0.0.27		Total 234 ± 15				3.22
Bauman (1976)	10.2- 10.6	0.470 ± 0.036		Total 236 ± 22				3.6 ± 0.2
	10.9- 11.4	0.468 ± 0.020		Total 223 ± 20				3.1 ± 0.15
	11.6 –12.4	0.540 ± 0.032		Total 214 ± 20				2.9 ± 0.2
Guissard and Duchateau (1990)	10.8-11.2	0.327 ± 0.013	925 ± 252	190.1 ± 48.8	0.140 ± 0.015	1247 ± 153	61.0 ± 11.9	
Henry (1952) 11" spacing	College and high school	0.312 ± 0.022	414 ± 144		0.163 ± 0.037	500 ± 143		2.02 ± 0.27
16" spacing		0.333 ± 0.035	427 ± 117		0.166 ± 0.031	575 ± 162		2.26 ± 0.27
21" spacing		0.353 ± 0.021	407 ± 89		0.165 ± 0.032	593 ± 150		2.29 ± 0.20
26" spacing		0.378 ± 0.023	420 ± 121		0.156 ± 0.035	560 ± 170		2.32 ± 0.27
Mero (1988)	10.45-11.07	0.342 ± 0.022	Total 1426 ± 213	Total 223 ± 18				3.46 ± 0.32

To maximise impulse in the blocks, Ludwig (1978) concluded that the following factors must be implemented:

- Complete extension at the knee of the front leg on takeoff,
- Complete extension at the ankle of the front leg on takeoff,
- Increased hip flexion of the rear leg on front leg takeoff,
- Forward (horizontal) drive of the hips whilst still in block contact.

2.7 Muscle Activation

Mero and Komi (1990) state "in the sprint it is clear that after the gun signal every leg extensor muscle must contribute maximally to the production of force and finally to the running velocity. Therefore the faster the electrical activity begins in every muscle, the faster the neuromuscular performance is maximised". It must be considered within this that the movement should remain coordinated. Table 7 provides each muscle's reaction time and is therefore also a measure of electromechanical delay (EMD). Here pre-motor time was the time from the gun sounding to the onset of EMG activity and motor time was the onset of EMG to the start of force production (Mero and Komi, 1990).

Table 7. Reaction times of muscle groups (adapted from Mero and Komi, 1990).

	Front Leg		Rear Leg	
	Mean	SD	Mean	SD
	(s)		(s)	
Total Reaction time	0.121	0.114	0.119	0.011
Pre-motor time				
GA	0.064	0.048	0.101	0.042
VL	0.079	0.036	0.090	0.014
BF	0.097	0.024	0.096	0.002
RF	0.110	0.019	0.099	0.040
GM	0.113	0.018	0.074	0.016
Motor Time				
GA	0.057	0.050	0.018	0.029
VL	0.042	0.049	0.029	0.004
BF	0.024	0.010	0.023	0.003
RF	0.011	0.019	0.020	0.028
GM	0.008	0.009	0.045	0.009

GA = gastrocnemius caput lateral muscle; VL = vastus lateralis muscle; BF Biceps femoris caput longum muscle; RF = rectus femoris muscle; GM = gluteus maximus muscle.

Guissard and Duchateau (1990) noted that the sequence of initial muscle activations was virtually the same in both legs with only the rectus femoris and medial gastrocnemius being recruited earlier in the rear leg than in the front (Figure 2.5). Interestingly Mero and Komi (1990) noted "muscle activation varied considerably between individuals" however for the subjects of Guissard and Duchateau (1990) it was stated "the pattern of EMG activity was relatively consistent between subjects". Each study used a similar standard and number of subjects.

Figure 2.5. Electromyography of the sprint start (Guissard and Duchateau, 1990)

2.8 Computer Simulation

Having considered the movements, forces and muscle activations which make up the sprint start, it will now be considered how the start may be replicated using computer simulation.

A computer simulation model is created in three parts; a segmented model of the human body, myoactuators (muscles/ force generators) and a controller system (nervous system to activate the muscles) (Hatze, 1983). When considering the design and creation of a simulation model it is important to begin by making a model which replicates the activity in the simplest manner possible. This may allow investigation of some underlying principals but also, the more complex a model becomes the more difficult the results are to interpret and the greater the risk of confusing interactions

and compensating errors (Hubbard, 1993). A model must represent the important components of real life however, all models are approximations because not everything can be included. The choice of what to include and to leave out requires much consideration.

2.8.1 Segmented Models

A segmented model simulates the performer by representing the body using geometric shapes connected by articulated or fixed joints; examples of segmented models are that of Yeadon (1990b), Dapena (1981), Hatze (1980b) and Jenson (1976). Each model has been designed to simulate a particular type of activity, for example twisting somersaults and jumping in the cases of Yeadon (1990b) and Hatze (1980b) respectively. Depending on the complexity of the model, segments may represent a number of body parts, for example models simulating symmetrical activities may combine the left and right sides and so use one arm segment and one leg segment e.g. the Hecht vault (King et al. 1999). Further, joints are often modelled as 'pin' joints and so neglect any translational movements (e.g. Mills et al., 2008, in gymnastic landings; Domire and Challis, 2007, in vertical jumping; King et al., 1999, in vaulting).

Despite seemingly large assumptions, many models still provide excellent representations of real life activities. The model of Yeadon et al. (1990) did not allow movement at the head, wrists or ankles as the actions the model was intended to analyse do not involve large movements at these joints. The model also assumed zero air resistance, equal moments of inertia of the left and right sides of the body, rigid body segments connected at a single point and equal angle of flexion at both thigh and knee. Despite this, the model was able to simulate various twisting somersaults to within 0.04 revolutions of a somersault, 7° tilt and 0.12 revolutions twist.

29

2.8.2 Model Actuators

Computer models may be driven using a number of methods, the most simple of which is to use joint angles based on that measured in a given performance. The joint angle time histories may then be manipulated in order to analyse the effect of changes on performance criteria (e.g. Hiley and Yeadon, 2003a). Such models are limited as it is not necessarily known if a real athlete is likely be able to perform the speed and strength of muscle activations needed to replicate optimised movements. Hiley and Yeadon (2003a) avoided this by obtaining subject specific joint torque data and prevented the model exceeding limits by use of penalties in the optimisation score. However, the problem may be averted or further investigated by using the subject's strength characteristics to drive the model. For example, Yeadon and King (2002) examined the effect of strength increases in tumbling.

When creating such a model of performance there are two main options as to how the muscles are represented. The researcher can either attempt to model each muscle individually (muscle driven model) or use a torque generator at each joint to represent the cumulative effect of all the muscles acting over the joint (torque driven model) (King and Yeadon, 2002b).

2.8.3 Muscle Models

In this method identified muscles are individually represented. It may therefore appear to be the more accurate of the two methods and it allows the examination of some neuromuscular diseases, muscle-tendon injuries and surgical interventions (Hawkins and Smeulders, 1999). However, recreating the effects of each muscle for every athlete raises difficulties in measuring the properties of each muscle in turn (Yeadon and King, 2002b).

The number of muscles used in a model varies immensely. Alexander (1990) used just one muscle in his model of jumping. Pandy (2003) created of model of human gait which included 54 muscles. Each muscle had a contractile element, series and parallel elastic components as well as passive stiffness properties. Movement ranges

30

were limited by the use of ligaments at each joint. In the same paper a more simple two segment model was presented based on an inverted two segment pendulum. The simple model predicted some of the basic concepts confirmed by the more complex one. However, the author warned that such a simple model may be likely to mislead in its conclusions. Pandy and Anderson (2000) noted that the 54 muscles lead to 846 unknown variables and hence a large amount of computational power was needed to obtain solutions

2.8.4 Torque Driven Models

The use of torque generators means that the subject's joint torque-velocity parameters can be measured with the use of an isovelocity dynamometer. A profile of the total of all the muscles acting on the joint can then be created. For a given joint angle and angular velocity, the torque the joint is capable of producing is known. Whilst physiologically limited, computer models that have used torque generators to simulate performances have matched well to the measured performances (e.g. Yeadon and King, 2002; King et al., 2006). One such limitation of this method is that it is difficult to account for the function of muscles which cross more than one joint. The length of a bi-articular muscle is affected by the angle at two joints. For example, when collecting torque data using an isovelocity dynamometer at the knee, results will be affected by the angle at the hip due to the bi-articular nature of the Rectus Femoris.

Bi-articular action also allows movement at joints whilst a muscle is acting isometrically (Kuo, 2001) and so transfers power to different joints for a more economical application of energy (Jacobs and Van Ingen Schenau, 1992). For the sprint start this means that the gastrocnemius could act isometrically (and therefore provide a stronger action than a concentric contraction) to extend the ankle whilst the knee extends. This in turn means a faster movement is possible than with monoarticular muscles alone. The same could also be said at the knee for the rectus femoris. Jacobs et al. (1996) examined use of bi-articular muscles in the second step of a sprint start and considered that the hamstrings (average of semitendonosus and biceps femoris), rectus femoris and gastrocnemius account for 11% 31% and 28% of

the relative work done during hip extension knee extension and plantar flexion respectively.

2.8.5 Model Control

Once an appropriate segmented model has been selected and method of driving it chosen, controller models are needed to move it (Hatze, 1983). Muscle activations have been modelled in several ways. Perhaps the most simple method is to use 'bang-bang' activation. In this method the muscle or torque generator is either off or maximally activated (e.g Chowdhary and Challis, 2001; Alexander, 1991). Pandy et al. (1990) and Selbie and Caldwell (1996) used this method to control models of vertical jumping but despite being 'bang-bang' the activation was made to ramp up. The main advantage of bang-bang techniques can be seen when optimising a simulation as much computer power is saved (Yeadon and Challis, 1994). When trying to replicate performances however it is likely that not all muscles or torque generators will act maximally. Yeadon and King (2002) allowed the level of activation to ramp up to maximum activation from the initial level in an 'S' shaped curve. Here the onset time, initial activation, ramp and maximum activation could all be specified. A minimum of 50 ms was allowed for the ramping period although no justification was provided for this. However, none of these models allow for activation levels to vary within the performance which may be due to their relatively short, maximal nature.

An alternative to 'bang bang' activation or using an 'S' shaped curve is to use a linear activation profile. Domire and Challis (2007) and Spagele et al., (1999b) used this method to control simulation models of vertical jumping. Domire and Challis (2007) set points (control nodes) every 0.05 s and joined them by interpolation. Excitation could then be altered or optimised by increasing or decreasing the activation at each control node. Methods such as this allow activation to both increase and decrease within the activation profile although in Domire and Challis (2007) and Spagele et al. (1999b) the beginnings of profiles also tended follow an 'S' shape.

32

2.8.6 Model Evaluation

A computer model is merely a set of equations and once created it must be evaluated to examine its closeness to reality, for example by comparison to experimental data (Hubbard, 1993). Even if a model does closely simulate real life under the conditions in which it is tested, there is still no certainty that the model can predict "behaviour in unknown situations" (Panjabi, 1979). This is of great importance as the ability to predict how an athlete is able to move is often the focus of a simulation model. This problem maybe overcome by comparing the model to high quality experimental data or by basing hypothetical movements on real data (Yeadon et al., 1990).

2.8.7 Optimisation

When modelling a system, exact input values to the model may not be known and so there are an infinite number of possible solutions that the model could achieve. This is known as indeterminacy, there are insufficient known variables in an equation to solve it. In these situations, if approximate values of variables are known, a process of optimisation may be used to find a potential solution. For example, this may be useful for determining visco-elastic parameters, finding parameters to match performances or finding 'optimum' performances (e.g. Yeadon et al., 2006 in diving or King and Yeadon, 2004 in Tumbling).

During the optimisation process a score function is maximised or minimised. In a model of the sprint start this may be velocity, acceleration or impulse against the starting block. If optimising the technique of throwing a ball the score function may be release velocity or distance travelled. When selecting an optimising algorithm to use, the computational costs (how quickly it finds the optimum) and how robust it is at finding the global minimum (the true minimum of the function as opposed to a local minimum which is the optimum solution for only a small part of the possible solutions overall, Figure 2.6) needs to be considered.

Matlab computing software utilises an optimisation toolbox which includes a number of functions including 'fmincon'. This operates in a similar fashion to a simplex

algorithm (Nelder and Mead, 1965) and is referred to as 'constrained nonlinear optimisation'. Simplex works by using the gradient of the surface created by possible solutions and is reliant on an initial estimate to 'point it in the right direction'. By always attempting to go 'downhill' the algorithm finds the best solution by getting to the lowest point on the surface. Problems occur in methods such as this when waves in the surface cause the algorithm to stop at a local minimum point as mentioned above. Figure 2.6. is an example cross section through the optimising surface. The initial guess is a little way off the global optimum solution so the algorithm finds solutions down the slope. However, as is demonstrated it may stop too early due to an uneven part of the surface and so does not reach the optimum solution.

Initial guess

False optimum-local minima

Optimum solution-global minima
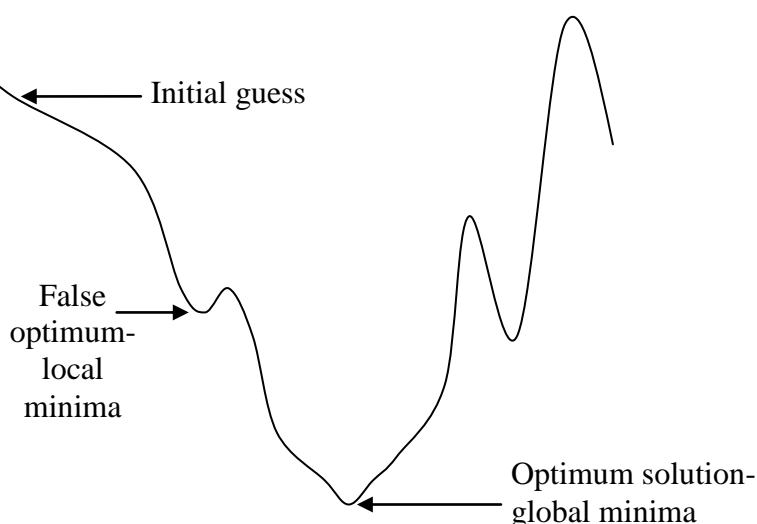
Figure 2.6. Cross section through a part of a surface of possible solutions to a problem.

Simulated Annealing (Corana et al., 1987) is an optimisation algorithm able to move both up and downhill, so can potentially explore the whole of the surface for that function. This takes greater computational power than the Simplex method but it is thought to be more robust as it is less likely to become 'stuck' in local minima (Goffe et al., 1994). As the name suggests there is an analogy to cooling metals; at high temperatures the molecules are free to move but as the metal cools, the molecules begin to become more structured (Brooks and Morgan, 1995). The 'temperature' at which the algorithm is run is an important feature. At a high temperature the

iterations are large and only a general picture of the overall function may be found. As the temperature becomes lower, the search can become more specific.

DIRECT optimisation (Finkel, 2003) attains its name from dividing rectangles. If the possible solutions are considered to be a surface, DIRECT splits the surface up into rectangles and samples in each rectangle. Rectangles with good solutions are further divided in order to find an even better solution in that area (figure 2). As the whole surface is sampled, no initial guess is needed, however the time taken to run this optimisation may be longer than some other methods.

Figure 2.7. Simplification of several iterations of DIRECT (Finkel, 2003). Each shade darker represents the next iteration.

2.9 Summary

In the past sprint start research has been experimentally based and as such it has been difficult to isolate relationships and interactions. Furthermore, studies were likely to be influenced by the level of athlete involved, motivation, experience, and preferred/ usual starting configurations.

Experimental research has also used various criteria to analyse the start and this seems likely to influence the results of any such research. Impulse appears be a more useful measure of starting performance than time or force alone and whilst variables such as block velocity have been shown to correlate to times further down the track (Mero et al., 1997), agreement as to how far is less clear (e.g. Mendoza and Schölhorn, 1993; Schot and Knutzen, 1992; Menely and Rosemier, 1969)

Computer models of athletic performances have been used to examine many activities including artistic gymnastics, tumbling, jumping and diving. A computer model of the sprint start does not yet exist but the need for such a model has been identified (Helmick, 2003). In order to construct a computer simulation model, authors note that consideration should be given to its ability to replicate real events and hence it's likely success in predicting interactions and optimum performances.

Chapter 3.

Methods of Data Collection

In order to construct and evaluate computer simulation models of the sprint start, knowledge of the kinetics, kinematics and muscle activations of an athlete's performance were required. This section begins by discussing how body coordinate systems may be calculated. This information was needed to inform the creation of an anatomic model which allowed 3D kinematic sprint start data to be collected. Kinetic data were recorded using an instrumented set of starting blocks, Section 3.2 discusses the construction and calibration of this apparatus. Finally how the anatomic model, instrumented starting blocks and other equipment were utilised to record an athlete's start is described.

3.1 Kinematic Modelling

In order to obtain movement data, the Vicon™ motion tracking system was utilised. This system tracks retro-reflective markers in three dimensions by combining views from multiple cameras. This section will consider how knowledge of marker movement may in turn allow the examination of human movement. Combined with knowledge of anatomy this allowed the creation of a whole body anatomic model for use in computer simulations.

3.1.1 Translation and Rotation

When recording movements of the human body it is recommended that local and global coordinate systems are used (Baker, 2003; Cappozzo et al., 1995). The global coordinate system provides a defined area in which the body moves. Attaching local coordinate systems to each segment helps to describe the location and orientation of each segment, individual joint movements and where features such as the CoM lie.

To know where a point in a local coordinate system lies in terms of a global coordinate system, the coordinate of the point in the local system is added to the point of origin of the local system in the global coordinate system.

Location of point P in the global coordinate system	Location of the origin of the local coordinate system in the global system	Location of point P in the local system	Location of point P in the global system

$$
\begin{bmatrix} P_X \\ P_Y \\ P_Z \end{bmatrix} = \begin{bmatrix} L_X \\ L_Y \\ L_Z \end{bmatrix} + \begin{bmatrix} P_x \\ P_y \\ P_z \end{bmatrix} = \begin{bmatrix} L_X & +P_x \\ L_Y & +P_y \\ L_Z & +P_z \end{bmatrix} \quad (3.1)
$$

Zatsiorsky (1998)

When examining the human body in motion it is unlikely that translation will occur without rotation of the segment and hence this must also be expressed. A direction cosine is the cosine of the angle between a vector and an axis (in 2D).
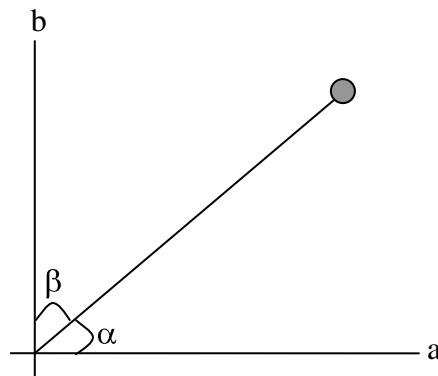
Figure 3.1. Direction cosines.

The direction cosines, cosineα and cosineβ, often termed *l* and *m,* can be calculated:

$$
l = \frac{a}{\sqrt{a^2 + b^2}} \quad (3.2)
$$

$$m = \frac{b}{\sqrt{a^2 + b^2}}$$ (3.3)

The vector P which rotates in the global frame can be described using

$$P_X = P_x \cos\alpha + P_y \cos(90 + \alpha)$$ (3.4)

$$P_Y = P_y \cos(90 - \alpha) + P_y \cos\alpha$$ (3.5)

Written as a matrix this becomes

$$\bar{P}_G = \begin{bmatrix} P_X \\ P_Y \end{bmatrix} = \begin{bmatrix} \cos\alpha & \cos(90+\alpha) \\ \cos(90-\alpha) & \cos\alpha \end{bmatrix} \cdot \begin{bmatrix} P_x \\ P_y \end{bmatrix} = \bar{R} \cdot \bar{P}_L$$ (3.6)

Where G and L represent global and local components and R is a rotation matrix which gives the local coordinate system in relation to the global one. R can be written as

$$\bar{R} = \begin{bmatrix} \cos\alpha & -\sin\alpha \\ \sin\alpha & \cos\alpha \end{bmatrix}$$ (3.7)

as 90° + α = -sin and 90°-α = sin.

The same can be done for vectors with 3-D coordinates.

$$l = \frac{a}{\sqrt{a^2 + b^2 + c^2}}$$ (3.8)

$$m = \frac{b}{\sqrt{a^2 + b^2 + c^2}}$$ (3.9)

$$n = \frac{c}{\sqrt{a^2 + b^2 + c^2}}$$ (3.10)

So for a 3-D rotation written in matrix notation

$$
\begin{bmatrix} P_X \\ P_Y \\ P_Z \end{bmatrix} = \begin{bmatrix} \cos_{Xx} & \cos_{Xy} & \cos_{Xz} \\ \cos_{Yx} & \cos_{Yy} & \cos_{Yz} \\ \cos_{Zx} & \cos_{Zy} & \cos_{Zz} \end{bmatrix} \cdot \begin{bmatrix} P_x \\ P_y \\ P_z \end{bmatrix} = \begin{bmatrix} P_G \end{bmatrix} = \begin{bmatrix} R \end{bmatrix} \begin{bmatrix} P_L \end{bmatrix} \tag{3.11}
$$

The equations for translation and rotation can be combined to provide a complete description of the location and orientation of a segment.

$$
\begin{bmatrix} P_X \\ P_Y \\ P_Z \end{bmatrix} = \begin{bmatrix} L_X \\ L_Y \\ L_Z \end{bmatrix} + \begin{bmatrix} \cos_{Xx} & \cos_{Xy} & \cos_{Xz} \\ \cos_{Yx} & \cos_{Yy} & \cos_{Yz} \\ \cos_{Zx} & \cos_{Zy} & \cos_{Zz} \end{bmatrix} \cdot \begin{bmatrix} P_x \\ P_y \\ P_z \end{bmatrix} \tag{3.12}
$$

3.1.2 Centre of Rotation in Human Joints

In order to use knowledge of marker movements to calculate human movements, an understanding of human anatomy is required. Joint centres and segment orientations must be predicted based on the locations or movements of markers attached to the surface of the body.

Finding the location of a joint centre is complicated by the various surrounding tissues. With this in mind, two approaches may used to find the centre of a joint. The functional method uses the movements of groups of markers in order to locate the centre of rotation of the segment (e.g. Besier et al., 2003). The other method requires identification of anatomic markers whereby the joint centre has previously been identified to be located at a known location nearby. This data may have been gained from studies which used scanning methods such x-rays and MRI scans (e.g. Chow et al., 1999), based on data from cadaver studies e.g. Seidel (1995) or using the functional method above.

Location of joint centres using technology such as radiography is not practical do to for every subject. Interpretation can be complex and it is also limited due to availability, expense and is not feasible for use with children due to radiation exposure (Bell et al., 1989). Use of this and data from cadavers may lead to inaccuracies in findings if subjects are not representative of the population studied (Chow et al., 1999).

Anthropometric data from cadavers are not widely available for sporting populations and so data from more general populations are often employed. To use segmental mass centres as an example, locations are often calculated based on studies such as that of Dempster (1955). Dempster's data was based on eight elderly cadavers but results have been applied to athletic populations from long distance runners to power athletes (e.g. Hobara et al., 2008), including sprinters (e.g. Kunz and Kaufmann, 1981). Sprinters possess different and less varied anthropometric characteristics compared to the general population (Uth, 2005) and so to use Dempster's data may introduce a source of error.

Functional methods may be "slightly more repeatable" for the lower limb, however, Besier et al. (2003) found few significant differences in axis identification (using the helical axis method). The main benefit of the functional method was thought to be for experimenters who are not experienced in identifying bony landmarks or for subjects who are obese or have a deformity which again might make feature identification more problematic.

The following examines various studies with the view to creating an anatomic model, called Anatomic, which may be used to examine an athlete's movements during a sprint start. This model needed to identify the locations where markers could be placed and then by tracked by a multiple camera, passive marker, automatic tracking system (Vicon™)

3.1.3 Whole Body Models

De Leva (1996b) used Chandler's cadaver study (Chandler et al., 1975) data in order to calculate longitudinal distances along each segment to find the joint centres. The result was a set of data stating the position of the joint centre for each major joint in the limbs (Figure 3.2). This was used in conjunction with a body segment inertia parameter model (Zatsiorsky et al., 1990a) in order to calculate joint centre locations (de Leva, 1996).

Figure 3.2. Joint centre locations (De Leva, 1996).

As measurements have only been calculated in one plane, this data is most relevant for use in 2-D studies. Use of this data is likely to contain at least two potential sources of error. Firstly it requires the scientist to have an excellent knowledge of anatomy in order to find the relevant bony landmarks. Secondly, because the data is based on cadavers and not the athlete of interest, it is unlikely that the distances stated will be exact. These problems are relevant to any anatomical study in this area. Their use must therefore be considered in terms of predicted accuracy and compared to other available methods.

Research has tended to focus on individual joints rather than whole body models. The remainder of this section will focus on how investigators have attempted to locate the rotation centres of individual joints. Further, these methods result in convenient location methods for use in practical situations.

3.1.4 The Hip Joint

The hip, or coxageal, joint is a ball and socket joint formed by the femoral head inserting into the acetabulum. An articular capsule is formed from the rim of the acetabulum to the neck of the femur and is reinforced by ligaments (iliofemoral, transverse acetabular, pubofemoral, ischiofemoral, ligamentum teres) (Seeley et al., 1992). It is flexed by muscles including the iliopsoas, rectus femoris, and extended by muscles including the gluteus maximus and the hamstring group (semitendinosus, semimembranosus and biceps femoris). Abduction, adduction and lateral and medial rotation are also possible. Due to the sphericity of the femeral head the joint axes are not displaced during joint movement (Zatsiorsky, 1998).

Palpation of the joint is difficult due to the surrounding musculature. The top of the greater trochanter can however be located. The joint centre is considered to be 1 cm proximal to this but passive movement of the joint is likely to aid the process of location (Palastanga et al., 2002). The ISB standardisation committee recommended standardised coordinate systems for the pelvis and hip joints. The origin is situated at the midpoint between the two ASIS (anterior superior iliac spine). The Z axis lies along this line and is positive towards the right ASIS. The Y axis is then perpendicular to this vertically with the X axis perpendicular in a horizontal plane. A similar system was also recommended for the femur. For this the Y axis is orientated as a line from the 'midpoint of the medial and lateral epicondyles' to the centre of the hip joint. As for the pelvis the Z axis is perpendicular to the right of the subject and the X axis perpendicular to both the Z and Y axes pointing forward from the subject (also Cappozzo et al., 1995).

Seidel (1995) examined the pelvises from the cadavers of 35 women and 30 men. The hip joint centre was found to be '14% (S.D. 3%) of pelvic width medially, 34%

(S.D. 2%) of pelvic depth posteriorly, and 79% (S.D. 5%) of pelvis height inferiorly. Predicted error was 0.58 cm in width, 0.30 cm in depth and 0.35 cm vertically. Interestingly the results were combined for males and females. The distances were also found as a percentage of inter ASIS distance which is a common definition of pelvis width. This could be particularly useful as the width is much more simple to find than the height or depth. The location given was 30% (S.D. 4%) distally, 14% (S.D. 3%) medially, 24% (S.D. 2%) posteriorly. This was however, noted to be somewhat unreliable but required fewer measurements to be taken.

Bell et al. (1990) compared similar studies, that of Tylkowski et al. (1982) and Andriacchi et al. (1980, 1982 and Andriacchi and Strickland, 1983). The studies by Andriacchi "predicted that the hip centre would lie 1.5 – 2 cm directly distal to the midpoint of a line between the pubic symphysis and the ASISs in a frontal plane projection, and directly medial to the greater trochanter in the sagittal plane. Tylkowski's (1982) group predicted that the hip centre would lie 11% of the distance between the ASIS medial to, 12% distal to and 21% posterior to the ASIS" (Bell et al., 1990). X-ray radiographs were used as a gold standard to compare the methods against each other on 7 male subjects. The replication of Andriacchi's method put the hip centre an average total error (combined from the three axes) 3.61 cm from its true location however just 0.73 cm of this was due to error in the anterior-posterior direction (Bell et al., 1990).

Lack of information concerning the position and orientation of the reference frame for Tylkowski's (1982) study meant that the percentages calculated from the average position in this study were, as a percentage of inter ASIS distance: 30% distally, 14% medially and 19% posteriorly. These values are extremely similar to that of Seidel (1995) above and Bell et al. (1989) (30, 14 and 22% respectively). Interestingly the only value that was different, the anterior-posterior value was the source of most error. This was the source of least error in the method by Andriacchi et al. (1980, 1982 and Andriacchi and Strickland, 1983) as the authors used an extra marker in order to help use this method in the AP direction. The combination of the two methods gave a total error of 1.07cm. The initial problem was thought to lie in locating the ASIS from markers (Bell, et al., 1990).

In their study Shea et al. (1997) defined the axis as x (anterior- posterior), y (medial-lateral) and z (superior- inferior). In order to locate the hip joint centre, markers were placed on the pelvis and thigh. Subjects circumducted the hip joint and the marker movements were used to find a centre of rotation. As with the studies mentioned above the location of a hip joint centre was expressed as a percentage of inter ASIS distance (X = -22.8%, Y = -38%, Z= 45%).

Davis et al. (1991) based their study on radiographs of 25 hip joints. This may not be especially accurate due to the comments above stating that radiographs are difficult to interpret for such matters. The results from this provided mean angles for which each PSIS (posterior superior iliac spine) is positioned relative to each ASIS (Figure 3.3). These were calculated to be 28.4° in the coronal (parallel to the face) and sagittal plane 18°. They also predicted inter ASIS distance as a function of leg length through a regression equation ($C = 0.115L_{leg} - 0.0153$, r squared = 0.90).

Figure 3.3 Calculation of hip joint centre by Davis et al. (1991)

3.1.5 The Knee Joint

The knee joint is composed of the tibiofemoral and patellofemoral joints. The tibiofemoral joint is a 'complex ellipsoid joint', although it is traditionally classified as a hinge joint (Seeley et al., 1992), formed where the distal end of the femur meets the proximal end of the tibia. It allows a range of approximately 145° of flexion-extension, also a small amount of rotation and abduction-adduction depending on the extent of flexion-extension (Zatsiorsky, 1998). The axis for flexion-extension

movements is also not perpendicular to the line of the femur. Hollister et al. (1993; cited in Zatsiorsky, 1998) put the angle at $84 \pm 2.4°$. Extension is initiated by the quadriceps group (rectus femoris, vastus lateralis, vastus intermedius and vastus medialis). Flexion is initiated via muscles including the hamstring group (semitendinosus, semimembranosus and biceps femoris).

The knee joint has many features which can be located by palpation: the circumference of the patella, "the articular margin of the femoral condyle; the articular margin of each tibial condyle; the joint line medially, anteriorly and laterally; the tibial tuberosity together with the ligamentum patellae attaching to it; the adductor tubercle, and the medial and lateral epicondyles of the femur" (Palastanga et al., 2002).

Besier et al. (2003) compared a helical axis method and an anatomical method for locating lower limb joints. For the anatomic method, the knee joint centre was positioned midway between the femoral lateral and medial epicondyles which are easily palpable. Interestingly significant kinematic differences were found only for knee rotation.

Cappozzo et al. (1995) recommended that the axes for the shank are orientated as follows. First they defined a plane formed by the medial and lateral malleoli and the apex of the fibula. This forms a 'quasi frontal plane' and a 'quasi sagittal plane'. From the origin this is orthogonal to the frontal plane and goes forward through the tibial tuberosity. The origin is at the midpoint between the two malleoli with the Y axis following intersection of the frontal and sagittal planes, the Z axis following the line of the frontal plane to the right and the X axis following the line of the sagittal plane ventrally.

3.1.6 The Ankle Joint

The ankle joint is a complex of two joints, the talocrural and subtalar or talocalcaneal joint. The talocrural joint is formed where the tibia and fibula meet the talus and only one degree of freedom is permitted, plantar flexion-dorsiflexion, which can be defined as rotation about a lateromedial horizontal axis (Zatsiorsky, 1998). The subtalar joint is formed by the talus and calcaneus and also has a single axis allowing inversion and eversion. Dorsiflexion at the ankle is performed by the Tibialis anterior and peroneus tertius. Plantar flexion is performed by the gastrocnemius, soleus and plantaris.

Cappozzo et al. (1995) recommended the following coordinate system for the foot: the origin is located on the calcaneus at a prominence on the posterior superior edge. A transverse plane is then made using this point and the first and fifth metatarsals. The sagittal plane is formed by the second metatarsal and the origin and is orthogonal to the transverse plane. The axes are situated as follows: the Y axis lies along the intersection of the two mentioned planes and is positive in a posterior direction to the subject, the X axis follows the line of the sagittal plane vertically and the Z axis follows the line of the transverse plane to the right of the subject.

The ankle (talocrural) joint centre is commonly taken as the medial or lateral malleolus due to ease of location during the digitising process. Inman (1976; cited in Zatsiorsky, 1998, p. 297) put the actual location 3 ± 2 mm distal to the lateral malleoli and 5 ± 3 mm distal to the medial malleoli however, Besier et al. (2003) placed the centre between the two malleoli. It is perhaps clear then why these are such useful reference points to use for manual digitisation. However, Palsatanga et al. (2002) locate the centre line of the joint centre a little further away from the malleoli, '1 cm above the tip of the medial malleolus and 2 cm above the tip of the lateral malleolus'.

3.1.7 The Shoulder (Glenohumeral) Joint

The shoulder joint is a ball and socket joint formed by the head of the humerus and the glenoid fossa of the scapular. In this joint stability has been somewhat sacrificed

in return for range of movement as the socket is quite shallow. Therefore three degrees of freedom (DOF) are allowed, flexion-extension, abduction-adduction and rotation. Flexion is performed by the coracobrachialis and anterior deltoid; extension by posterior deltoid, teres major, infraspinatus and subscapularis; abduction by deltoid and supraspinatus; adduction by coracobrachialis, latissimus dorsi, teres major and teres minor.

A simple method to find the centre of rotation for the shoulder was used by de Luca and Forrest (1973). They took 3 frontal plane x-rays with the shoulder abducted at different angles all on the same film. To find the joint centre they traced an outline of the humerus and, by trial and error rotated the radiograph to find the centre of rotation. 'In all cases, the instantaneous centre of rotation was situated medially and inferiorly to the greater and lesser tuberosities of the humerus, but not necessarily on the head of the humerus'. This is similar to some mathematical methods which are based on rigid body movement such as the Reuleaux method or Spiegelman and Woo (1987). Although this helps locate a rotation centre it is only 2-D, requires the use of an x-ray machine and no information was provided on how accurate this method was expected to be.

Meskers et al. (1998) presented a regression method based on bony landmarks. This method has also been compared with sphere fitting and helical axis techniques (Stokdijk et al., 2000, Table 8). The coordinate system was defined using the acromial angle, trionum spinae and angulus inferior, though no more information was given.

Table 8. Predicted location of the glenohumeral joint centre of rotation using three different methods, Stokdijk et al. (2000), standard deviations in brackets.

Method	Joint Centre Location (cm)		
	X	Y	Z
Regression	0.92 (0.48)	-2.60 (0.26)	-3.52 (0.35)
Sphere fitting	-1.01 (0.34)	-4.76 (0.32)	-3.84 (0.41)
Helical Axis	-1.35 (0.38)	-4.84 (0.26)	-3.94 (0.42)

The study (Stokdijk et al., 2000) was conducted from a clinical perspective and so the helical method was preferred as this allowed the centre of rotation to move. A method which relies on finding bony landmarks, which then do not move in relation to the point of interest becomes less useful if there is instability in the joint and the point moves. Importantly this was minimised by not allowing abduction greater that 45°. The helical axis technique can also calculate rotation at any joint whereas the sphere technique is limited to ball and socket joints. The regression method was also considered less accurate due to differences between observers, particularly in locating bony landmarks, as well as the comments above relating to movements about fixed points.

Veeger et al. (1997) also found the glenohumeral joint centre using helical axes. They considered that, although the shoulder has been examined in some detail, no quantitative description is available to help find the joint centre. Results presented were only based on one subject (cadaver), with little mention of measurement accuracy and also in terms of a global reference frame, which should be carefully examined if using the results.

3.1.8 The Elbow Joint

The elbow is composed of two joints, the humeroulnar and humeroradial joints, where the humerus meets the ulna and radius. The humeroulnar is a hinge joint and the humeroradial is a ball and socket joint. Only two DOF are permitted; flexion-extension and pronation-supination. Flexion is performed by the brachialis, bicep brachii and brachioradialis; extension by triceps brachii and anconeus; pronation by pronator quadratus and pronator teres; supination by biceps brachii and supinator.

The axis of rotation for the flexion – extension at the elbow has been identified using cadaver studies as the centre of the trochlea (Morrey and Chao, 1976) or at the centre of the arcs formed by the trochlea sulcas and the capitellum (London, 1981). Whilst these may form a useful location for defining the rotation centre, it is not easy to locate.

ISB recommendations (Wu et al., 2005) define the long axis for the humerus as between the glenohumeral rotation centre and the mid point of the medial and lateral epicondyles. The Z axis is between the epicondyles, to the right and this forms the axis of rotation for flexion at the elbow. The medial and lateral epicondyles of the humerus are easily palpated and Schmidt et al. (1999) used this convention for locating the joint centre although no justification was provided. Palastanga et al. (2002) placed joint centre 1 cm distal to the lateral and 2 cm distal to the medial epicondyles. No explanation was provided as to how these measurements were made and as they are provided to 0 d.p., can only be taken as estimates. For men, Shiba and Sorbie (1985; cited in Zatsiorsky, 1998) placed the axis at 15.2-15.3% of the interepicondyler distance. A line drawn 45° from the line of the humerus would run through the centre of rotation. Stokdijk et al. (1999) placed the elbow centre of rotation 0.81 cm cranially and 1.86 cm ventrally of the epicondylus lateralis at 15.3° to the frontal plane. This was found from calculations using helical axes.

3.1.9 The Wrist Joint

The wrist, or carpus, is composed of eight carpal bones, meaning that it comprises many individual joints 'including the radiocarpal joint, several intercarpal joints, and five carpometacarpal joints' (Zatsiorsky, 1998). Only two DOF are permitted, flexion-extension and abduction-adduction. When combined with pronation-supination from the elbow, the hand appears to be connected by a ball and socket joint, however this configuration allows for much greater stability (Palastanga et al., 1989). Flexion is performed by muscles including; flexors carpi radialis and ulnaris, and extension by muscles including; extensors carpi radialis brevis, carpi radialis longus, carpi ulnaris and digitorum. Abduction is performed by muscles including; flexor carpi radialis, extensor carpi radialis brevis, extensor carpi radialis longus, and adduction is performed by muscles including flexor carpi ulnaris and extensor carpi ulnaris.

Schmidt et al. (1999) located the centre of the wrist by placing markers either side of the line of the joint. The mid point was then used as the centre. Whilst this appears a

logical location, numerous equations were provided on calculation of joint angles (including the elbow) and reduction of noise due to marker movement, but there was no mention of justification for this initial position.

3.1.10 Anatomic Models

The aim of this part of the present study was to create an anatomic and marker set specifically designed for analysis of sprint starts. Cappozzo et al. (1995) made several recommendations for the placement of markers used in tracking human movements: at least three markers are required per segment in order to locate its position and orientation; the position of each marker should be considered in order that it can be seen from sufficient cameras, the markers should not form a straight line and should not be placed close together, markers should be placed on areas of skin that are not likely to move in relation to the underlying bone, markers should be quick and easy to place.

3.1.10.1 Golem Model

This is the model and marker set that is part of the basic Vicon package. The model assumes that, with the exception of the shoulder and hip, the centre of each joint in the limbs lies at half of the joint width. The calculation of the hip joint centre uses the findings of Davis et al. (1991) from their study of 25 hip radiographs (see above for details). The reasoning for other joint orientations and definitions is less clear.

In order to define a segment's movement, a minimum of three markers are required to provide a three dimensional position and orientation, however, the Golem model assumes that movement at the knee and elbow are 2-D hinge joints. This assumption reduces the total number of markers needed for the limbs but also means that the location of all proximal points in the chain must be known. Consequently, should the position of the hip joint centre be lost in tracking, then so are the locations of the knee and ankle joint centres. Furthermore, as stated above, the knee does allow some adduction/abduction movement, so whilst the 2-D assumption may be useful to save on markers, it is only advantageous if it is considered acceptable.

51

3.1.10.2 Anatomic Model

To create a sprint start specific model, analysis of the research in section 3.1 was used in order to select and justify methods of locating joint centres. Further consideration was also given to the spine, shoulder, hip and foot.

3.1.10.3 Spine

During bending, the vertebrae in the upper spine, move along an arc and therefore the relative movements of each vertebrae should be described through rotation and translation (Zatsiorsky, 1998). Movement in the thoracic section of the spine is limited due to structures such as the ribs and flexion in the lumber spine is nearly always accompanied by pelvic tilt (particularly past 30° flexion) (Zatsiorsky, 1998). It may be considered that a multi-segment spine or even modelling each vertebra would be the most appropriate method of segmentation but this would have added greatly to the complexity of the model and time taken to run simulations. Modelling methods for the spine have been considered by Pandy (2003) who connected a trunk to a pelvis segment at L3 when examining walking. Hatze (1980a) and Ferdinands et al., (2008) used a pelvis and lower spine segment and a chest segments although the focus of the later was rotational movements in cricket bowling.

Markers were positioned to allow for three possible trunk segments: a pelvis, abdomen and chest. The pelvis segment was defined using the ASIS and PSIS markers. The abdomen used the sternum and T10 markers, and the chest used the T10 and C7 and mid-clavicle markers (Appendix A for Vicon model code). Start data collected revealed ranges of movement of: 12.8° for pelvis – abdomen, 14.1° for abdomen – chest and 20.0° for pelvis – chest. As might be expected, the largest range of movement was found between the pelvis and chest with the least movement between the pelvis and abdomen. The spine was therefore split into a pelvis-abdomen segment and a chest.

3.1.10.4 Shoulder Joint Centre

Two different methods for determining the shoulder joint centre were considered. First a method using three markers on the scapular (Stokdijk et al., 2000). The second method used markers anterior and posterior of the shoulder in line with the joint centre (located by asking the subject to abduct and adduct) in a similar method to Luca and Forrest (1973) but without the use of x-rays, taking the mid point as the joint centre. A comparison was made over a sprint start trial. The RMS difference was 17.524 mm in the x direction, 5.990 mm in the y direction and 10.807 mm in the z direction. Figure 3.4 below displays the two trajectories.
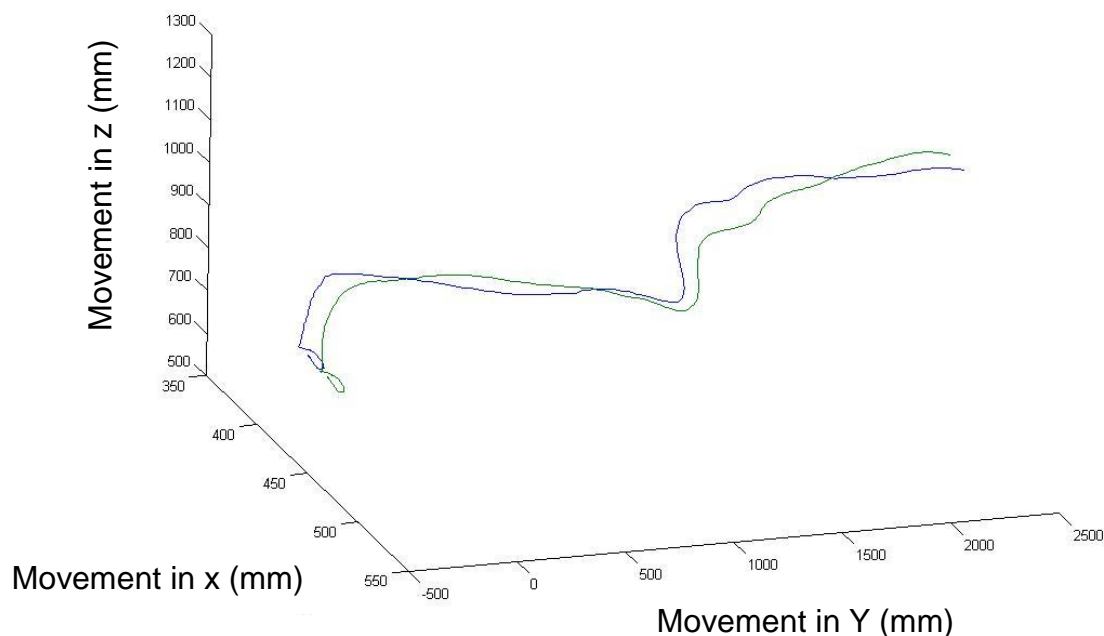
Figure 3.4. Comparison of shoulder joint centre trajectories using two marker systems. The green line is the two marker method and the blue line, the three marker method.

It is unclear which method is most accurate. It can be seen that the three marker method displays a slightly less smooth pattern. As the markers are placed on the scapular, they are influenced by scapular movements which occur as the shoulders move. The two marker method is less affected by this. Which method is the more accurate of the two is determined by whether scapular movement reflects the movements of the shoulder joint centre. It was decided to use the three marker

method due its previous justification, the large RoM that occurs at the shoulder and notable scapular movements that occur during the sprint start.

3.1.10.5 Hip Joint Centre

One problem with the athlete in the set position is that both hips are flexed and the trunk is close to horizontal. This can block the cameras view of the Anterior Superior Iliac Spine (ASIS) markers. Several methods were attempted to help solve this. The most simple of these was to add four more cameras lower down to the floor, Figure 3.5 below. This improved the amount of both hip and foot markers that could be identified by the system.
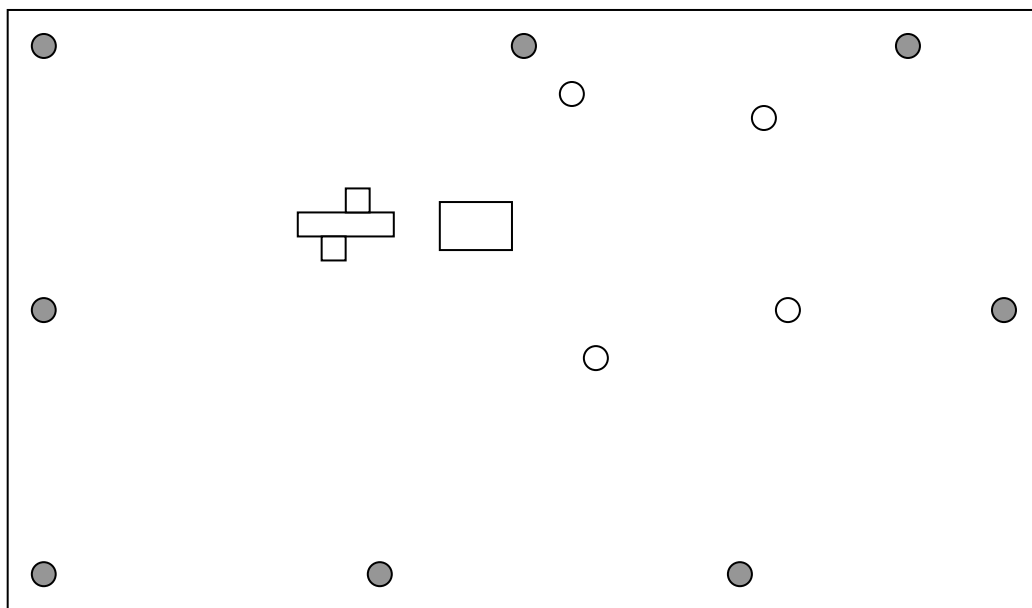
Figure 3.5. Plan view of experimental set up. Gray circles represent wall mounted cameras, white circles represent low down cameras.

Two modelling methods were also used. The first involved placing two extra markers on the pelvis, one on each superior iliac crest at the most lateral point on each side. Positioned here the cameras have the most chance of seeing them unless blocked by

the arms (which does not happen in the set position). A static trial was then taken. In the model, two new coordinate systems were created for use in a static trial based on the Posterior superior-illiac (PSI) markers and the two new hip markers, one for each side. The position of the anterior superior-illiac (ASI) was then saved to the parameter file so that if one should disappear during a trial, its location could be calculated based on the location saved from the static trial.

The second method used the two extra markers from the previous method and code from the Golem model. The Replace4 macro is able to find a markers location should it disappear from a rigid segment which has at least 3 other markers visible. This would work if only one of the ASI markers disappeared at any one time however testing revealed that it was likely both may disappear in the set position. By adding the 2 extra markers, the pelvis has 6 markers in total. This meant that 2 extra lines of the Replace4 macro could be added in order that the two ASI markers could be calculated based on the remaining marker locations. The macro works by finding the position of the missing marker in relation to the other markers over the trial and then uses this to predict its location when it goes missing. The two methods are therefore relatively similar only the first works based on a static trial, the second on the current trial.

3.1.10.6 Foot Modelling

The original model was adjusted to have a marker on the second toe as well as markers on the 1st and 5th MPJ's (metatarsal-phalangial joint) as used by Lee (1997, cited in Oleson at al., 2005). This allowed a segment for the toes and one for the rest of the foot. The joint and toe end position was taken as half the distance from the marker centre to the floor in a static trial. This method only allowed for calculation of flexion/ extension movements at the toes because two of the three markers needed to calculate the joint angle lay across the line of the joint. Testing showed that placing more markers in this area was likely to lead to occlusion of the markers and further problems of markers falling off during trials.

3.1.10.7 Model and Outputs

The methods selected for calculation of joint centres are displayed in Table 9. A marker set and model called Anatomic was created using BodyLanguage (Oxford Metrics Ltd., 2002a), Appendix A. Anatomic used 54 markers and the marker file was created so that the model could be labelled using the same names as for Golem. This was to allow some comparison although it should be noted that some of the markers are in slightly different locations. For example, Anatomic places the shoulder marker on the acromion angle (according to Stokdijk et al. 2000) whereas Golem is less specific. As far as possible axes were defined according to ISB guidelines (Wu and Cavanagh, 1995) in order to aid comparison to other studies. Figure 3.6 displays the marker locations and Figure 3.7 reveals the resulting model in BodyBuilder.

Table 9. Studies used to define joint centres

Joint	Study used to define the joint centre location
Hip	Seidel (1995)
Knee	Churchill et al. (1998)
Ankle	Inman (1976)
Shoulder	Stokdijk et al. (2000)
Elbow	Stokdijk et al. (1999)
Wrist	Not sufficient information found to justify a specific location – Markers placed laterally and mediolaterally of the joint centre
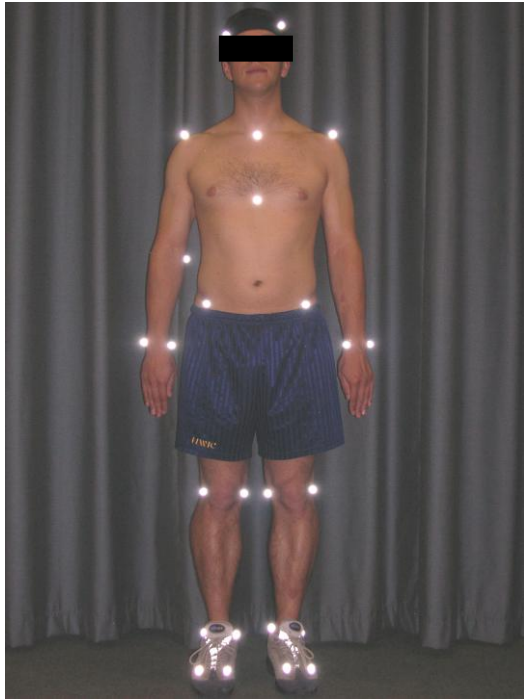
Figure 3.6a. Marker placements
- anterior view.

Figure 3.6b. Marker placements
 - posterior view.
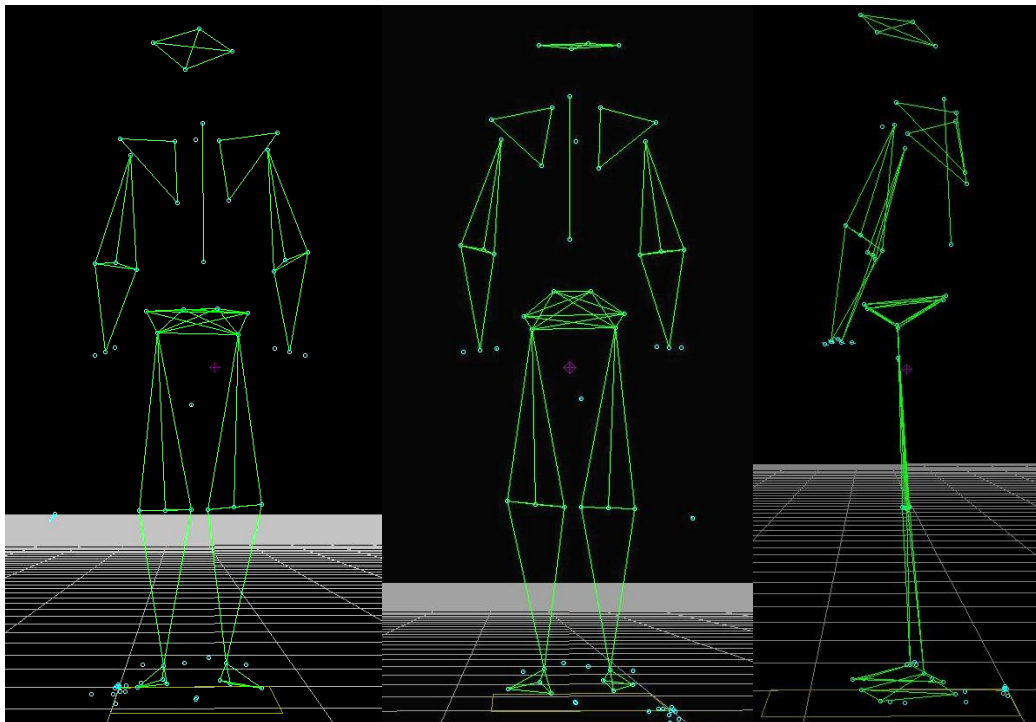
a.   b.   c.

Figures 3.7 a, b and c. Anatomic model run in bodybuilder anterior, posterior and
sagittal views respectively.

Joint centre coordinates, marker coordinates, global segment orientations, joint angles and CoM could all be output from the model. To check the model worked as expected, trials were performed with a subject performing pure flexion/extension, abduction/adduction and rotation movements at each joint. The output could then be examined. When comparing joint angles to the Golem model, similar results can be seen (Figure 3.8).
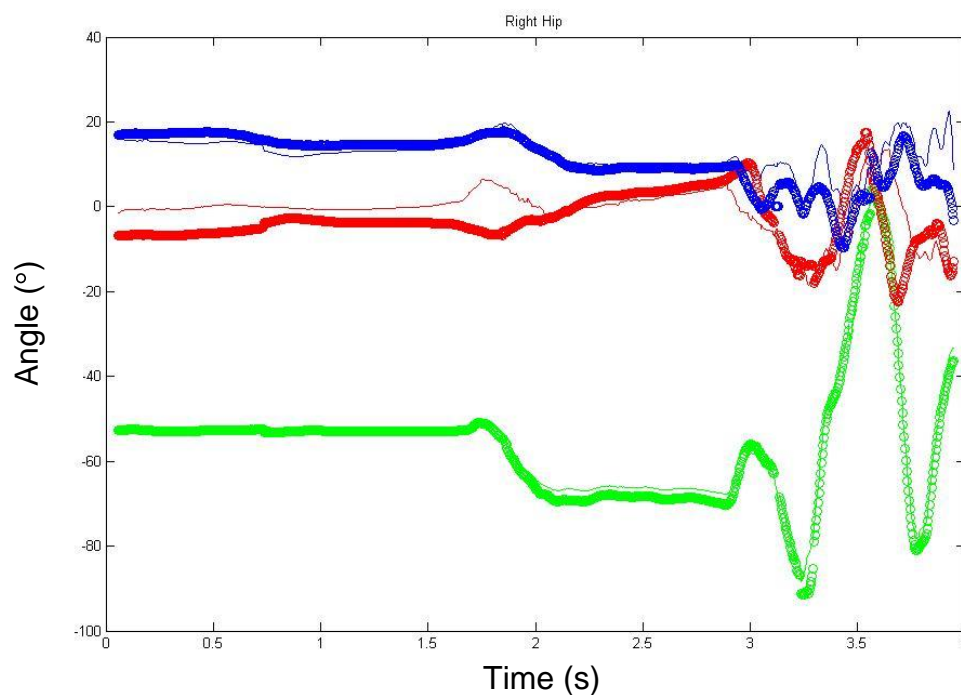
Figure 3.8. Right hip angles. Circles represent the Golem model output, solid lines represent Anatomic model output (x = green, y = red, z = blue).

It can be seen from figure 3.8 that for the right hip, flexion/ extension movements (movement around the z axis) is approximately equal and opposite. Rotation and abduction/adduction movements can also been seen to be relatively similar.

Importantly, during trials where subjects flexed/extended, abducted/adducted and rotated at each joint in turn, outputs appeared to be reasonable. Further, the marker system/ model allowed for the Golem model to also calculate joint angles. Table 10

displays a comparison of the lower limb angles outputted on a sprint start trial using Anatomic and then the Golem models.

Table 10. Comparison of angles calculated by Golem and Anatomic models.

Joint	RMS difference (°)		
	X	Y	Z
Left MPJ	27.64	0	0
Right MPJ	50.53	0	0
Left ankle	69.89	8.62	13.31
Right ankle	116.40	12.64	177.22
Left knee	9.04	17.92	18.46
Right knee	9.04	11.79	13.13
Left Hip	5.39	7.76	8.27
Right Hip	5.17	6.61	3.98

The comparison displayed in Table 10 was performed to help develop the Anatomic model and reveal potential errors. At the metatarsophalangial joints it can be seen that there is zero difference in the Y and Z axes. This would be expected as this was modelled as a hinge joint and so there is zero movement about these axes. Figure 3.9 displays the angles at the right ankle. It can be seen that whilst the error is 177.22°, the actual difference is 2.78° as this is due to contradictory definitions of the joint orientation. Similar can also be seen around the X axis for both ankles and at the right toe (Figure 3.9).
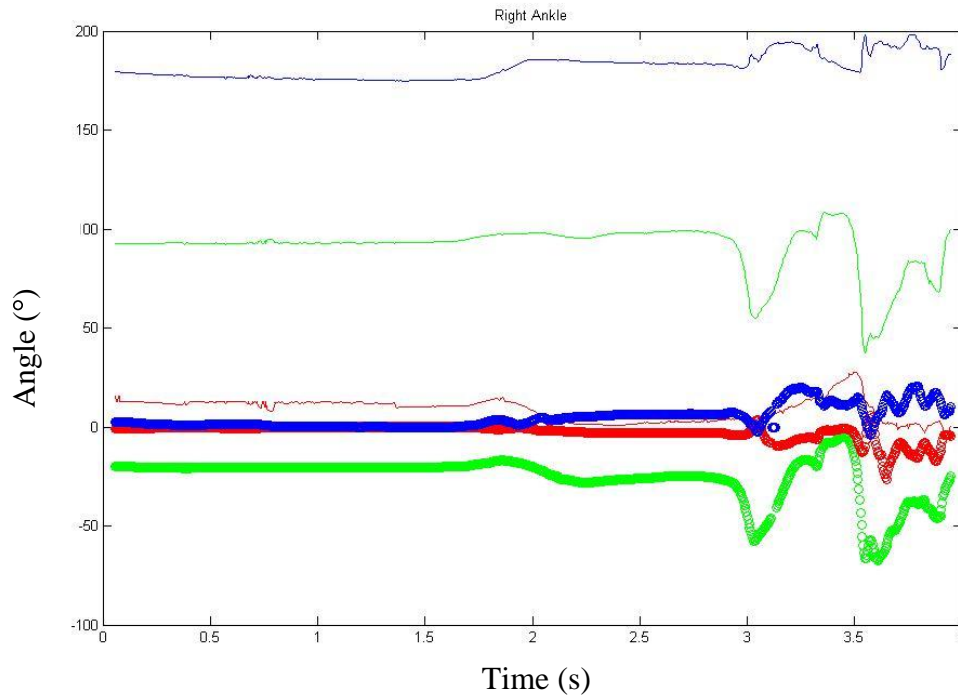
Figure 3.9. Right ankle angles. Circles represent the Golem model output, solid lines represent Anatomic model output (x = green, y = red, z = blue).

3.2 Force Measurement

In order to examine interactions with the starting block and obtain a kinetic analysis of the sprint start, a method of force measurement was required. Section 3.2 examines how previous studies have gained force data after which a method is presented for use in this study.

3.2.1 Force Data Acquisition Methods

The methods used to calculate the forces exerted during sprint starts vary tremendously. The first method used by Kistler (1934) used some customised scales installed under each starting block. Unfortunately these compressed during loading but were an important step in the collection of force data. Perhaps the most simple methods were those used by Mero et al. (1983) and Mero (1988). These used a starting block positioned on top of a tri axial force plate and could therefore measure

60

the total horizontal and vertical forces. Guissard and Duchateau (1990) implemented force transducers into each foot block and could therefore measure the forces exerted by each foot, however these only measured forces perpendicular to each block. Gander at al. (1994) designed starting blocks to measure vertical and horizontal but not lateral forces in each block. The studies by Bauman (1976) and Čoh et al. (1998) used tri axial force transducers in the foot blocks of each starting block. This is perhaps the ideal method as vertical and horizontal and lateral forces may be examined for both legs independently.

As with any measurement device, calibration of instrumented starting blocks is essential. A method for calibrating dynamic forces was given by Fujii and Fujimoto (1999). This method involved using measuring the change in velocity of an object impacting the transducer and using the impulse-momentum relationship to calculate force. Uncertainty in the estimation of impulse was considered to be 10^{-3} N·s. However, as the sprint start contains both static and dynamic phases, a static and dynamic approach to calibration seems appropriate. To do this Gander et al. (1994) used a series of static weights in order to calibrate for horizontal and vertical force independently. Dynamic calibrations were also conducted using an impulse hammer used to strike the transducer and a shaker system working at 5 and 7.5 times gravity.

In order to gain the most information possible for the forces exerted during a sprint start, instrumented starting blocks should contain tri-axial force transducers in each side of the starting block. Ideally a minimum of three transducers should be used, creating a force plate on each side capable of measuring force in each direction as well as centre of pressure. In order that the measurements are valid the system should be calibrated in a manner that reflects the use that the system will undergo.

3.2.2 Instrumentation of Starting Blocks

A set of Sure-Start 3 starting blocks were adapted for use in the study by allowing the installation of up to three force transducers (PCB Piezotronics ICP 260A01) in each foot block (Figures 3.10 and 3.11a and 3.11b). These starting blocks were preferred over some other starting block designs as they were flat faced and had a relatively

simple design which facilitated installation of the transducers. The rubber face was removed and remounted on a solid metal plate (front plate). Holes were then drilled through the front plate and the foot plate of the starting block. This allowed a tensioning bolt to be threaded through the back of the foot plate and into the front plate, sandwiching the transducer in between. Mounts were also attached onto the foot plate to ensure that the transducers remained aligned during application of a preload via tightening of the nut.
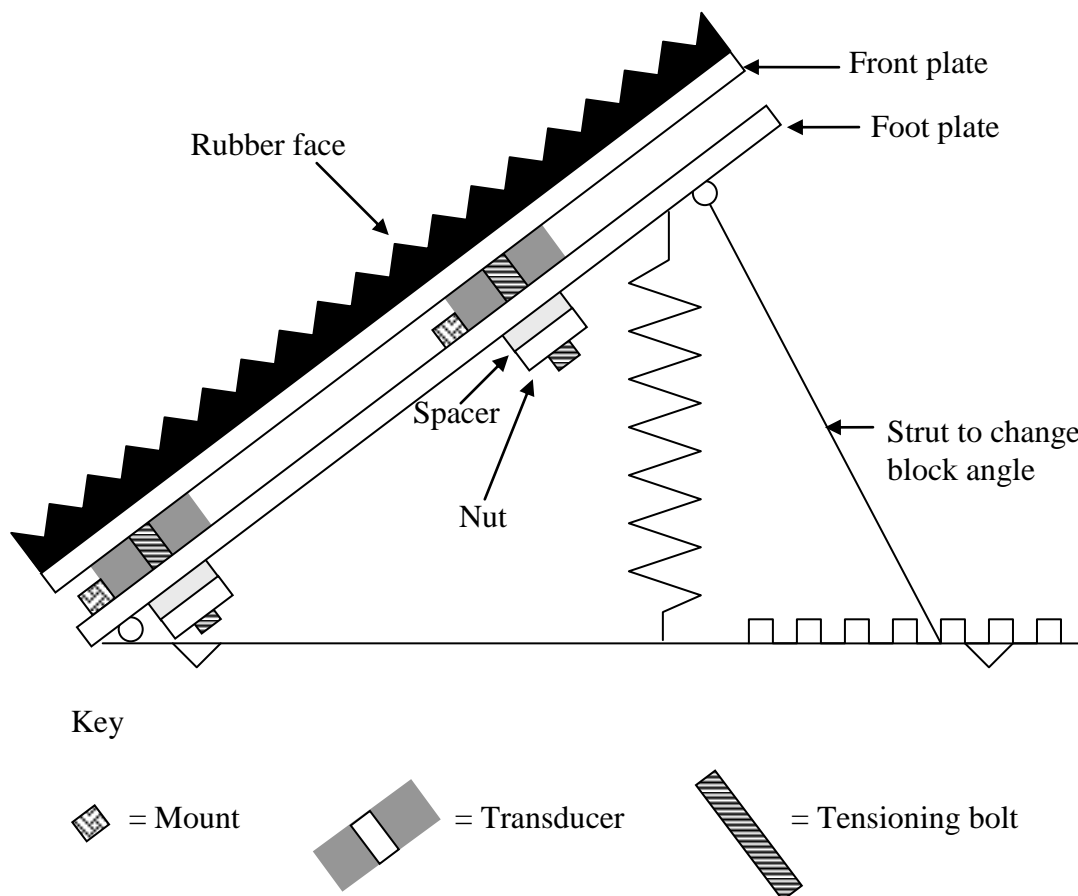
Figure 3.10 Instrumented starting block design. Note, not to scale.
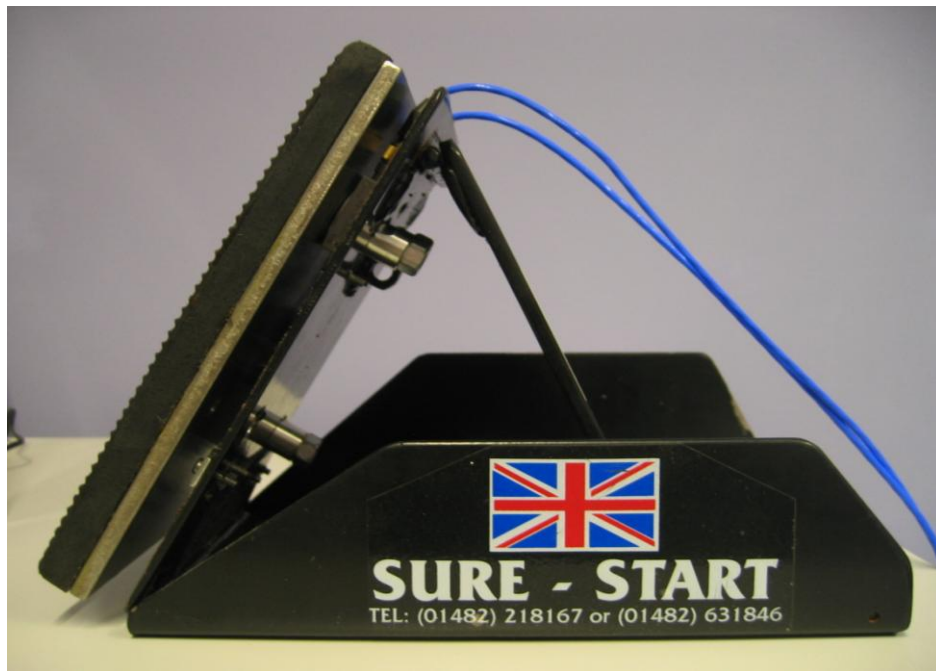
Figure 3.11a Instrumented starting block.
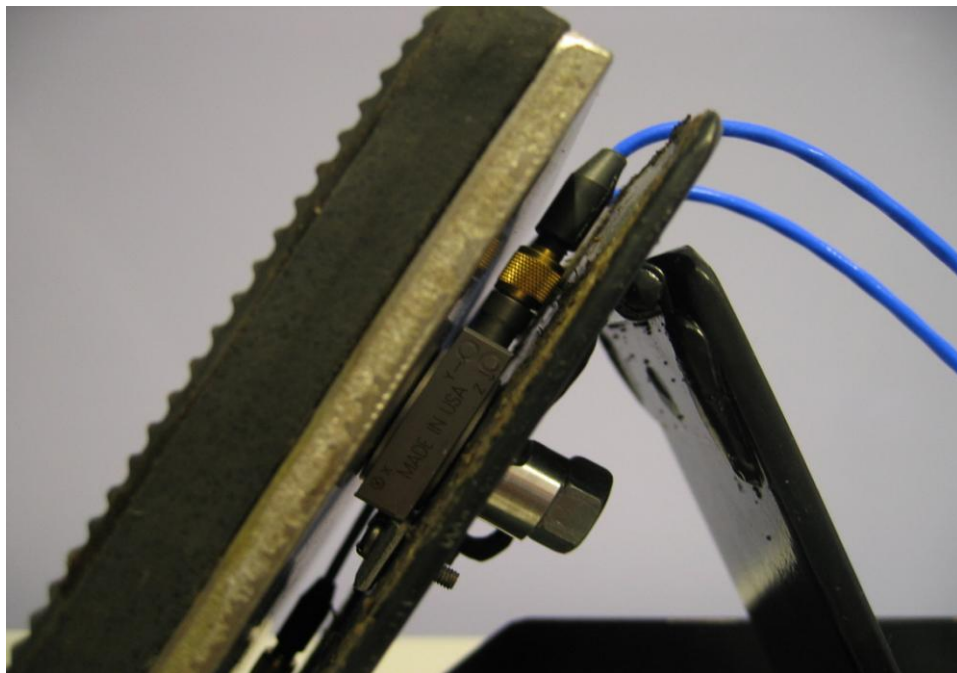
Figure 3.11b Transducer installation in starting block.

A total of four transducers were available for collection of starting block reaction forces. Three holes were drilled in each plate to allow for either three transducers in one block and none in the other, or two in each. Figure 3.12 (below) displays the locations of the transducers; locations A to D were used when two transducers were being used in each block.
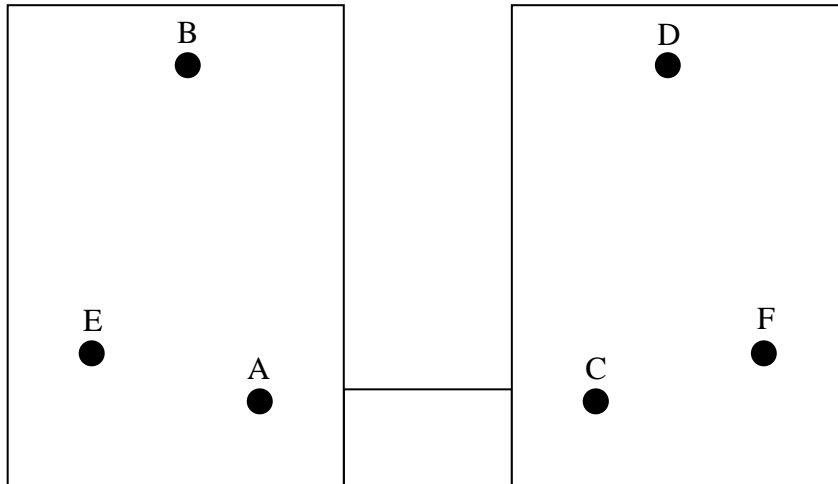
Figure 3.12 Front view of starting blocks and transducer locations

In order that forces may be output in a global orientation, i.e. true vertical and horizontal, the angle of each foot plate was measured relative to its base. To check that the angle of the transducers did not change through the plates bending, high speed video of sprint starts using the blocks was recorded at 200 Hz.

3.2.3 Calibration

The PCB Piezotronics ICP 260A01 force transducers used required a preload of 22239 N. This was applied by tensioning the bolt connecting the front plate and foot plate. The suppliers recommend using:

$$P_1 = M_T / 0.2 \cdot b \qquad (3.13)$$

Where P_1 is bolt tensile load, M_T is applied torque and b is bolt diameter (m). Rearranging and inputting the relevant numbers resulted in a tightening torque on the nut of 27.9 Nm.

Voltage output was converted into Newtons based on information provided in the calibration certificates. The nature of piezoelectric transducers meant that when a constant force was applied, the signal drifted. The rate at which this occurs is known as the discharge time constant (DTC). The signal conditioning box used meant that this was much shorter than suggested in the manual and hence needed to be recalculated. This was of particular importance due to the amount of time an athlete spends in the starting blocks before commencing the start itself.

3.2.3.1 Calibration Method 1

The force at any point can be calculated using

$$q = Qe-t/RC \tag{3.14}$$

Where:

q   = instantaneous charge (pC)

Q   = initial quantity of charge (pC)

R   = Bias resistor value (ohms)

C   = Total capacitance (pF)

t   = time after t0

e   = base of natural log (2.718)

To calculate the values for the later part of the equation, a 25 kg weight was placed on each block with the face flat to the floor. The output voltage was then recorded for 60 s. MatLab version 6.0 was then used to calculate the natural log of the curve and correct the data.

Figure 3.13 displays the raw voltage output from a starting block instrumented with two transducers and the loss of charge is clearly evident. Figure 3.14 displays the same graph, but adjusted using the DTC calculated from figure 3.13 and converted into Newtons.
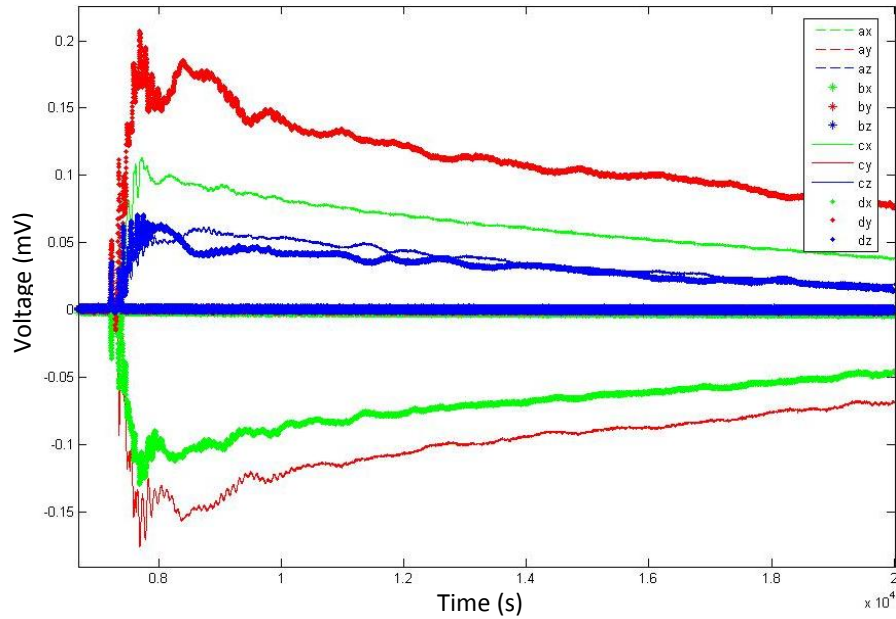
Figure 3.13. Raw voltage output from force transducers
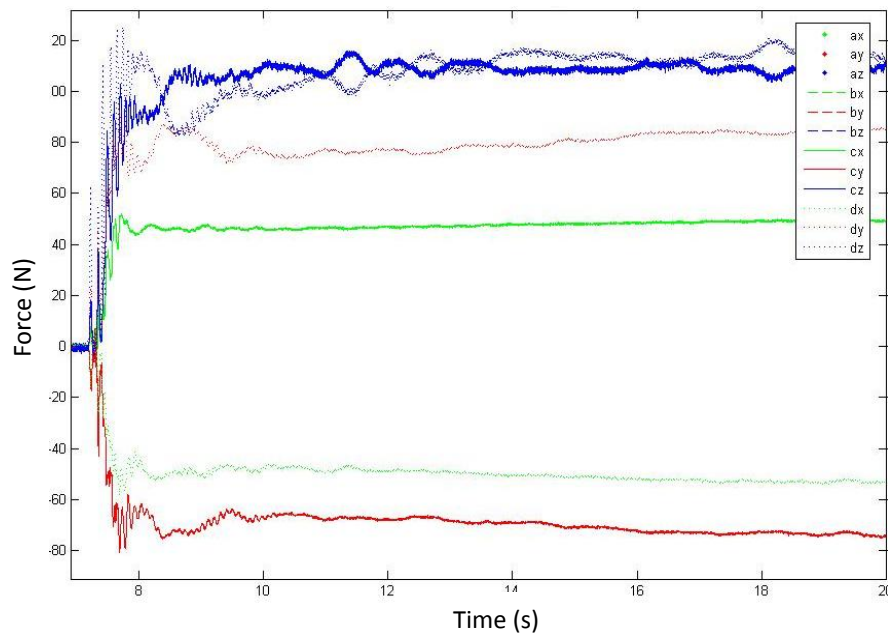
Figure 3.14. Data shown in Figure 3.13 adjusted for DTC.

In order to test further, the starting blocks were placed individually face down on a force platform (Kistler, 9281B). In a series of tests, weights of increasing mass were then loaded on top. When comparing the resultant force to that given by the force plate however it can be seen in Figure 3.15 that whilst the line is approximately flat, it is not the correct force measurement.
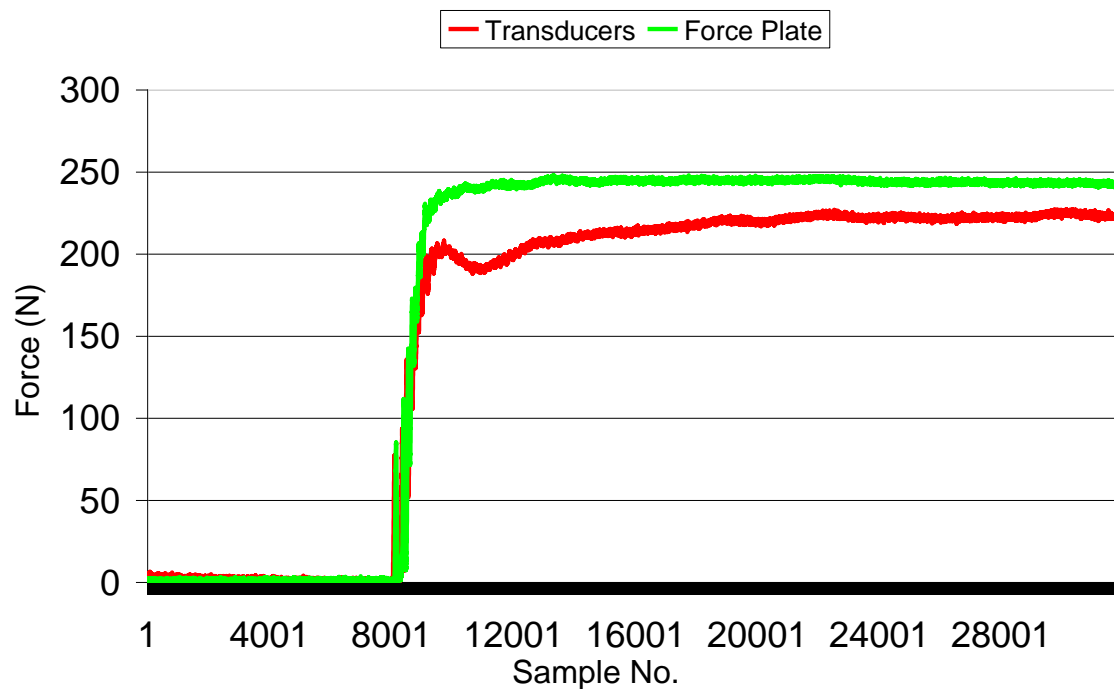
Figure 3.15. Resultant force from force transducers and force plate.

3.2.3.2 Calibration Method 2

A dynamic calibration method was investigated. For this method the individual foot blocks were bolted (in turn) to the force plate through the base of the block. A series of sprint starts were then performed ensuring that the athlete's foot did not contact the force plate itself. Data were recorded from both the force plate and starting blocks at 1000 Hz synchronised by manually matching the peaks at the beginning and end.

Using graphs for the output of each channel during a start, the first and last peaks (one positive and one negative) were identified. The first peak represented Q in the equation above and the last peak (x) is the amount the voltage returned past zero due

to the loss of charge during constant force phases. Equation 3.15 was then used to adjust the data by adding the lost charge back on over the trial.

$$q = q_i + \left(\frac{-x}{T} \cdot t \right)$$
(3.15)

Where:

T = the time between peaks,
q_i = output voltage.

The result of this method is shown as the red line on Figure 3.16. The green and blue lines display the raw data and force plate data over the same period respectively. As expected the raw data line falls over time compared to the force plate data. This method succeeded in removing the drop due to the DTC but the error score was higher due to the line now being constantly much higher than the force plate data. It was considered that this is likely to be due to rotational forces against the transducers causing coupling forces, resulting in the over calculation of horizontal forces.
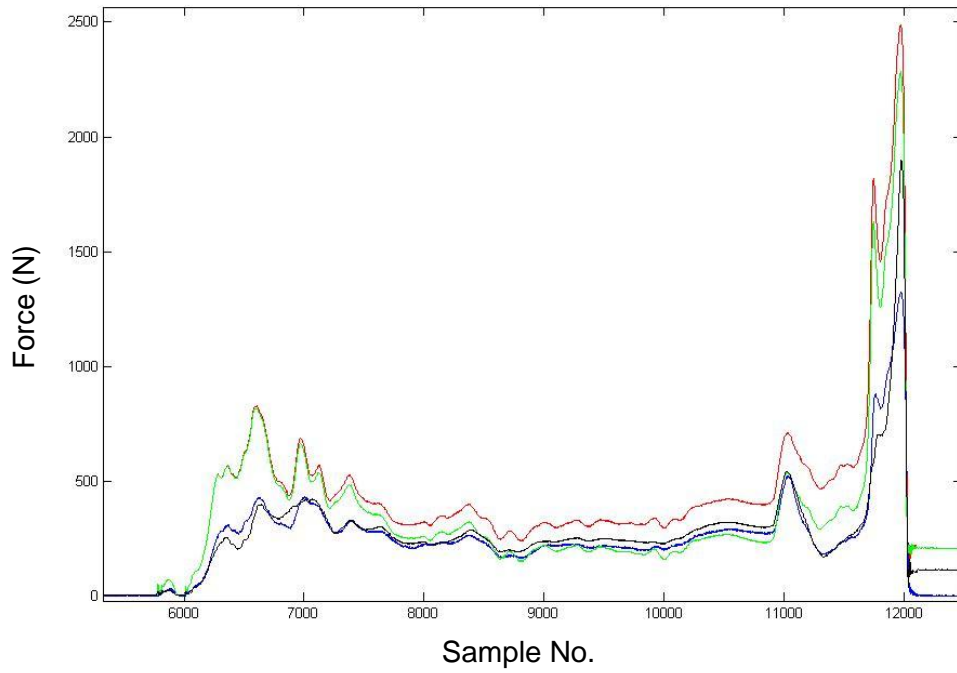
Figure 3.16. Comparison of force transducer and force plate output during a sprint start. The blue line is the force plate, green is the raw transducer data, red is the DTC adjusted transducer data and black is the completely processed transducer data.

To account for the overestimation of horizontal forces, data calculated using equation 3.15 was adjusted using:

$$q_n = q - x_{fun} \left(x_a + y_a \right) \div \left(|x| + |y| \right)$$
(3.16)

Where

q_n	= adjusted resultant force data
x_a	= summation of absolute x values
y_a	= summation of absolute y values
$|x|$	= absolute value of the sum of the x values
$|y|$	= absolute value of the sum of the y values
x_{fun}	= optimised value with bounds, $0 < xfun < 1$

x_{fun} is therefore the fraction of the horizontal force data to be removed from the signal. This resulted in the black line on Figure 3.16 (above). RMS error scores for this method were 39.7 ± 23.2 N over a whole trial. This was still considered to be too

high as most of the error occurs during the actual start as opposed to in 'set' phase. It was therefore decided to optimise x_{fun} based on the start phase only and then use this part to match to the force trace. This reduced the mean RMS error score over this phase from 112.5 ± 40.2 to 68.3 ± 52.1 N. However for use in a practical situation the force plate would not be present. In this case it would not be possible to optimise each trial. It is therefore important to know what x_{fun} to use and the likely error margins to be expected. The average x_{fun} over ten trials was different for each block, for the left the average was 0.66 ± 0.05 N and 0.53 ± 0.01 N for the right. Using these averages to recalculate q_n over the start phase resulted in an RMS scores of 113.4 N for the left block and 93.3 N for the right.

3.3 Data Collections

One male sprinter age 22, height 1.86 m, mass 83 kg, 100 m personal best 10.80s, 200 m personal best 21.56 s gave consent (Appendix B) to take part in the study which was performed in accordance with Loughborough University Ethical Advisory Committee. The two collections took place in the Biomechanics Laboratory at Loughborough University. They were six days apart and timed to occur at the end of the subject's competitive season in order to prevent clashes with his training schedule, but so that he would be at the end of his peak in terms of training for the start.

The data collections were split into two as initial testing showed that it would not be possible to collect all the data in one day due to the time needed and the amount of equipment attached to the subject at any one time. In the first session, data were recorded for 3-D joint coordinates, starting block reaction forces and forces on first foot touch down. For the second session, data were collected on the forces as above and muscle activations. Some data were also collected for 3-D joint coordinates but this was reduced from the first session. For external validity, collecting data on an athletics track may have been more appropriate. This however was not possible due to the time needed for setting up equipment. The surface was a thin carpet which allowed negligible compression and was non-slip. This also meant that the athlete performed starts wearing trainers rather than sprint spikes.

In order that the computer model replicated the performer's anthropometry, knowledge of the athlete's inertial parameters was required. Calculation of inertial parameters was achieved using the method set out by Yeadon (1990b). This method was selected due to the relative ease of taking the required measurements, predicted and the resulting segmentation which would be appropriate for creating the simulation model. The calculated segment lengths and moments of inertia were input directly into the model and can be found in Appendix C.

3.3.1 Data collection 1

Figure 3.17 displays a plan view of the experimental set up. Data were collected to examine 3-D joint kinematics, reaction force from each foot in the starting blocks and ground reaction force on first foot contact.
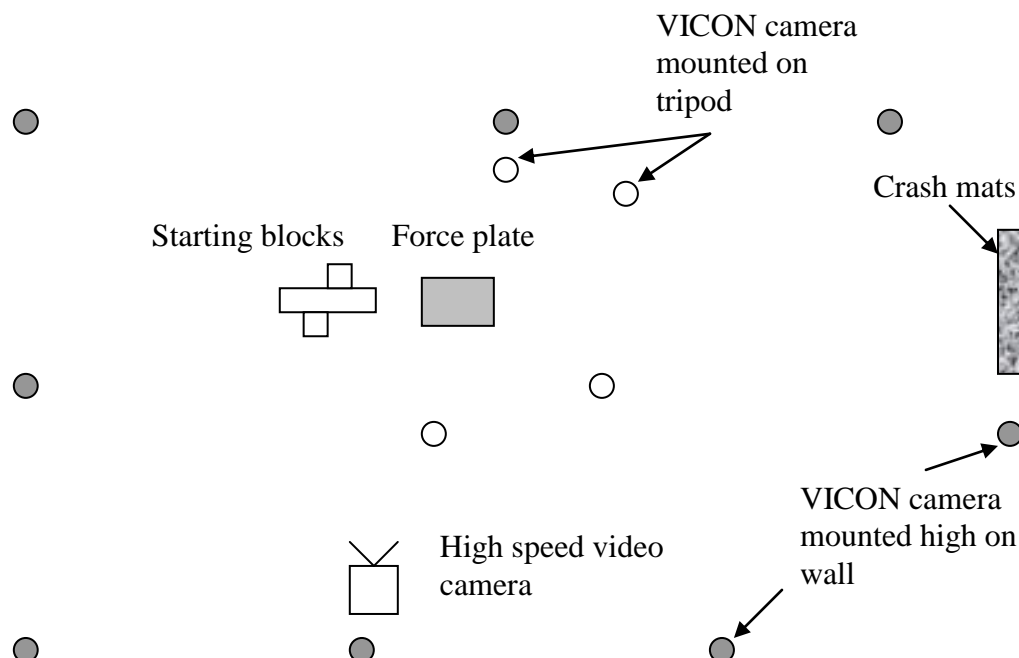
Figure 3.17. Plan view of experiment (not to scale).

Initially the markers for the anatomic model were applied using double-sided tape and spray-on glue. Markers on the shoes were also taped on by piercing the screw of the maker base through the adhesive side of black electrical tape, and screwing the marker on top of it. Reflective parts of the athlete's shoe were covered in black electrical tape to prevent interference with the camera system. A static trial was then performed to calculate marker positions in rigid segment reference frame such as the pelvis. The athlete then performed a set of pure flexion-extension, abduction adduction and rotation movements for reference purposes. After performing his own warm up, the subject performed five starts to approximately 8m using his own block configurations. Finally the foot blocks were screwed into the force plate to aid in the calibration process as discussed in Section3.2.3

3.3.2 Motion Analysis

3-D marker coordinate data were collected using the Vicon™ motion analysis system and Workstation software. This is a passive marker system which records movement through infra red light reflecting off retro-reflective markers. Twelve Vicon™ M2 MCam cameras (1280 x 1024 pixels) were used to collect data. Eight of these were mounted at various heights on the wall around the laboratory, the other four were placed low down to the floor with the specific aim of aiding capture of the hip and chest markers (see Figure 3.17 above). The calibrated volume was approximately 8 m long, 2.2 m high and 1.4 m wide (a little wider than a lane on the track). Cameras were calibrated with a residual error of approximately 0.84 mm and were set to record at 200 Hz. A higher sample frequency would have reduced the size of the capture area and pilot research suggested this would be sufficient (a maximum error of 0.03 $m \cdot s^{-1}$ in velocity data).

To track the athlete's movements, 14 mm rigid based retro reflective markers were placed on the subject in accordance with the Anatomic model described in Section 3.1.10. Figure 3.18 displays the marker locations. As there was no restriction on the number and placement of markers, extra markers were added. This was to compare the two methods of assessing shoulder joint centre and between the Anatomic and Golem models.
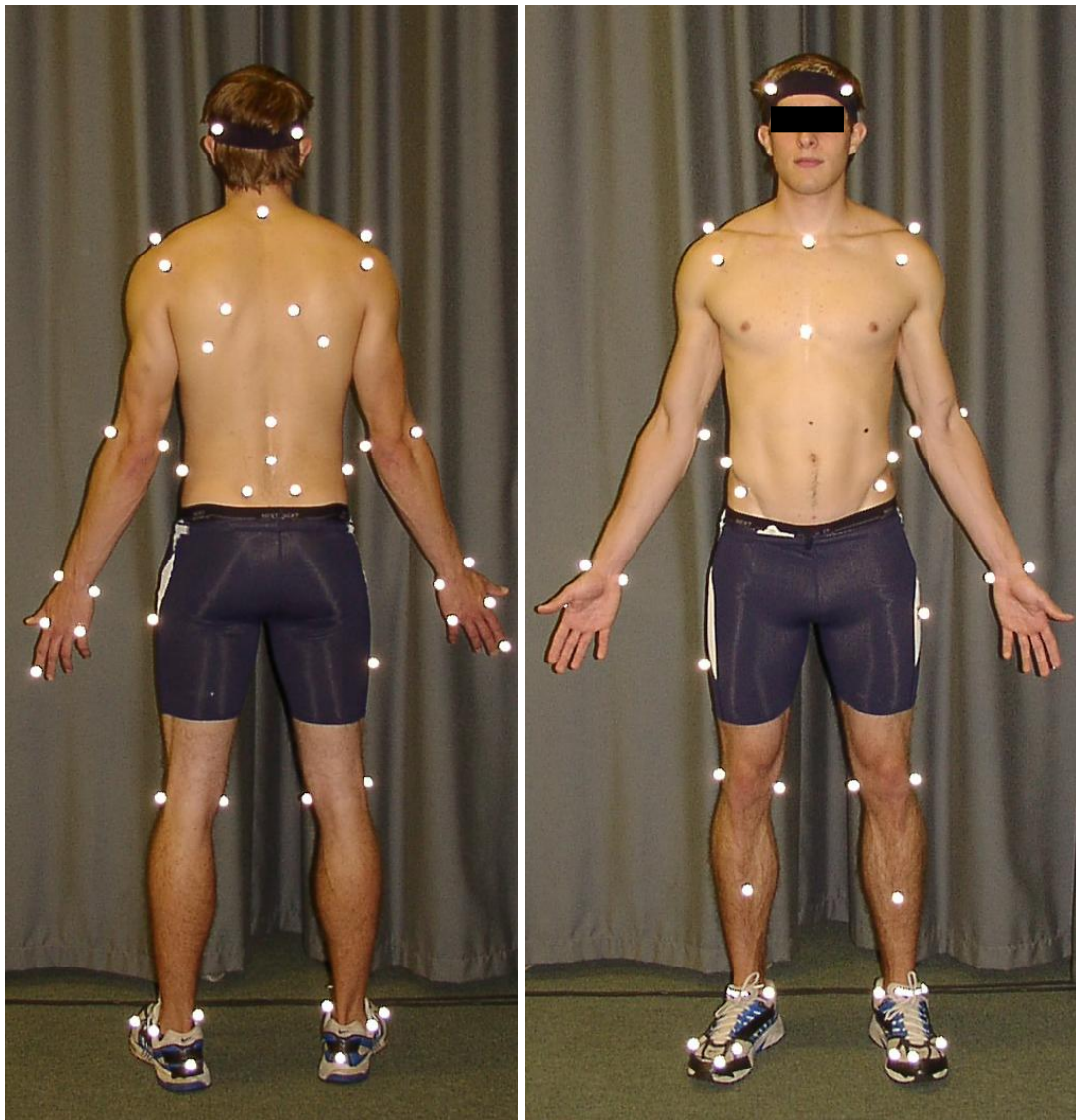
Figure 3.18. Marker placement.

3.3.3 Kinetic Data

The instrumented starting blocks described in Section 3.2 recorded starting block reaction forces for each foot during the start. They were connected to three ICP® Sensor Signal Conditioner units (482A22) and in turn connected to a BNC junction box. This was connected to a Toshiba Pro 4600 laptop computer with a National Instruments DAQ Card (A1-16-XE-50) and data were recorded on National Instruments LabVIEW 6 as text delimited files. The forces at touchdown on the first

step were recorded on a Kistler force platform (type 9281B, 0.4 x 0.6 m) mounted in the floor. The force platform and transducers both recorded at 1000 Hz. The athlete performed some trial starts during their warm up and positioned the starting blocks so that the first step would contact the force platform. A start line was marked on the floor to correspond to this and any trials in which the foot missed the platform were rejected. Synchronising the force plate to other data provided a record of first step duration.

3.3.4 Start and Synchronisation.

Trials were started using a starting procedure as would be used in a race and 'go' was signalled by electronic beep. Synchronisation was achieved using an infrared transmitter. This triggered the force platform, produced a square wave pulse through the same ADC (analogue to digital converter) as the force transducers and also on a VICON synch channel (and the EMG in the second data collection). It also triggered a bank of twenty LED lights which came on at millisecond intervals for synchronisation of the high speed camera.

3.3.5 Data Collection 2

Initial testing revealed that placing all the markers required for the anatomic model as well as all the parts for the EMG (electromyography) equipment (such as wires, electrodes, data logger and synchronisation box) was not achievable. The second data collection used the instrumented starting blocks as in the first data collection, Vicon motion capture system but this time with a reduced marker set (see Appendix D for marker file and model), the EMG and the synchronisation equipment. After the subject had warmed up, he completed a series of maximal contractions against an immovable object in order to examine EMG for a maximal effort. Examples of the movements included shoulder flexion and extension with resistance provided by the researcher or hip extension against a wall (upper body support was also provided by the researcher). Following this the starting blocks were put in the same position as for the first five trials in the first data collection. Again five good starts were recorded.

The new reduced marker set, where possible, used the positions of markers for the original anatomic model. In the new model the ASIS marker became the hip joint centre. Whilst this is not near the actual position, it provided a consistent position to compare joint angles. It was considered that this combination of markers would allow sufficient information to input into the model as well as comparison to some other studies which have examined EMG of the sprint start, e.g. Mero and Komi (1990) and Guissard and Duchateau (1990).

The EMG data from this data collection were synchronised to a trial from the first collection in post processing using angle data from two trials (see Chapter 5). Whilst performing two separate data collections to collect data for one simulation was not ideal, it did help ensure a higher quality of initial data as the subject was less hampered by an excessive amount of equipment attached during trials.

3.3.6 Electromyography (EMG)

A Bio-Vision EMG system set to record at 2000 Hz was used to record muscle activity. Surface electrodes were placed on the following muscles (for left and right sides unless indicated, Figure 3.20):

Gastrocnemius

Tibialis Anterior

Vastus lateralis

Rectus Femoris

Biceps Femoris

Gluteus Maximus

Left Anterior Deltoid

Right Posterior Deltoid

Right Illiopsoas.

A sixteenth channel was used for synchronisation with other equipment and so the maximum number of channels available were used. Data were recorded on a palm top computer which fitted into a bum bag around the subject's waist. Loose wires and the synchronisation unit were also placed in the bum bag.
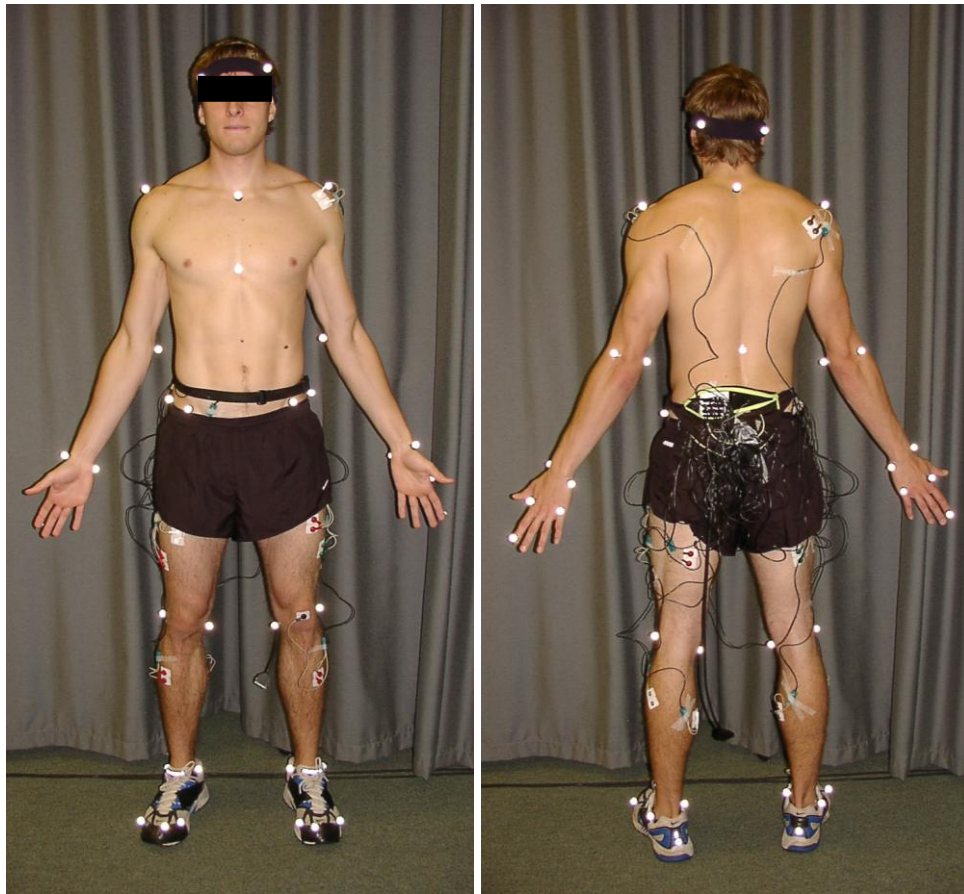
Figure 3.20. Electrode and marker placement.

In order to find the periods of muscle activation, raw EMG data were rectified (REMG) and plotted against time. The on and off times were then located from each plot. Appendix H displays the periods during which muscles were active for each joint movement and a summary is given in Table 11 below. The first two on/ off phases were recorded for each muscle. This ensured sufficient data was available for a torque driven model of the start to replicate up to 0.6 s, and hence was more than enough to replicate the first step.

Table 11. Identified periods of muscle activation.

Movement	Time (s)			
	Activation period 1		Activation period 2	
	Start 1	End 1	Start 2	End 2
Left hip extension	-0.0245	0.3055	0.5065	0.829
Right hip extension	-0.0325	0.043	0.304	0.58
Left hip flexion	0.3055	0.5065	0.829	0.5844
Right hip flexion	0.065	0.29	0.5685	0.791
Left knee extension	-0.045	0.4295	0.558	0.849
Right knee extension	-0.0435	0.13	0.2933	0.647
Left knee flexion	0.1535	0.4475	0.662	0.9685
Right knee flexion	0.134	0.287	0.4365	0.606
Left ankle extension	-0.0715	0.324	0.5795	0.8545
Right ankle extension	-0.07	0.0328	0.311	0.5844
Left ankle flexion	0.373	0.734	0.91	1.45
Right ankle flexion	0.19	0.359	0.613	0.9035
Left shoulder flexion	0.05	0.2715	0.5155	0.7875
Left shoulder extension	0.1715	0.6155	0.6875	0.5844
Right shoulder flexion	0.266	0.611	0.7	0.5844
Right shoulder extension	0	0.366	0.511	0.8

Chapter 4

Modelling Ground Contact and Four Segment Models

This chapter begins by investigating how ground contact may be reproduced in computer simulation models of the sprint start, and also the effects of including varying numbers of body segments in such models. This information is then used as a foundation for creating simple four segment angle and four segment torque driven sprint start models.

4.1 Modelling Ground Contact

When an athlete is in the starting blocks or contacts the floor, ground reaction forces are exerted back on the athlete. Computer simulation models can reproduce these forces with the use of springs which act horizontally or vertically and with this in mind, the equation used to represent the spring is of interest. Some studies have used linear spring dampers (e.g. Yeadon and King, 2002; King et al., 2006 (vertically only)) but few things in nature act in a linear manner for example, a nonlinear response can be seen for the sole of running shoes (Verdejo and Mills, 2004) and heel pads (Pain and Challis, 2001), Figure 4.1. It is perhaps therefore more appropriate to model athlete- ground interactions using nonlinear springs such as done successfully by Gittoes et al. (2006) to replicate drop landings.

Figure 4.1. Force deformation curve for the heel pad (Pain and Challis, 2001).

Simulation models for this study, including the springs to represent ground contact, were created using Matlab and Simulink with SimMechanics. SimMechanics includes spring blocks that can be connected to joints or bodies. These are simple linear springs and are of little use for modelling the sprint start as they cannot be released mid-simulation to replicate events such as takeoff and flight phases. As this was essential, the springs were written into the model manually and used an If Statement block to release the foot on take off (Appendix E displays the spring subsystems developed). This allowed for much greater flexibility as the spring equation could be customised, although initially the springs were developed on a linear spring equation:

$$f = -kx - r\dot{x} \qquad\qquad (4.1)$$

Where:

k   = spring stiffness

x   = displacement

r   = spring damping

The spring was tested by removing the 'if statement' and comparing it to SimMechanics' own spring function. This was done by creating a point mass model and running it twice, once with SimMechanics spring and once with the spring created. No differences could be seen between either model and with predicted theoretical values. Further, the mass came to rest at the point mg = kx.

As discussed above, a non-linear spring better represents foot-ground interaction. With this in mind, the following non-linear spring was adopted:

$$f = -kx^2 - r\dot{x}x \tag{4.2}$$

Whilst the x^2 part of the equation made it non-linear, multiplying the velocity component by displacement prevented negative forces occurring should velocity be large near takeoff.

At the hands, the horizontal spring only released once the vertical spring length became zero in order to reflect the hands leaving the ground. At the feet, the vertical spring only released once both the vertical and horizontal spring lengths were zero as this represented the foot pushing back against the starting block.

In order to compare the effect of the different springs on a computer simulation model of the sprint start, investigations were carried out using the linear and non-linear spring and also varying the number of segments in the model. Table 12 displays the models and spring types tested. The 11 segment model comprised a head and trunk, upper arms, forearms and hands, thighs, shanks, and feet. Creating toe segments joined by a metatarsal-phalangeal joint increased the number of segments to 13 and a two segment spine as described in Section 3.1.10.3 provided 14 segments. It can be seen that the 14 segment model with non-linear springs provided the best match, calculated by RMS error of the neck joint, to the measured data (Table 12).

Table 12. Segmented models and spring types.

Model	Spring type	Match[+] (m)	Stiffness (Nm^{-1})		Damping (Nsm^{-1})	
			X	Y	X	Y
11 segment	Linear	0.052	304,649	245,322	1,759	4,087
13 segment	Linear	0.042	125,057	185,584	156	8,306
14 segment	Linear	0.023	337,226	21,671	293	317
14 segment	Non-linear	0.012	196,391*	181,273*	2,565[#]	53[#]

[+] Match was determined through RMS comparison of the resultant neck joint movement.

* Units = Nm^{-2}, [#] units = Nsm^{-2}

With the number of segments and spring type for a full computer simulation model of the sprint start considered, it was decided to begin investigation proper by using a simple four segment model as has been used by several authors to investigate activities such as jumping (e.g. Domire and Challis, 2007, Selbie and Caldwell, 1996, Pandy et al., 1990). Furthermore, results obtained from models with added complexity would be more difficult to interpret due to the possibility of compensating errors.

4.2 Four Segment Angle Driven Model

Following the recommendation of Hubbard (1993), the four segment model was created to represent the start in as simple manner as possible. Simple models have been used successfully to examine the fundamental and generic characteristics of jumping activities. For example, the model of Alexander (1990) was able to identify the relationship between takeoff velocity and jump height/ distance despite the lack of leg mass, a foot segment or any compliance.

The sprint start can be seen as a form of squat jump but here it is the trade-off between impulse and time that is of interest. The four segment model comprised a head and trunk, thigh, shank and foot segments (Figure 4.2), and so only represented

the forward leg in the starting block. This could also be seen as similar to a 'bullet start' where each leg obtains the same orientation in the set position. Each segment was given inertial properties based on that of the subject and no parameters were combined. For example, the mass of the leg segments were only that of a single leg and did not represent that of both legs. Joint angles were driven by the angle data taken from one representative trial selected from data collection 1. The model started at the point the left starting block resultant force began to rise and terminated as soon as a segment contacted the ground. Contact with the starting block was modelled by means of the horizontal and vertical non-linear spring described in by Equation 4.2. In order to match the reaction forces at the starting block in the model to those measured, the measured forces were resolved to provide true global horizontal and vertical forces. In the model this allowed simple insertion of horizontal and vertical springs.
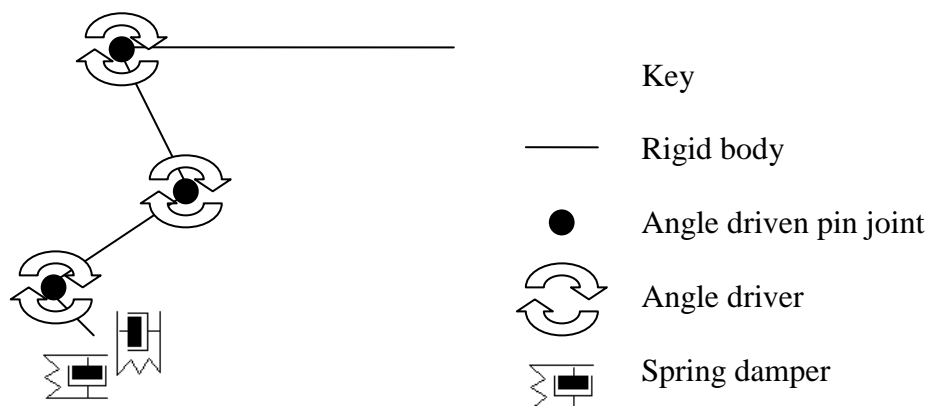
Figure 4.2. Four segment angle driven model of the sprint start.

The spring parameters were optimised using Direct optimisation and bounds were set as shown in Table 13. Direct optimisation was used in preference to Simulated Annealing due to time allowances and over Simplex in order to cover a larger portion of the optimising surface. Large bounds were set due to lack of existing information on parameter values for an interacting foot/ shoe and starting block.

Table 13. Spring bounds for optimisation and results.

Spring	Stiffness (Nm^{-2})			Damping (Nsm^{-1})		
	Upper bound	Lower bound	Result	Upper bound	Lower bound	Result
Horizontal	80000000	1000000	1805911.60	10000000	5000000	3306819.20
Vertical	80000000	1000000	6851182.60	10000000	5000000	9844269.10

The score for the optimisation was based on the location of the toe. The spring was given an initial length of 0.01 m and was optimised to allow a further 0.015 m increase in length before shortening. This was to replicate the compression of the foot, shoe, starting block and ground. Penalties were added for vibrations in the spring and 1% of the maximum force over 1200 N was also added to the score in order to make the forces realistic. Finally the difference in time in losing contact with each spring was also added to the score. The resulting score after 50 iterations was 9.021, (see Appendix F for relevant code) and provided 1805911.6 Nm^{-2} and 3306819.2 Nms^{-1} stiffness and damping for the vertical spring and 6851182.6 Nm^{-2} and 9844269.1 Nms^{-1} stiffness and damping for the horizontal spring.

Whilst the spring parameters allowed the model to perform the movement (Figure 4.4), the pattern of force production was not typical of a real sprint start. Figure 4.3 below shows that force dropped greatly in the middle of the movement and negative forces occurred towards the end of contact. The negative vertical force occurred as take off had not yet happened in the horizontal direction. The smaller negative force in the horizontal direction occurred before take off due to the high velocity at the toe causing the damping part of the spring equation to become greater than the stiffness part. In an attempt to provide a closer match to reality, the optimisation was re-run with added penalties however, this did not improve the overall result and the graph did not appear to be substantially different. Therefore the initial spring parameters were used.
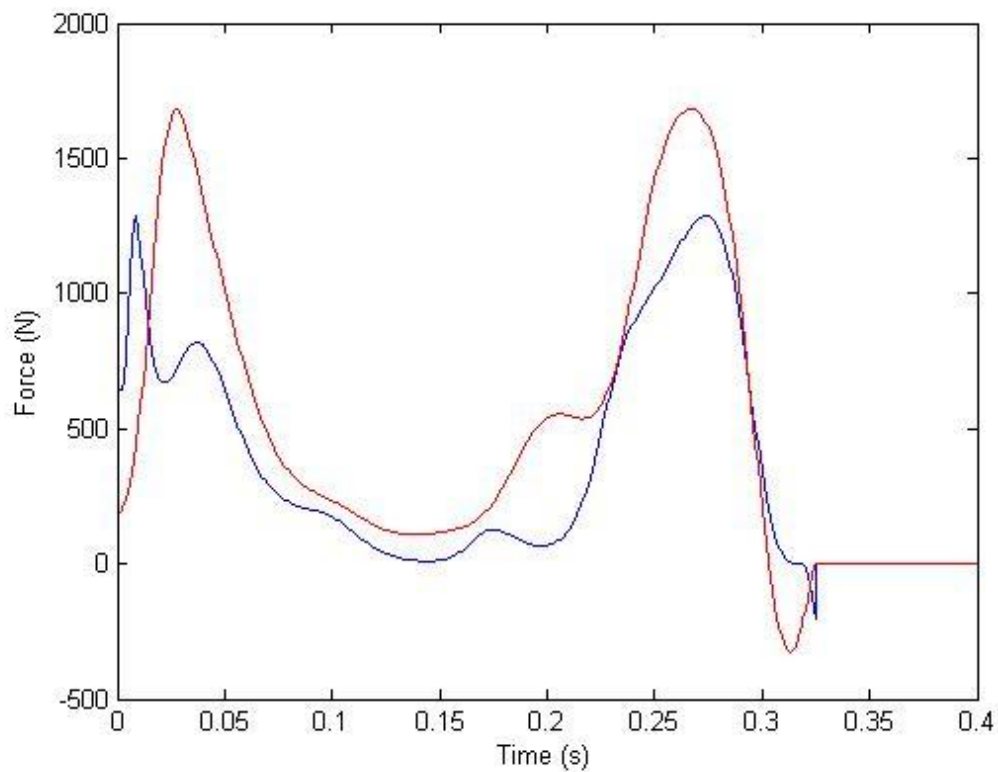
Figure 4.3. Horizontal and vertical ground reaction force. Blue = horizontal force, red = vertical force.

Figure 4.4 shows the simulation model driven using the 100% RoM (range of movement) data. It can be seen that the hip is lower than head height which would not usually be expected. This is because the hip angle has been taken based on the two segment spine hip joint angle. Whilst this is likely to have consequences in terms of angular momentum on during the movement, it was considered important to use this angle in order for the correct torque values to be used in the torque driven model. Not using this angle put the trunk almost 45° lower which also put the head on the ground in simulations where a large RoM was used.
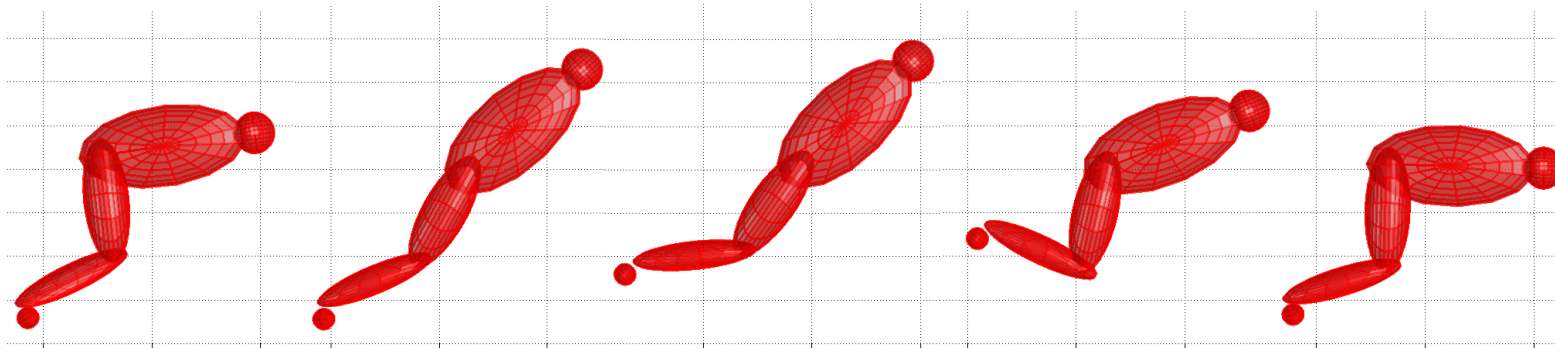
Figure 4.4 Four segment model starting using 100% RoM.

4.2.1 Effects of Changes to the Angle Driven Model Set Position

The four segment angle driven model was re-run using the optimised spring parameters in order to investigate the effect of changing the athlete's RoM and also the amount of time spent pushing against the starting block (Ptime). Increasing the RoM produced a similar effect to a more bunched start where the starting block is closer to the line, however, it also represented greater flexibility in extension. Each original joint movement pattern was used as a baseline and then changes were made using:

$$\theta_n = \theta_h + \left(\frac{j-100}{100} \right) \cdot \theta_h - \overline{\theta}_h \qquad (4.3)$$

Where:

θ_n = New joint angle

θ_h = Original joint angle

j   = Percent of joint RoM to be used

Figures 4.5a - 4.5c display the joint angles at the ankle, knee and hip over the start and first step. At 150% it can be seen that some hyperextension occurs at the knee and peak dorsiflexion is very small, otherwise joint angles appear to occur within feasible limits.
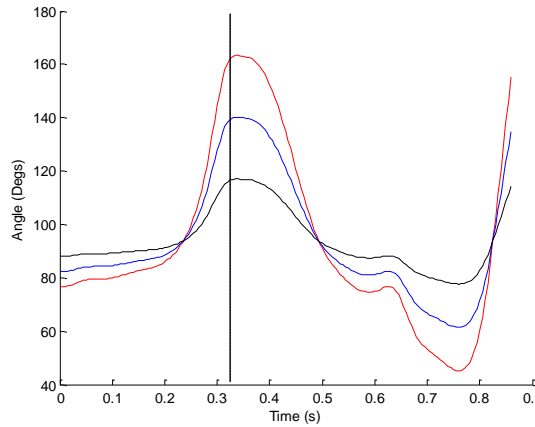
Figure 4.5a. Ankle angles for four segment model.
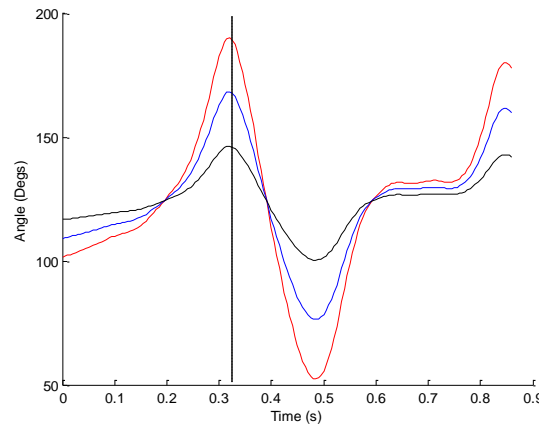
Figure 4.5b. Knee angles for four segment model.

Figure 4.5c. Hip angles for four segment model.
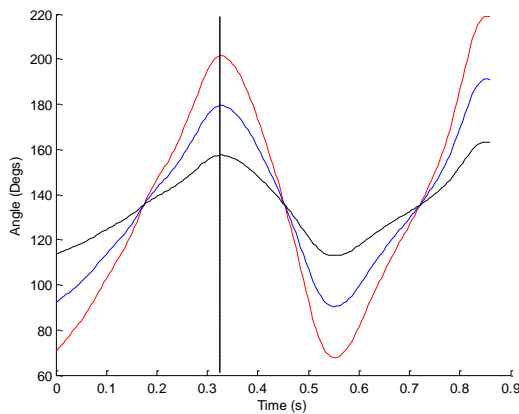
Key for Figures 4.5a – 4.5c

— RoM = 50 %

— RoM = 100 % (original data)

— RoM = 150 %

– – – Loss of contact with starting block in measured data

Changing the push time (Ptime) was accomplished by adjusting the time column corresponding to the angle data driving the simulation. Therefore 50% Ptime represents half the movement time recorded in the measured data. The following 3-D graphs depict what happened to the model as both the RoM and time changed. Black lines are plotted along 100% of RoM and 100% Ptime, and the original start is shown where these lines intersect.

Horizontal displacement increased with increases in both RoM and Ptime, although Figure 4.6 shows increases in time to have a much greater effect. The increase gained through performing the start over a greater time peak at 115% Ptime for 150% RoM,

87

118% Ptime for 100% RoM and 120% Ptime for 50% RoM. Achieving a large horizontal displacement is at the expense of vertical displacement. Beyond the ridge insufficient vertical velocity was generated and the athlete begins to fall out of the starting blocks shown by zero peak vertical displacement in Figure 4.7. These simulations all terminated due to the head or knee hitting the ground before the foot. At very small Ptimes horizontal displacement becomes negative and vertical displacement very large. Here the athlete jumped straight up from the starting blocks and rotated backwards.
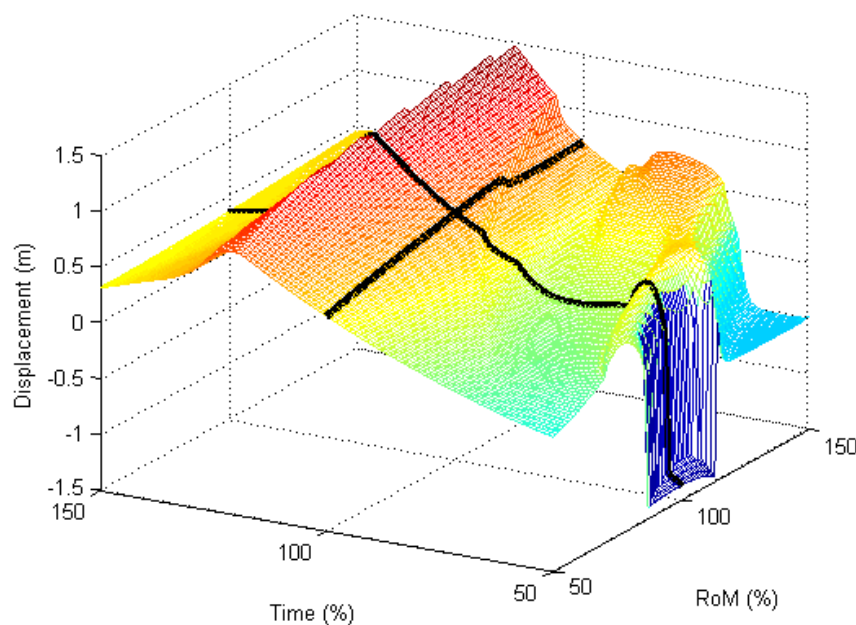
Figure 4.6. Horizontal displacement from the start line. Black lines denote 100% RoM and Ptime.
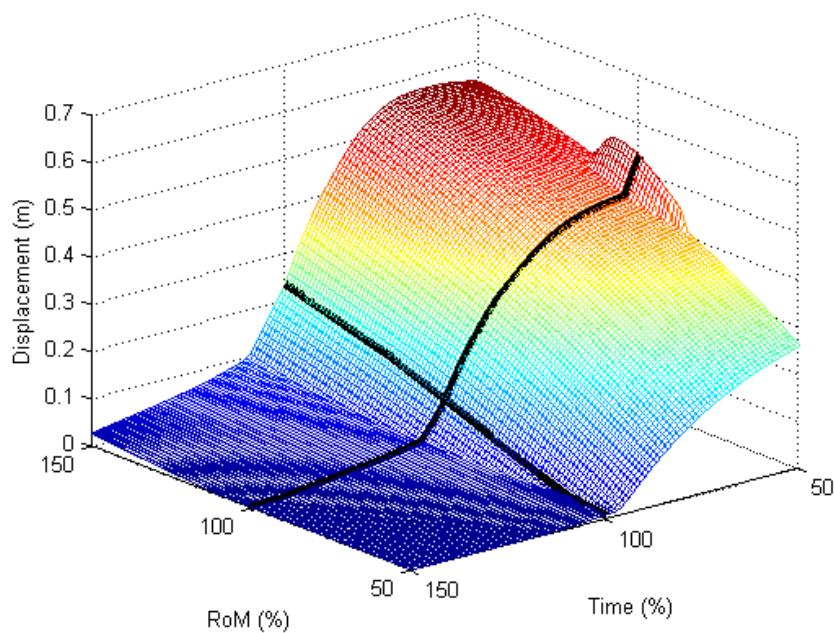
Figure 4.7 Maximum vertical displacement. Black lines denote 100% RoM and Ptime. Note the axes have been switched for ease of viewing.

Horizontal velocity on takeoff (Figure 4.8) corresponded well to horizontal displacement and increased with increases in Ptime and RoM. It may be expected that the highest horizontal velocity would be achieved using the longest Ptime. At long Ptimes, vertical velocity on take off (Figure 4.9) became negative as the athlete fell out of the starting blocks or began to flex before takeoff had occurred. This caused a rotational velocity and reduced horizontal velocity. The large increase in horizontal velocity around 50% Ptime and 150% RoM in Figure 4.8 was also due to the springs not releasing and the athlete jumping up quickly. Furthermore, the occasional spikes seen in this and other graphs were caused when the horizontal spring released later than the vertical spring (allowing a large negative vertical force on takeoff).
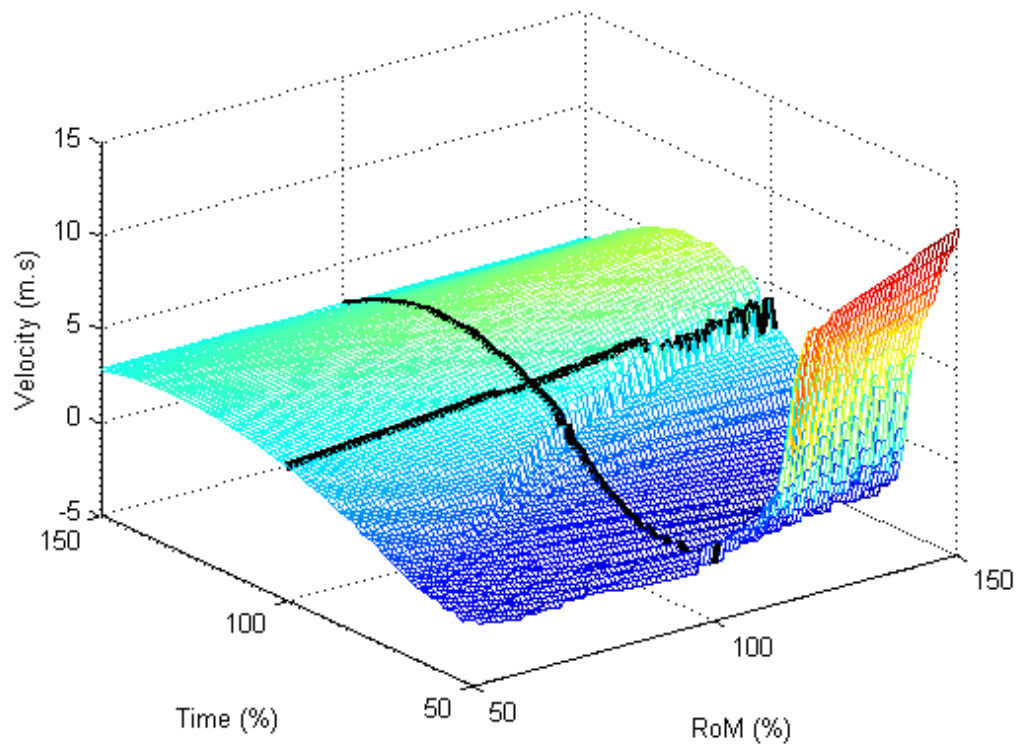
Figure 4.8. Horizontal velocity on take off. Note, for ease of viewing axes have been switched. Black lines denote 100% RoM and Ptime. Peak seen at around 50 % time and 150 %. RoM is caused by insufficient stiffness in the ground contact springs.
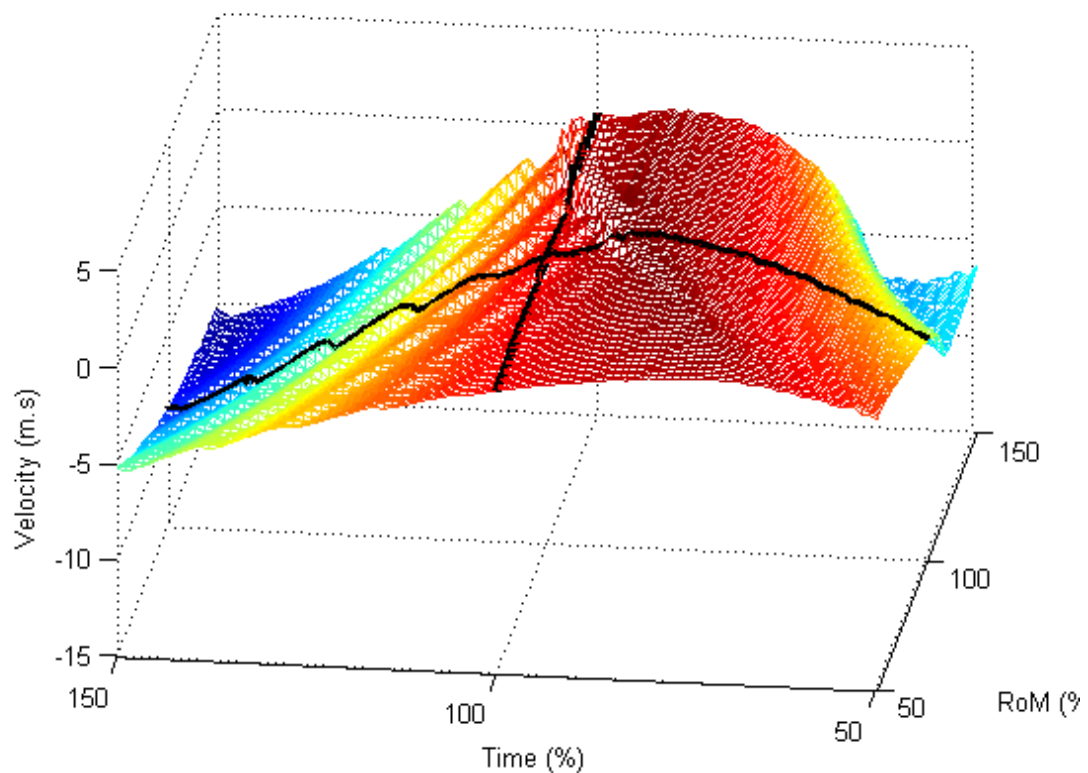
Figure 4.9. Vertical velocity on takeoff. Black lines denote 100% RoM and time.

Time in contact with the starting block (Figure 4.10) increased almost linearly with Ptime and decreases in RoM. As previously eluded to, during longer Ptimes and smaller RoM trials, insufficient velocity was generated to allow takeoff and therefore long contact times resulted.
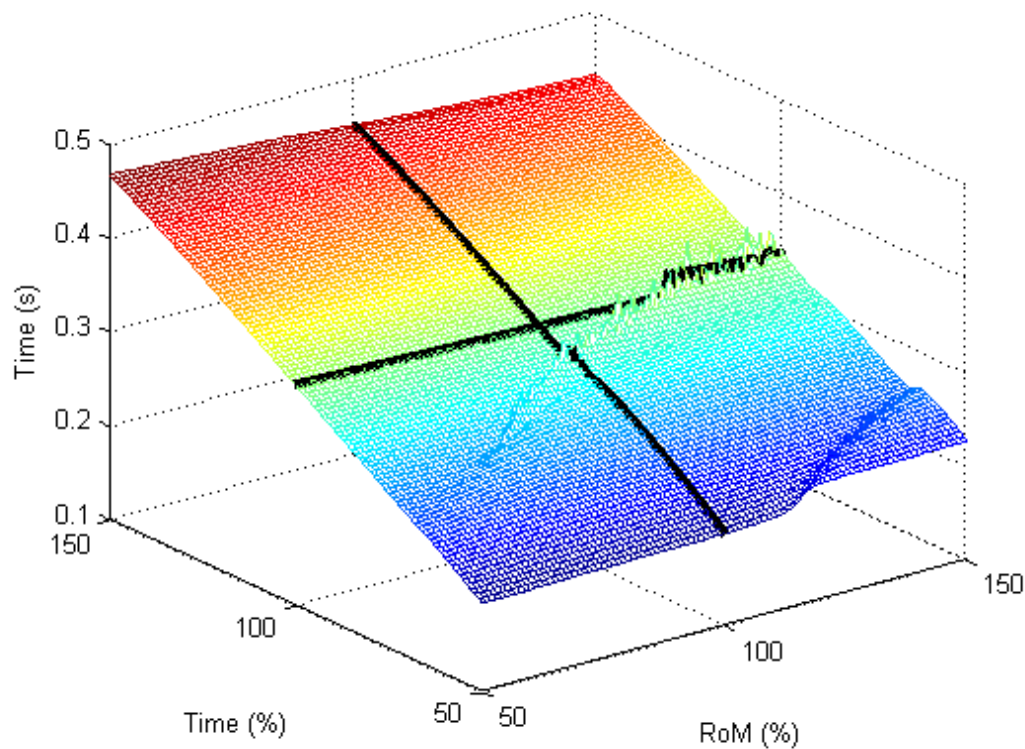
Figure 4.10. Block contact time. Black lines denote 100% RoM and Ptime..

Graphs of horizontal and vertical force, Figures 4.11 and 4.12 reveal quite similar patterns with the largest peak forces occurring at 150% Ptime and 150% RoM. The forces recorded were very high and it can be seen that for many of the trials, an athlete would be unlikely to create these forces.
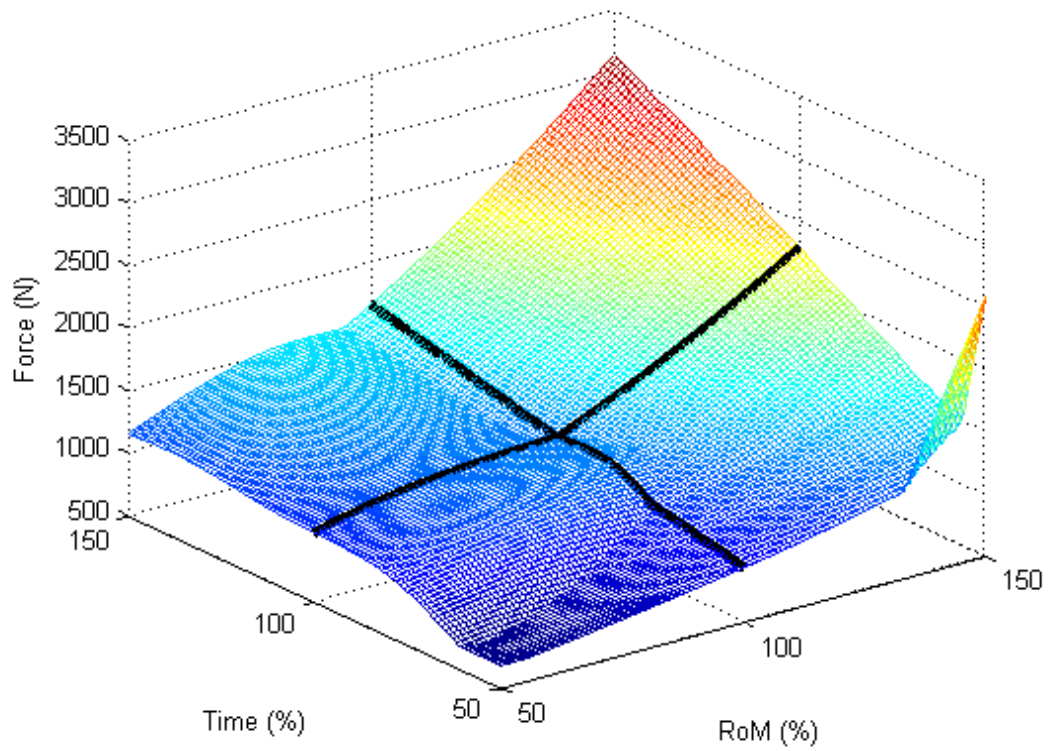
Figure 4.11. Peak horizontal force. Black lines denote 100% RoM and Ptime.
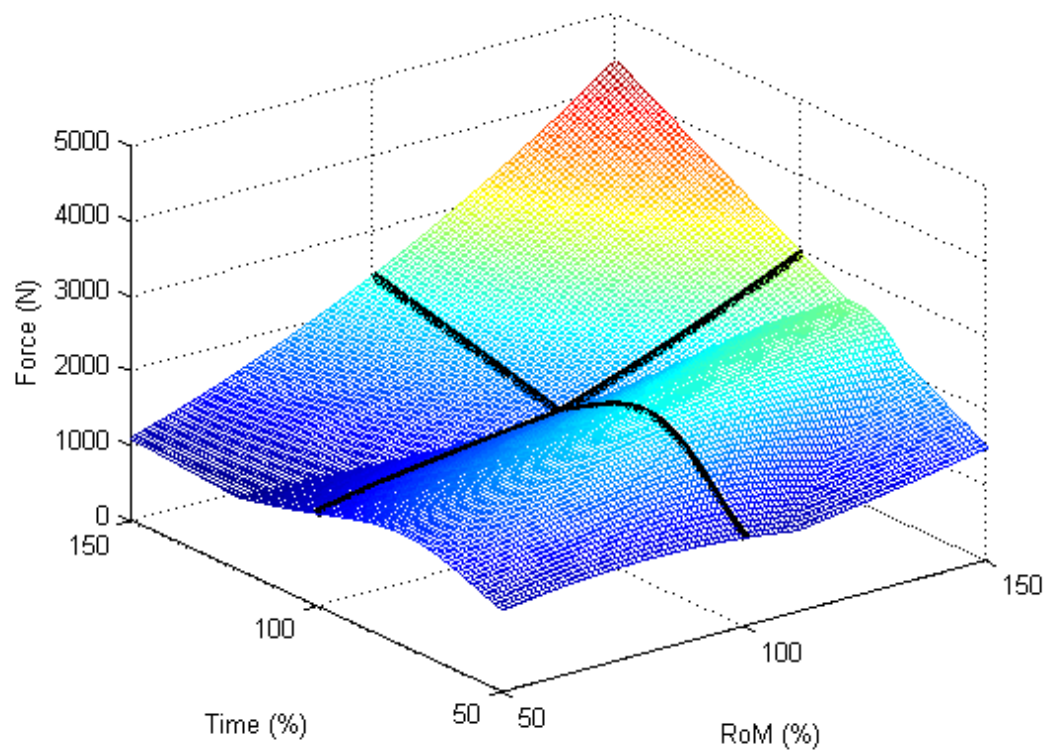
Figure 4.12. Peak vertical force. Black lines denote 100% RoM and Ptime.

At 150% Ptime and 150% RoM, high forces and a long contact time resulted in the largest horizontal and vertical impulses (Figures 4.13 and 4.14). Horizontally the smallest impulse was also at 50% Ptime and 50% RoM. It appears that this should also be the case for vertical impulse however, the large negative force created when springs did not release before the flexion phase also caused reductions in impulse.
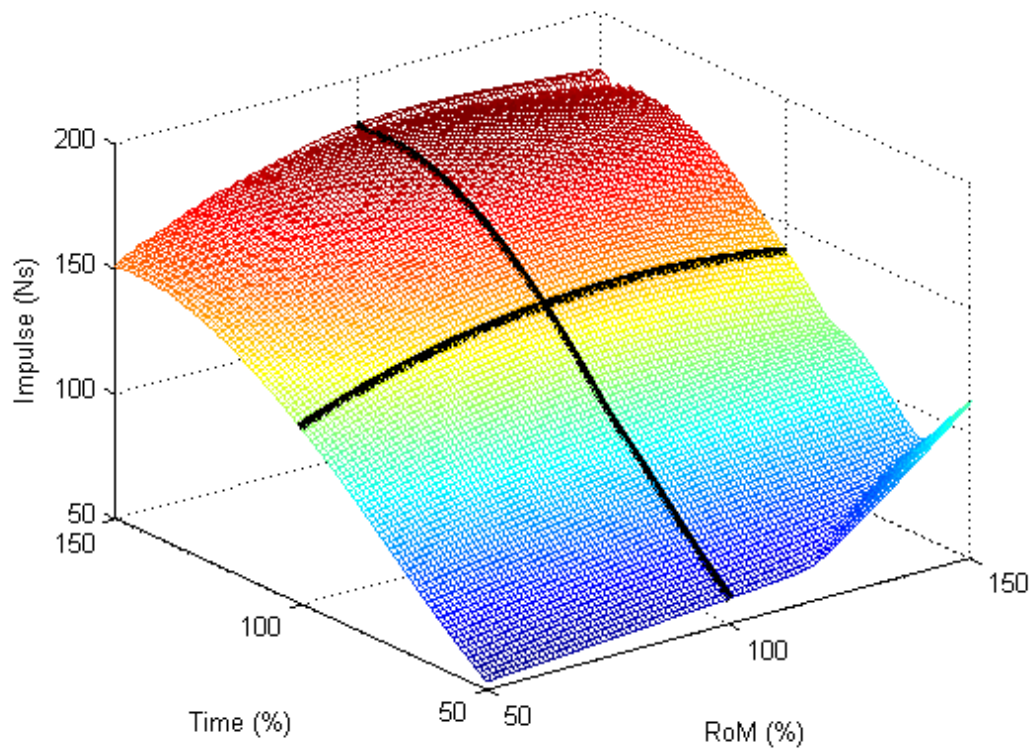
Figure 4.13. Horizontal impulse. Black lines denote 100% RoM and Ptime.
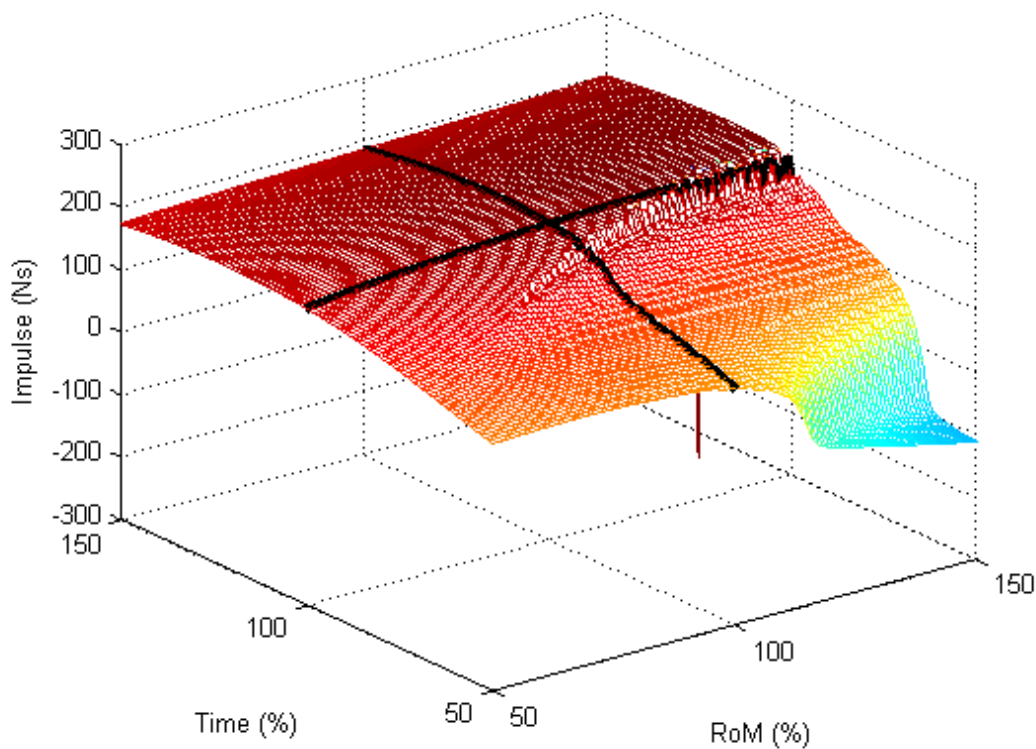
Figure 4.14. Vertical impulse. Black lines denote 100% RoM and Ptime.

By combining the results above it can be seen that the best start the athlete could perform (based on contact time and horizontal velocity on takeoff) used 115 % Ptime and 150 % RoM. In this case the athlete travelled 1.82 m with a horizontal takeoff velocity of 5.41 m·s^{-1}, a contact time of 0.35 s compared to 1.02 m, 2.82 m·s^{-1} and 0.32 s for the matched start respectively. It seems therefore that spending an extra 0.03 s in contact with the starting block could reap large benefits. These results should be viewed with some caution. As mentioned, the large forces and ranges of movement as well as the position in which the athlete landed meant that most of the starts which were considered better than the original may not be achievable in reality. Figure 4.15 below displays a region of trials that may be possible within set limitations. The red areas were considered possible whereas the blue areas were rejected due to one or more of the following: a knee angle greater than 180°, the final vertical position of the head less than 0.5 m, the final horizontal position of the head less than 0.2 m (suggesting that the athlete jumped straight up or did a back flip), the peak force either horizontally or vertically being over 2400 N (approximately 1.5 times the peak forces given after optimisation of the springs in the 100 % trial).
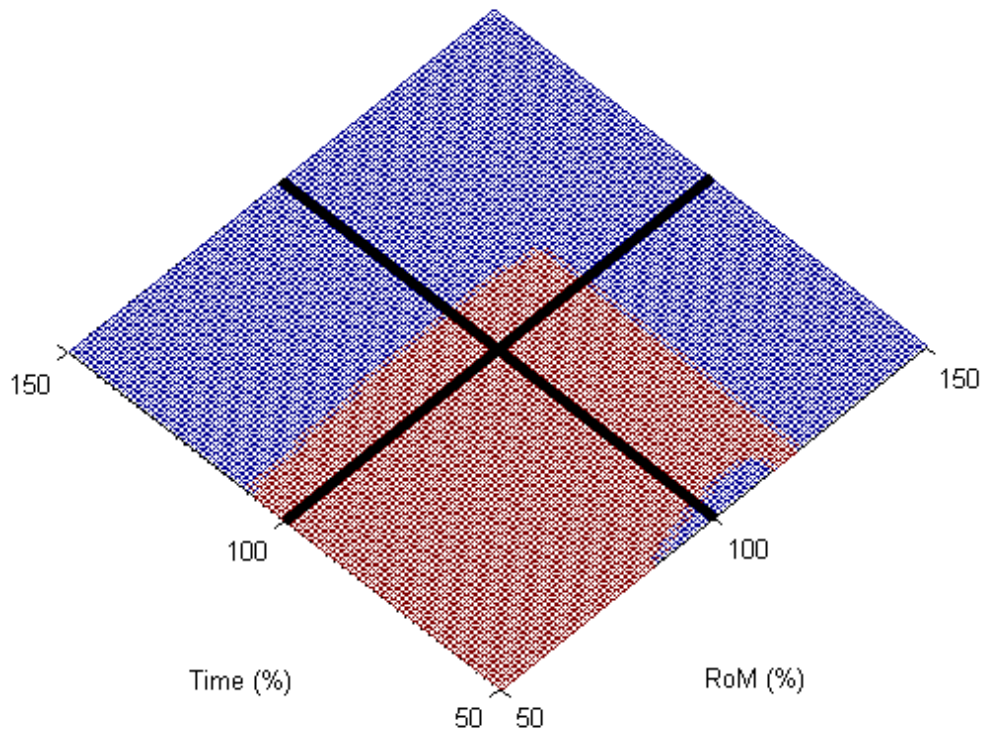
Figure 4.15. Surface plot of possible trials. Red areas indicate feasible trials, blue areas indicate trials have been rejected.

Despite some of the limits being quite loosely set, it is interesting to see that a large portion of the trials are rejected. Even the optimum trial above would be rejected meaning the optimum under these conditions would be 109% Ptime and 120% RoM. Trials above 120% RoM used a knee angle over 180° and trials using more than 109% Ptime failed to generate sufficient vertical velocity for the athlete to continue. The matched start, optimum start and limited start are compared in Table 14.

Table 14. Comparison of noted starts by the four segment model.

Start	Ptime (%)	RoM (%)	Time in block (s)	Starting angle (°)			CoM Displacement (m)		Velocity at take off (m·s⁻¹)		Impulse (Ns)		Maximum joint torque during extension (Nm)		
				Ankle	Knee	Hip	X	Y(peak)	X	Y	X	Y	Ankle	Knee	Hip
Matched start	100	100	0.325	82	109	92	1.07	0.12	3.03	-0.17	142.75	200.97	377	269	762
Optimum start	115	150	0.354	76	102	70	1.82	0.08	5.41	-3.91	159.04	213.91	799	654	1525
Limited start	109	120	0.345	80	106	84	1.43	0.06	4.43	-2.05	157.66	210.19	495	403	894

The focus here however was to examine the relationships involved and to understand more about limitations for athletes performing the sprint start. Whilst RoM and coordination are shown to be important, the model suggests that the athlete's strength may be a limiting factor which will take affect before the athlete is limited by RoM or coordination. In order to investigate this further, a torque driven model was created.

4.3 Four Segment Torque Driven Model

As previously discussed, an angle driven model does not account for limitations such as the athlete's muscle strength throughout the RoM and speed of contraction. A four segment torque driven model of the sprint start (Figure 4.16) was created by replacing the angle driven components of the angle driven model with torque generators (joint torque data provided by Forrester, 2006 who used a data collection method based on that of Yeadon et al., 2006). These reproduced the athlete's strength characteristics for each joint as displayed in Figures 4.17 – 4.19 and a full description is provided in Chapter 5.5. Initial segment orientations were again based on one representative trial from data collection 1.
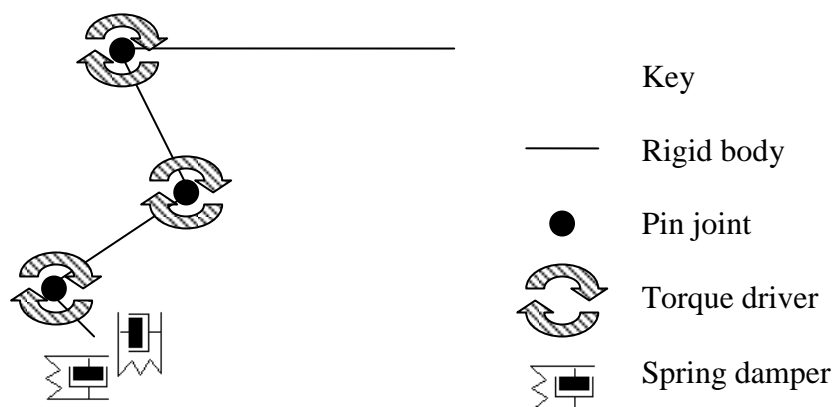
Figure 4.16. Four segment torque driven model of the sprint start.
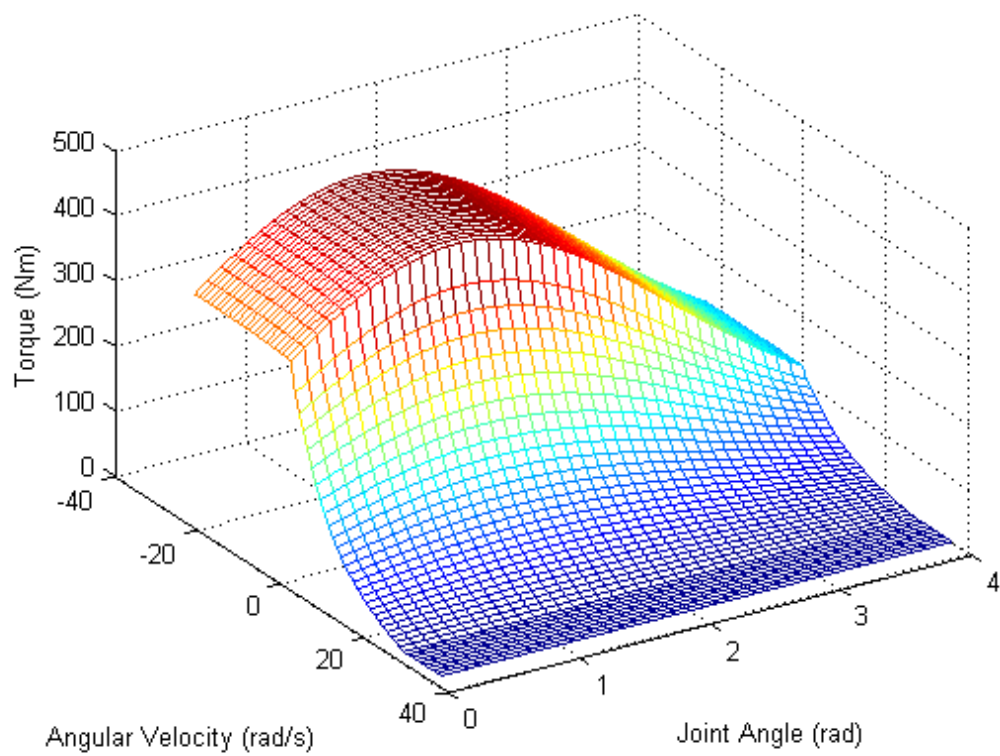
Figure 4.17. Hip extension torque, angle, angular velocity profile.
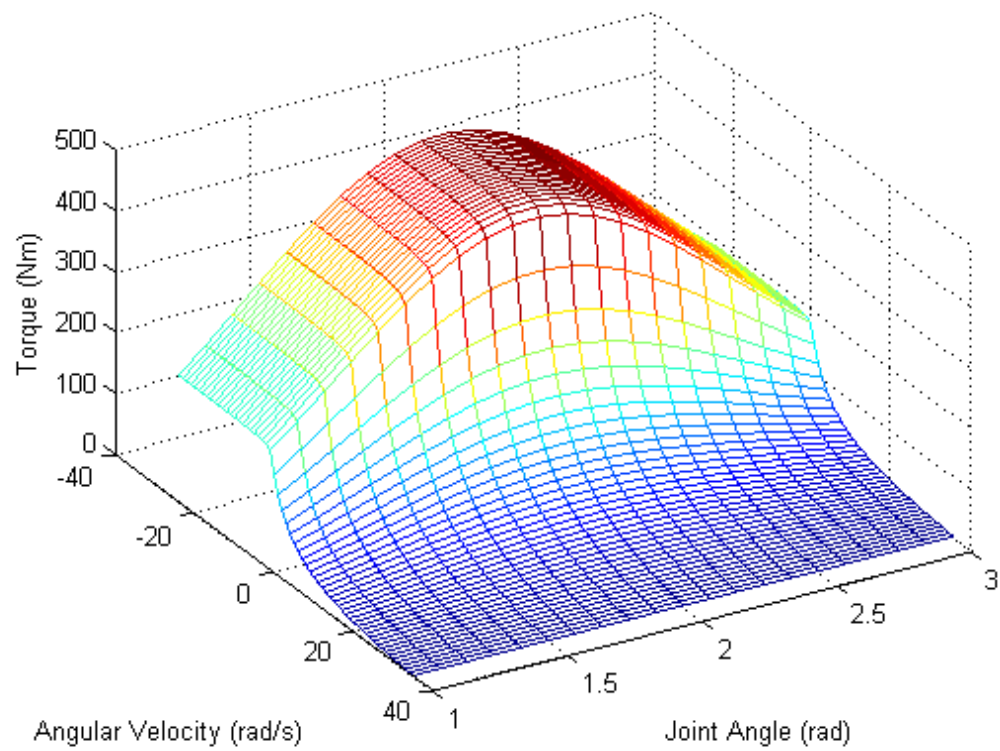
Figure 4.18. Knee extension torque, angle, angular velocity profile.
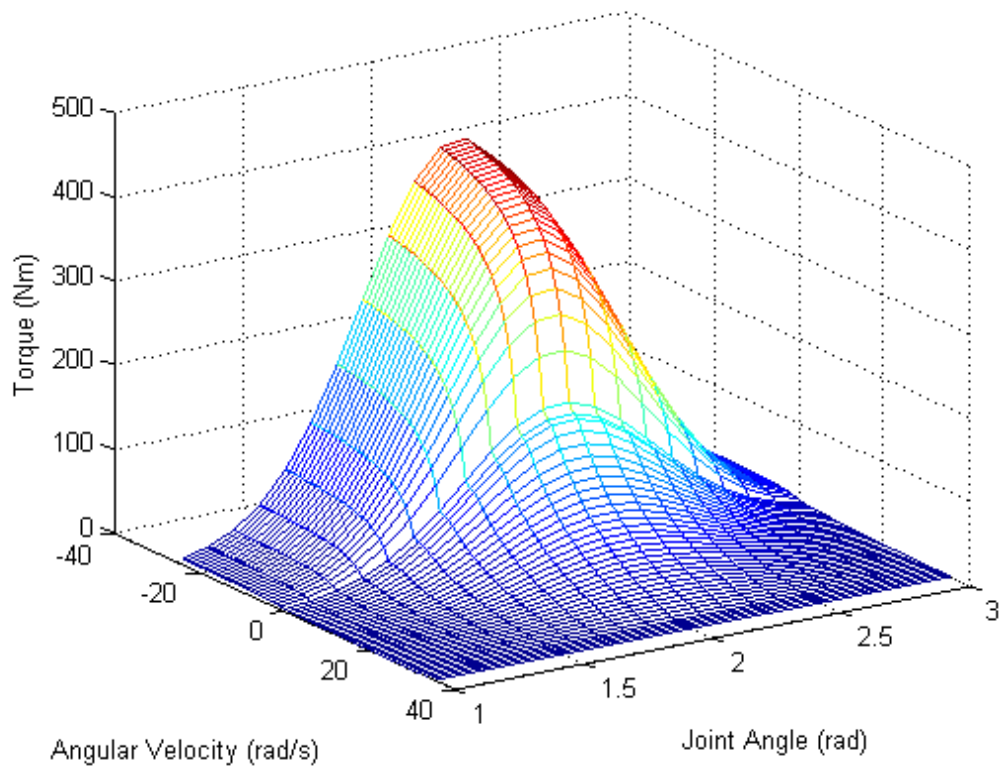
Figure 4.19. Ankle plantar flexion torque, angle, angular velocity profile.

Allowing each joint to extend maximally throughout the simulation resulted in the ankle collapsing and overall uncoordinated movement, illustrating that a greater level of control was required in the model. In order to improve coordination, activation was governed using a sigmoid curve, equation 4.4. The typical curve, as shown in Figure 4.20, had asymptotes at 0 and 1. Activation was then multiplied by the relevant subject specific torque data to input joint torque into the model.

$$a \left(t \right) = \frac{m}{1 + e^{-ts}} \qquad (4.4)$$

Where:

a   = level of activation

m   = maximum level of activation possible (asymptote)

e   = number 'e'

t   = time

s   = steepness of the curve
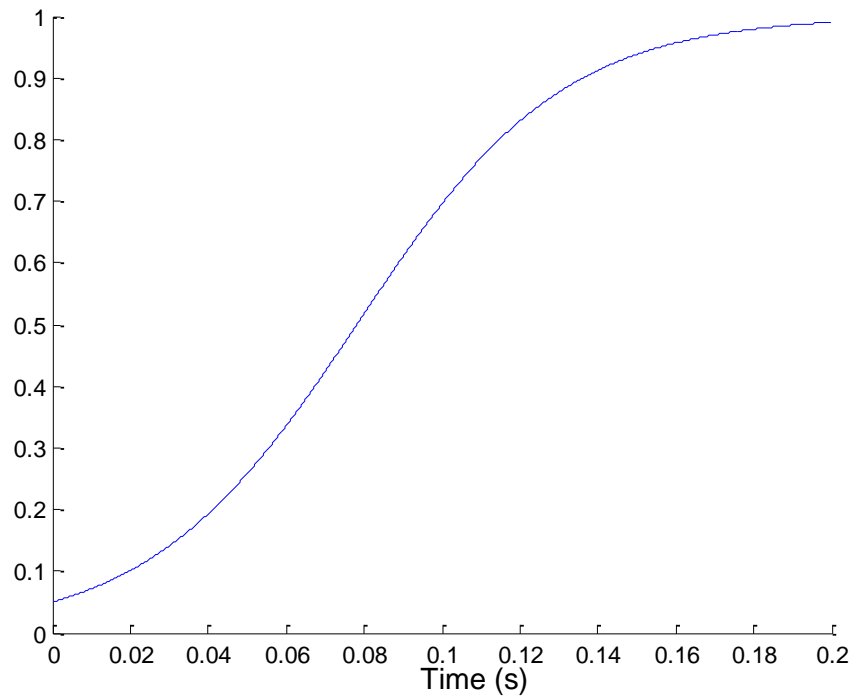
Figure 4.20. Sigmoid curve.

For each simulation of the start, activation profiles were optimised (using DIRECT optimisation, (Finkel et al., 2003)) by allowing three parameters to vary, these were: initial level of activation, maximum level of activation and time at which maximum activation was reached. Bounds were 0.1 - 0.7 for initial activation, 0. 1 − 1 for maximum activation and 0.07 - 0.7 s for time to reach maximum activation. Once maximum activation had been reached, the level was maintained for the remainder of the simulation.

The simulation terminated on takeoff or when a joint exceeded 180°. The score was composed based on penalties for RoM used, velocity on takeoff and a penalty should the model fail to takeoff (Figure 4.21). Whilst there was no set penalty for a joint attempting to exceed 180°, this was not required as the simulation stopped early and the penalty for not taking off was large.
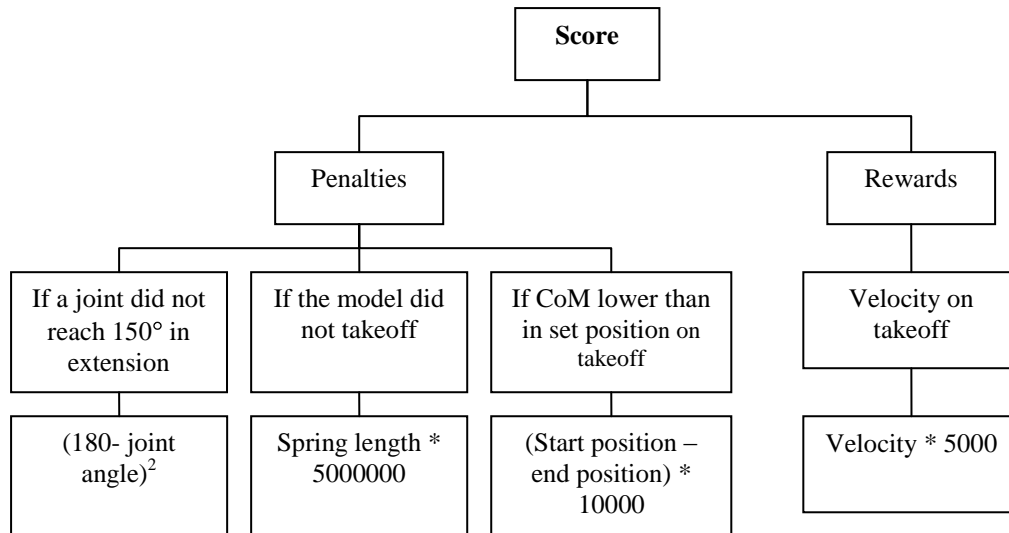
Figure 4.21. Score composition for four segment torque driven model.

The formulation of the score for optimising parameters and simulations appeared to influence results during initial testing. The use of adding a set number as a penalty was avoided except where the likelihood of the instance occurring was small (such as when a simulation was stopped prematurely to prevent it crashing). If set penalties were given during regular occurrences, such as when the knee joint attempted to hyper extend in torque driven models, the result was that the optimisation took longer to reach a minima or was more likely to find a local minima. Helping to create a slope for the optimisation routine was therefore important. Taking this a stage further, it was interesting to note that when optimising the torque driven four segment model, squaring the error in joint angle resulted in an approximately 20° average better total error in score over taking the error alone (based on DIRECT optimisation).

4.3.1 Effects of Optimisation Criteria

One of the aims of the study was to examine the effects of using different optimisation criteria on simulations of the sprint start. Horizontal velocity on takeoff was used as a baseline to compare contact time, horizontal acceleration and impulse as other possible measures. It was expected that impulse should be a good indicator of starting performance given the impulse momentum relationship, however, time was

optimised to be both as short and long as possible. A short time would be of interest for the athlete attempting to leave the starting block as quickly as possible whereas a long time should relate to a high velocity on takeoff given its role in the calculation of impulse. Finally horizontal acceleration is based on horizontal velocity and time and obtaining a high velocity in a short time could be seen as the priority of the sprint start. The null hypothesis was that the same start performances would be found irrespective of the criteria used to optimise the model due to the variables all being mechanically linked. It is appreciated however that this is unlikely to be the case for both short and long contact times.

The initial optimisation of all 125 simulations using velocity showed the fastest simulation reached 2.96 m·s^{-1} on takeoff. In the score equation, this was multiplied by 5000 (14800) and subtracted from the score. In order that similar weightings be applied for contact time, horizontal acceleration and horizontal impulse, contact time was multiplied by 36585, acceleration by 1429 and impulse by 93 and based on maximums of 0.41 s for contact time, 10.53 m·s^{-2} for acceleration and 163 Ns for horizontal impulse. Table 15 below displays some of the variables for the original start (100Sim) when optimised using different criteria.

Table 15. Effect of using different optimisation criteria on simulations of the sprint start.

Value obtained on or accumulated up to take off	Optimisation criteria				
	Short time	Long time	Velocity	Accelera-tion	Impulse
Contact time (s)	0.24	0.38	0.27	0.25	0.27
Horizontal Distance (m)	0.97	0.85	1.26	1.28	1.26
Horizontal velocity (m·s^{-1})	1.92	2.49	2.61	2.53	2.61
Vertical velocity (m·s^{-1})	0.78	-0.41	0.64	0.86	0.64
Horizontal acceleration (m·s^{-1})	8.00	6.56	9.54	10.19	9.54
Horizontal impulse (Ns)	105.97	137.13	143.72	139.51	143.72
Vertical Impulse (Ns)	172.94	181.95	182.49	178.32	182.49

As seen in Table 15, the starts found based on velocity and impulse are exactly the same but differences can be seen when optimising for contact time and acceleration. The use of optimising for a long contact time seems small as whilst the optimisation did find a longer contact time, velocity on takeoff was no better than when optimising for velocity alone. Optimising for a short start time reduced the contact period by 0.03 s but with a loss in velocity of 0.69 m·s^{-1} as well as 1.54 m·s^{-2} lower in acceleration than the start optimised for velocity. Perhaps not surprisingly the start optimised for acceleration used slightly more time than the start optimised for a short contact period but shorter than the start optimised for impulse. This start was 0.08 m·s^{-1} slower than the starts optimised for impulse and velocity but went furthest due to a higher vertical velocity on takeoff. This all shows that the criteria used for optimising sprint start will affect the results obtained.

If the model included the opposite leg and a second step it would be possible to begin predicting if a shorter contact time would allow the athlete to start the second step sooner and compensate for a lower velocity on takeoff. As the simulation lasts until takeoff it is difficult to make predictions about how this would affect the athlete beyond the simulated time which is a limitation of the study. Future work may be able to examine this, however, it is acknowledged that changing the criteria used for optimising will affect the starts found. In the follow part of the study, horizontal velocity was used to optimise simulations in each case.

4.3.2 Changes to the Set Position

The first area investigated was the effect of changes to the 'set' position. This was achieved using five initial joint angles for each of the ankle, knee and hip based on measured angle data $\pm$ 5° and 10°, Table 16. Henceforth, where joint angles are referred to as -10, -5, 0, 5 or 10, this refers to the values presented in Table 16. This method provided 125 possible combinations for the initial body configuration and is based on the method used by Selbie and Caldwell (1996) in their four segment model of vertical jumping. As was done for the angle driven model, the change in angle at

the ankle was added to the foot-ground angle to help the simulation maintain orientation.

Table 16. Joint angles examined in four segment torque driven model

Joint	Joint angle in Set position (°)				
	-10	-5	0	5	10
Hip	72.57	77.57	82.57	87.57	92.57
Knee	97.84	102.84	107.84	112.84	117.84
Ankle	76.77	81.77	86.77	91.77	96.77

Once optimised, all trials obtained an extended position on takeoff without hyper-extension at any joint. Figure 4.22 shows the simulation where initial joint orientations were all the same as the found in the measured data (100Sim).
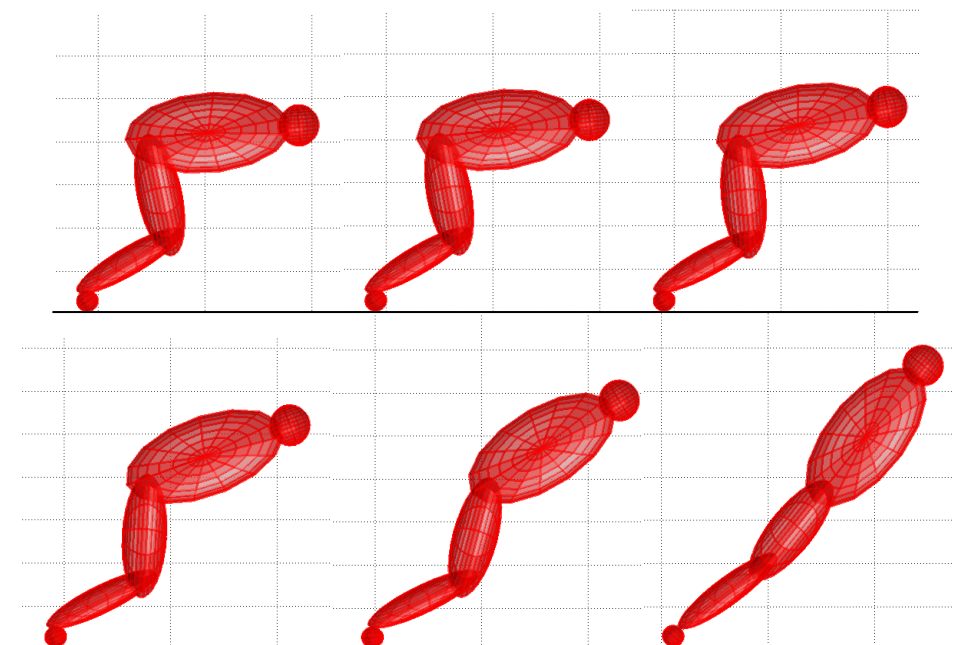
Figure 4.22. Four segment torque driven model of the sprint start.

In order to examine the influence varying joint angles on the start variables, analysis of variance was conducted using an ANOVA or Kruskal-Wallis test following a Lilliefors test for normality. Figures 4.23 – 4.25 below display the results and

relationships for some of the variables of interest. Significant positive relationships can be seen between horizontal velocity and start distance, vertical velocity and CoM height on takeoff and horizontal impulse and contact time although this list is not exhaustive. Such relationships may be expected due to the variables being mechanically linked but it can be seen that in no case did the simulation with the highest value for one variable also have the highest value for the other. Figure 4.23 shows a large variation from the regression line and a simulation with an average horizontal velocity obtained the largest distance and vice-versa. This further demonstrates that the sprint start cannot be represented as a single segment or mass. Whilst overall mechanical relationships hold true, variations away from the regression line show the involvement of more complex relationships when modelled using even just four segments. This also reflects the non linear surfaces shown by the angle driven model in the previous section.
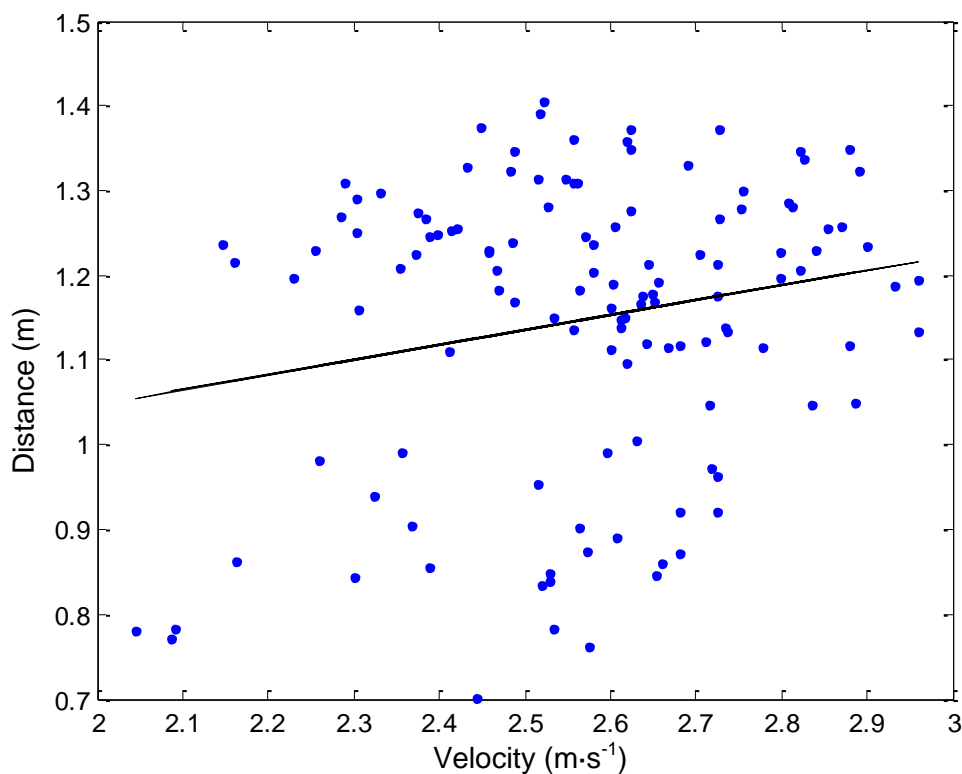
Figure 4.23. Horizontal velocity and start distance. R = 0.2058, P = 0.0213, Y = 0.1765 * x + 0.6943.
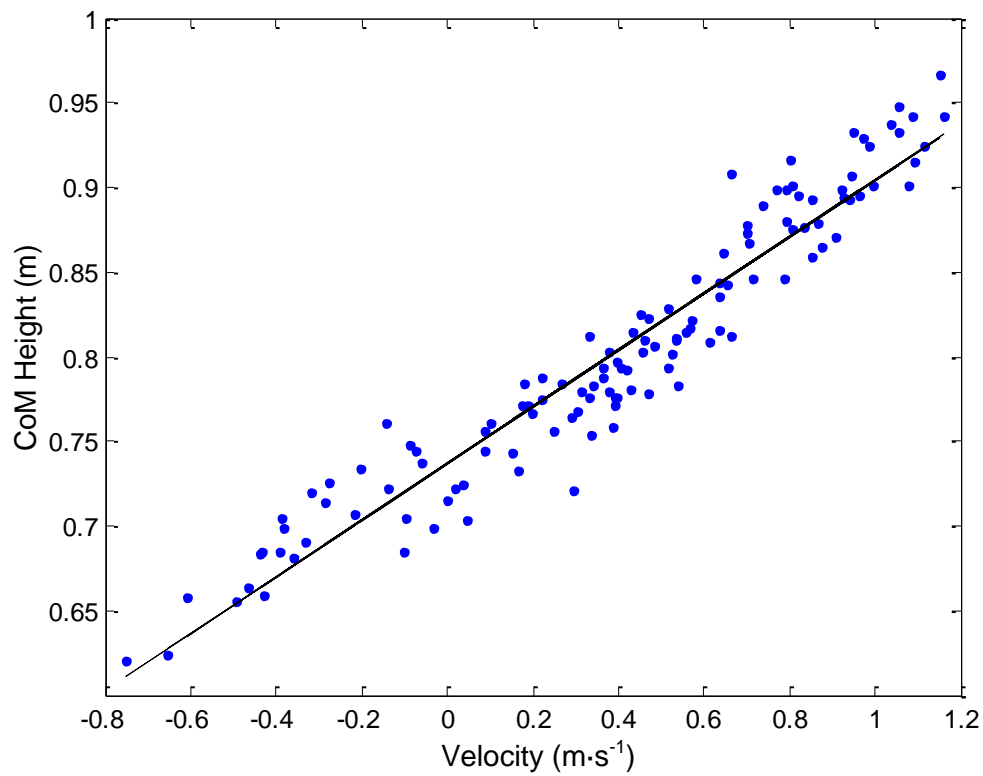
Figure 4.24. Vertical velocity and CoM height on takeoff. R = 0.9597, P = 0.0000, Y = 0.1674 * x + 0.7369.
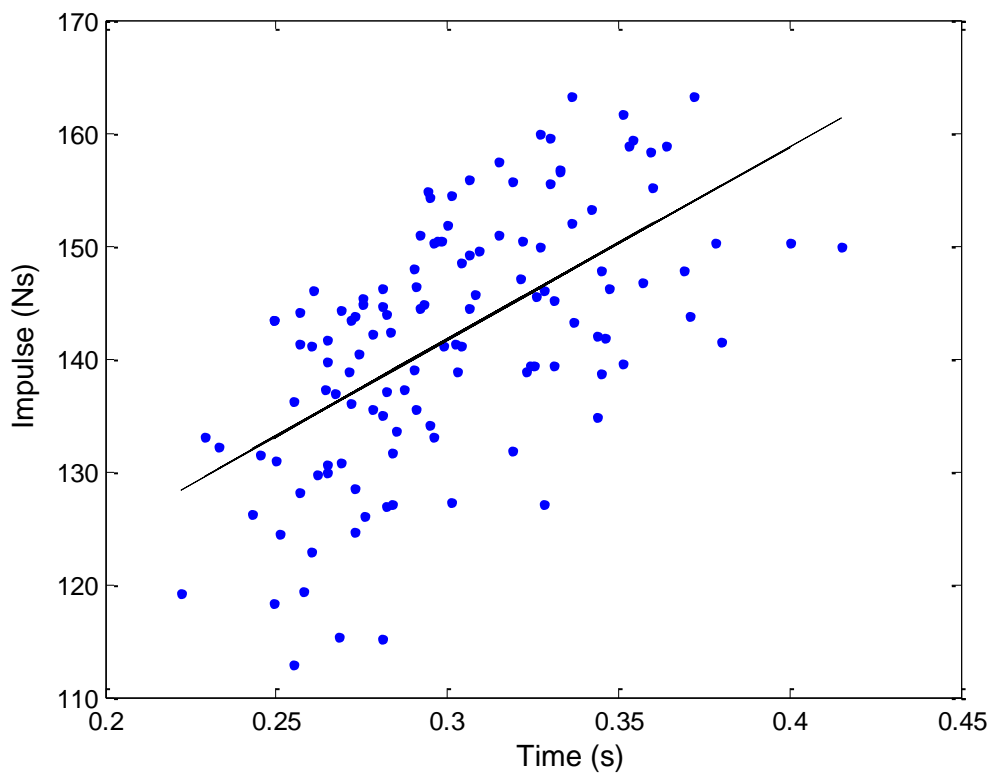
Figure 4.25. Contact time and horizontal impulse. R = 0.5979, P = 0.0000, Y = 170 * x + 90.4470.

The effect of changing the starting position can be examined more closely when examining the individual joint angles. Figure 4.26 below displays the effect of varying joint angles in the set position on horizontal impulse on takeoff. Whilst the differences between conditions were relatively small, Table 17 reveals which starting angles at the hip and knee were significantly different at $P < 0.05$ based on the ANOVA analysis. Examining the joints in isolation, the smallest angle at the hip (-10°), 0° at the knee and -5° at the ankle resulted in the fastest (highest horizontal velocity) starts. Therefore, the fastest start would be one with the smallest possible hip angle, an optimum angle at then knee of approximately 107° and the ankle angle being of little consequence. Interestingly the simulation which exerted the highest horizontal impulse used -10° (72.6°) at the hip, -5° (102.8°) at the knee and 0° (86.8°) at the ankle.
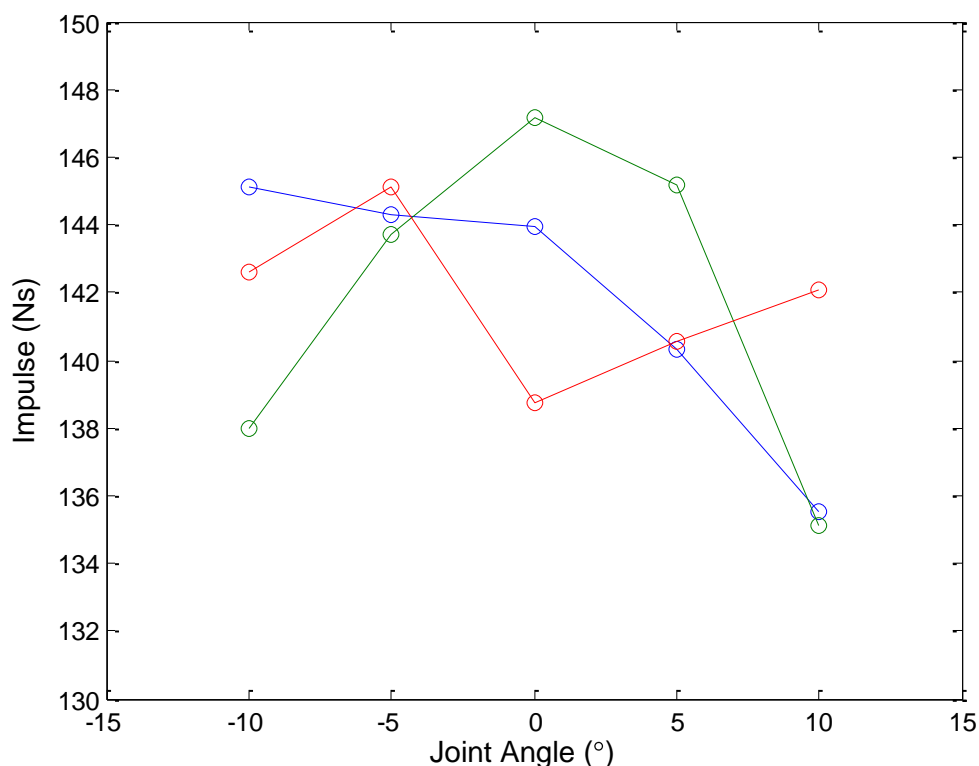
Figure 4.26. Joint angle and horizontal impulse. Blue = hip, green = knee, red = ankle.

Table 17. Horizontal impulse with changing joint angle.

Joint	Mean Horizontal Impulse (Ns)				
	Start Position (°)				
	-10	-5	0	5	10
Hip	145.12 ± 13.79	144.30 ± 11.91	143.92 ± 8.12	140.31 ± 8.25	135.50 ± 9.34
Significantly different to	10	none	none	none	-10
Knee	137.97 ± 10.15	143.70 ± 12.02	147.15 ± 10.27	145.19 ± 6.86	135.14 ± 10.63
Significantly different to	0	10	-10, 10	10	-5, 0, 5
Ankle	142.63 ± 11.42	145.13 ± 9.92	138.76± 10.46	140.56 ± 10.80	142.07 ± 11.91
Significantly different to	none	none	none	none	none

Lilliefors test showed velocity data to be normally distributed ($p = 0.1671$), therefore an ANOVA was used to calculate differences.

Significance level, $p < 0.05$

Figure 4.25 displays a significant positive linear relationship between horizontal impulse and contact time and in turn, plots of contact time with joint angle (Figure 4.27) are similar to that for horizontal impulse. The differences between conditions are quite small but significant in cases such as the knee where the most extended position used significantly less time in contact with the starting block (Table 18).
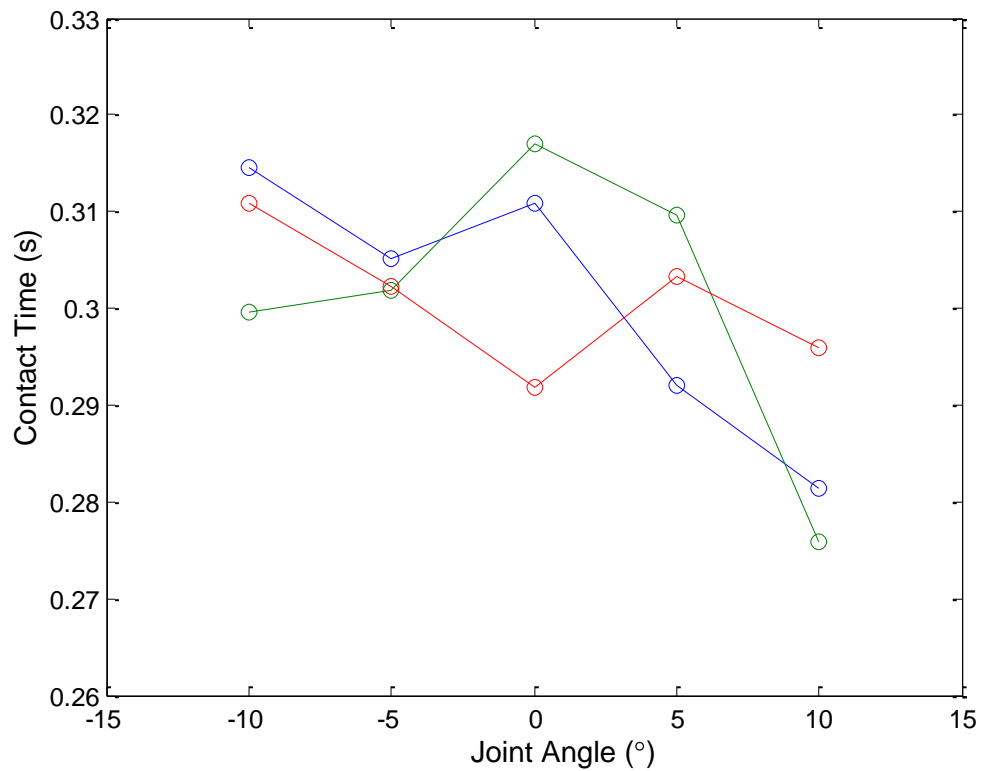
Figure 4.27. Mean contact time with starting position. Blue = hip, green = knee, red = ankle.

Table 18. Contact time with changing joint angle.

Joint	Mean Contact Time (s)				
	Start position (°)				
	-10	-5	0	5	10
Hip	0.31 ± 0.03	0.31 ± 0.03	0.31 ± 0.04	0.29 ± 0.04	0.28 ± 0.03
Significantly different to	10	none	10	none	-10, 0
Knee	0.30 ± 0.03	0.30 ± 0.04	0.31 ± 0.04	0.31 ± 0.03	0.28 ± 0.03
Significantly different to	none	none	10	10	0, 5
Ankle	0.31 ± 0.05	0.30 ± 0.03	0.29 ± 0.04	0.30 ± 0.05	0.30 ± 0.03
Significantly different to	none	none	none	none	none

Lilliefors test showed velocity data to be normally distributed ($p = 0.0634$), therefore an ANOVA was used to calculate differences.

Significance level, $p < 0.05$

Results for peak horizontal forces (Figure 2.28 and Table 19) follow a somewhat different pattern to that seen so far, although it is still the angle at the knee which causes the largest changes. For both the knee and ankle, the highest peak forces are seen in more extended positions whilst the opposite appears to be the case at the hip (result was not significant).
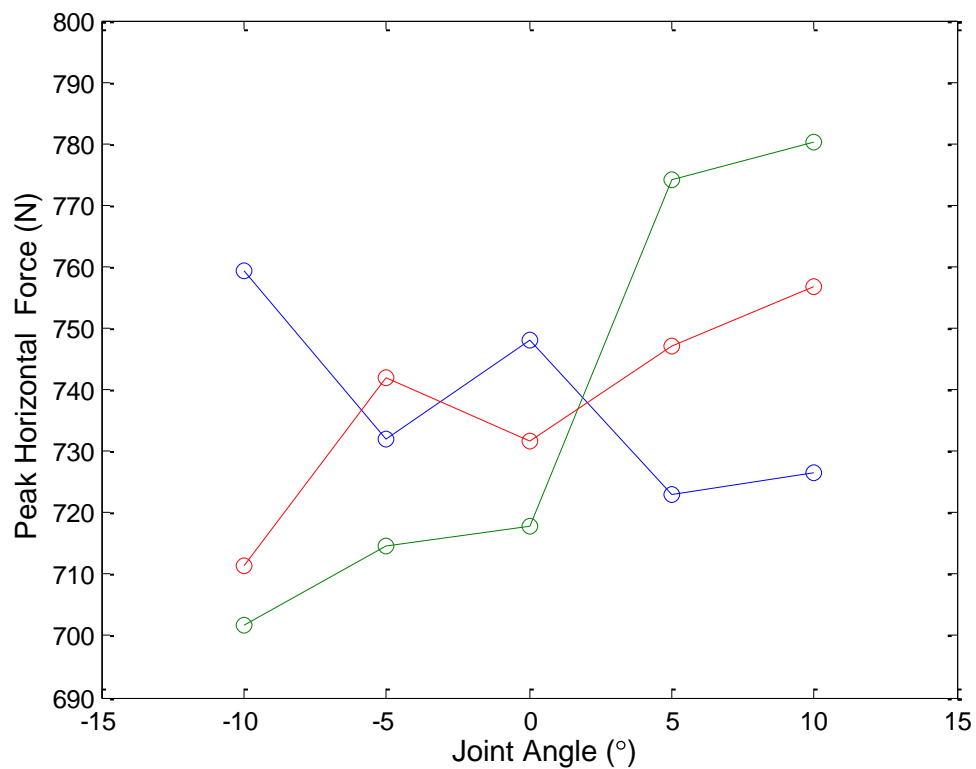
Figure 4.28. Joint angle and mean peak horizontal force. Blue = Hip, green = knee, red = ankle.

Table 18. Mean peak horizontal force with changing joint angles.

Joint	Peak Horizontal Force (N)				
	Start Position				
	-10	-5	0	5	10
Hip	759.25 ± 114.27	732.06 ± 48.72	747.98 ± 101.18	723.03 ± 31.03	726.38 ± 35.87
Significantly different to	none	none	none	none	none
Knee	701.82 ± 18.93	714.73 ± 25.03	717.76 ± 32.54	774.19 ± 112.86	780.21 ± 92.45
Significantly different to	5, 10	10	10	-10	-10, -5, 0
Ankle	711.40 ± 29.56	741.93 ± 56.71	731.63 ± 81.68	747.13 ± 99.95	756.60 ± 83.12
Significantly different to	10	none	none	none	-10

Lilliefors test showed velocity data to not be normally distributed ($p = 0.001$),

therefore a Kruskal-Wallis was used to calculate differences.

Significance level, $p < 0.05$

Three simulations were selected in order to undertake a closer examination of results. These were; a simulation which obtained a high horizontal velocity on takeoff (FastSim), the simulation which matched the original measured joint angles (100Sim) and one of the simulations with a low horizontal velocity on takeoff (SlowSim).

Table 20 compares variables from the three starts. The fastest start also had the highest horizontal impulse and contact time however it had the least vertical velocity on takeoff, CoM height on takeoff and horizontal and vertical peak forces. The anomaly is vertical impulse which is also highest for FastSim and doesn't relate to the low vertical velocity seen for this start. Conversely, SlowSim used the highest CoM position on takeoff, least horizontal impulse, highest peak forces and shortest contact times.

Table 20. Start variables for simulations.

	Simulations					
	FastSim	100Sim	SlowSim	Mean	Range	S.D.
Hip Angle (°)	72.57	82.57	92.57	82.57	20	7.10
Knee Angle (°)	102.84	107.84	112.84	107.84	20	7.10
Ankle Angle (°)	81.77	86.77	86.77	86.77	20	7.10
Contact time (s)	0.35	0.27	0.26	0.30	0.19	0.04
Distance (m)	1.19	1.26	1.18	1.15	0.70	0.17
CoM height on takeoff (m)	0.74	0.84	0.85	0.80	0.35	0.08
Horizontal velocity (m·s^{-1})	2.93	2.61	2.47	2.57	0.92	0.20
Vertical Velocity (m·s^{-1})	0.15	0.64	0.58	0.39	1.92	0.46
Horizontal Acceleration (m·s^{-2})	8.35	9.54	9.68	8.63	3.98	0.85
Peak Horizontal force (N)	698.44	709.47	728.76	737.74	429.01	74.79
Peak vertical force (N)	670.48	847.34	875.16	851.58	477.87	102.54
Horizontal impulse (Ns)	161.71	143.72	136.23	141.83	50.42	10.96
Vertical Impulse (Ns)	198.11	182.49	169.68	184.04	97.61	21.52

Note. Range and standard deviation are for all 125 simulations.

Figures 4.29a-f present joint angles and angular velocities for simulations presented in Table 20. The general pattern of movements is the same for each trial revealing proximal to distal sequence. In each case the hip is extended to 180° on take off but interestingly FastSim shows the smallest angle is at the ankle on takeoff.

Furthermore, this simulation used lower peak angular velocities at the hip and knee than either 100Sim or SlowSim.

The pattern of muscle activation is also similar for the three simulations, Figures 4.29g-i. Furthermore, the three simulations all begin using similar level of activation level at each joint. As the simulations progress, the knee becomes most active and the hip the least. Interestingly, peak activation was lowest for each joint in FastSim perhaps suggesting it was capable of going faster still. This perhaps also demonstrates the importance of coordination and the role of muscle force-length/ velocity relationships in the movement.
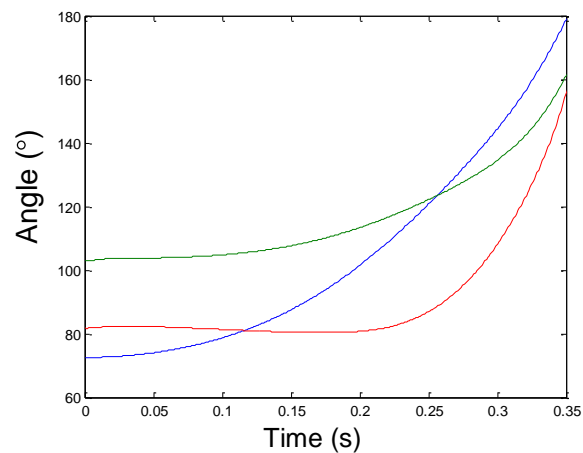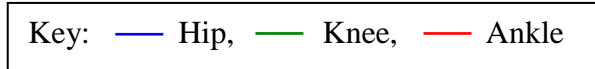
Figure 4.29a. Joint angles during FastSim.
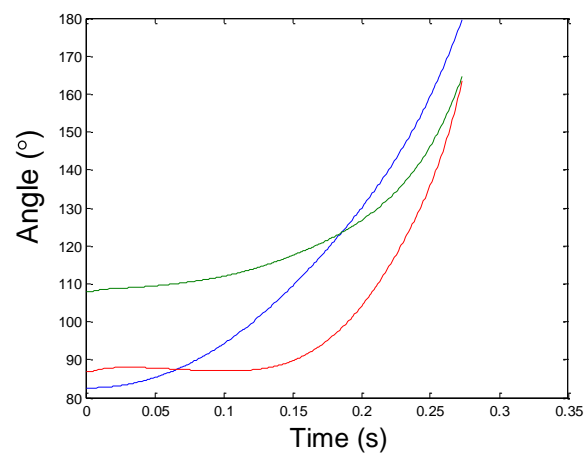
Figure 4.29b. Joint angles during 100Sim.
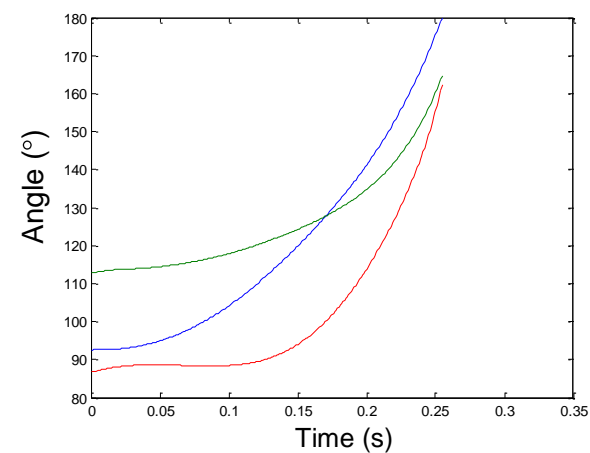
Figure 4.29c. Joint angles during SlowSim.
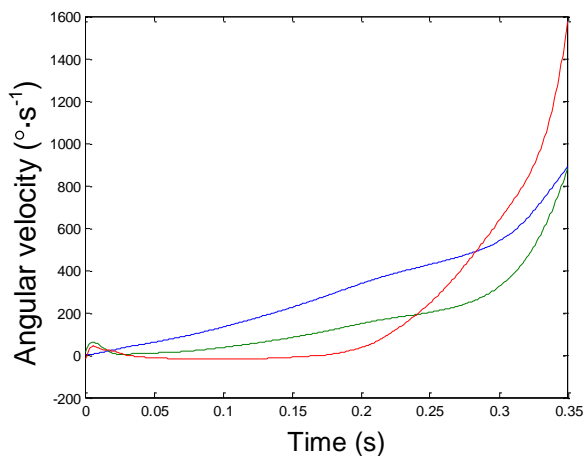
Figure 4.29d. Joint angular velocity during FastSim.
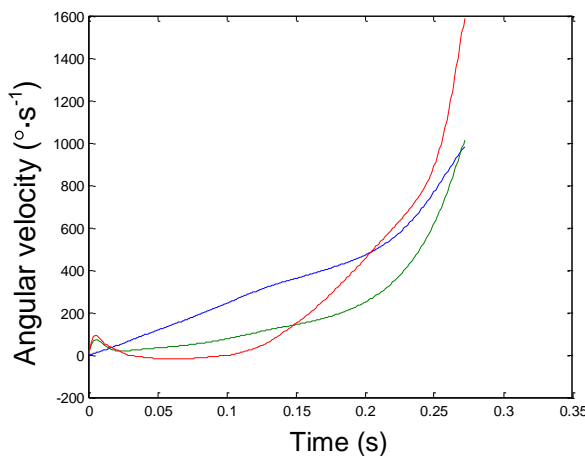
Figure 4.29e Joint angular velocity during 100Sim.
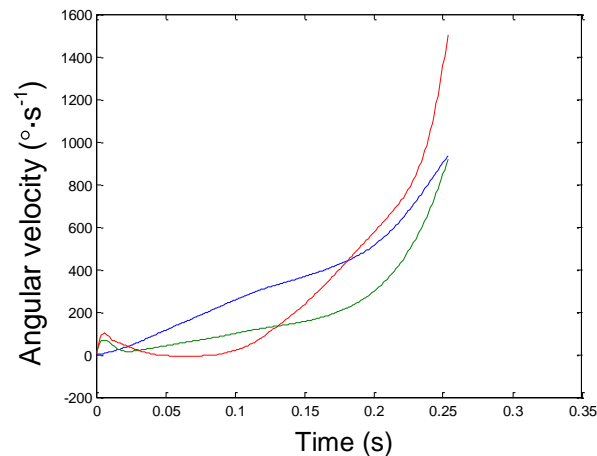
Figure 4.29f Joint angular velocity during SlowSim.

Key: — Hip, — Knee, — Ankle
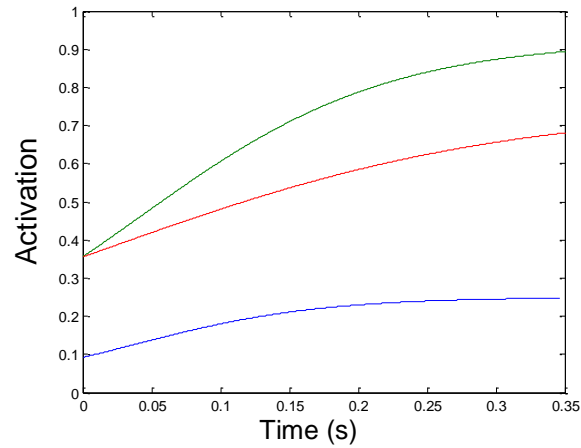
Figure 4.29g Joint activations input for FastSim.
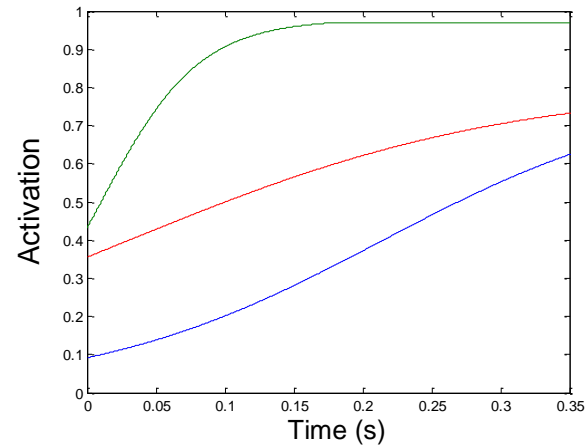
Figure 4.29h Joint activations input for 100Sim.
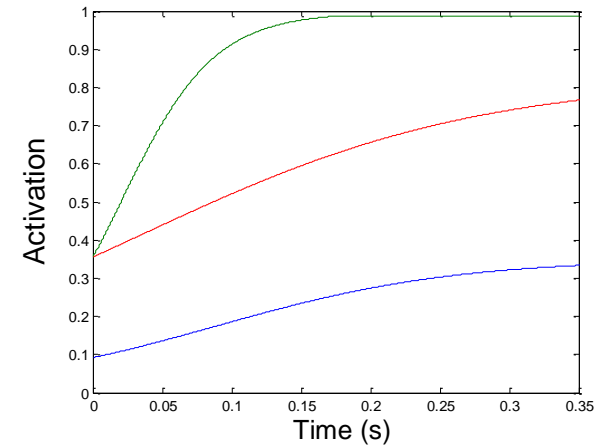
Figure 4.29i Joint activations input for SlowSim.

On closer inspection of the simulations it was found that two different techniques had been adopted. Ninety three of the simulations followed the technique shown above in a proximal to distal movement sequence. The other thirty two simulations used almost the opposite technique; large extension at the ankle to begin followed by extension at the hip and knee. An example of this is shown in Figures 4.30 a-c where it can be seen that the hip and knee initially flex but by takeoff each joint reaches approximately 170°. Peak angular velocity at the ankle appears to be somewhat less than for the simulations above, peak angular velocity at the hip is higher and is comparable at the knee.

Guissard et al. (1992) showed that a normal sprint start technique would be expected to show some delay in ankle extension over the first 100-150 ms as their results depicted that the Soleus muscle does not shorten compared to its initial length in the set position during this time. Furthermore peak joint torques and energy flow is expected to move down the limb in a proximal to distal sequence (Mero et al., 2006).

Key: —— Hip, —— Knee, —— Ankle
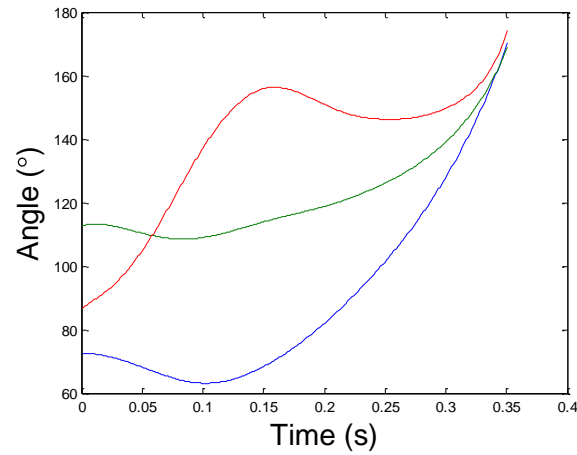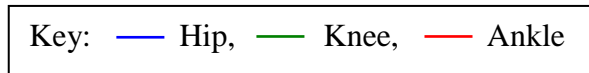
Figure 4.30a Joint angles during AnkSim.
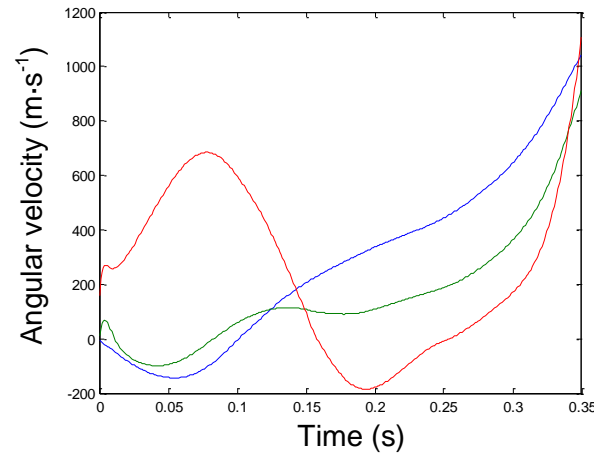
Figure 4.30b Joint angular velocity during AnkSim.
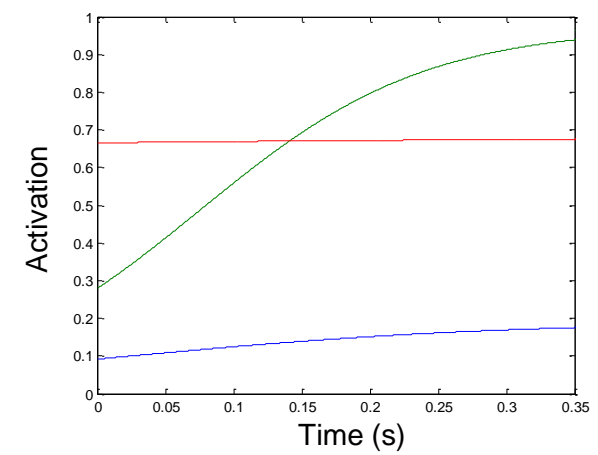
Figure 4.30c Joint activation during AnkSim.
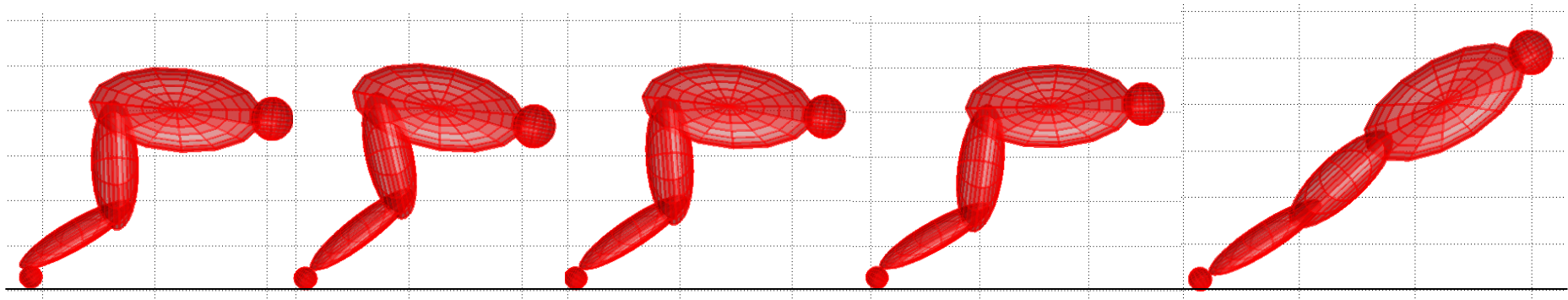
Figure 4.31. Four segment model using an ankle first strategy.

Figures 4.32-4.34 below show the effect of this ankle first strategy on the overall results. The blue points show simulations which used the ankle first strategy and it can be seen that generally whilst horizontal velocity was similar to the proximal-distal strategy, vertical velocity, distance, and CoM height on takeoff were generally lower. Interestingly contact time tended to be higher but the lack of increase in horizontal velocity compared to proximal-distal strategy suggests that this is less efficient. On closer inspection, for the thirty two simulations represented by the blue points, all but two had a knee angle at 0, 5, or 10°. Indeed the general pattern appeared to be that these simulations used a small hip and ankle angle with a large knee angle although this wasn't always the case.
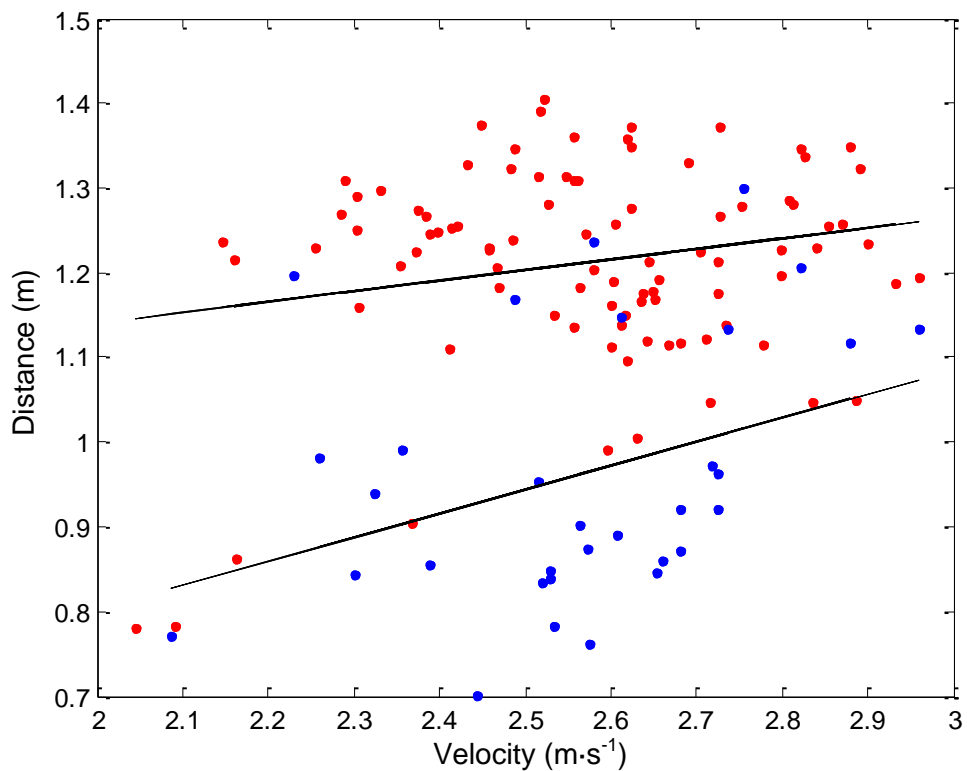
Figure 4.32. Horizontal velocity and distance for proximal to distal and ankle first strategies. Red points = proximal to distal strategy, R = 0.2082, P = 0.0452, Y = 0.1248 * x + 0.8910. Blue points = ankle first strategy, R = 0.3503, P = 0.0494, Y = 0.2830 * x + 0.2365.
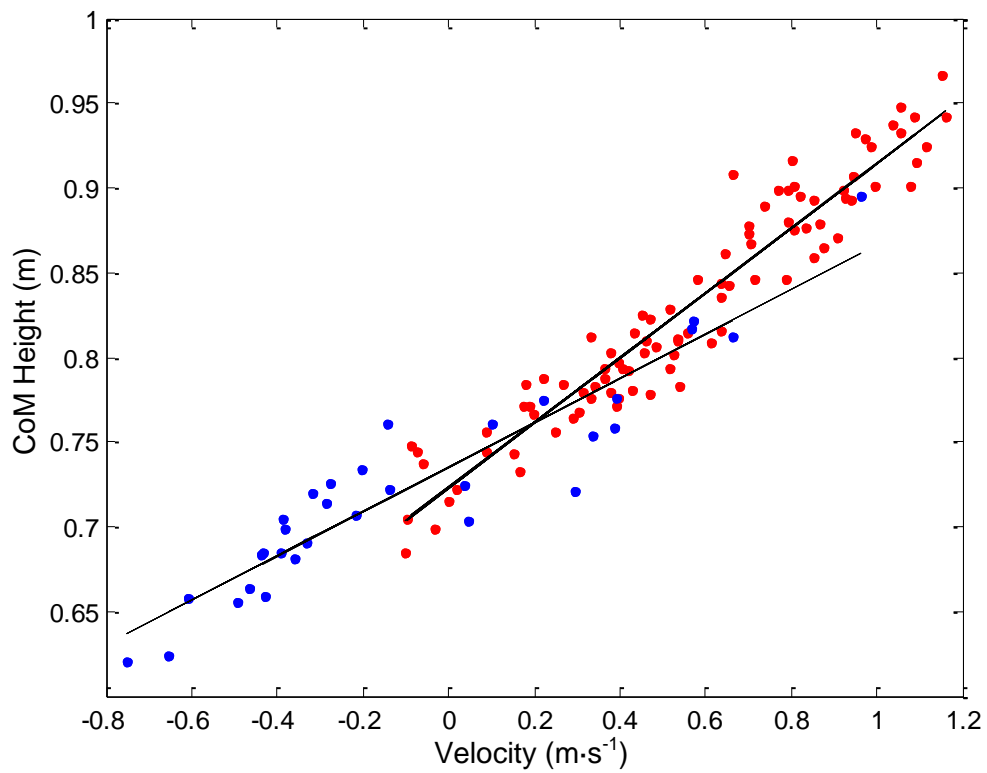
Figure 4.33. Vertical velocity and CoM height on takeoff for proximal to distal and ankle first strategies. Red points = proximal to distal strategy, R = 0.9565, P = 0.0000, Y = 0.1913 * x + 0.7230. Blue points = ankle first strategy, R = 0.9344, P = 0.0000, Y = 0.1307 * x + 0.7351.
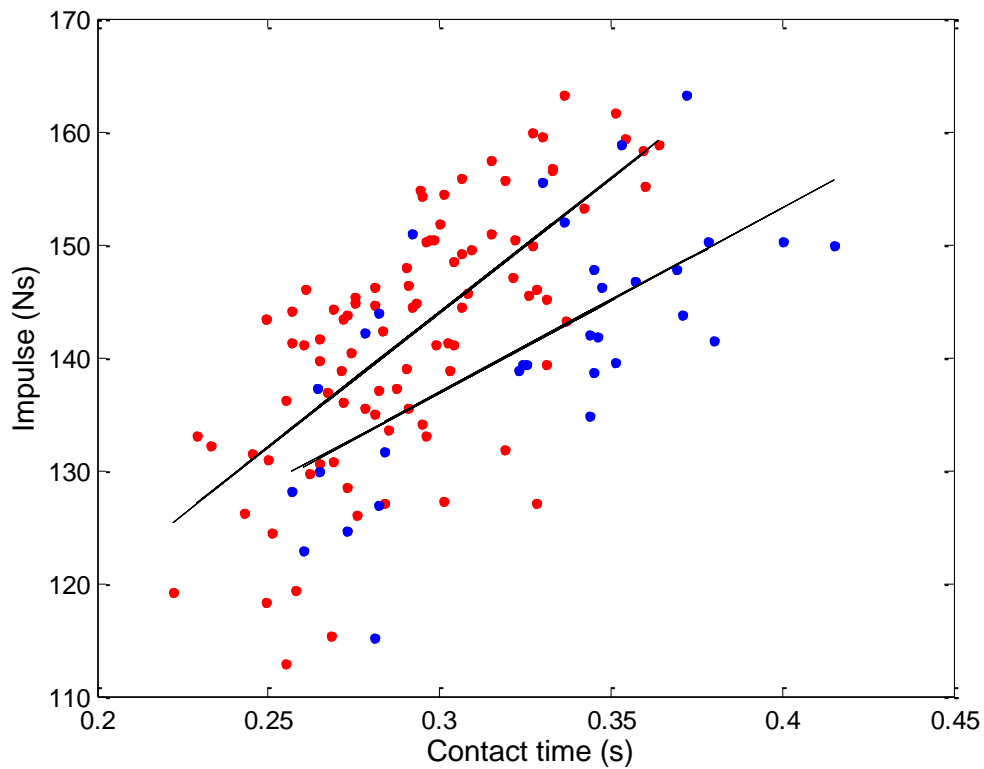
Figure 4.34. Contact time and horizontal impulse for proximal to distal and ankle first strategies. Red points = proximal to distal strategy, R = 0.6788, P = 0.0000, Y = 237.7910* x + 72.6361. Blue points = ankle first strategy, R = 0.6709, P = 0.0000, Y = 163.4827 * x + 87.8098.

These simulations were reoptimised with an added penalty in the score function in an attempt to make these simulations use the proximal to distal technique. This had little effect as simulations either produced extremely slow starts or failed to find a solution. This shows the importance of initial position on finding the optimum start in this model.

4.3.3 Increased Activation

To examine the effects of increasing muscle activation during the start, seven simulations were selected for further investigation. These were the five simulations which used the same initial condition joint angle conditions for each joint (for example, -10° at the hip, knee and ankle), and FastSim and SlowSim used above. Ideally, if time had permitted, all 125 simulations would have been used but it was thought that this provided an interesting and useful sample. The optimisation was run with the same score equation as previously used however the initial activations were given higher bounds. Concurrently, the lower bound for maximum activation was also made to be higher, see Table 21. It can be seen that the hip was permitted to begin using a minimum activation of 0.4 compared to 0.7 at the knee and ankle. This was based on the highest initial activation at the hip being 0.35 under normal conditions therefore, starting at this level would still represent increased activation but also help to maintain coordination in the movement. Finally, as the bounds for initial and maximum activation now overlapped, an 'if' statement was added to the code so that maximum activation was always greater then initial activation.

Table 21. Bounds for investigation into increases in activation.

Joint	Time to maximum activation (s)		Initial activation		Maximum activation	
	Lower	Upper	Lower	Upper	Lower	Upper
Hip	0.07	0.7	0.4	0.9	0.9	1
Knee	0.07	0.7	0.7	0.9	0.9	1
Ankle	0.07	0.7	0.7	0.9	0.9	1

Table 22 displays information for the new starts with increased activation and compares the means of the seven simulations optimised with the original starts (for ease of viewing only FastSim, 100Sim and SlowSim are shown in detail). Increasing activation resulted in slower starts by an average 1.01 m·s^{-1} although vertical velocity and horizontal acceleration increased by 0.79 m·s^{-1} and 0.78 m·s^{-2} respectively. Horizontal and vertical impulse were also lower with increased activation but despite this peak forces were much higher and contact time was lower.

Table 22. Start variables for starts with increased activation and comparison to the original starts.

	Simulations				
	FastSim	100Sim	Slow Sim	Mean differe-nce[*]	S.D.
Hip Angle (°)	72.57	82.57	92.57	0	0
Knee Angle (°)	102.84	107.84	112.84	0	0
Ankle Angle (°)	81.77	86.77	86.77	0	0
Contact time (s)	0.19	0.18	0.17	-0.13	0.03
Distance (m)	1.14	1.06	1.03	-0.25	0.27
CoM height on takeoff (m)	0.89	0.90	0.91	0.08	0.06
Horizontal velocity (m·s^{-1})	1.91	1.84	1.79	-1.02	0.37
Vertical Velocity (m·s^{-1})	1.46	1.29	1.25	0.79	0.38
Horizontal Acceleration (m·s^{-2})	10.03	10.20	10.63	0.78	1.70
Peak Horizontal force (N)	964.18	1066.30	1102.50	335.68	158.92
Peak vertical force (N)	1402.20	1509.50	1552.40	685.74	156.01
Horizontal impulse (Ns)	104.97	101.11	98.27	-56.24	20.52
Vertical Impulse (Ns)	182.91	168.07	159.59	-28.02	23.22

[*] From equivalent 'normal' starts

Figures 4.35a-f reveal that the simulations with increased activation all adopted ankle first strategies which is concurrent with the drop in horizontal velocity and contact time but increase in vertical velocity when compared to the original simulations. All three simulations achieved complete extension at the knee and ankle but used comparatively small ranges of movement at the hip. FastSim is again the fastest of the three simulations and this appears to be due to greater contact time and angular velocity and the ankle towards takeoff. FastSim also used the greatest level of activation at the knee throughout the simulation. Indeed patterns of activation were similar for all three simulations (Figures 4.35g-i). Each started with almost the minimum hip extension allowed with constant high knee and ankle activation throughout. The main difference to any of the activation profiles is that SlowSim

used higher activation at the ankle compared to the knee whereas FastSim and 100Sim used higher knee activations.
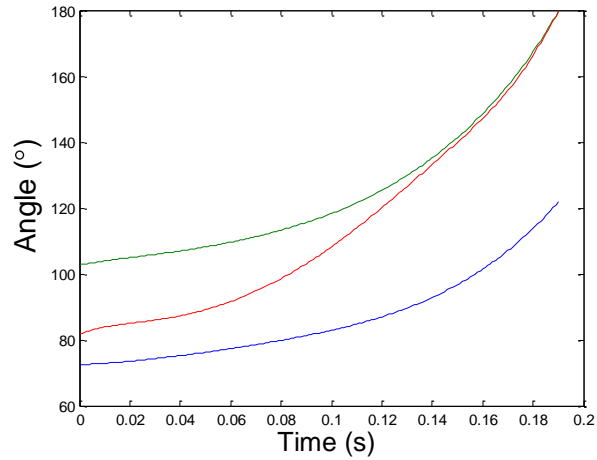
Figure 4.35a. Joint angles during FastSim with increased activation.
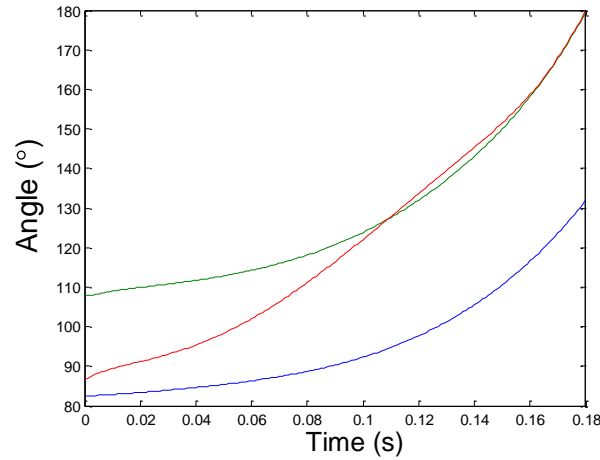
Figure 4.35b. Joint angles during 100Sim with increased activation.
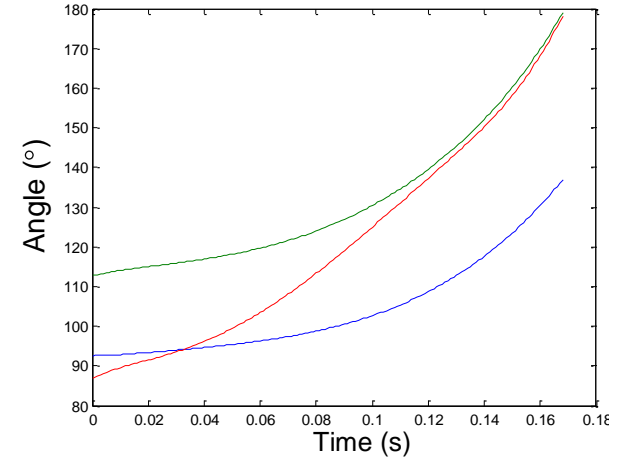
Figure 4.35c. Joint angles during SlowSim with increased activation.
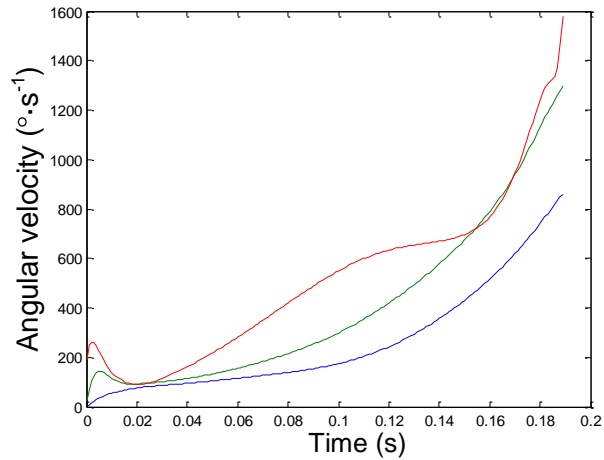
Figure 4.35d. Joint angular velocity during FastSim with increased activation.
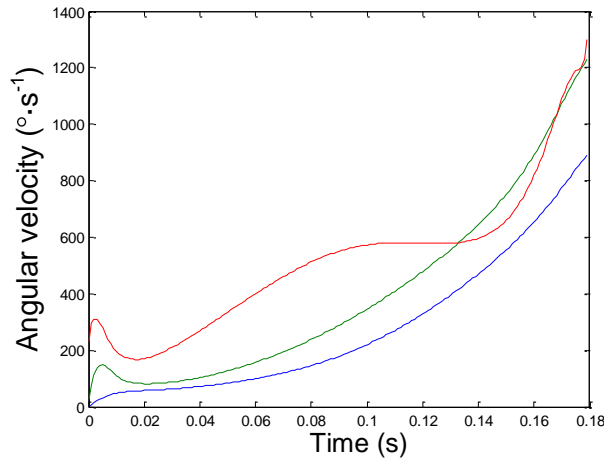
Figure 4.35e. Joint angular velocity during 100Sim with increased activation.
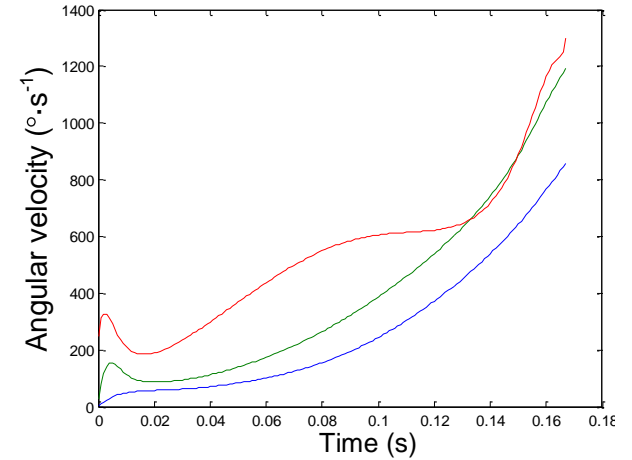
Figure 4.35f. Joint angular velocities during SlowSim with increased activation.
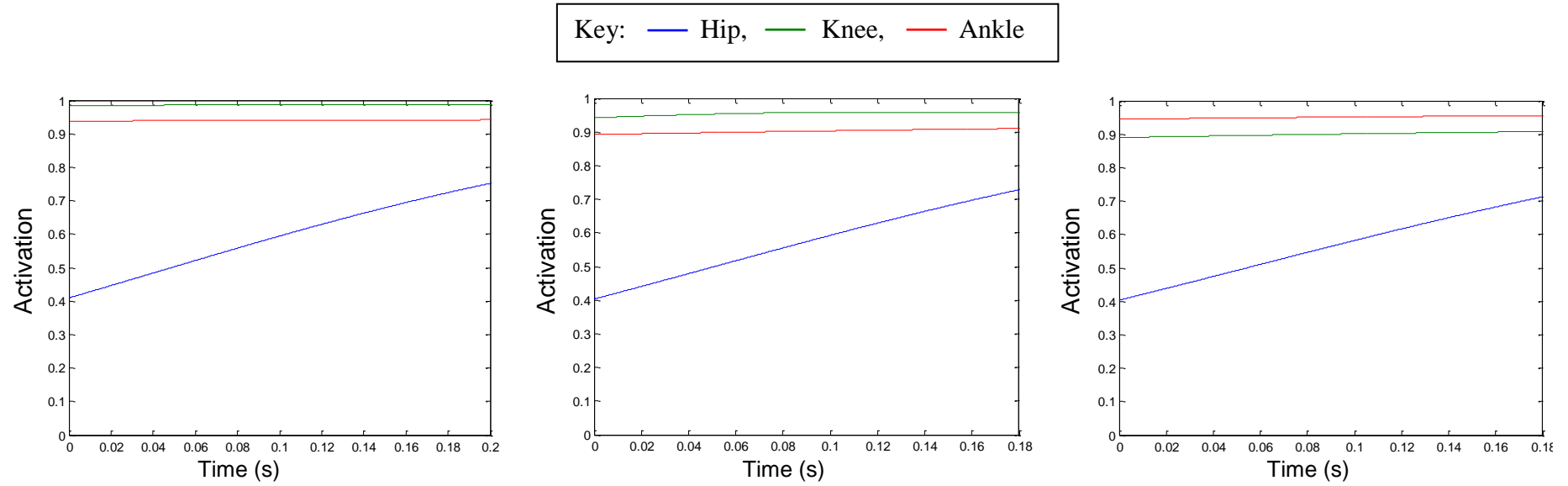
Figure 4.35g. Joint activations during FastSim with increased activation.

Figure 4.35h. Joint activations during 100Sim with increased activation.

Figure 4.35i. Joint activations during SlowSim with increased activation.
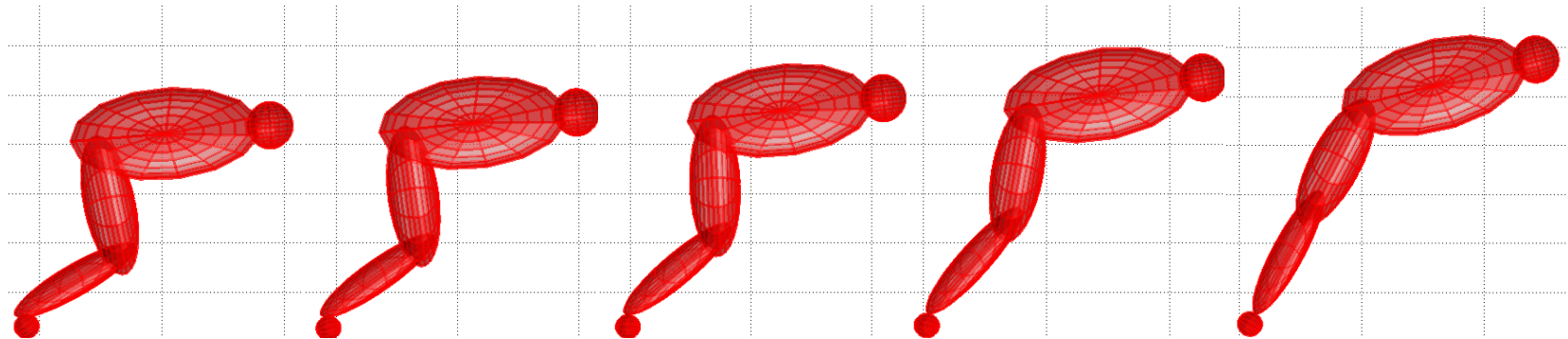
Figure 4.36. Four segment model (100Sim) with increased muscle activation.

4.3.4 Increased Strength

To investigate increases in strength, each joint was made 10% stronger (by multiplying t_{max} and t_0 by 1.1) and the same seven simulations were used for investigation as for investigations into increases in activation. These were: the five simulations which utilised equal changes in joint angles as well as FastSim and SlowSim.

Initially the same joint activation profiles as found for the normal simulations were used to drive the stronger simulations. Five of the seven simulations produced poorer starts than found initially, however, the two simulations which began in the most extended positions, SlowSim and the simulation with 10° added at each joint, were 0.33 and 0.12 $m·s^{-1}$ faster respectively. It is to be expected that the optimal control solution will change with changes in strength (Bobbert and van Soest, 1994) and therefore the seven simulations were re-optimised using the same bounds and score equation as previously employed.

Table 23 reveals that the increase in strength resulted in slightly slower horizontal velocity on takeoff for the three simulations presented but overall an average increase of 0.04 ± 0.12 $m·s^{-1}$ was seen for the seven simulations which were optimised. The largest increases were seen in the simulations which used -10° and +5° at each joint where there were increases of 0.18 and 0.24 $m·s^{-1}$ respectively. A greater average increase of 0.18 ± 0.14 $m·s^{-1}$ was seen for vertical velocity. Increases in velocity combined with a small average decrease in contact time also resulted in an average increase of 0.57 $m·s^{-2}$ in horizontal acceleration. Corresponding increases in vertical impulse as well as peak forces could also be seen.

Table 23. Start variables for starts with increased strength and comparison to the original starts.

	Simulations				
	FastSim	100Sim	Slow Sim	Mean difference[*]	S.D.
Hip Angle (°)	72.57	82.57	92.57	0	0
Knee Angle (°)	102.84	107.84	112.84	0	0
Ankle Angle (°)	81.77	86.77	86.77	0	0
Contact time (s)	0.31	0.25	0.25	-0.01	0.03
Distance (m)	1.36	1.28	1.23	0.09	0.06
CoM height on takeoff (m)	0.80	0.85	0.86	0.02	0.02
Horizontal velocity (m·s^{-1})	2.89	2.57	2.47	0.04	0.12
Vertical Velocity (m·s^{-1})	0.52	0.74	0.71	0.18	0.14
Horizontal Acceleration (m·s^{-2})	9.35	10.03	10.35	0.57	0.29
Peak Horizontal force (N)	778.74	709.17	768.84	34.59	32.76
Peak vertical force (N)	777.11	908.43	924.04	51.42	83.56
Horizontal impulse (Ns)	159.15	141.66	136.00	2.37	4.25
Vertical Impulse (Ns)	191.13	178.99	167.67	2.7	10.87

[*] From equivalent 'normal' starts

Figures 4.37a-i display the joint angle, angular velocity and activation time histories. As for the original simulations, joint movement patterns followed a proximal to distal sequence with the hip extending to almost 180° on takeoff. Joint angular velocity profiles also follow similar patterns.
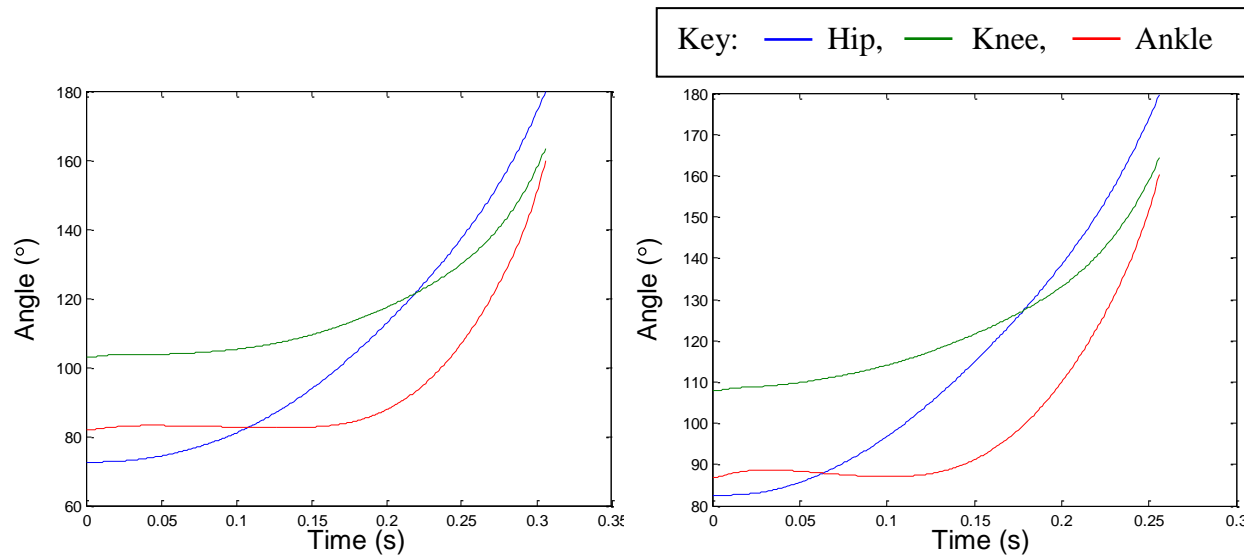
Figure 4.37a. Joint angles during FastSim with increased strength.
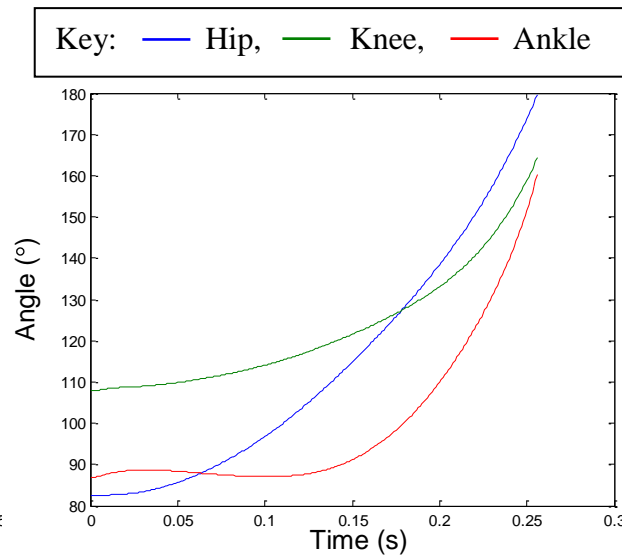
Figure 4.37b. Joint angles during 100Sim with increased strength.
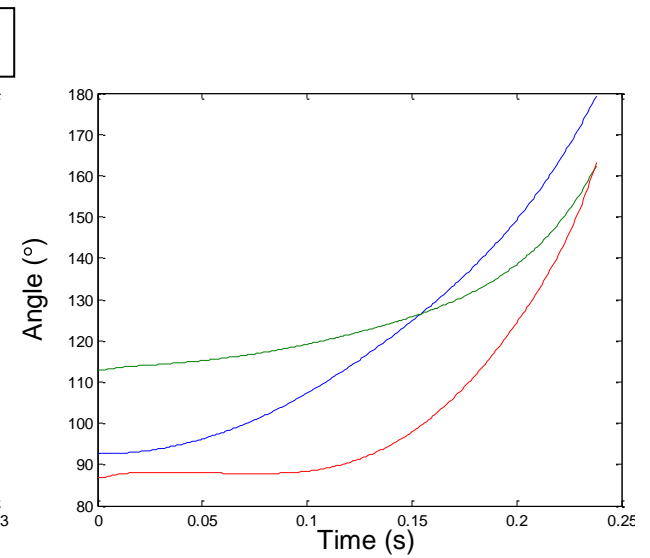
Figure 4.37c. Joint angles during SlowSim with increased strength.
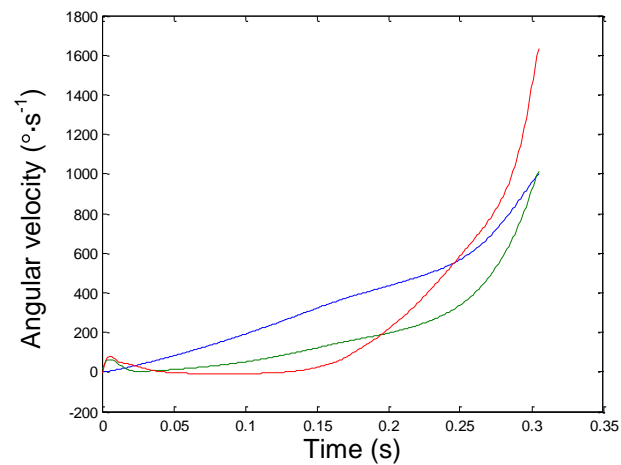
Figure 4.37d. Joint angular velocity during FastSim with increased strength.
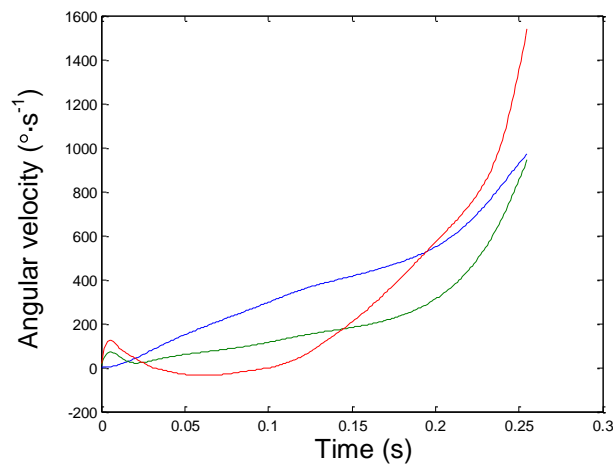
Figure 4.37e. Joint angular velocity during 100Sim with increased strength.
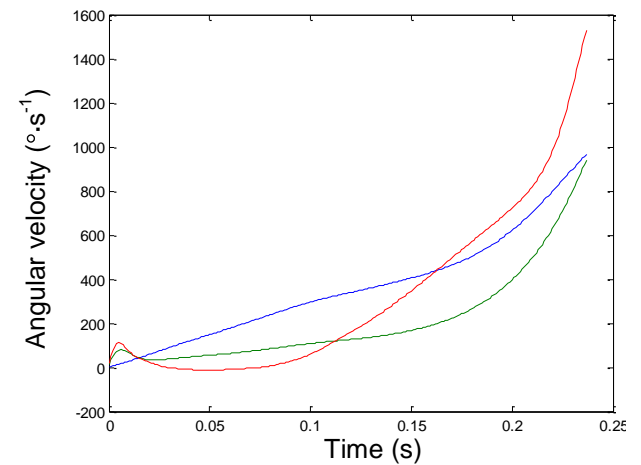
Figure 4.37f. Joint angular velocities during SlowSim with increased strength.

128
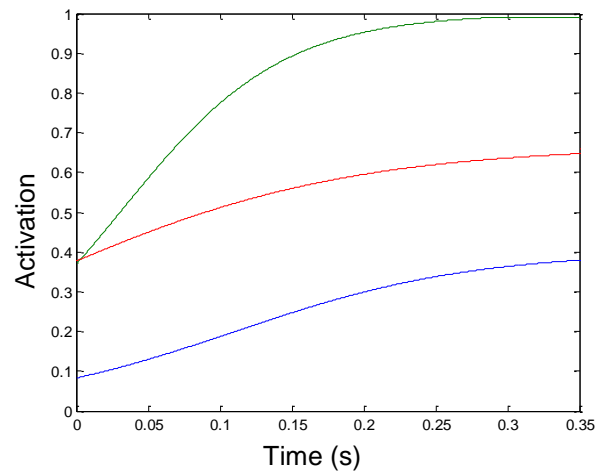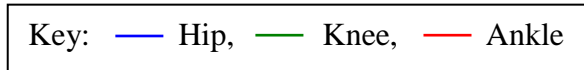
Figure 4.37g. Joint activations during FastSim with increased strength.
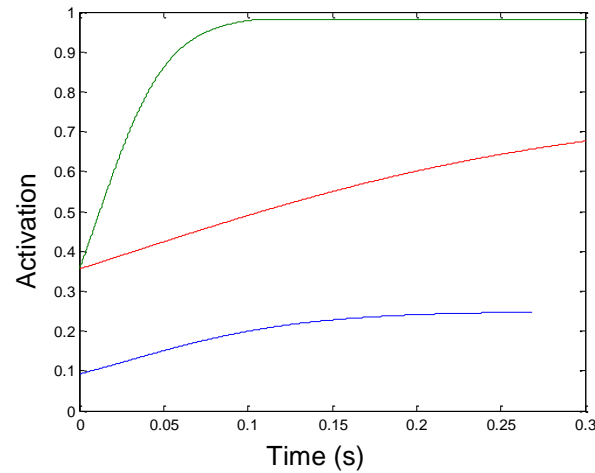
Figure 4.37h. Joint activations during 100Sim with increased strength.
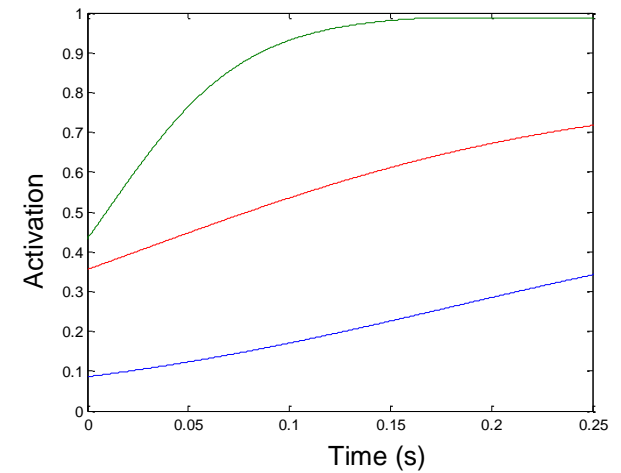
Figure 4.37i. Joint activations during SlowSim with increased strength.
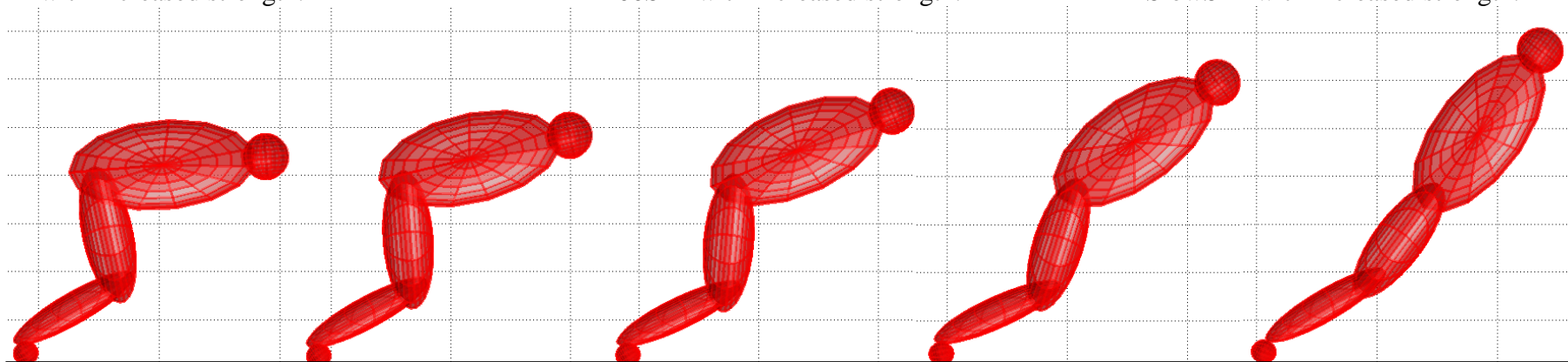
Figure 4.38. Four segment model (100Sim) with increased strength.

4.4 Discussion

The aim of this part of the study was to study the sprint start using simple computer simulation models generated in Matlab and Simulink. A four segment model was successfully generated and it revealed various limitations for athletes performing a sprint start. These came under the categories of joint constraints, strength constraints, body orientation constraints and control constraints. Horizontal velocity on takeoff was used as the criteria to optimise the simulations although it was acknowledged that the criteria used will influence results.

The number of segments included in a model of the start influenced the model's closeness to reality. The need for a foot segment was realised early on as without a foot, simulations appeared to lack coordination. Whilst takeoff will always occur once sufficient vertical velocity has been achieved, the lack of a foot segment made maintaining ground contact difficult during the push off. Similar issues have not been noted in models of vertical jumping but Gittoes and Kerwin (2006) observed that exclusion of the foot segment may lead to excessive ground reaction forces. Without plantar flexion at the ankle, the ability to produce force over a time is also reduced and concurrently impulse is diminished. As the use of a two part foot was also shown to improve the match of the model to a measured performance, these features seem important for inclusion in more sophisticated models of the sprint start.

Results from the four segment angle driven model showed that an increased RoM increased horizontal velocity on takeoff. This suggests that the athlete would benefit from using a more bunched starting position. Similar results have also been found in jumping research, also using a four segment model (Domire and Challis, 2007). Domire and Challis (2007) showed that a deeper squat led to a 7 cm increase in jump height and 44 % increase in movement time with optimum squat angles of 90° at the hip and 105° at the knee. This compares to joint angles of 92° and 109° measured for the subject in this study so it may be that the subject is already close to an optimum configuration. However, the best position for the sprint start was more flexed than this (Limited start = 84° and 106°, Optimum start = 70° and 102°) and it may be

130

considered that this is more achievable here than for jumping due to the athlete not pushing directly against gravity.

It was noted that the angle driven model simulated many performances that would not be possible for a real athlete to attempt. It was therefore essential to examine simulations in order to assess the likelihood of the performance being achievable by athletes. The overriding limitation in the angle driven model was RoM which was reached in extension, particularly at the knee. In a highly flexed 'set' position, it is the subject's ability to generate large forces quickly, rather than flexibility itself, which limits performance. This was particularly apparent at the ankle where the rate of the decline in maximum isometric torque from the optimum angle was much greater than at the hip or knee. The starting angles for the Limited start were 84° at the hip and 106° at the knee, where joint torques were 1.2 – 1.5 times joint torques in the matched trial. It is therefore likely that the athlete would need to improve their strength in order to achieve this situation. Interestingly Domire and Challis (2007) found experimentally that subjects noted the greater effort required to start from a more flexed position and the results from their model were not repeated. Furthermore, a model by Selbie and Caldwell (1996) found jump height to be insensitive to starting position.

When the four segment model was torque driven, it was the angle at the knee and hip rather than the ankle which appeared to have the greatest effect on the start. An approximate optimum angle at the knee was the found during 100Sim and performance dropped with angle changes away from this. The same might be seen at the hip as the results presented may have found only the falling limb of an otherwise larger relationship. Indeed, the ideal situation would be to have examined many more angle combinations over larger movement ranges however, the time taken for this would have been great. It was interesting that the initial angle at the ankle seemed to have relatively little influence on the start. This is particularly so considering that the model seemed to struggle to stop the ankle collapsing even after the joint torque profile had been increased.

Mero and Komi (1990) state "in the sprint it is clear that after the gun signal every leg extensor muscle must contribute maximally to the production of force and finally to the running velocity. Therefore the faster the electrical activity begins in every muscle, the faster the neuromuscular performance is maximised". Despite the need for large and fast muscle activations, the model did not work using 'bang-bang' activation profiles as the knee hyper-extended and the ankle collapsed. This suggested that not all leg extensor muscles act maximally during the start and/or that the role of bi-articular muscles (which were not represented), is key to sprint start performance.

Even when a greater level of control was implemented in the model, peak angular velocities for all trials were reached on takeoff and still appeared to be increasing. This is unrealistic for sprint starts and even for vertical jumping where there is no urgency to begin flexion. Bobbert and Van Ingen Schenau (1988) observed that peak knee velocity in the vertical jump occurred 30 ms before peak extension was reached and considered that bi-articular muscles are likely to aid in this slowing whilst also allowing high levels of activation in the extensor muscles around peak extension. Furthermore, van Ingen Schenau et al. (1987) noted that, near full knee extension, the bi-articular Gastrocnemius not only prevents the knee hyper-extending but also allows continuation of knee extensor activation to aid planar flexion. Interestingly, in the four segment models of jumping mentioned above, Domire and Challis (2007) included the action of the Gastrocnemius whereas Selbie and Caldwell (1996) did not. This may go some way to explaining their differences in findings.

The evidence presented suggests that the start is influenced by initial joint configurations, however, it was surprising that to control the model and obtain the fastest starts, neither the hip or ankle were maximally active at any point. This suggests several possible occurrences; firstly that the control needed for the sprint start is more complex than represented here, secondly that the knee was not strong enough to cope with maximum torques at the hip and ankle, or finally that limitations caused by segments not represented in the model have affected the findings. Each possibility has merit as inclusion of the rear leg is likely to aid knee extension in the early part of the movement due to earlier high peak forces furthermore, modelling individual muscles would include bi-articular muscle actions. Just as ankle extension

would usually be aided by the bi-articular Gastrocnemius, knee extension is aided by the bi-articular action of Rectus Femoris. As this lack of bi-articular action is least likely to effect the hip, this is likely to account for the hip being uninhibited by decreases in joint angle and need to use apparently little activation. In a real start, bi-articular muscles transfer energy from the hip down the lower limb which would therefore require greater activations to maintain performance.

Forcing an increase in the levels of muscle pre-activation when in the set position did not help to improve velocity out of the starting block but it did improve acceleration. Given the discussion so far around this, it seems likely improved model complexity and control would increase this difference. Examining the effects of increased activation without including the arms may also be an over simplification. When the use of the arms is included, negative forces exerted at the hands must counter the increases from the legs. Unless this force is removed quickly, the net effect produces little gain (Guitérrez-Dávila et al., 2006). Experimental results have shown that in order to exert added force when in the set position, athletes tend to position their CoM further back from the start line and the end result is a little different from a 'normal' start (Guitérrez-Dávila et al., 2006). The subjects in Guitérrez-Dávila et al's study had personal best 100 m times 11.09 ± 0.3 s and did not practice a pre-activated start prior to the day of testing. It would therefore be of interest to observe data for elite athletes and/or athletes who had practised this start over a prolonged period.

Neuro-muscular activity is also likely to affect the success of pre-activation in the sprint start and particularly where little training in this new position has occurred. Pain and Hibbs (2007) observed 40% longer pre-motor times in starts were pre-activation was increased. They considered that this was due to interactions regarding reduced postural stability and reaction time (De Wolf et al., 1998 cited in Pain and Hibbs, 2007). The need for prolonged specific training in order to utilise a pre-activated and/or more bunched start is further supported by rate of force development (RFD) research showing that voluntary contraction increases result in increased RFD (Andersen and Aagaard, 2006) and also increased muscle activation increases rate of torque development (De Ruitter et al., 2007).

Previous studies have suggested that increasing muscle tension in the set position may improve starting performance (e.g. Pain and Hibbs, 2007). Pain and Hibbs (2007) took the view that that this was due to increased muscular-tendinous stiffness and so decreased EMD. Similarly Mero et al. (2006) noted that an increase in muscle length, brought about by a reduction in block angle allowed a higher block velocity through greater joint moment and power (particularly at the ankle). However, they also noted that a greater block angle resulted in a shorted contact time and so, to some extent negated this increase and no difference was visible at 20m. This experimental data further shows that much training may be needed to utilise concepts found through simulation modelling.

Increasing strength slightly improved horizontal takeoff velocity but it was surprising that this was not the case for all simulations. The reasons why an increase in velocity was not seen may again be one of model control, model complexity or local minima in the optimisation surface. Local minima may provide much of the answer given that two simulations were faster before re-optimisation but not after. Optimisation effects aside, the hip was again barely active throughout the beginning of the starts and this may have been the maximum activation it could produce before the knee or ankle began to collapse. However, as the ankle was not maximally active it may suggest that knee strength is a limiting factor especially as an optimum angle was seen in relation to velocity and impulse. Furthermore, knee strength but not ankle strength has been shown to correlate with 40 m sprint performance (Nesser et al., 1996).

Studies into jumping have found increases in strength to result in increased jump height (e.g. Bobbet and van Soest, 1994). Bobbert and van Soest (1994) found a 0.039 m increase in jump height following a 10 % increase in strength which compares to a 0.09 m increase in horizontal displacement in this study. For jumping, a higher velocity on takeoff means a higher jump but for the sprint start this isn't necessarily the optimum solution. Simulations with increases in strength all achieved greater acceleration, so despite not necessarily achieving as high velocity on takeoff they spent proportionately less time in the starting block. This leads to the question of what should the athlete aim to do in the starting blocks, obtain a high average acceleration throughout the push-off or a high velocity on takeoff? Bezodis et al. (2007 & 2010) examined the starts of an athlete to 30 m in order to answer this

question. They suggested that the use of horizontal velocity on takeoff or horizontal impulse could be misleading due to the possibility of increases occurring through increased block time (spending longer in the starting blocks doesn't directly help the sprinter finish in the fastest possible time). Their opinion was one that power provides the best indicator as this comprises all of displacement, velocity and time. The question would perhaps best be answered theoretically by simulating the start with both legs and further into the race.

4.4.1 Limitations

Where models of jumping have been shown to be useful using just three or four segments, the equivalent assumptions are somewhat greater for the sprint start. This is due to the sprint start representing the beginning of the overall activity whereas a model of jumping represents the end or all of the activity. With this in mind, the end position must be considered in order to ensure that the athlete is able to continue in the race. Knowledge of the role of the rear leg must therefore be considered, particularly as the best starts used a low or negative vertical velocity on takeoff. In these starts it seems likely that the rear leg will touch down early to prevent that athlete falling. Indeed, the current fastest sprinters in the world can be seen to drag the rear foot on the ground during the first step from the blocks meaning that there is no flight phase.

The level of coordination represented must also be considered. The angle driven model assumed that joint angles could be scaled and the resulting start would maintain relative coordination. In the graphs it can be seen that a number of peculiarities occurred as coordination lessened towards the extremes of the movement ranges examined. For example, this combined with the spring model meant that large ankle extension resulted in a back flip. This also shows a limitation of any angle driven model as the joint torque required to perform this was unfeasibly large and so not replicable by human performers.   Further, the torque model suggests that the hip, knee and ankle don't all work maximally throughout the movement and that a greater level of coordination is present.

The spine was modelled as a single rigid segment. Bobbert and van Soest (1994) noted that extension in the spine during jumping contributes to the work done and consequently the height jumped. The same is therefore likely during the sprint start and inclusion of a multi segment spine in more complex models of the start will help to further examine such contributions.

4.4.2 Conclusions

The sprint start is influenced by initial joint configurations particularly at the hip and knee. Initial positions which have small joint angles will increase velocity on takeoff providing that sufficient strength exists at the relevant joints to cope with the reduced angle. This shows that the optimum start for individual athletes is likely to be different based on their joint torque/ angle/ angular velocity profile. Increasing strength and initial muscle activations at each joint allowed for greater acceleration in the torque driven model however, small increases in velocity were only seen in some simulations with increased strength.

The graphs produced which compared simulations suggested many relationships and interactions, whilst these may hold true for overall relationships, the simplistic nature of the model may not fully reflect events in reality. The ability of the four segment models to replicate the sprint start was limited due to the number of segments involved as the arms, spine and other leg all play an important part in the start. Furthermore it has been argued that a greater level of complexity in the control of sprint start models is needed to replicate real performances. Models of the sprint start in the next section will address these issues in order to further investigate the sprint start.

Chapter 5

Fourteen Segment Computer Simulation Models

This chapter presents fourteen segment angle driven and fourteen segment torque driven computer simulation models for use in investigating the sprint start. A fourteen segment model was chosen based on data in Section 4.1 which suggested that fourteen segments and non-linear springs for ground contact would provide the most realistic results. The angle driven model was created in order to calculate spring parameters which could then be used in the torque driven model. The torque driven model was used to simulate the push off phase of the start, and then to investigate the effects of using a more bunched starting position.

5.1 Angle Driven Model

The model comprised a head and trunk, pelvis and lower spine, two upper arms, two forearms and hands, two thighs, two shanks, two feet and two toe segments. Data processing and computer simulation were conducted using MatLab and Simulink with SimMechanics, and the model represented one start (trial) performed during data collection 1. Raw force and kinematic data were synchronised and the marker data were filtered using a Butterworth low pass filter at 14 Hz based on visual inspection of acceleration plots of various joints. Joint angles were entered into the simulation models based on segment angles which were output as part of the Anatomic model and using the subsystem shown in Appendix G.

Figure 5.1 shows the simulation model with all angles and translations specified.
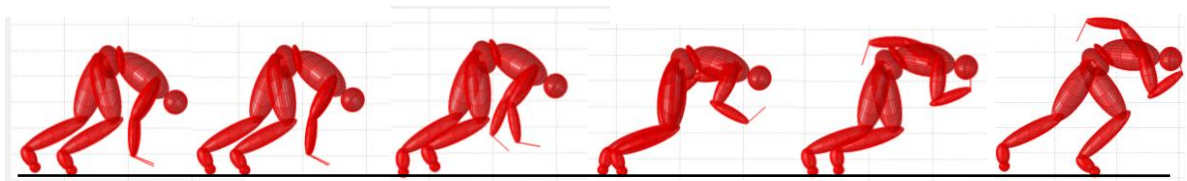
Figure 5.1. Fourteen segment model.

In order for the model to simulate ground reaction forces, horizontal and vertical spring dampers were inserted at each foot and hand. A diagram of the model is shown in Figure 5.2 and the Simulink block model can be found in Appendix G In Figure 5.1, it can be seen that the hands appear not touch the ground in the 'set' position and subsequently the reason for this was investigated.

Key

—— Rigid body

● Pin joint

Angle driver

Spring damper

Rotational spring damper
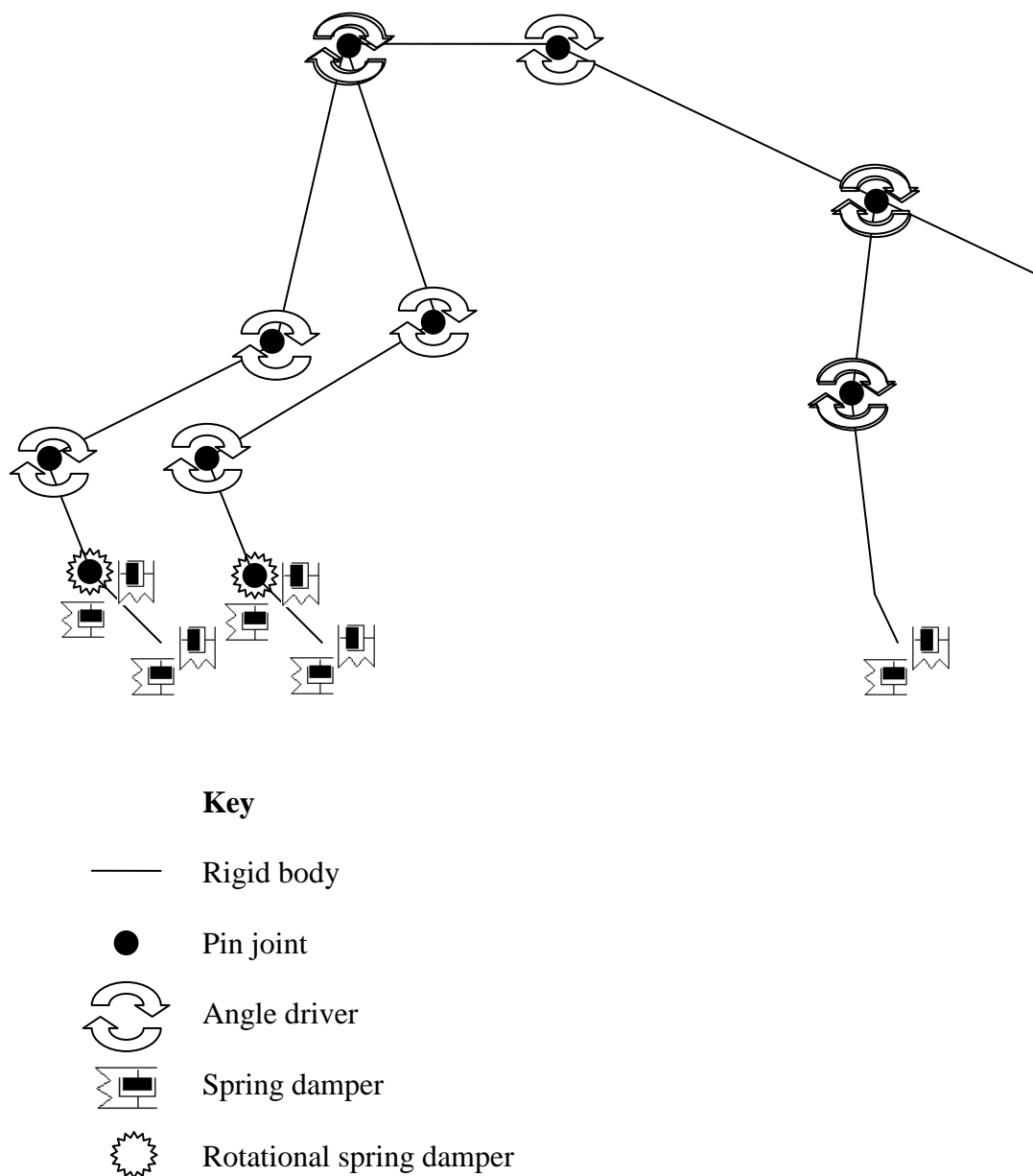
Figure 5.2. Fourteen segment angle driven model of the sprint start. Note that the left arm is hidden by the right.

5.1.1 Upper Limb Modelling and Hand Springs

The reason for the hands not meeting the ground in the 'set' position was found to be due to the calculation of the shoulder position and also hand orientation. The difference in hand-floor height was partially due to 'rounding' of the shoulders whilst in the 'set' position. Anatomic calculated trunk orientation based on the C1, clavicle and sternum markers, not the shoulder. This meant that the shoulder joint centre in the model started the simulation nearly 5 cm vertically above the joint centre calculated originally using Anatomic. Figure 5.3 demonstrates that this could be corrected in the 'set' position using a constant offset, but it can be seen that as soon as that athlete began to move, the shoulder moved dorsally and the original version was then a closer match.
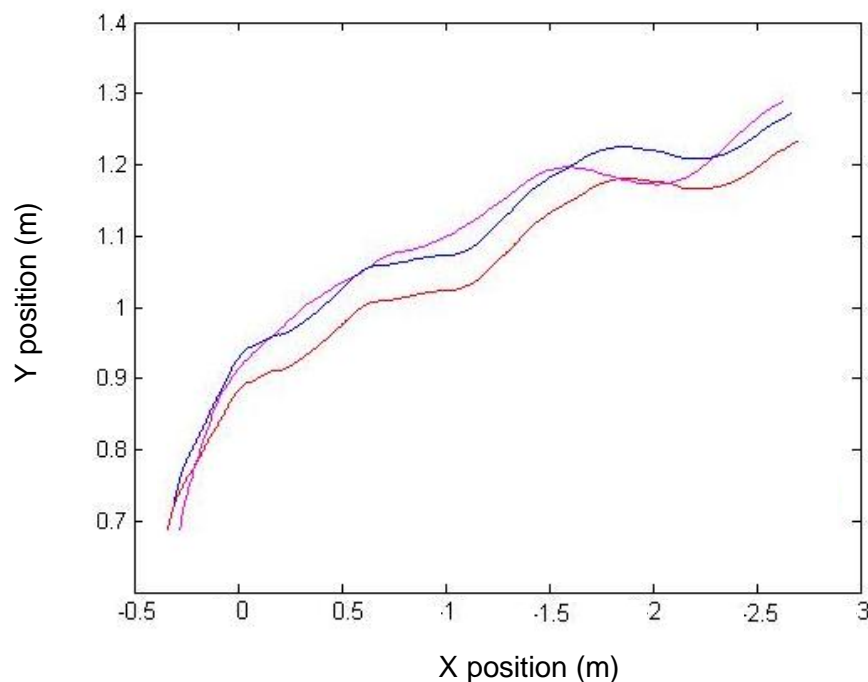
Figure 5.3. Shoulder offsets. Pink = shoulder joint centre from Vicon, blue = shoulder joint centre from model, red = shoulder joint centre with constant offset. Note, 0 in the X direction is the start line.

It was therefore decided that anterior-posterior translational movement of the shoulders would not be accounted for and instead a different floor height was stated for the hands. Modelling the shoulder with a more complex joint that allowed translation would help to account for this and so further consideration may be given in future projects.

Hand and finger locations were also adjusted to place them in a more realistic orientation. Based on the static trial, the locations of the finger and knuckle joint centres were moved to be the middle of the finger and knuckle rather than the marker position. This was accomplished by calculating the midpoint of the finger tip and knuckles using calculations for stadium sections used with measurements taken for use in Yeadon's inertia model (1990b). Here the perimeters and widths were both measured for input into the model. Figure 5.4 below shows how the width of the segment can be calculated as:

$$w = 2t + 2r \qquad\qquad\qquad\qquad (5.1)$$

and the perimeter can be calculated as:

$$p = 4t + 2\pi r \qquad\qquad\qquad\qquad (5.2)$$

Figure 5.4. A stadium section (Yeadon, 1990b).

This meant the distance r is the distance to the mid point of the cross section which was taken as the knuckle and finger tip centres. The radius r could be calculated using $p - 2w$ to remove t from the equation:

$$p - 2w = \left(\!-4t + 2\pi r\right) - \left(\!-4t + 4r\right)$$
$$p - 2w = 2\pi r - 4r$$
$$\frac{p - 2w}{2\pi - 4} = r$$

Using the coordinate system of the hand, Figure 5.5 shows how the distance $r + r_m$ could be used to move the coordinate for the finger tip and knuckle from the marker centres to the relevant anatomic centre.

Marker Centre r_m

r

Finger Centre

Marker Centre r_m

r

Finger Centre
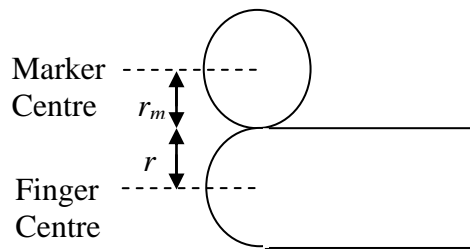
r_m = Marker radius (7mm)

Figure 5.5a. Side view of finger coordinate adjustment.
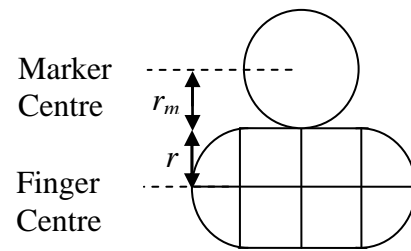
Figure 5.5b. End view of finger coordinate adjustment

Wrist angles were also adjusted so that they came closer in the horizontal direction to the start line. The angle of the hand to the wrist was calculated whilst the sprinter was in the 'set' position. This was input in to the model as a constant angle throughout the simulation.

Horizontal and vertical linear spring dampers were implemented at the fingertips using the non-linear springs described previously in Section 4.1. Both the horizontal and vertical springs released as soon as the vertical spring length became zero. Optimisation bounds for stiffness and damping were allowed to be large and maximum initial spring lengths of 1.8 cm were to allow for compression of the finger pads, floor and hyperextension at the finger tips.

5.1.2 Foot Modelling and Springs

Rotational spring dampers based on the linear spring formulae were inserted at the MPJs. Initial bounds for these were based on Oleson et al. (2005) who found a value of approximately 1.8 Nm/deg during barefoot running (4 m·s^{-1}) and 0.2- 0.6 Nm/deg for a male's training shoe. This was noted to be extremely time dependent and represented maximum values. Interestingly Stefanyshyn and Nigg (2000) noted stiffness in very stiff shoes to be 0.38 Nm/deg. Damping was set to be critical damping based on the mass of the forefoot. Initial testing of the model suggested that these values may be too low with excessive movement occurring at the MPJ. Consequently the maximum bound was increased to 50 Nm/deg but penalties were also added should the sum of the starting block reaction forces at the toe be greater than at the MPJ or less than 1/3 that of the MPJ.

5.1.3 Matching Optimisation

Spring parameters were found through optimisation using a Simulated Annealing (Corana et al., 1987) algorithm in Matlab (code written for MatLab by van Soest, 1999). Bounds for the initial spring lengths were set using the initial position and initial position minus 0.025 m based on the distance from the calculated joint centre to the rubber face of the starting block. Bounds for stiffness and damping were set and allowed to be large due lack of existing data but based on initial experimentation with the model. In order to help the simulation match measured forces, penalties were included which are summarised in Figure 5.6

```
                        ┌──────────────┐
                        │    SCORE     │
                        └──────┬───────┘
          ┌────────────────────┼────────────────────┐
     ┌────┴────┐          ┌─────┴─────┐         ┌────┴────┐
     │   CoM   │          │   Hands   │         │  Feet   │
     └────┬────┘          └─────┬─────┘         └────┬────┘
```

RMS error calculated as percent of distance travelled * 5	Initial Y force less than 200N add 100 + (200- Yforce)	Initial X force less than 50N add 50 + (50 – Xforce) *3

RMS error of total resultant force expressed as % of maximum force	Toe force less than 1/3 or greater than MPJ GRF, add 250	Vibrations or zero force, add 5000	Initial forces 10% different to measured forces, add 2 * RMS error

Figure 5.6. Composition of 14 segment model score.

The resulting score was 15,926 and the forces for the front (left) foot were much more realistic than for the rear (right). To improve the match at the rear foot, various optimisations were run which focused solely on the rear foot spring parameters. These included using a linear spring and adjusting displacement in the stiffness part of the equation to one half power rather than squared but each were unsuccessful. It was therefore decided that, due to time limitations, the parameters for the front block would be used for the rear. This resulted in Figures 5.7a-f below and a score of 16,188 and improved results for the rear block.
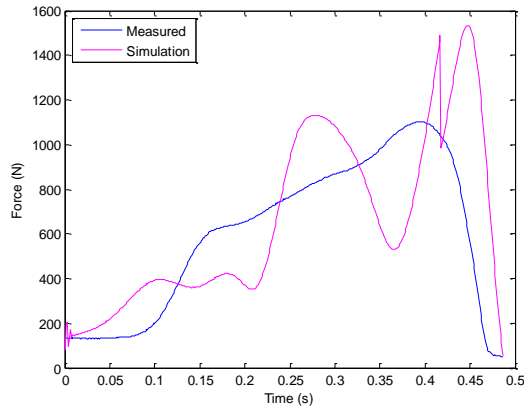
Figure 5.7a Left block resultant force
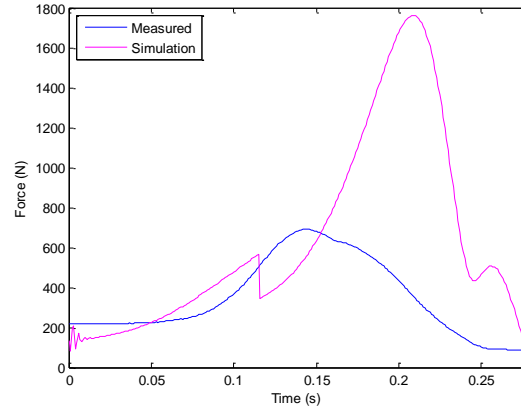
Figure 5.7b. Right block resultant force
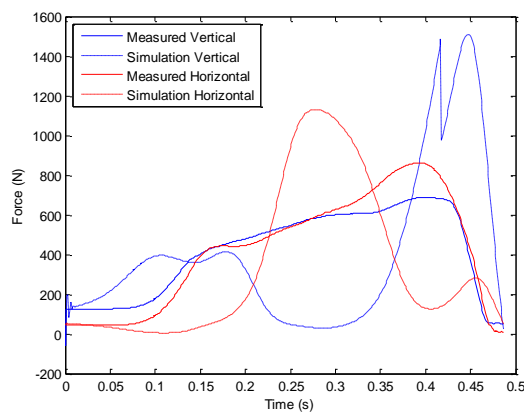
Figure 5.7c. Left block horizontal and
vertical forces
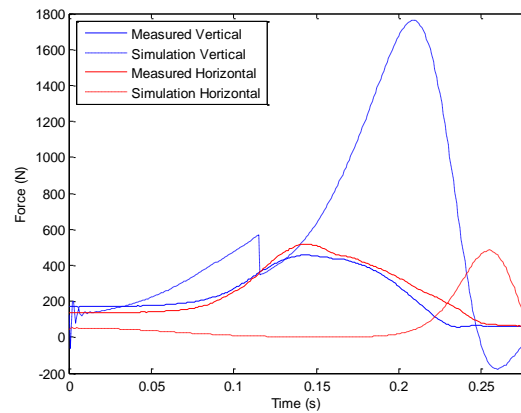
Figure 5.7d. Right block horizontal and
vertical forces
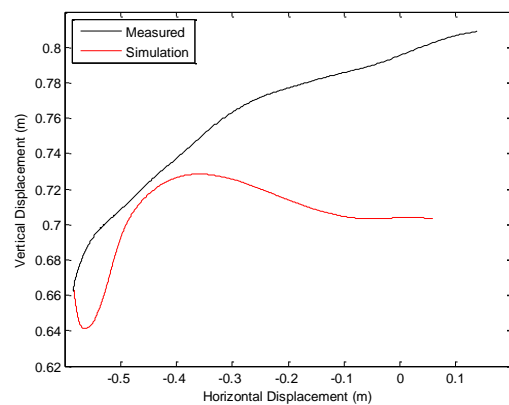
Figure 5.7e. CoM position
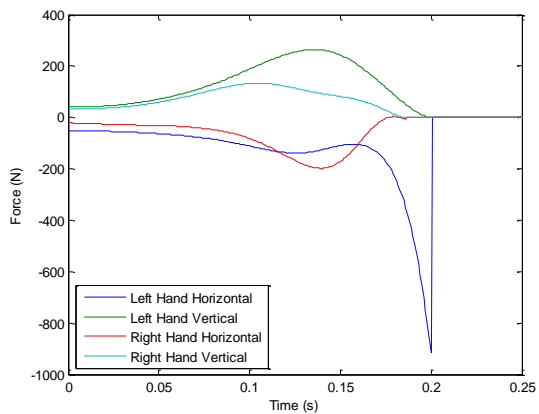
Figure 5.7f. Forces at the hands

Combined vertical forces at the hands peaked at 368.8 N which was approximately
45% body weight although initial forces were only 73.2 N. In Figure 5.7f it can be
seen that horizontal force at the left hand is extremely low (a negative force meant

that the arms were pushing backwards against the body). This is likely to be due to the large drop in CoM delaying takeoff at the hands.

The spring parameters selected for use in the model are presented in Table 24 along with the bounds which were used for optimisation.

Table 24. Spring optimisation bounds and results.

Spring Parameter	Lower Bound	Upper Bound	Result
Feet			
Horizontal			
Stiffness (Nm^{-2})	90000	200000	182100
Damping (Nsm^{-1})	0	5000	1025.5
Initial length (m)	0.01	0.03	0.0126
Vertical			
Stiffness (Nm^{-2})	50000	300000	89599
Damping (Nsm^{-1})	4000	100000	67587
Initial length (m)	0.01	0.03	0.0214
MPJ (rotational spring)			
Stiffness ($Nm \cdot °^{-1}$)	1	50	47.9403
Damping ($Ns°^{-1}$)	0	5	2.0940
MPJ zero (°)	135	180	177.5
Hands			
Horizontal			
Stiffness (Nm^{-2})	5000	150000	97599
Damping (Nsm^{-1})	0	5000	665.0225
Initial length (m)	0.01	0.03	0.0224
Vertical			
Stiffness (Nm^{-2})	5000	150000	150000
Damping (Nsm^{-1})	0	5000	150.0006
Initial length (m)	0.01	0.018	0.0165

5.2 Fourteen Segment Model with Sprung Spine

The final stage in the development of the angle driven model was to insert a rotational spring damper into the L1 joint in the spine. This was needed to drive the angle at the spine for the torque model as lack of torque data for the spine prevented it being torque driven.

Extension at the spine was modelled using a linear spring damper such as used at the MPJ's. Parameters for the spring were optimised using the same method as shown above. Stiffness bounds were set (based on trial optimisations) between 40 and 1000 N·° and maximum damping was set to critical damping. The natural angle at the joint was allowed to vary between 0° and 45° from straight, and the score was based on the RMS error in joint angle throughout the trial, final joint angle and angular velocity. This was to encourage the optimisation to find a solution which would allow the athlete to continue as use of the RMS error in joint angle alone resulted in a position of greater flexion than in the set position. Figure 5.8 compares the angle in the spine throughout the trial. Initially the match does not appear to be good but the RMS error based on joint angle was 3.2° and the spine steadily extended throughout the simulation. Furthermore, the apparently small changes in the joint angle measured experimentally may also be due to noise in the data.
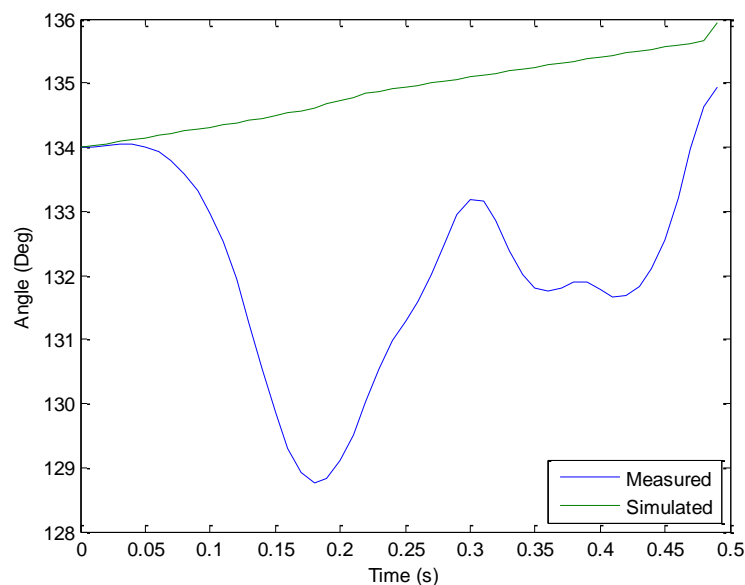
Figure 5.8. Comparison of measured and simulated spine angle using a linear spring damper.

5.3 Fourteen Segment Torque Driven Model

Sprinting is a maximum effort activity; maximal force, velocity and power of the lower limbs is significantly ($p \leq 0.05$) related to whole body acceleration in the 100 m sprint (Morin and Belli, 2002). Further, Meckel et al. (1995) showed 100m time in women to be positively related to maximum muscle strength (cited in Andersen and Aagaard, 2006). In order to investigate and for the simulation model to reflect the characteristics of muscles, all angle inputs were removed (other than those which described the initial joint and fixed joint configurations) and replaced with torque inputs (see Appendix G for Simulink subsystem). To help simplify the model, the elbow angle was fixed in its initial orientation relative to the upper arm. Further, the horizontal springs at the hands were removed due to problems when running the simulations. This was due to insufficient vertical movement in the upper body during push-off which in turn caused large forces at the finger tips and consequently the shoulder rapidly circumducted. Figure 5.9 depicts the structure of the torque driven model and the Simulink block diagram can be seen in Appendix G.

Key

——— Rigid body

● Pin joint

Torque driver

Spring damper

Rotational spring damper
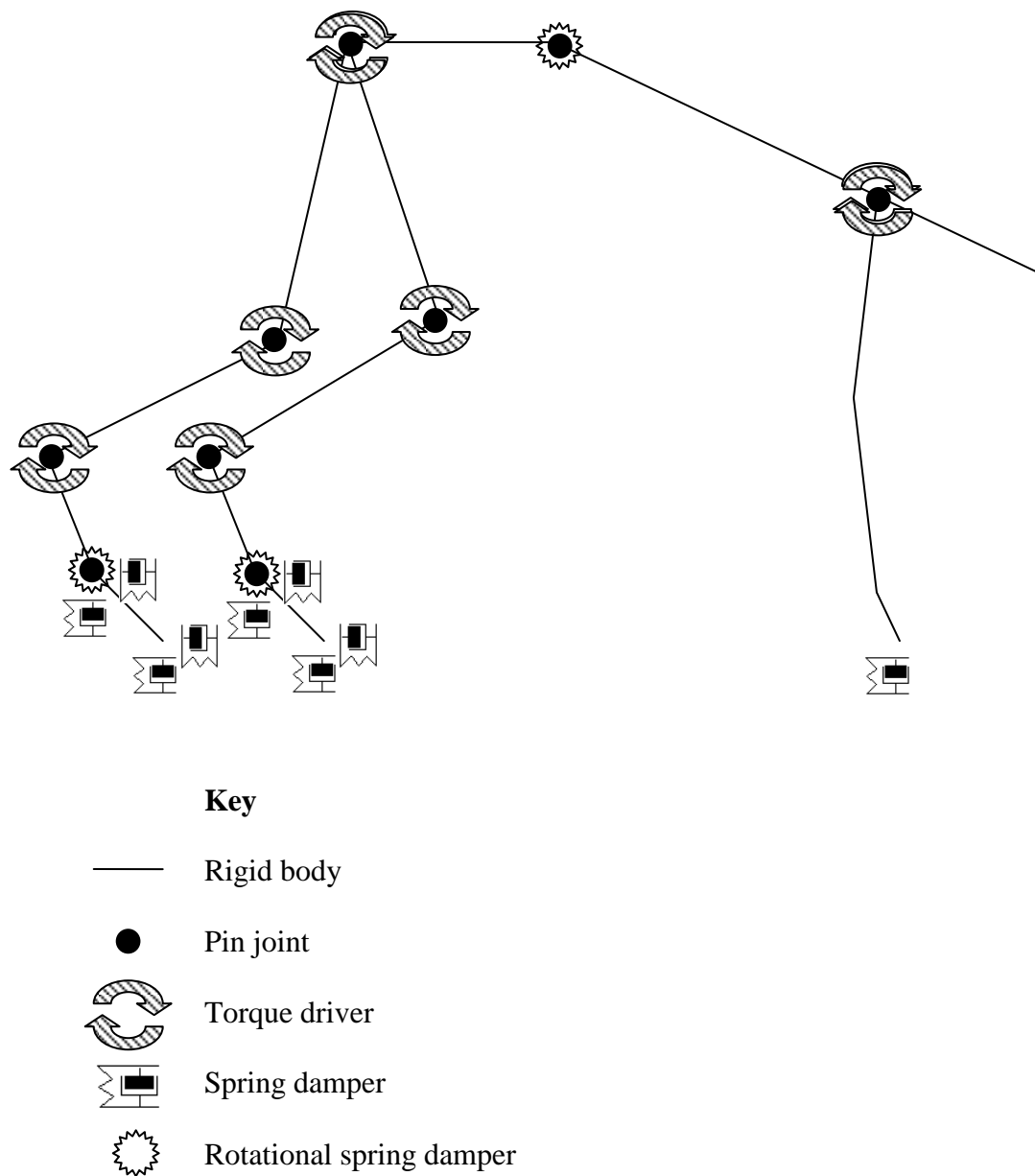
Figure 5.9. Fourteen segment torque driven model of the sprint start. Note that the left arm is hidden by the right.

The following sections consider characteristics of muscle and muscle activations. These characteristics were then combined with measured joint strength and muscle activation data in order to create the inputs to drive the new model.

5.3.1.1 Electromechanical Delay

Electromechanical delay (EMD) is the time taken by a muscle to exert measurable tension having been stimulated (Cavanagh and Komi, 1979). During this time several processes occur: "conduction of the action potential along the T-tubule system, release of calcium by the sarcoplasmic reticulum; cross-bridge formation between actin and myosin filaments, the subsequent tension development in the contractile component and stretching of the series elastic component" (Cavanagh and Komi, 1979). It is the final part of this process that is considered to take the most time (Vos et al. 1991). Here the tendon becomes taut and then stretched enough to transmit the force of contraction in order to move the limb and produce an external force (Winter and Brookes, 1991).

Varying amounts of time have been recorded for EMD; Cavanagh and Komi (1979) recorded average times of 49.4 ms for eccentric contractions, 53.9 ms for isometric contractions and 55.4 ms for concentric contractions. Vos et al. (1991) found values of 93-112 ms in quadriceps muscles and longer values were found when the percent of maximum voluntary contraction was lower. When reviewing research in the area, Komi (1984) found times recorded between 20-100 ms although Tillin et al. (2010) noted times as low as 6 ms. Whilst these differences may reflect differences in methodologies, it is clear that when examining explosive activities, EMD could make up a large portion of the EMG data recorded (Gourgoulis et al., 2003; Vos et al., 1990). For example, during sprint starts, Baumann (1976) recorded that it took 302 ms for the rear leg to leave the starting block.

It is thought that the time for EMD may also vary under different speeds of movement and with the involvement of the stretch shortening cycle (Cavanagh and Komi, 1979). Further, the greater compliance of tendons that may be seen in sprinters (Kubo et al., 2000) and the expected higher proportion of type II muscle fibres (e.g. Maughn et al., 1983; Gregor, 1979) should also be considered as this may reduce possible expected differences between populations. Therefore EMD should always relate to the individual muscle (or even individual where possible) but may make it more difficult to measure as part of an experiment (Mero and Komi, 1990).

5.3.1.2 Rate of Force Development

Rate of force development (RFD) describes how quickly force is produced at a muscle or joint and it may take humans up to 1.0 s to generate maximum isometric force (Komi, 1984). A number of factors are thought to influence this rate including neural factors and contractile properties of the muscle-tendon unit. Tillin et al. (2010) noted explosive power athletes to have a greater RFD due to the greater levels of muscle activation. Indeed, De Ruitter et al (2007) also observed a positive correlation between muscle activation and initial rate of torque development. Interestingly RFD increases with maximum voluntary contraction (Andersen and Aagaard, 2006) but short term strength training may cause an increase in fascicle length and hence decrease RFD (Blazevich et al., 2009). It also makes sense that RFD should be influenced by the tendon stiffness as it is through these that the load is transmitted. Indeed, Bojsen-Møller et al. (2005) noted a positive correlation between tendon stiffness and RFD.

5.3.1.3 Force Velocity Relation

Figure 5.10 demonstrates the relation between the rate of muscle shortening and the force which it is able to generate during concentric contraction.

Figure 5.10. Force-velocity relation (Nigg and Herzog, 1999)

Nigg and Herzog (1999) presented a version of the equation of Hill (1938). This equation is solved to find the force generated rather than the velocity.

$$F = (F_0 b - av)/(b + v) \tag{5.3}$$

Where:

F	=	Instantaneous force
F_0	=	Maximal force at zero velocity and optimal sarcomere length
v	=	velocity of shortening
a,b	=	constants with force and velocity, respectively.

If *v* is zero then this equation represents events under isometric conditions. However Edman (1979, cited in Nigg and Herzog, 1999) considered that the upper and lower range boundaries were poorly predicted by Hill's equation from results gained on experimental data. It was considered, at least in part, due to it being difficult for all cross-bridges to be attached simultaneously during isometric contractions and attaching and detaching with greater regularity during high velocity contractions.

The speed of muscle lengthening has received less attention in the literature. Figure 5.11 demonstrates how during eccentric contractions at high velocities, the muscle is still able to generate higher force than at low velocities. Differences in in-vivo and in-vitro measurements means eccentric values may be overestimated and therefore demonstrates the importance of testing subjects where possible (e.g. Yeadon et al., 2006; Westing et al., 1991; Dudley et al. 1990).

Figure 5.11. Force velocity relation during eccentric and concentric contraction (adapted from Zatsiorsky, 2000).

5.3.1.4 Force Length Relationship

Based on the cross bridge theory, first identified by Huxley (1957), it is the overlap of actin and myosin filaments that determines the maximum force a muscle can generate. It is generally assumed that each cross bridge is capable of generating the same amount of force and that they are evenly spaced. This means that the greater the overlap of actin and myosin filaments, the greater the force that can be generated (Nigg and Herzog, 1999). Figure 5.12 depicts the overall relationship of muscle fibre length and force.

Figure 5.12. Force-length relation for isometric measures of force at given lengths (derived from frog skeletal muscle) (Nigg and Herzog, 1999).

Hof (1984) expressed this relationship using:

$$F_c = f(x_c)F_0 \qquad\qquad (5.4)$$

Where:

$f(x_c) =$ is a parabola (Woittiez et al. 1983)

$F_0 =$ active state of the muscle. It is the maximum force that can be generated when the force length relation is at its optimum.

This therefore plays an important role in "the individual characteristics of leverage" (Donskoi, 1975; cited in Hoster and May, 1979) and along with moment arms means that an individual's optimal joint angles during the sprint start may be different. For the sprint start, improvements in performance have been seen with increases in gastrocnenius length created through the use of lower block angles (Mero et al., 2006; Guissard et al. 1992). Indeed, in Chapter 2. it was noted that all research to have examined block angles has seen the best starts from the lowest block angle tested.

Whilst the above is a brief and basic description of the behaviour of muscles, it should be appreciated that if measuring muscle strength curves, a number of factors will influence the results. Kulig et al. (1985) categorised these as population studied, psychological factors, physiologic factors (e.g. muscle fiber type, cross sectional area,

fatigue), geometric factors (e.g. range of motion, line of action), exercise conditions (e.g. type of contraction, speed of contraction, number of joints involved).

5.3.2 Combining Data

As noted in Section 3, two data collections were used in order to gain the joint angle and muscle activation data. This meant there was the need to find similar starts from the two data collections in order to drive the torque driven simulation model. Selected angles for trials from data collection two were compared to the trial selected for the angle driven model from data collection one. The results for the trial with the smallest RMS differences can be seen in Table 25, graphs maybe found in Appendix H.

Table 25. Comparison of joint angles for the starts used for kinematic and EMG data collection.

Joint	RMS difference (°)
Left Hip	7.58
Left Knee	7.61
Left Ankle	4.68
Left Shoulder	9.51
Right Hip	6.29
Right Knee	5.41
Right Ankle	4.76
Right Shoulder	7.37
Mean	6.65

5.4 Muscle Activation Profiles

Two different approaches were used to replicate the muscle activation profiles; a sigmoid function and a linear function. The method selected (Table 26) depended on the shape of the REMG curve. Curves that rose to a maximum level and then after a time fell back to a resting level were replicated using the sigmoid function. For profiles that were more complex (which often occurred during longer periods of activation) activation patterns were replicated using a linear function. Here the curve could rise and fall several times within a single period of activation. The two approaches were performed using methods described below.

Table 26. Identified muscle activation times.

Movement	Function used to created activation profile	
	Activation period 1	Activation period 2
Left hip extension	Sigmoid	Sigmoid
Right hip extension	Sigmoid	Sigmoid
Left hip flexion	Linear	Sigmoid
Right hip flexion	Linear	Sigmoid
Left knee extension	Sigmoid	Sigmoid
Right knee extension	Sigmoid	Sigmoid
Left knee flexion	Sigmoid	Sigmoid
Right knee flexion	Sigmoid	Sigmoid
Left ankle extension	Linear	Sigmoid
Right ankle extension	Sigmoid	Sigmoid
Left ankle flexion	Sigmoid	Sigmoid
Right ankle flexion	Linear	Sigmoid
Left shoulder flexion	Sigmoid	Sigmoid
Left shoulder extension	Sigmoid	Sigmoid
Right shoulder flexion	Sigmoid	Sigmoid
Right shoulder extension	Sigmoid	Sigmoid

5.4.1 Sigmoid Function

The sigmoid function was based on the Equation 5.5.

$$a = \frac{m}{1 + e^{-ts}}$$

(5.5)

Where:

a   = level of activation

m   = maximum level of activation possible (asymptote)

e   = 2.71828

t   = time

s   = steepness of the curve

To make the whole activation curve, two sigmoid functions were used, one for the upward slope and one for the downward slope. This approach allowed for a different upward and downward slopes such as shown in Figure 5.13 below.
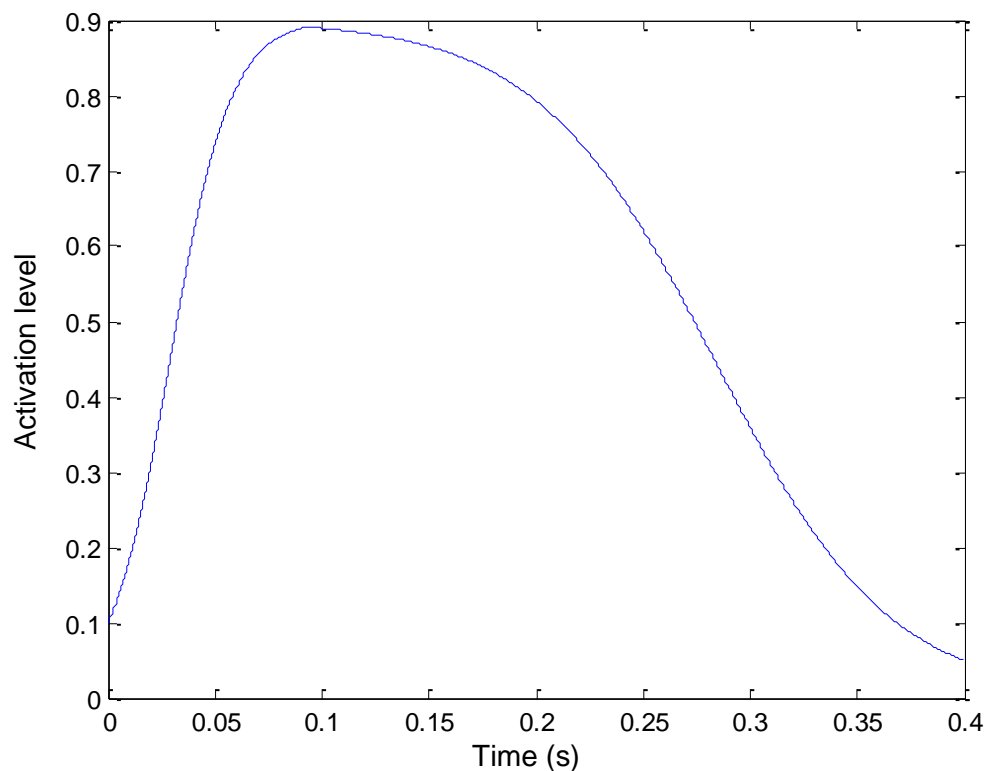
Figure 5.13. Sigmoid activation curve using different upward and downward slopes.

Seven parameters were needed to define the curve: start time, end time, initial level of activation, final level of activation, maximum level of activation, steepness of the curve and peak level of activation. Peak level of activation differed from maximum activation in that maximum activation was the asymptote of the curve whereas peak activation was the activation level set before the downward curve started. Figure 5.14 below displays the same curve but the blue line has a peak activation of 0.9 whereas the red line has a peak activation of 0.999.
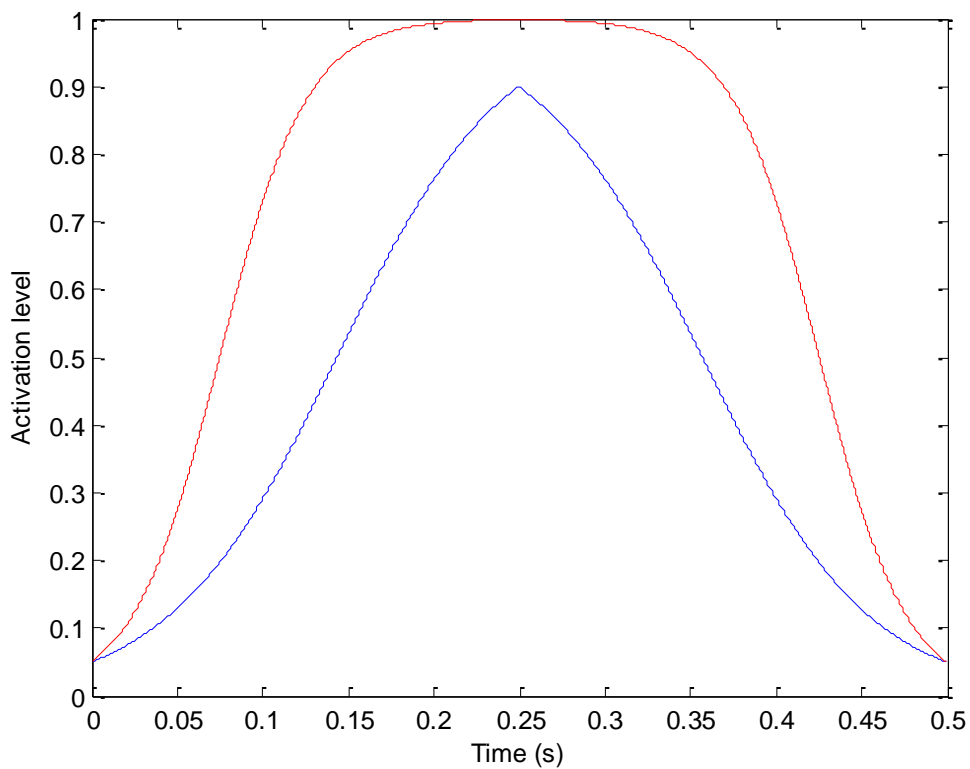
Figure 5.14. Sample activation curves. Blue line, peak activation = 0.9, red line, peak activation = 0.999.

Once the parameters were defined, a generic curve was created and locations of important times were found, these were time of; start (equation 5.6), peak activation for the upward curve (equation 5.7), peak activation for the downward curve (equation 5.8) and end activation (equation 5.9). To limit the maximum level of activation, equations were divided by one over the maximum level set. Time was then made the subject of the equation in order to identify specific activation levels such as the maximum and minimum:

$$t_{start} = -\log \frac{\left(-\left(\frac{-1+n}{n}\right)\right)}{\frac{\log e}{s_u}}$$ (5.6)

$$t_{peaku} = -\log \frac{\left(-\frac{(-1+p)}{p}\right)}{\frac{\log e}{s_u}} - t_{start}$$ (5.7)

$$t_{peakd} = -\log \frac{\left(-\frac{(-1+p)}{p}\right)}{\frac{\log e}{s_u}}$$ (5.8)

$$t_{start} = -\log \frac{\left(-\left(\frac{-1+n_e}{n_e}\right)\right)}{\frac{\log e}{s_d}}$$ (5.9)

Where:

t_{start} = sample corresponding to the defined start time and initial activation

t_{peaku} = sample corresponding to maximum activation on the upward curve

t_{start} = sample corresponding to maximum activation

t_{start} = sample corresponding to the defined end time and end activation

n   = initial activation divided by maximum activation

s   = steepness of slope

u   = upward slope

d   = downward slope

p   = peak activation

The upward and downward curves were then created using:

$$a_u = \cfrac{\cfrac{1}{1 + e^{\left(+t_{start}\right)s_u}}}{\cfrac{1}{m}} \qquad (5.10)$$

$$a_d = \cfrac{\cfrac{1}{1 + e^{\left(+t_{peak}+t_{peakd}\right)*s_u}}}{\cfrac{1}{m}} \qquad (5.11)$$

The two curves were then combined to provide one activation profile and plotted to fit the real time activation duration. To help save on parameters in the matching/ optimisation process, the ratio of the steepness for upward and downward slopes were used rather than optimising slopes separately.

To ensure that the curve did not ramp in an unrealistically steep manner, a limit of 0.07 s (multiplied by the maximum activation level) for the curve to reach 97 % of maximum activation was placed. Hatze (1981) allowed 89 ms for the ramp and Komi (1984) noted times of 50 ms for up to 40 % maximum contraction and 1000 ms for 100 %. This is therefore somewhat faster that quoted but it was noted that these times shorten with training such as might be seen in sprinters. The limit was checked using Equation 5.12 below and if the curve violated the limit, the steepness of the upward curve was reduced until the condition was met.

$$a_{check} = \cfrac{-\log\cfrac{\left(\left(1+r\right)\right)}{r}}{\cfrac{\log e}{s_u}} - t_{start} \qquad (5.12)$$

5.4.2 Linear function

This method was adopted if the shape of the REMG trace increased as well as decreased within one activation period. The activation period was divided in to ten sections and the slope of each line defined. This was then adjusted using Equation 5.13 in order to make the slopes similar even if the total time of activation or number of sections were different.

$$s = \frac{n}{t_{total}} \cdot s_{def} \qquad (5.13)$$

Where:

s = slope

n = number of sections

t_{total} = total activation time

s_{def} = defined slope

Activation for each slope was then calculated using Equation 5.14:

$$a = s \cdot t + c \qquad (5.14)$$

Where:

a = activation

t = time

c = constant (end activation from previous section)

If the slope defined for a particular region caused it to violate the maximum activation or the 97% maximum activation limit, the slope was reduced using:

$$s = \frac{m - c}{t_s} \tag{5.15}$$

Where:

t_s = time for one section

m   = maximum activation

If the activation of the first section, or up to the first four sections combined caused a violation of the 97% maximum activation in 0.07s limit, the slopes were limited using one divided by 0.07 before insertion to the above equations. Figure 5.13 displays an example activation curve using this method.
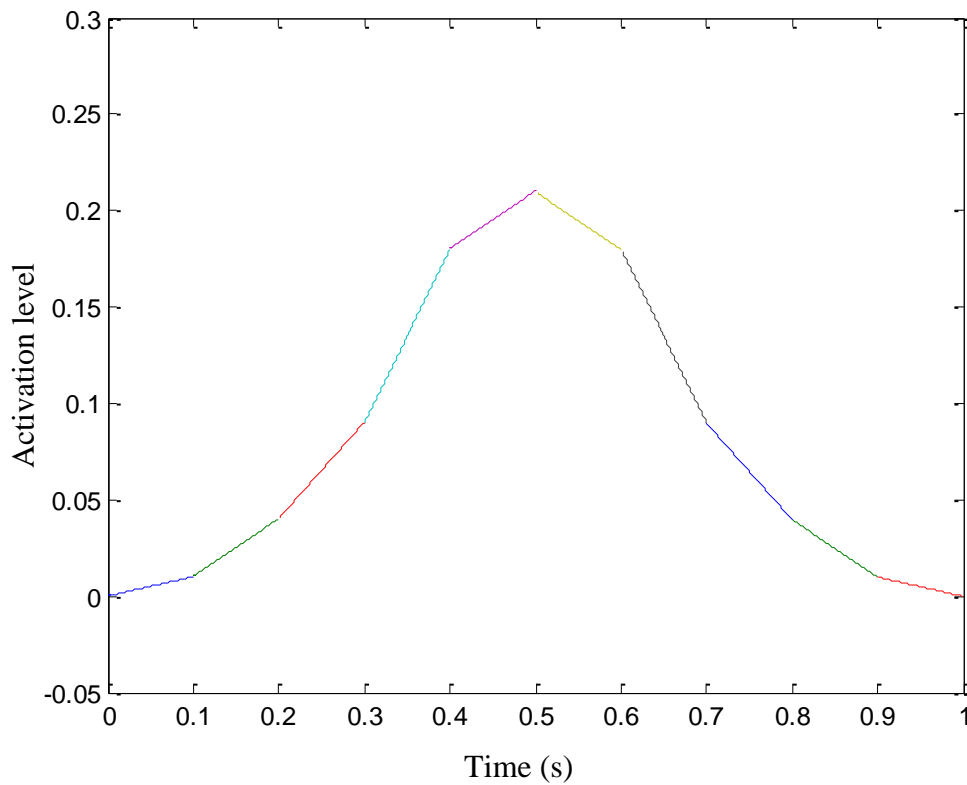
Figure 5.15. Example of the linear activation method.

As the period of activations had been identified from the REMG graphs, activations from this method were not permitted to fall to zero before the end of the final section. Instead a lower limit of 0.1 was set for the first nine sections.

This method required fourteen parameters to optimise a profile; time of initial activation, time of end of activation, initial level of activation maximum activation and the individual slopes for the ten sections.

5.4.3 Model Control

Initial guesses for the input of activation profile parameters into the torque driven model were created based on optimised curves through the RMSEMG data which had been normalised to the maximum voluntary contractions. The figures below are sample activation curves matched to the RMSEMG using the linear (Figure 5.16) and sigmoid (Figure 5.17) functions. Initial activations seen in these graphs are high as sample zero represents the start of the simulation. Further, activation was not allowed to decrease for the first two sections of the linear profile as the muscle had been identified as being active, and in all EMG plots, rose greatly at the beginning of the trace. Matches for the other muscles/ joints can be found in Appendix I.
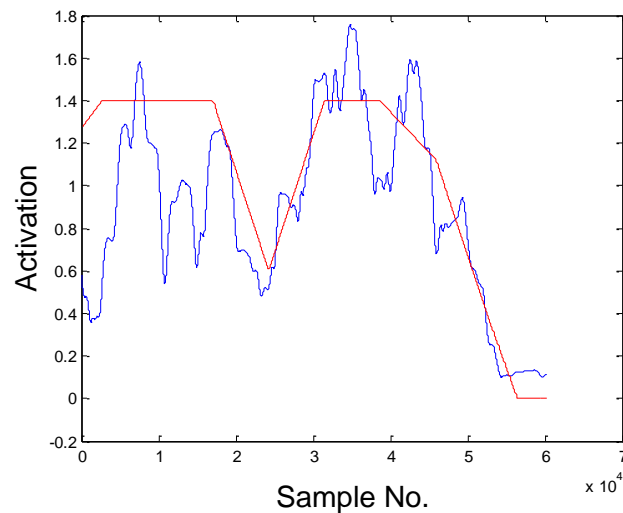
Figure 5.16. RMSEMG of the left Gastrocnemius and recreated using the linear function. Note, blue line = RMSEMG, red line = matched activation profile, maximum contraction = 2 although this was made to be 1 for the model.
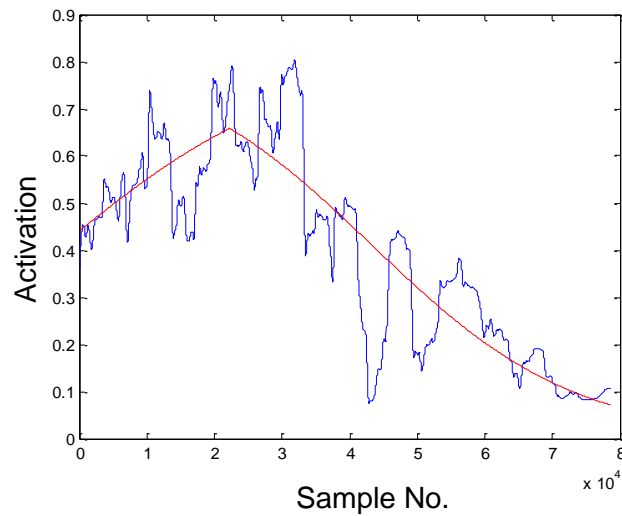
Figure 5.17. RMSEMG of the left Rectus Femoris and recreated using the sigmoid function. Note, blue line = RMSEMG, red line = matched activation profile, maximum contraction = 1.

This process was also used to reduce the number of sections needed for recreating the profiles which used linear the function. This was done by inspection of the curves and parts which used the same slope consecutively were merged into one larger section.

Once created, the profiles needed a time column and corresponding column of zeros to define no activation before the defined period. Importantly an extra zero was inserted as close as possible to the start time. This was to ensure that activation did not start prematurely due to interpolation performed by Simulink. The same procedure was also performed to combine activation profiles where both periods of activation occurred within the simulated time. The Matlab code for this can be found in the Score file in Appendix J. There was no need to define another time and zero column post activation as "Form output after final data value by: Setting to zero" was selected in the 'From Workspace' box which was used to import the numbers into Simulink.

5.5 Torque Modelling

Due to a previous injury, it was not possible to collect isovelocity torque data for the subject. Consequently, existing data (Allen, 2009) was used which had been collected on an athlete of similar build. Torque/ angle/ angular velocity had been calculated using the method of Yeadon et al. (2006) involving a nine parameter function and the results are shown in Table 27. Figures 5.18 and 5.19 display the resulting torque/ angle/ angular velocity profiles for the knee. Equivalent plots for the remaining joints may be found in Appendix K.

It can be seen that in maximum extension torque values for hip, knee and ankle were 594, 498 and 351 Nm respectively. The values for the hip and knee compare favourably with that used by Selbie and Caldwell (1996) for two legs with their simulation model of jumping (600 and 500 Nm respectively). However, the value for the ankle is 200 Nm less than that used by Selbie and Caldwell (550 Nm) who also used a spring at the heel in case it touched the floor. This suggests that the subject had weak plantar flexors or was not able to perform their maximum effort during testing. Similar studies to this one (Kong, 2005 and Mills, 2005), using the same measurement apparatus, have also noted seemingly low values measured at the ankle. Accordingly Tmax at the ankle was set to 550 Nm and the To was also increased accordingly.

Table 27. Torque parameters.

Parameter	Hip		Knee		Ankle		Shoulder	
					Plantar Flx	Dorsi-Flx		
	Ext	Flx	Ext	Flx	Flx	Flx	Ext	Flx
Tmax	594	269	498	574	351[*]	107	147	147
To	457	207	383	361	206[#]	64	113	113
ω_{max} (rad s^{-1})	26	28	36	34.1	30.8	26	36	36
ω_c (rad s^{-1})	7.94	4.2	5.44	5.18	15.38	3.9	5.83	5.83
a_{min} (-)	0.77	0.75	0.99	0.74	0.88	0.99	0.84	0.84
ω_r (rad s^{-1})	1.06	0.26	0	0.83	0.4	0.44	0.3	0.3
ω_l (rad s^{-1})	0.81	0.06	-0.36	1.57	1.38	-1.57	-0.18	-0.18
r (rad // rad^{-2})	1.64	1.64	0.74	0.52	0.37	0.44	1.08	1.08
θ_{opt} (rad)	4.93	3.02	4.31	2.19	2.06	2.13	1.78	0.39

Note. Ext = Extension, Flx = Flexion, * - Tmax was increased to 550 Nm, [#] - To was increased to 380 Nm.
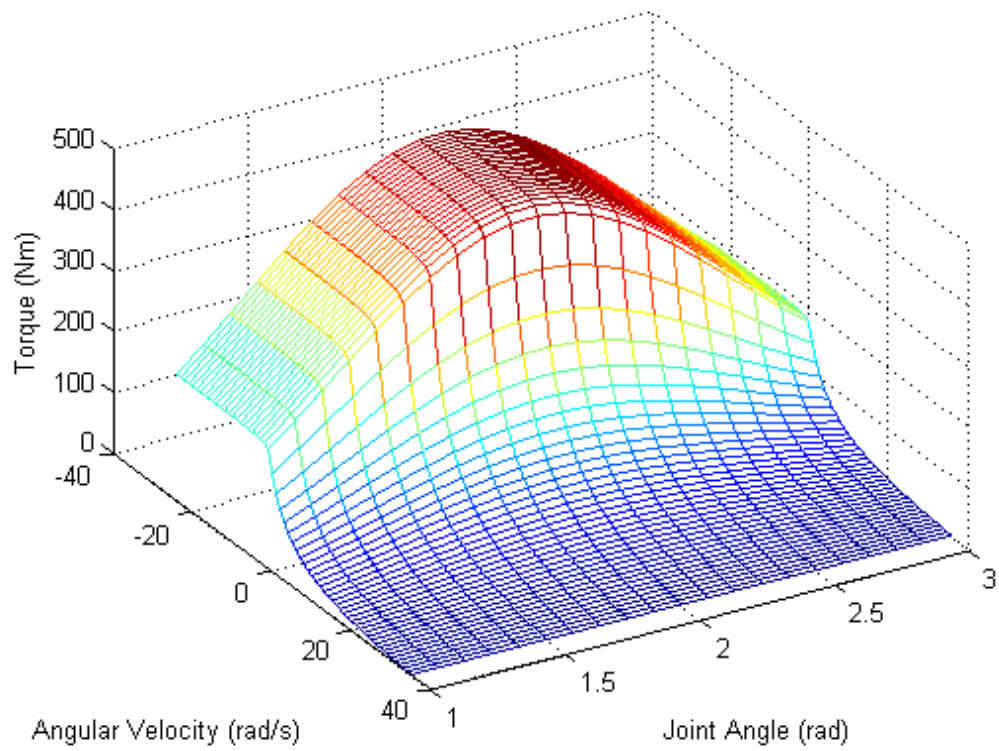
Figure 5.18. Hip extension torque, angle, angular velocity profile.
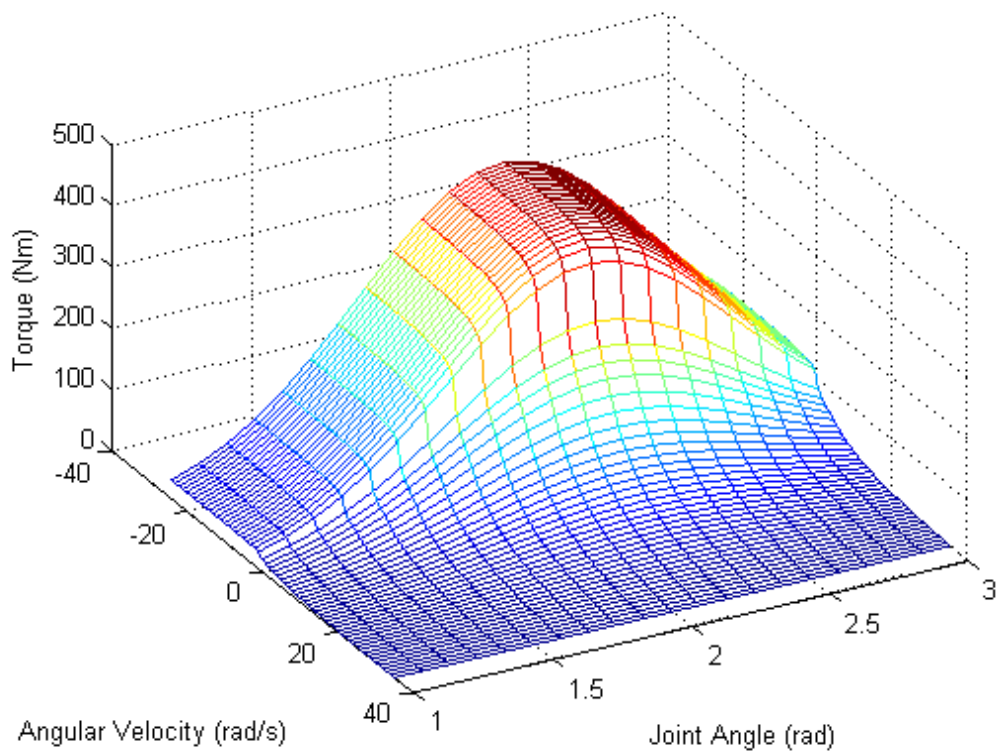
Figure 5.19. Knee flexion torque, angle, angular velocity profile.

The activation profiles were stated as inputs into the simulation. This along with angle and angular velocity data was then output from the model via an S-Function in order to calculate joint torque at a given moment, e.g. in Appendix L.

5.5 Reducing Simulation Running Time.

When running simulations it quickly became apparent that they took a long time to run. Whilst using multiple fast computers in order to run different optimisations at the same time, improvements were made in several areas.

Vibrations in the model often caused the model to slow as the time step decreased to cope. In the worst cases this could cause the model to crash. The solution was to provide a time limit for each simulation based on real time. This was done using the 'clock' function in Malab which provided the current time and date through a subsystem in Simulink with built in S-function shown in Appendix M. If the simulation took longer than the stated time limit, it was stopped and a large penalty was given in the score function. This eliminated the problem of simulations crashing due to the step size becoming too small. The limitation of this was that no useful information was gained from the simulation as if the simulation had completed, a reasonable score may have been achieved despite the vibration. To give the simulation every possible chance of finishing, the time limit was set relatively long and was based on experience of how long a simulation should take (which was outputted every simulation using the 'tic toc' functions around the line of code which called the simulation).

Experimenting with different blocks in Simulink also resulted in time reductions. This was particularly the case for the spring subsystems used for calculation ground reaction forces. One used a Custom Joint connected to a Ground block in order for a Joint Sensor to calculate the displacement of the segment from the ground. Force could then be calculated and applied using a Joint Actuator. The other method used a Body Sensor and Body Actuator to do the same job. The two subsystems provided exactly the same results but the second version ran approximately 10% faster over one simulation of the fourteen segment angle driven model (which took 7.7 s).

Surprisingly a rotational spring created in a similar way also ran much faster than the Rotational Spring block provided in Simulink.

Using 'Constant' block where possible as opposed to 'From workspace' block also helped the simulation run faster (see subsystem in Appendix G). These were also easier to code as they didn't require a time to accompany them. As many S-functions as possible were also rewritten using Simulink blocks. These included functions for calculation of CoM location and also joint torque calculations. The effect this was a reduction in simulation time of approximately ten seconds per S-function.

Separate versions of each model were made to run optimisations and to view the results of the optimisations. In versions which ran optimisations, all unnecessary outputs from the model were removed. These included blocks such as Scopes, To Workspace and Displays. The effect of this was relatively small compared to any of the adaptations mentioned above.

For the four segment models and fourteen segment torque model, simulations were stopped as soon as any body part struck the ground (as opposed to just the foot). A penalty was also then added to the score function to reflect this (See appendix N).

To speed up the time taken for optimisations for the torque models to run reductions in the number of parameters were made by; defining all initial and end activation levels at 0.05; attempting to remove sections of linear functions that occurred before zero (in practise this had no effect as no whole period could be removed due to the small time periods involved); and finally allowing more activation profiles to be created using the sigmoid function method (including all second part activations, most of which started little before the simulation finished).

Inserting springs at the MPJ vastly increased the time taken for each simulation. Outputting the time and score revealed that each simulation took between 120 – 6500 s to run meaning that a full optimisation using Simulated Annealing could take years to complete. Time was therefore spent attempting to make it run faster. Both the method of inputting the current variables into Simulink and the way the equation was written in the program affected the time taken to run each simulation. The fastest

method is shown in Figure 5.20 below. Here using a 'constant' block made the program run faster than the usual 'from workspace' block. This reduced the time taken for simulations using the angle driven model from to 5.9 – 2.4 s.
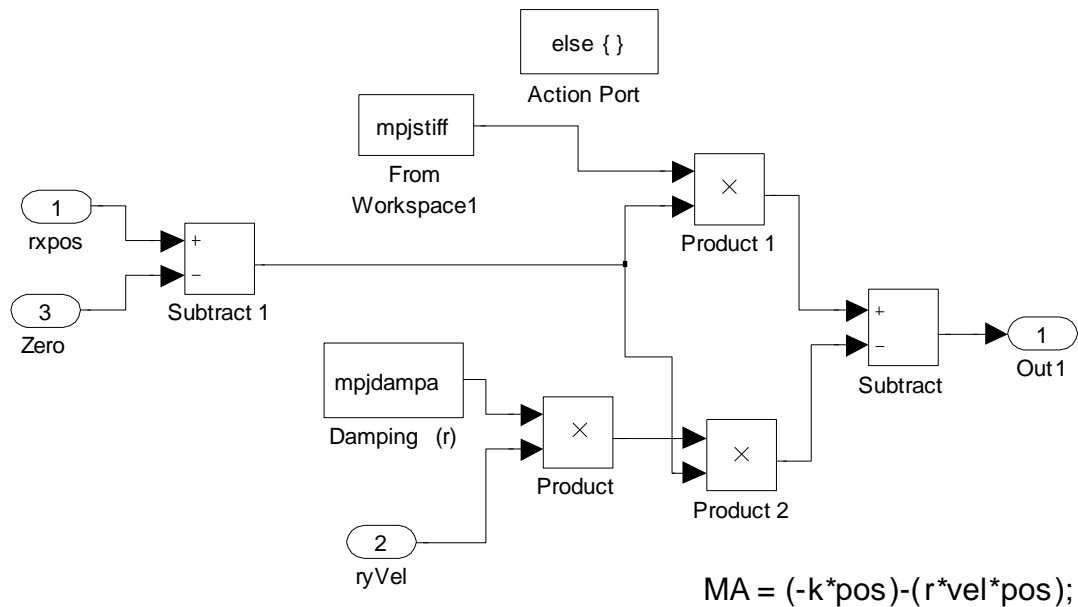
Figure 5.20. Linear MPJ spring programming in Simulink.

The initial version of the spring worked by specifying spring parameters within the model. This meant much intrusion into the model whilst developing it which led to mistakes. To make it more user friendly, all spring parameters, including the point from which they act, were written as From Workspace inputs. This also allowed the spring parameters to be optimised using MatLab.

Despite all these efforts to make simulations run faster, the final fourteen segment torque driven model took 350 – 850 s to run one simulation, and furthermore the computer ran out of memory after approximately 8000 – 10000 simulations. To make the most of the data gained from simulations which had run, a number of save points were included in the score code (Appendix N). For each optimisation, three sets of numbers were saved after every simulation. The first set 'currentparams' were the current set of parameters being tested. If these caused the simulation to crash, they could be used to aid in the debugging process. The second set of numbers saved were the parameters for every simulation that had been attempted as well as the resulting

score. Unfortunately for more complex problems this was reduced to the last 1000 simulations as the large file resulted in memory problems. Again this information was useful if the optimisation stopped early or to examine what sort of scores were achieved by certain parameters. The final set of numbers were the set of parameters that provided the best score to that point as well as the score itself. This was useful in case the optimisation crashed but also if the best score had been achieved more than 1000 simulations beforehand.

5.7 Matching Optimisation

To match the torque driven model to the original performance, 120 parameters were optimised for controlling the model. For each joint these were; the on and off times for the torque generators based on the EMG data $\pm$ 5 ms, initial level of activation $(0.00001 - 0.1)$ and maximum activation $(0.5 - 1)$. For joint activations modelled using the sigmoid function a further three parameters were optimised, these were; end activation $(0.00001 - 0.1)$, the ratio of the steepness of the upward and downward curve $(0.1 - 0.9)$ and peak activation see Section 5.4.1 for difference to maximum activation, $0.8 - 0.99995)$. For joint activations modelled using the linear function, the slopes of the ten sections were also optimised $(-0.7 - 0.7$ apart from the last section, $-0.9 - 0.1)$ although as previously mentioned, the number of sections were reduced where appropriate. Table 28 displays the method used for modelling activations at each joint. These activations provided control for the model to perform the first step out of the start block.

Table 28. Methods used to create joint activation profiles.

Joint	Activation method			
	Left limb		Right limb	
	Extension	Flexion	Extension	Flexion
Hip 1	Linear	Linear	Sigmoid	Linear
Hip 2	n/a	n/a	Sigmoid	n/a
Knee 1	Sigmoid	Sigmoid	Sigmoid	Sigmoid
Knee 2	n/a	n/a	Sigmoid	n/a
Ankle 1	Sigmoid	Linear	Sigmoid	Linear
Ankle 2	n/a	n/a	Sigmoid	Sigmoid
Shoulder 1	Sigmoid	Sigmoid	Sigmoid	Sigmoid

The score for matching the torque driven model is set out in Figure 5.21. As can be seen, it was decided not to match ground reaction forces. This was to reduce complexity in finding a solution and it was considered that the use of joint torques to drive the model and the use of previously optimised spring parameters should allow a good match to obtain realistic forces.
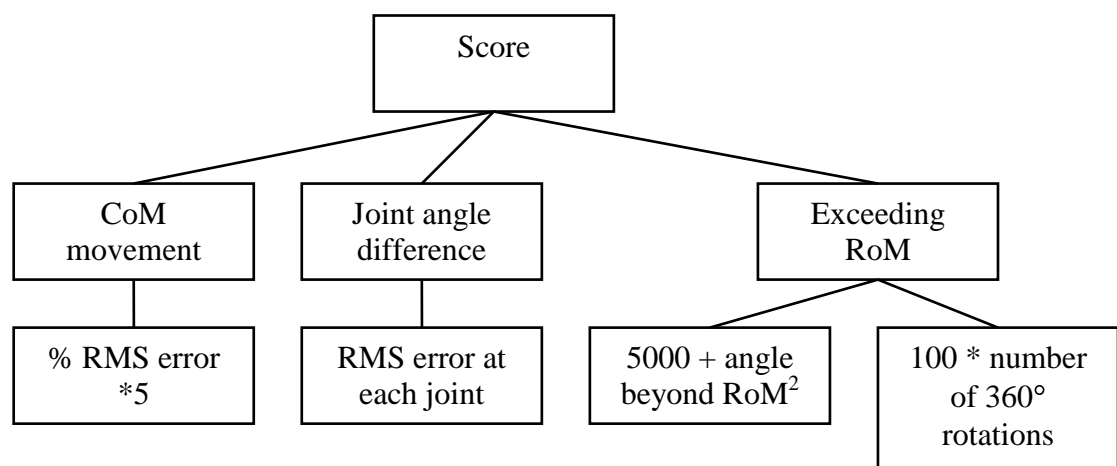
Figure 5.21. Score function for matching the 14 segment model.

As discussed above, the matching optimisation was repeatedly restarted when the computer crashed due to running out of memory. This was done using the best

solution previously found but after 10 months the matched start still did not represent as start over the whole first step. In order to try and find a solution the simulation length was reduced to stop on takeoff. It was matched manually, reducing the score from over 80,000 to 31619. A comparison of the torque driven model to the measured start can be seen in Figures 5.22 and 5.23 The match represents 15° average error in joint angles.
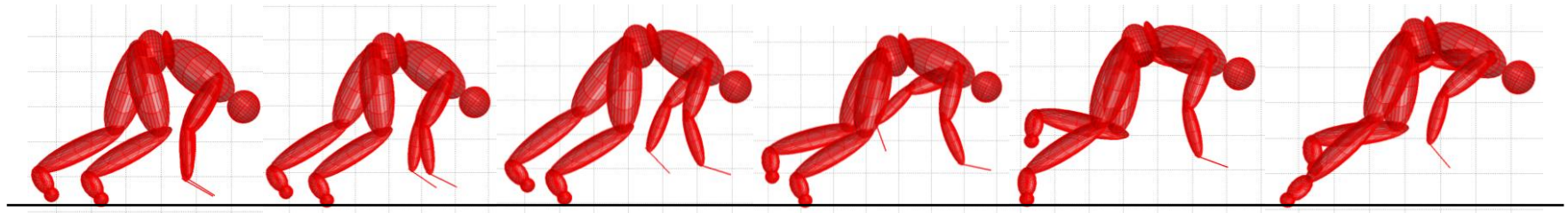
Figure 5.22. Matched start at 0.07 s intervals.
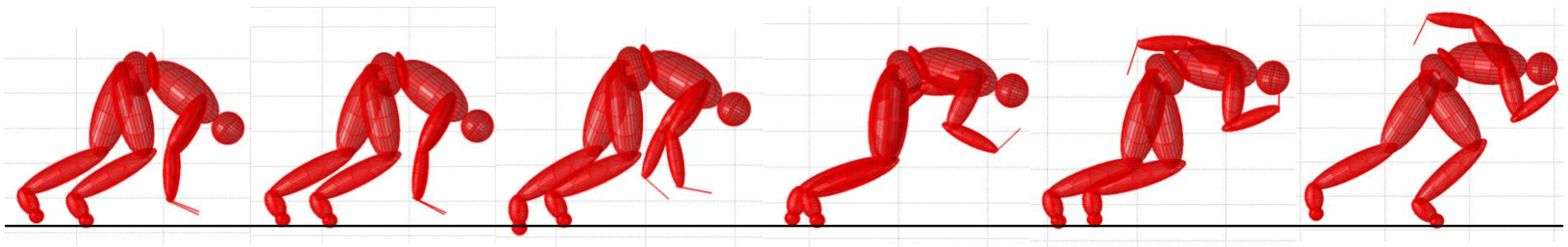
Figure 5.23. Measured start at 0.07 s intervals.

The following plots (Figures 5.24 – 5.33) provide joint angle time histories of the original and matched start along with RMS error scores over the first 0.354 s. The pattern of movement is generally for each joint although large extension at the left ankle and a poor match at the left shoulder are notable exceptions. The left ankle has an RMS error of 19.53° and the left shoulder does not appear to follow recorded movement pattern well. The push off phase lasted 0.354 s compared to 0.403 in the measured start and therefore the plots show the whole push off phase for both sets of data. To further investigate the data, Table 29 compares the measured start after 0.354 s and 0.403 s to the matched start.
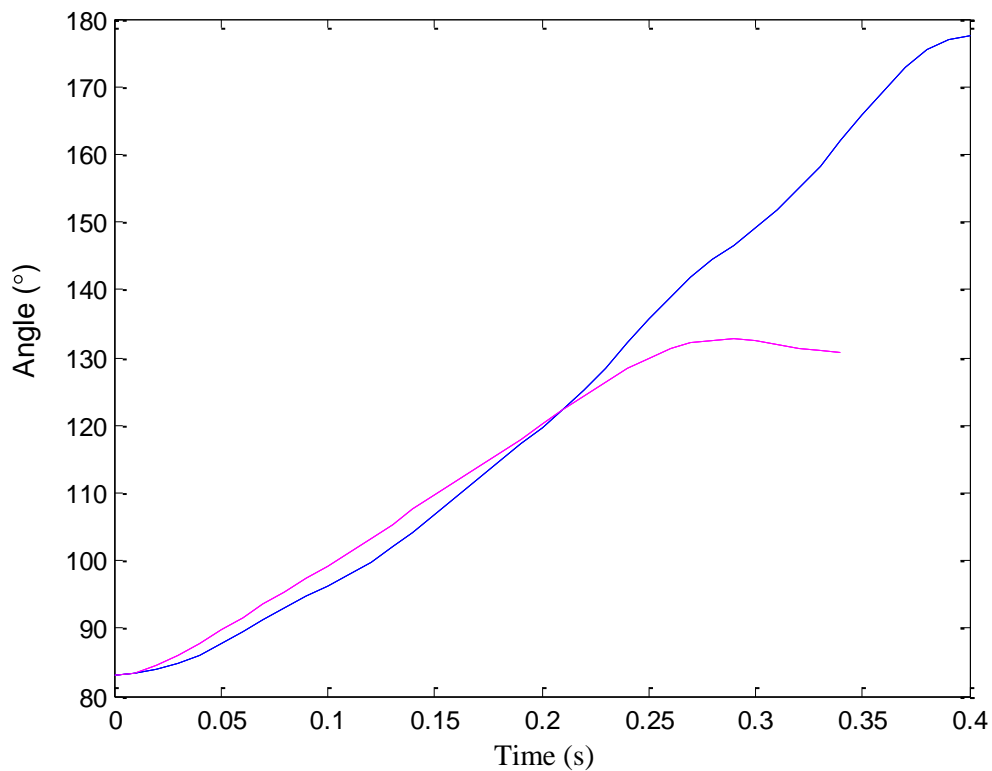
Figure 5.24. Comparison of left hip angles in the measured and matched starts. Blue = measured, pink = matched. Match = 10.11° RMS error.
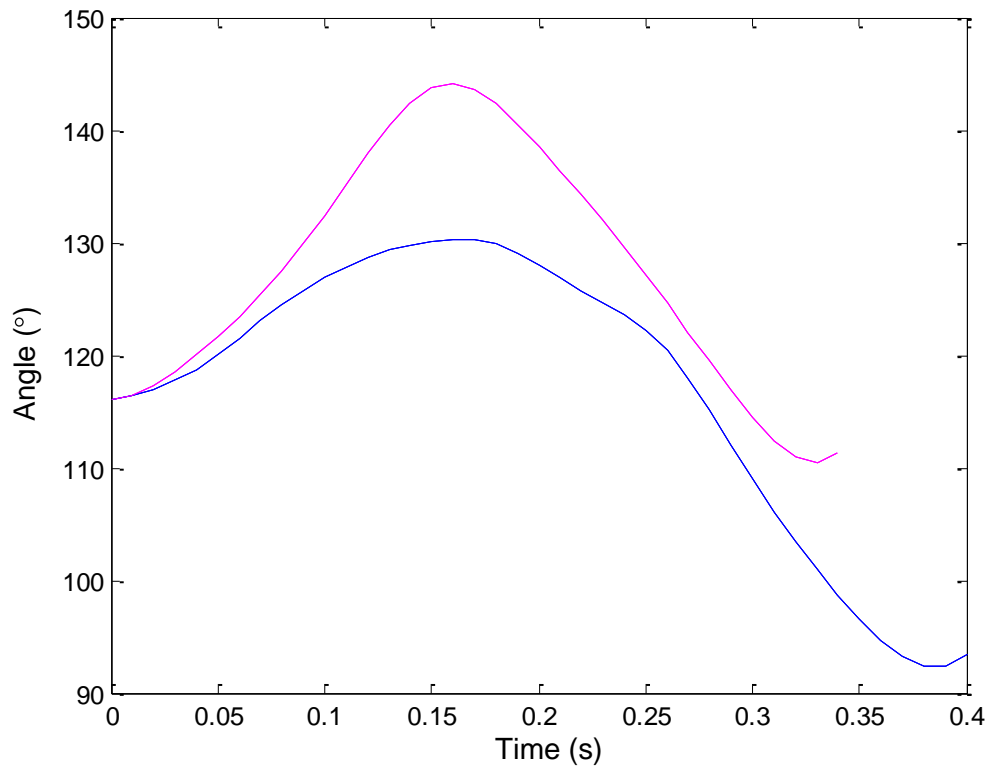
Figure 5.25. Comparison of right hip angle in the measured and matched starts. Blue = measured, pink = matched. Match = 7.89° RMS error
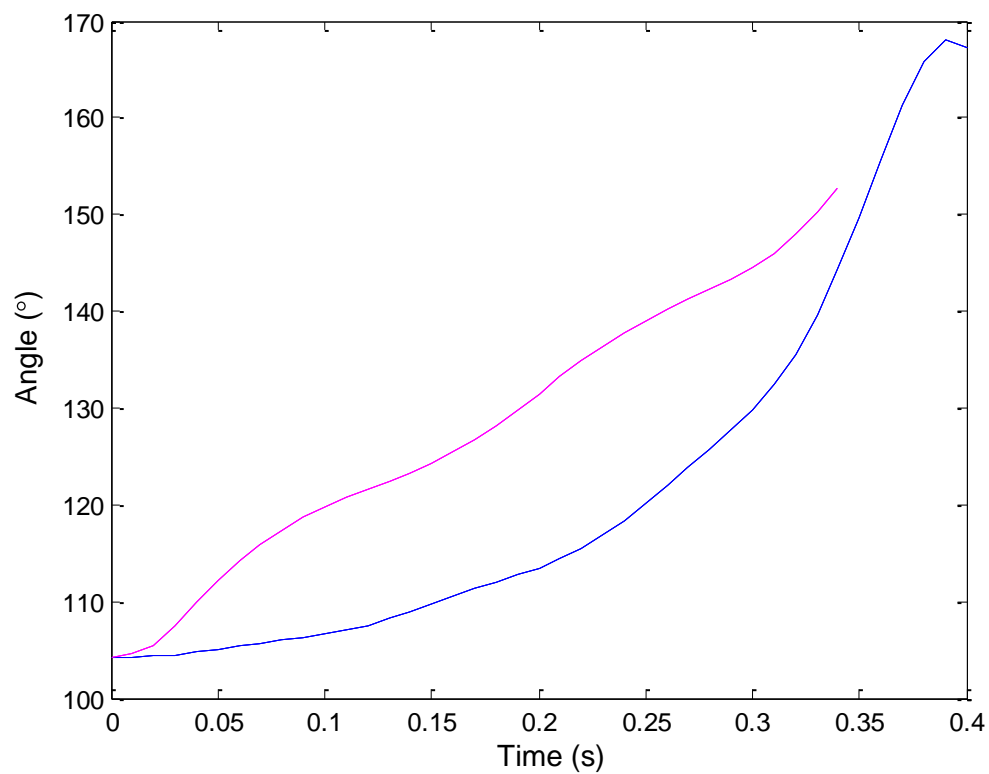
Figure 5.26. Comparison of left knee angle in the measured and matched starts. Blue = measured, pink = matched. Match = 13.96° RMS error
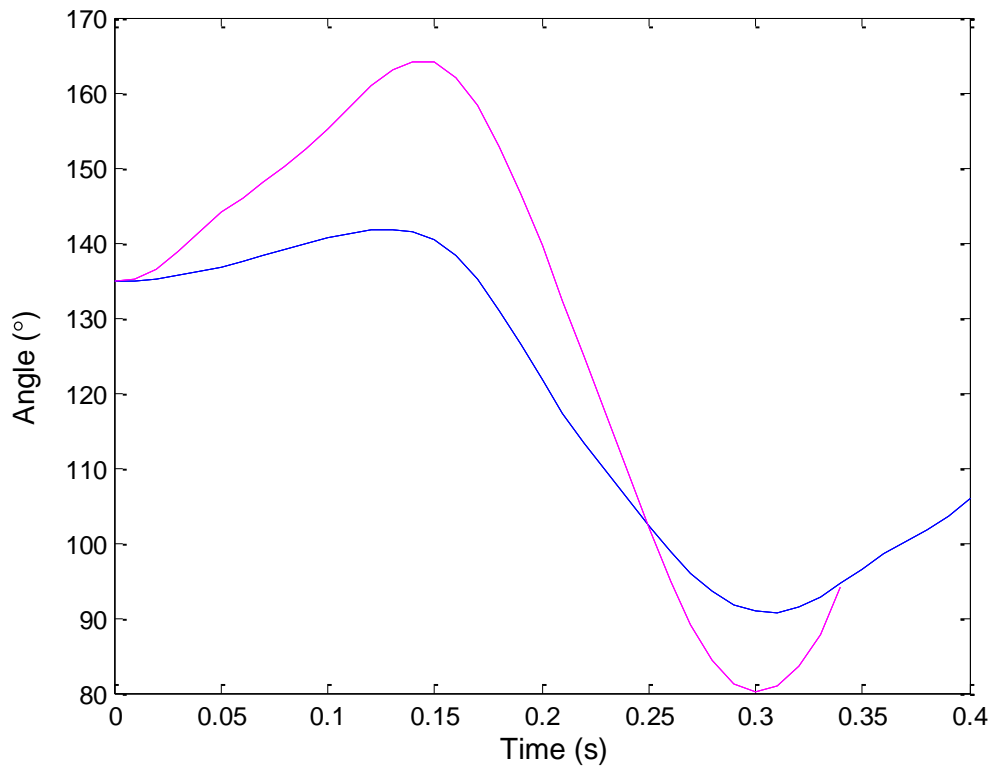
Figure 5.27. Comparison of right knee angle in the measured and matched starts. Blue = measured, pink = matched. Match = 13.30° RMS error
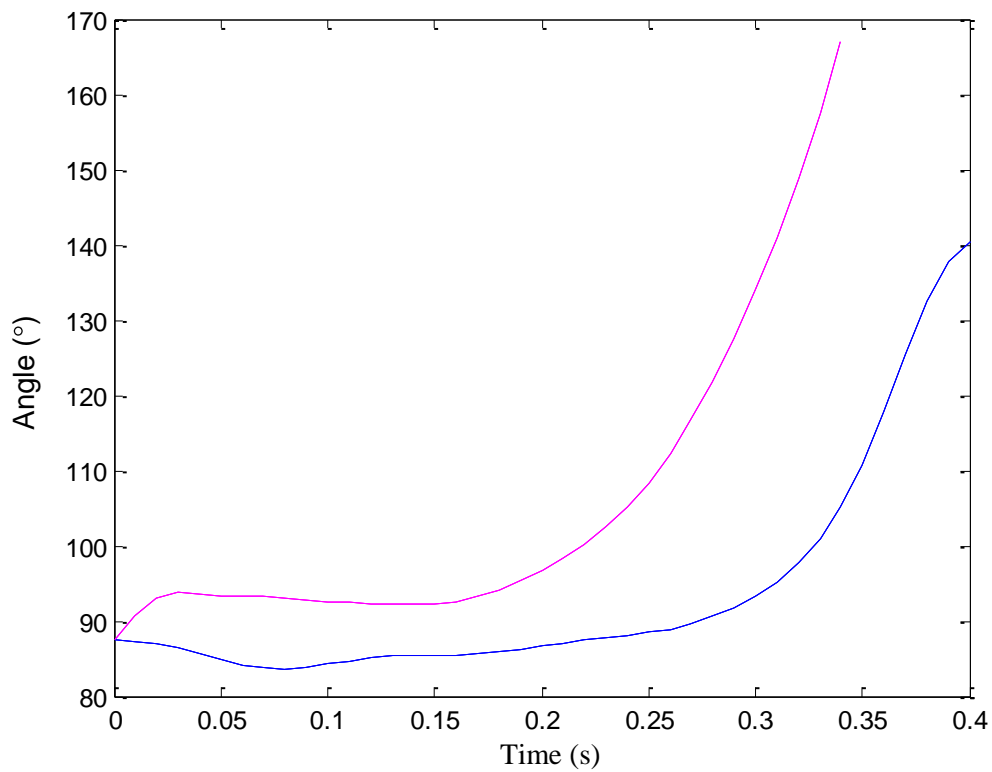
Figure 5.28. Comparison of left ankle angle in the measured and matched starts. Blue = measured, pink = matched. Match = 23.53° RMS error
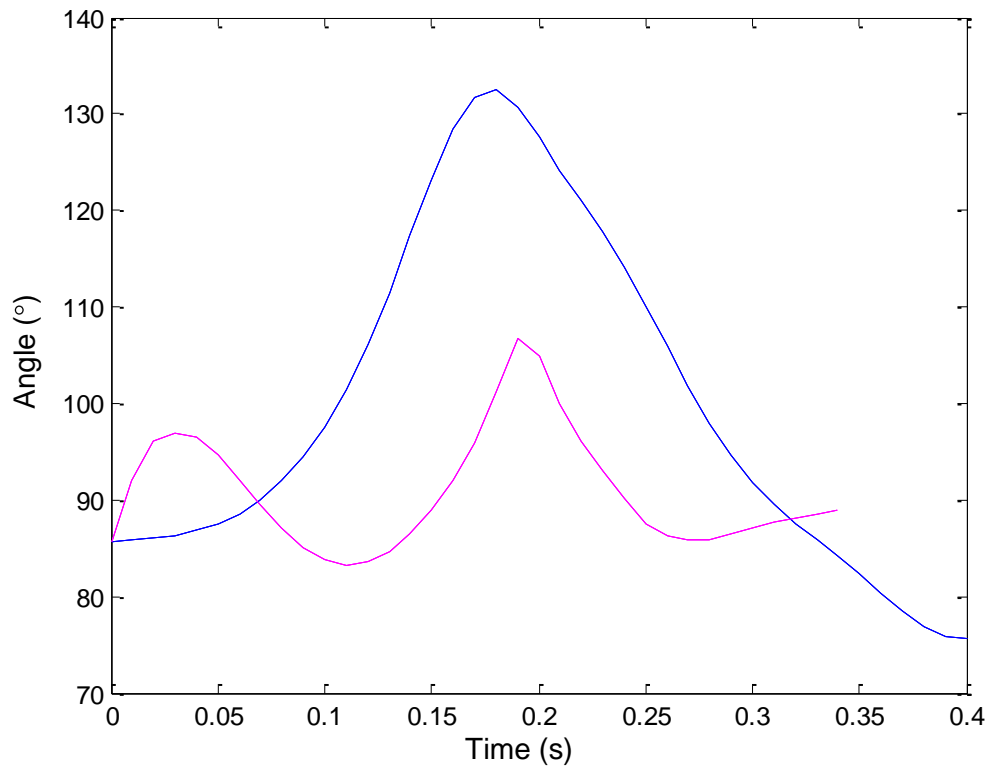
Figure 5.29. Comparison of right ankle angle in the measured and matched starts. Blue = measured, pink = matched. Match = 19.21° RMS error.
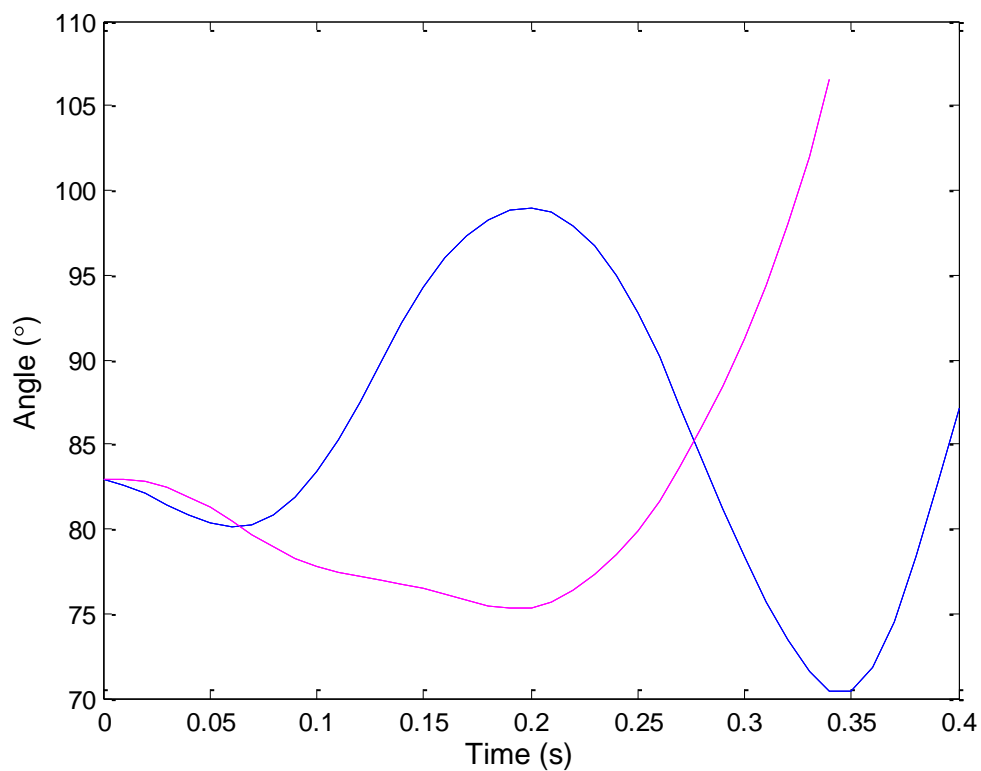
Figure 5.29. Comparison of left shoulder angle in the measured and matched starts. Blue = measured, pink = matched. Match = 15.81° RMS error
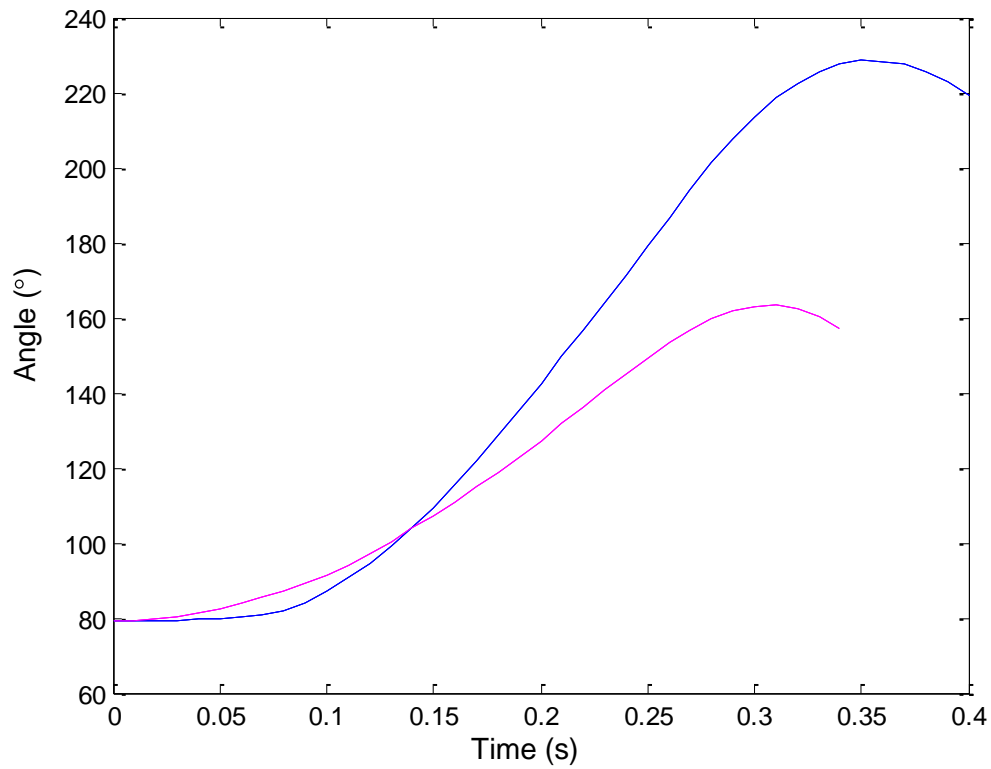
Figure 5.30. Comparison of right shoulder angle in the measured and matched starts. Blue = measured, pink = matched. Match = 28.45° RMS error.
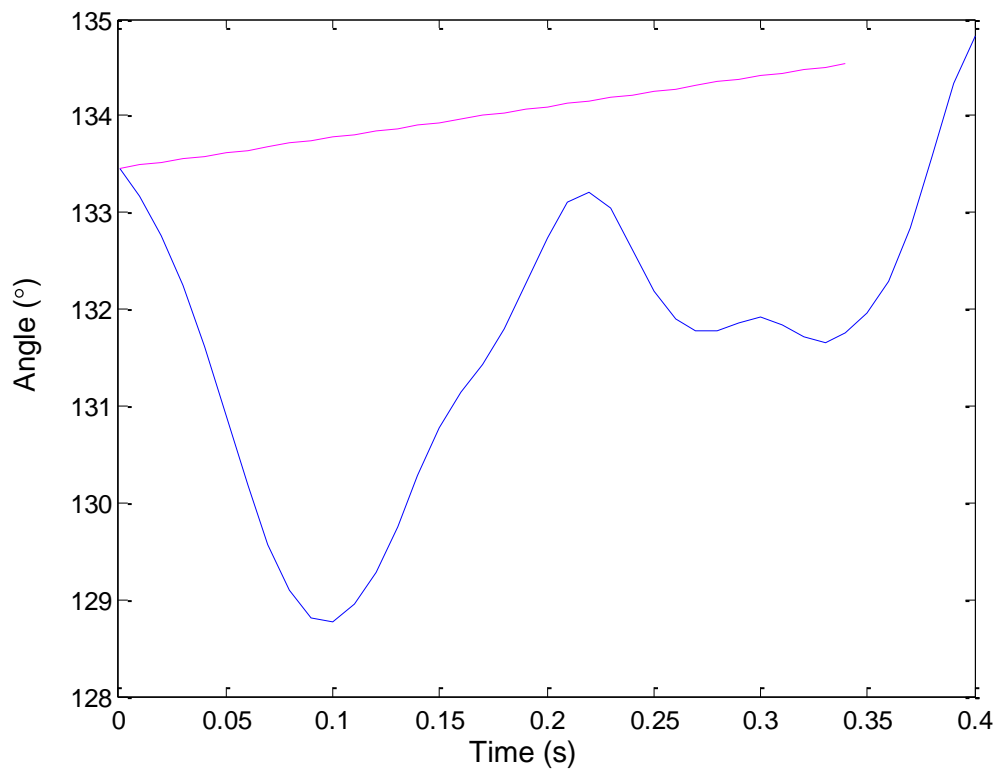
Figure 5.31. Comparison of spine angle at T10 in the measured and matched starts. Blue = measured, pink = matched. Match = 2.90° RMS error.
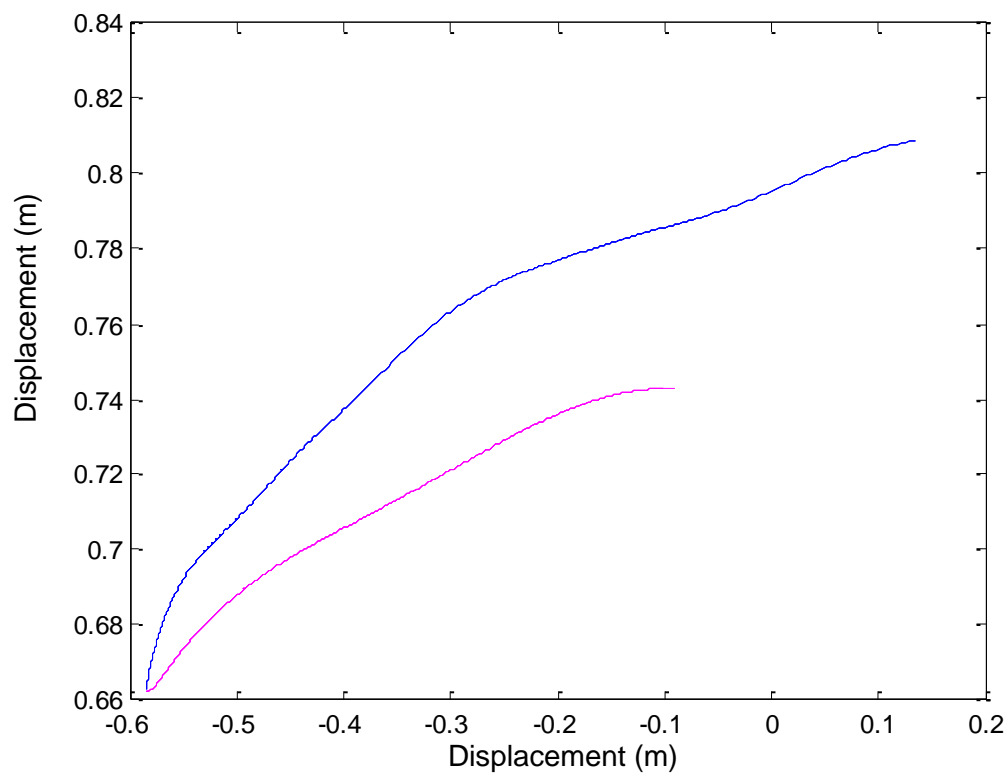
**Figure 5.32.** Comparison of CoM position in the measured and matched starts. Blue = measured, pink = matched. Match = 0.01 m RMS error horizontally and 0.03 m RMS error vertically.

Table 29. Comparison of matched start to measured data.

Start Variable	Matched start	Measured start	
Time (s)	0.354	0.354	0.403
CoM Height (m)	0.74	0.79	0.81
CoM horizontal Displacement (m)	0.49	0.46	0.69
Horizontal Velocity (m·s^{-1})	2.50	3.30	3.40
Vertical Velocity (m·s^{-1})	0.10	0.30	0.30
Average Horizontal Acceleration (m·s^{-2})	7.06	9.32	8.44
Front Foot Peak Horizontal Force (N)	803.88	861.40	861.40
Front Foot Peak Vertical Force (N)	985.32	689.00	689.00
Rear Foot Peak Horizontal Force (N)	592.04	519.07	519.07
Rear Foot Peak Vertical Force (N)	706.59	457.88	457.88
Front Foot Horizontal Impulse (Ns)	192.02	192.63	203.29
Front Foot Vertical Impulse (Ns)	249.14	183.50	193.29
Rear Foot Horizontal Impulse (Ns)	21.01	57.29	71.75
Rear Foot Vertical Impulse (Ns)	31.53	50.79	63.71

The data in Table 29 above shows that the matched start was less efficient in all key areas over both the whole of the push off and also when compared to the measured start at 0.354 s. Much of the data at 0.354 s is quite similar, particularly CoM height, horizontal displacement and horizontal impulse however, a reduction in horizontal velocity of 0.8 m·s^{-1} and 2.26 m·s^{-2} slower in horizontal acceleration reveals a poorer performances. The area where there does seem to be an increase is vertical impulse where impulse is 65.64 Ns greater for the matched start. This is reflected in the ground reaction force plots in Figure 5.33 where it can be seen that despite the shorter contact time, higher forces were maintained throughout the period. This may therefore show that the front leg is compensating for the low impulse produced by the rear.
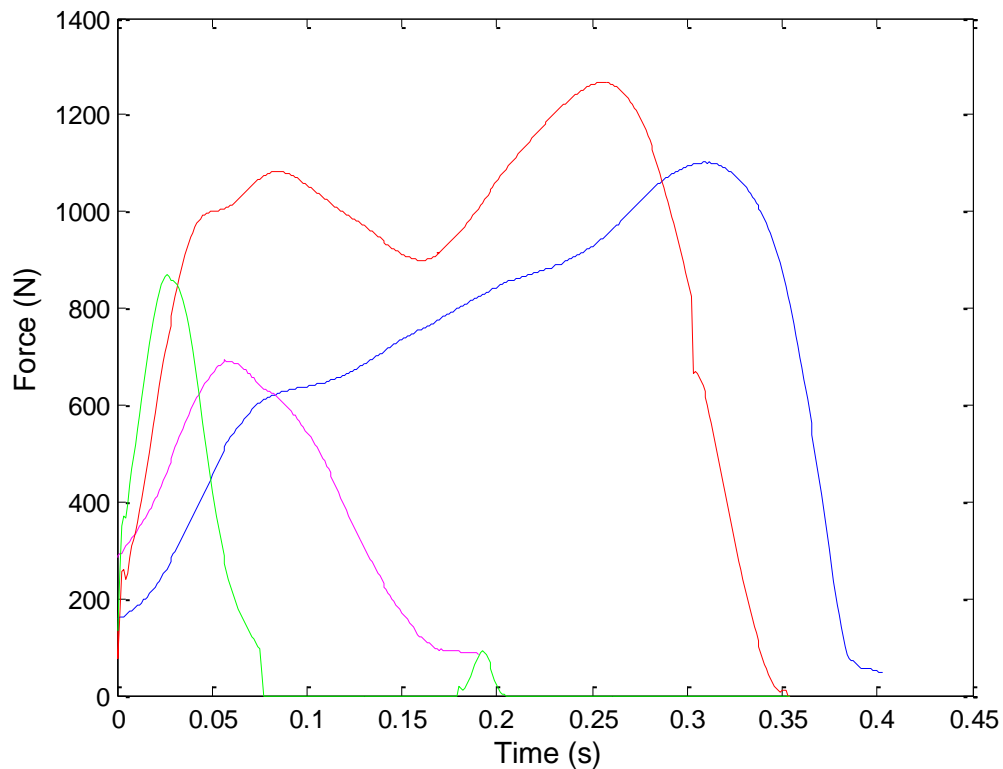
Figure 5.33. Resultant ground reaction forces for the matched start and measured data. Blue = front foot measured, pink = rear foot measured, red = front foot matched, green = rear foot matched.

Figures 5.34a – h display activation profiles for flexion and extension torques at each joint over 0.6 s. Whilst this goes beyond the end of the simulation many of the variables that created these profiles, such as slope steepness ratio, will have influences in the simulated times. It can be seen that activations for the knee are extremely small when compared to the ankle and hip which are 99 % maximally activated. Furthermore it is interesting that of the linear activation patterns, only hip flexion both rose and fell more than once within a single period of activation.

Figure 5.34a. Activation at the left hip.

Figure 5.34b. Activation at the left knee.

Figure 5.34c. Activation at the left ankle.

Figure 5.34d. Activation at the right hip.

Figure 5.34e. Activation at the right knee. Blue = extension, green = flexion

Figure 5.34f. Activation at the right ankle. Blue = extension, green = flexion
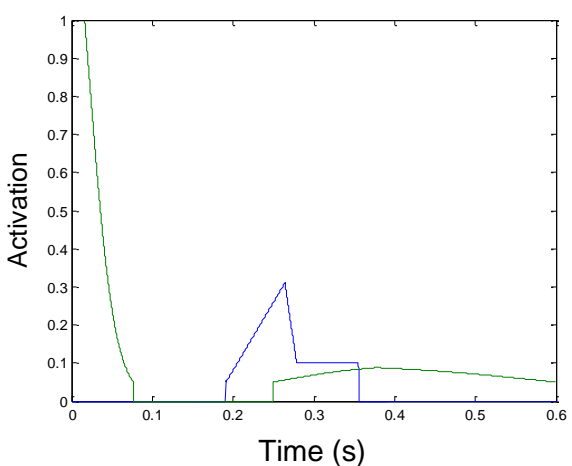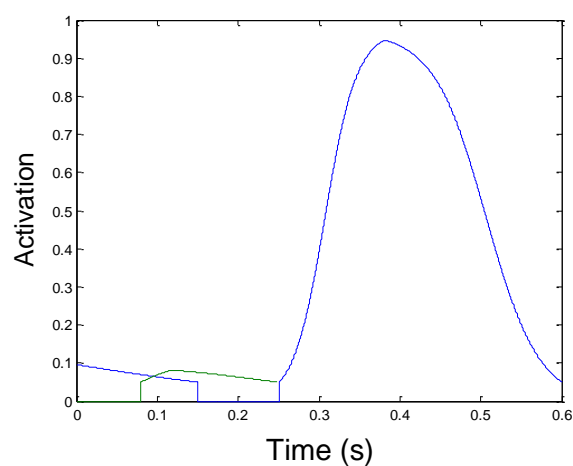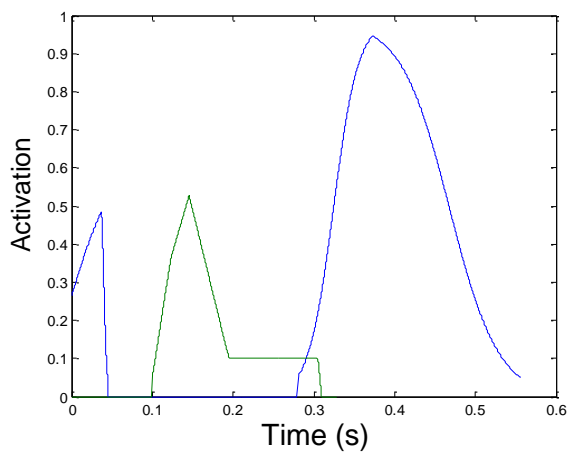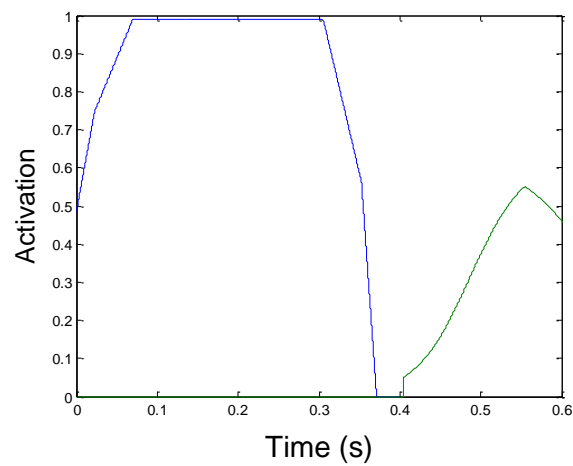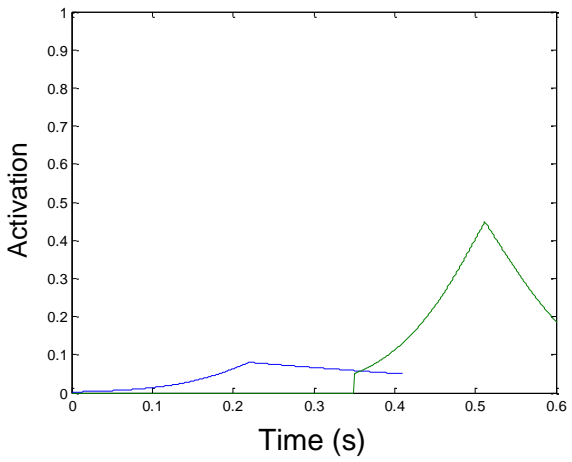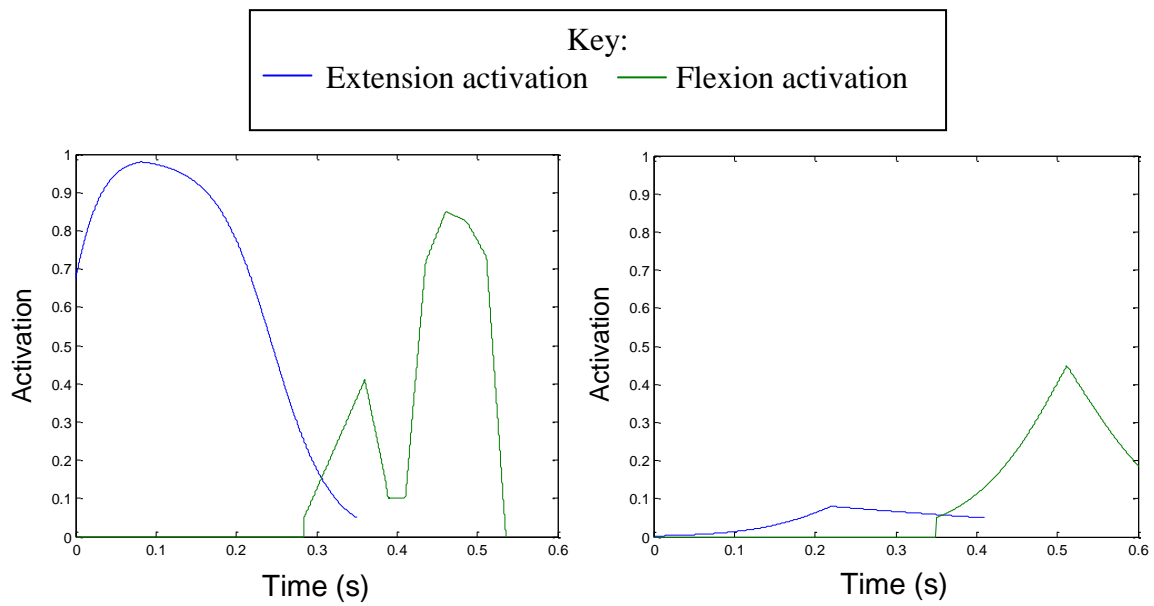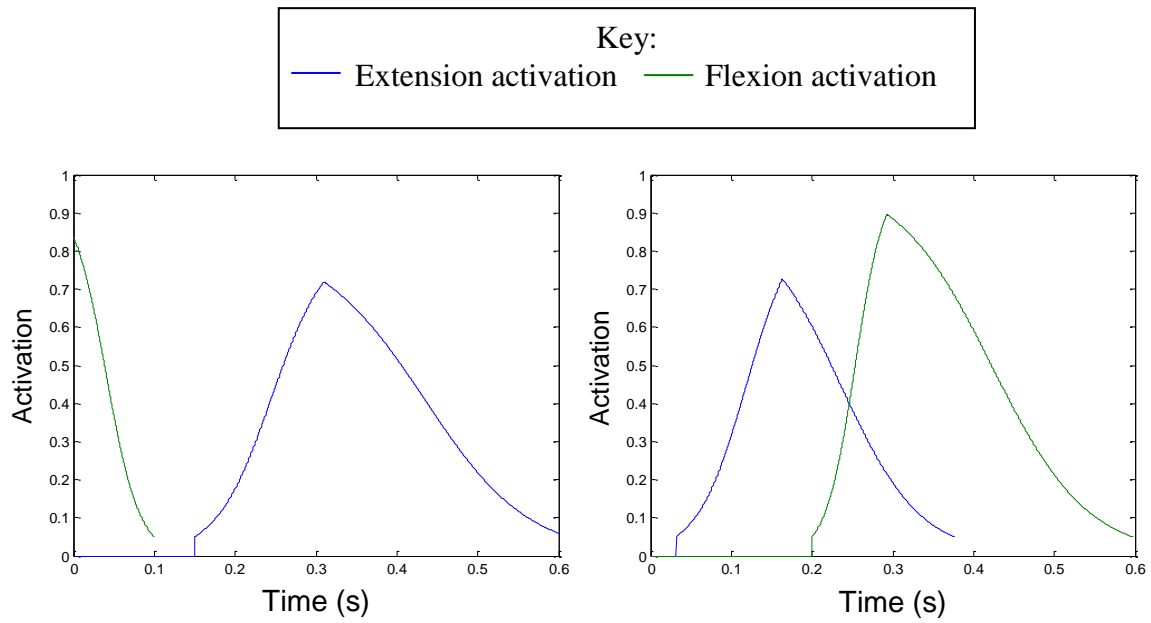
Figure 5.34g. Activation at the left shoulder.

Figure 5.34h. Activation at the right shoulder.

Figures 5.35 – 5.38 display joint torques during the matched start. As can be seen the torques are generally quite low particularly at the beginning when high torques are expected due the static start. Where torques profiles appear to change suddenly, this is likely to be due to the changes that occur during linear activation profiles.
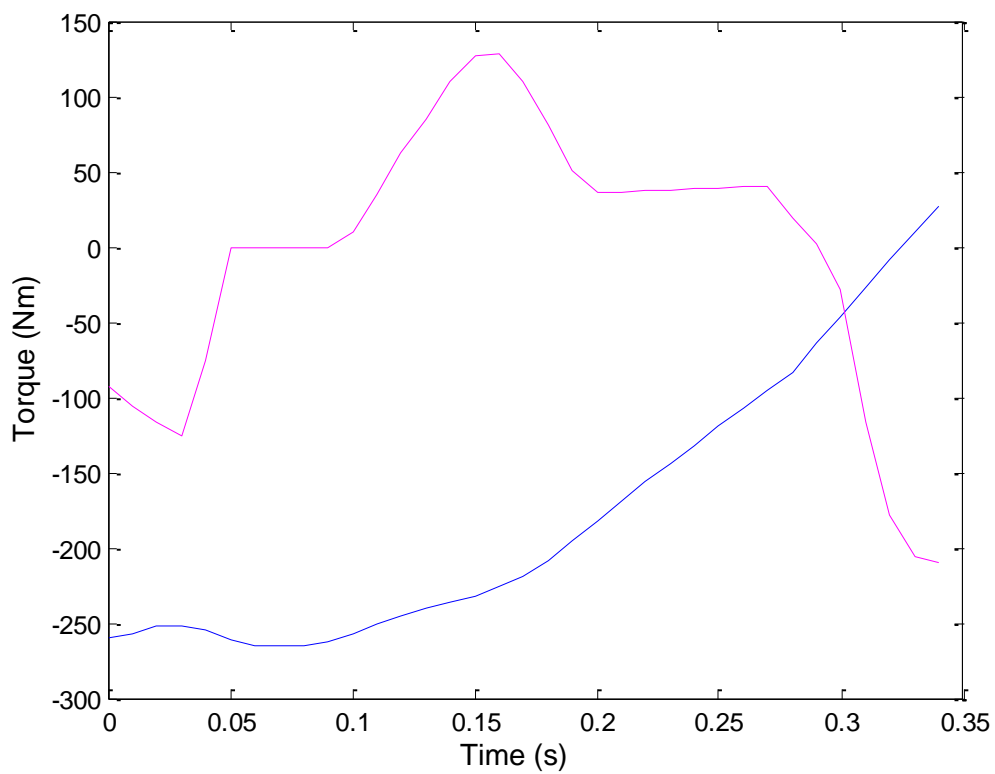
Figure 5.35. Joint torque at the hips. Blue = left, pink = right.
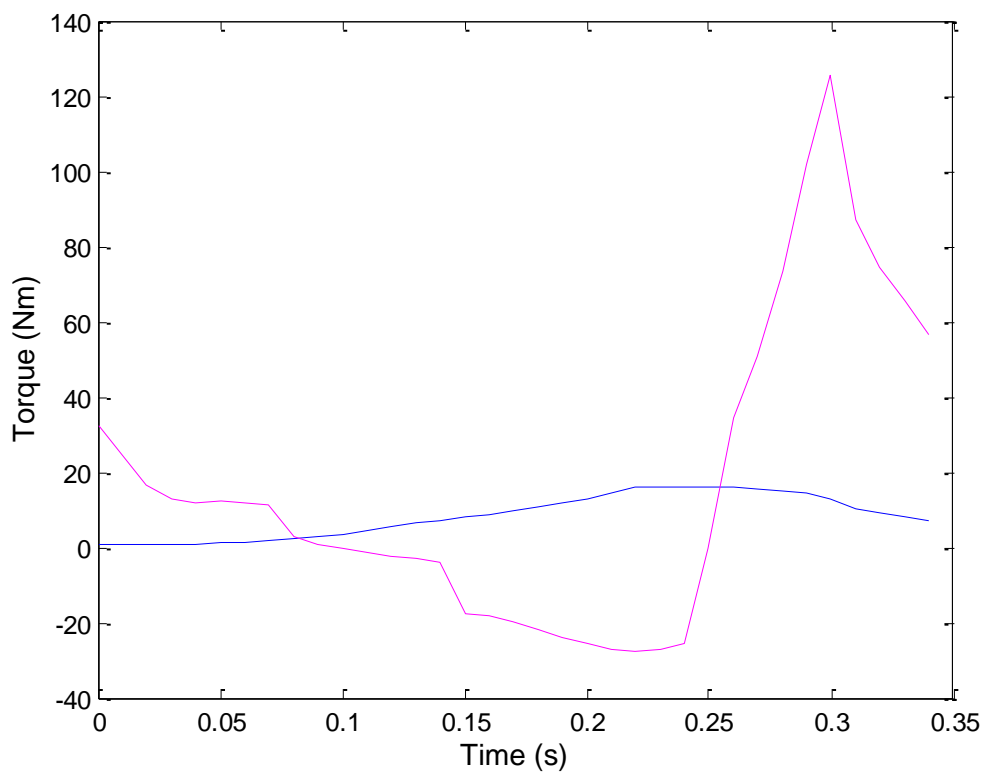
Figure 5.36. Joint torque at the knees. Blue = left, pink = right.
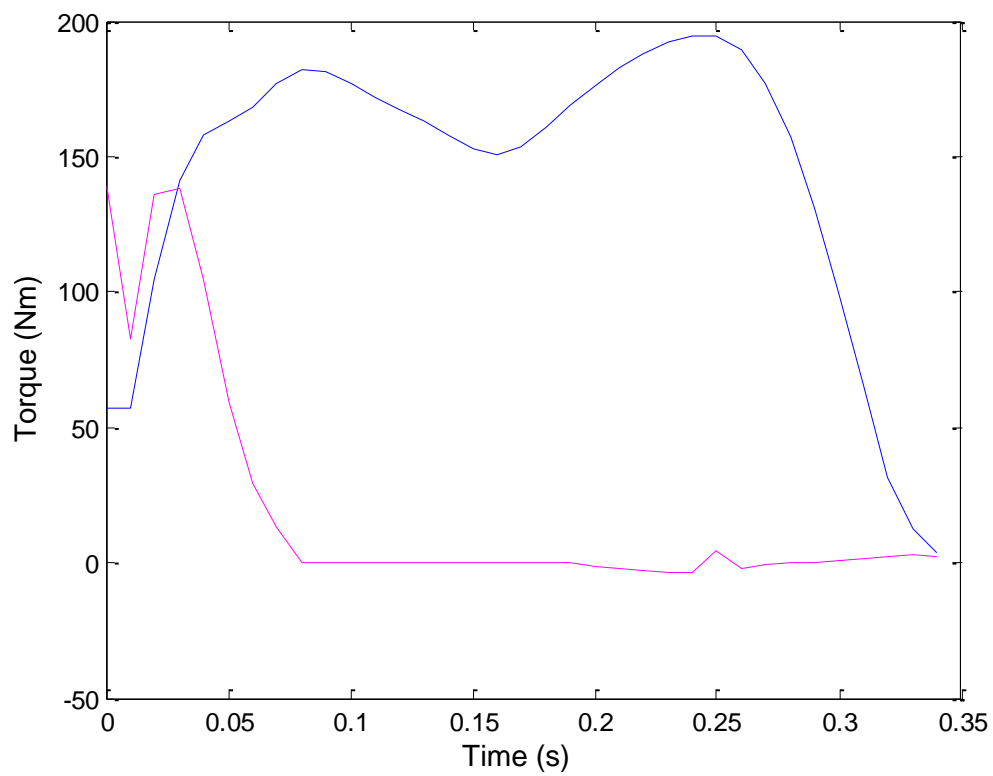
Figure 5.37. Joint torque at the ankles. Blue = left, pink = right.
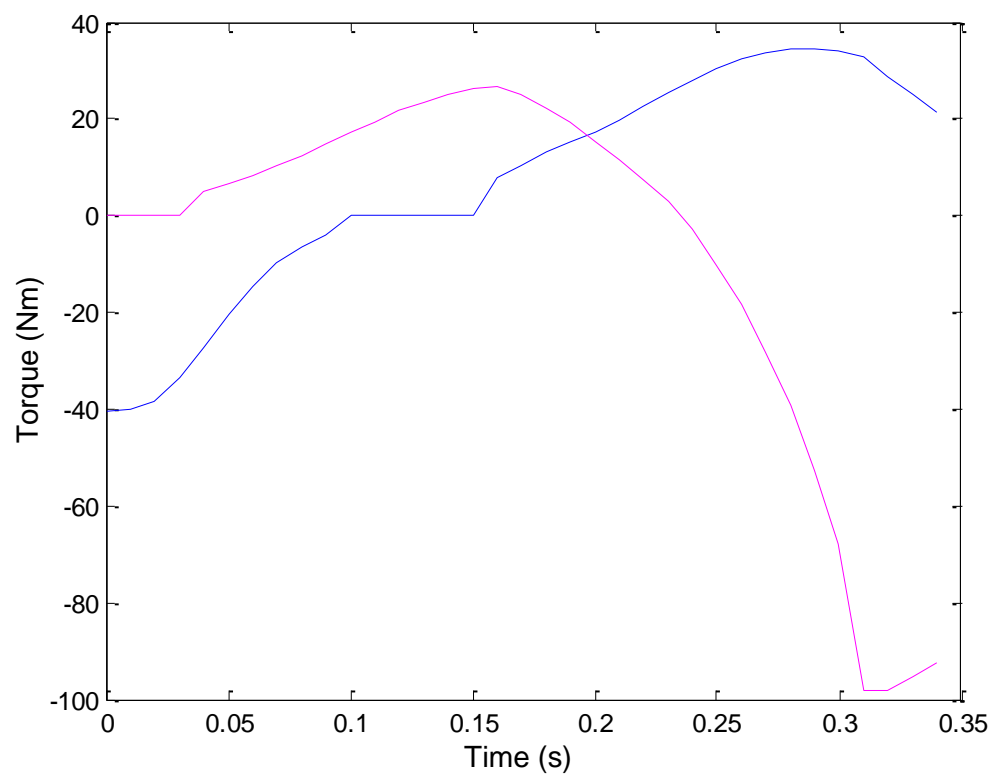
Figure 5.38. Joint torque at the shoulders. Blue = left, pink = right.

The data from Table 28 and joint angle comparisons show that the whilst the matched start was not particularly close, given more computing capacity and time to optimise, it seems capable of producing realistic and useful results. With this in mind computers ran optimisations to see if the athlete could improve their start using the same initial position. Optimisations were also run to examine the effect of a very elongated start and a very bunched start. Little success was obtained optimising the matched start as the best solution was no better than the matched optimisation provided. The result was similar for the elongated start as the movement gave little resemblance to coordinated movement. Some success was however obtained analysing a bunched start.

5.8 Bunched position

Initially a bunched start was examined by placing both feet closer to the start line. The input parameters from the matched solution were input into the bunched simulation but despite many of the movements resembling the start, both ankles collapsed even when made to be two times maximally active throughout the simulation. As a result the effect of bunching the start by placing the legs closer together was examined. The most bunched position possible would place both feet together and therefore the rear leg was given the same conditions and activations as the front. As the simulation only lasted until takeoff, both legs were allowed to leave the starting block at the same time. This type of start is sometimes referred to as a Bullet start and results are comparable to the four segment model and may also be of interest for swimming sprint starts.

To help ensure the start still performed within human capabilities the score function for this optimisation retained the RoM penalties created in the function used to match the starts. Velocity was then multiplied by 500 and subtracted from the score to provide an objective function. The resulting start can be seen in Figure 5.39.
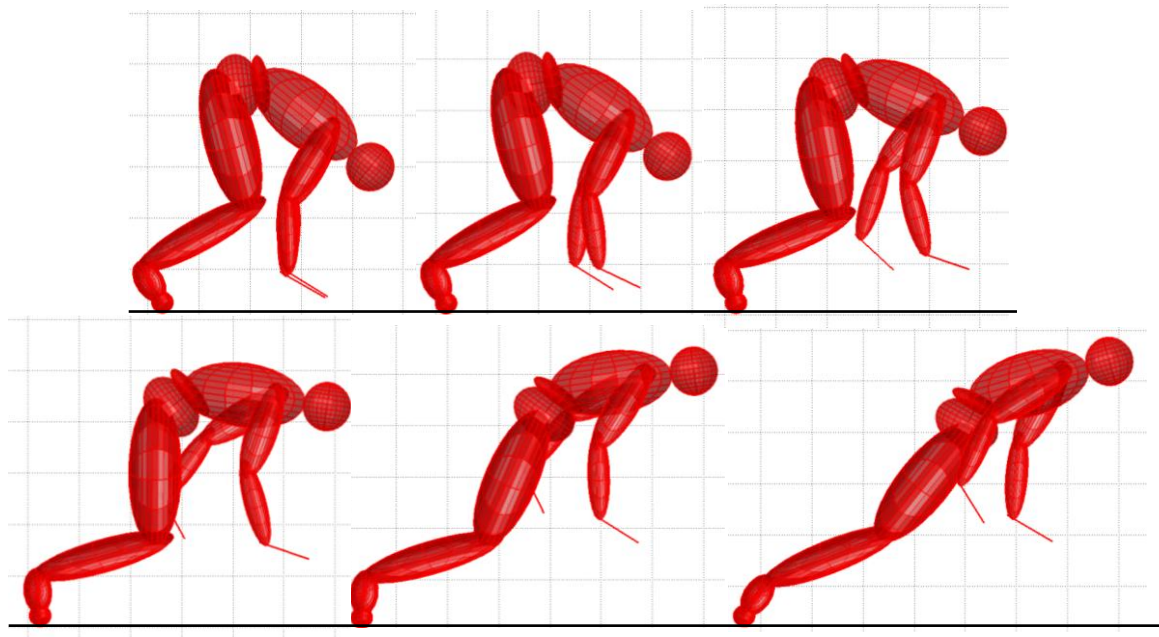
Figure 5.39. Bullet start output at 0.0758 s intervals.

It can be seen in Table 30 that the bullet start provided a somewhat improved performance when compared to the matched start but still less effective than the measured start. The combined horizontal impulse provided by the two legs together in the bullet start is also still 55.52 Ns less than that for the front and rear foot combined in the measured start. It is also only 6.49 Ns greater found in the matched start despite the 0.02s longer contact time. This resulted in 0.1 m·s^{-1} greater velocity than for the matched start on takeoff but still 0.04 m·s^{-1} at the same point in the measured data. Whilst this is interesting, it would have been more valuable if the matched model had achieved a close match to the measured start and then been optimised to examine if improvements could be made.

Table 30. Comparison of bullet start to matched start to measured data.

Start Variable	Bullet start	Matched start	Measured start	
Time (s)	0.374	0.354	0.374	0.403
CoM Height (m)	0.74	0.74	0.80	0.81
CoM horizontal Displacement (m)	0.54	0.49	0.59	0.69
Horizontal Velocity ($m \cdot s^{-1}$)	2.60	2.50	3.50	3.40
Vertical Velocity ($m \cdot s^{-1}$)	-0.1	0.10	0.50	0.30
Average Horizontal Acceleration ($m \cdot s^{-2}$)	6.95	7.06	9.36	8.44
*Peak Horizontal Force (N)	438.31	803.88	861.40	861.40
*Peak Vertical Force (N)	599.56	985.32	689.00	689.00
*Horizontal Impulse (Ns)	109.76	192.02	201.02	203.29
*Vertical Impulse (Ns)	147.28	249.14	191.02	193.29

* Forces and impulse are for the front foot for the matched and measured start but represents both in the bullet start.

For comparison the joint angles (Figures 5.40 – 5.45) for the bunched start are plotted along side those of the front leg during the measured start. Interestingly the leg angles appear to provide a close match to the left leg in the measured start (although this is still 30° mean RMS error). Some hyperextension can be seen at the hip however this is still likely to remain within the limits of the athlete's RoM. The ankle appears to follow a very similar pattern to the measured data apart from during the first 0.05 s where it extends rapidly compared to the measured data which slightly flexes. This put the ankles an average 14° more extended throughout the whole simulation. The movements at the shoulders appear almost unchanged from the matching simulation and this seems quite likely due to the incomplete optimisation and the relatively small effect arm movements are likely to have had on the score compared to the legs.

Finally, the plot for CoM for bullet start (Figure 5.46) is also lower than the measured start throughout the simulation and also fails to go as far. When examining the reason for this it seems that this is likely to be partly due to the knees not extending in the first half of the simulation. It seems more likely however that this is due to the high

vertical forces compared to the horizontal. In the measured data the horizontal peak forces and impulse are higher than they are vertically although the impulse data are relatively equal (10 Ns different at the front foot). In the bullet start this difference is 37.52 Ns but the proportionate difference is greater due to the lower impulse involved and results in a negative vertical velocity on take off.
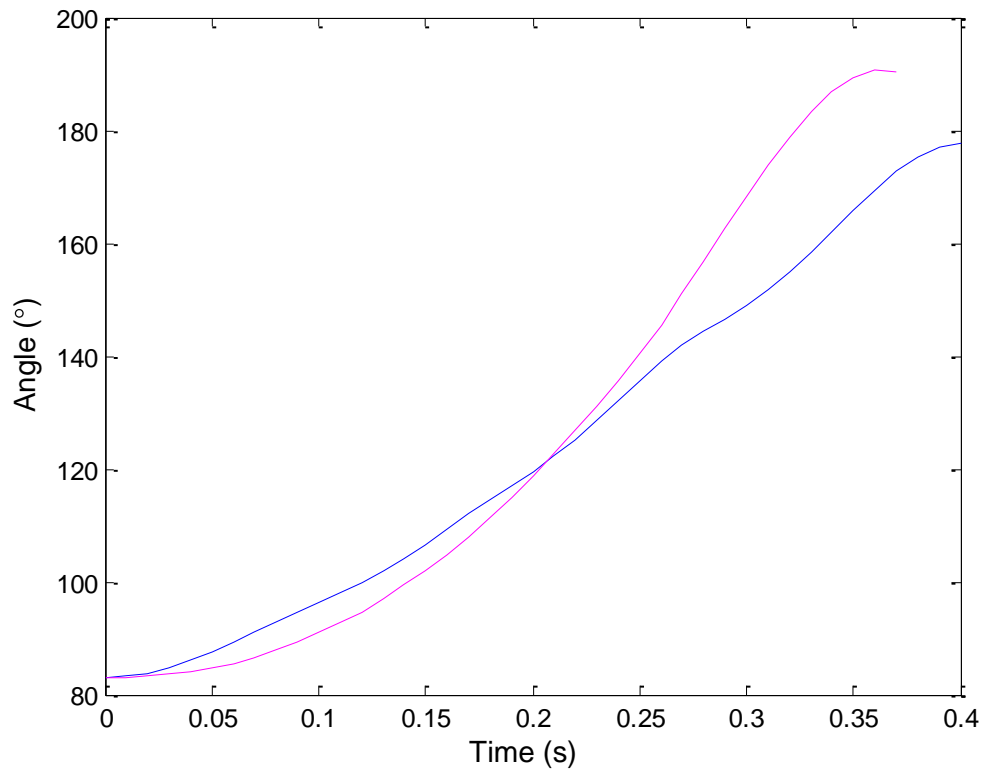
Figure 5.40. Comparison of hip angle during the measured start and modelled bullet start. Blue = measured start, pink = bullet start. Match = 11.32° RMS error.
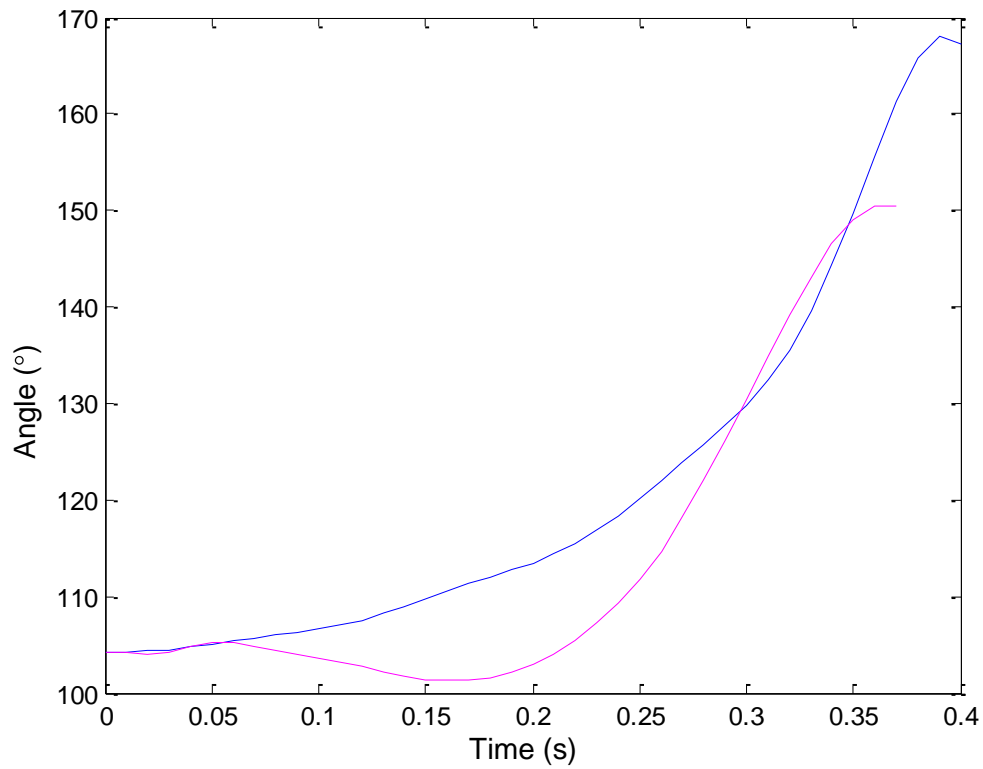
Figure 5.41. Comparison of knee angle during the measured start and modelled bullet start. Blue = measured start, pink = bullet start. Match = 6.20° RMS error.
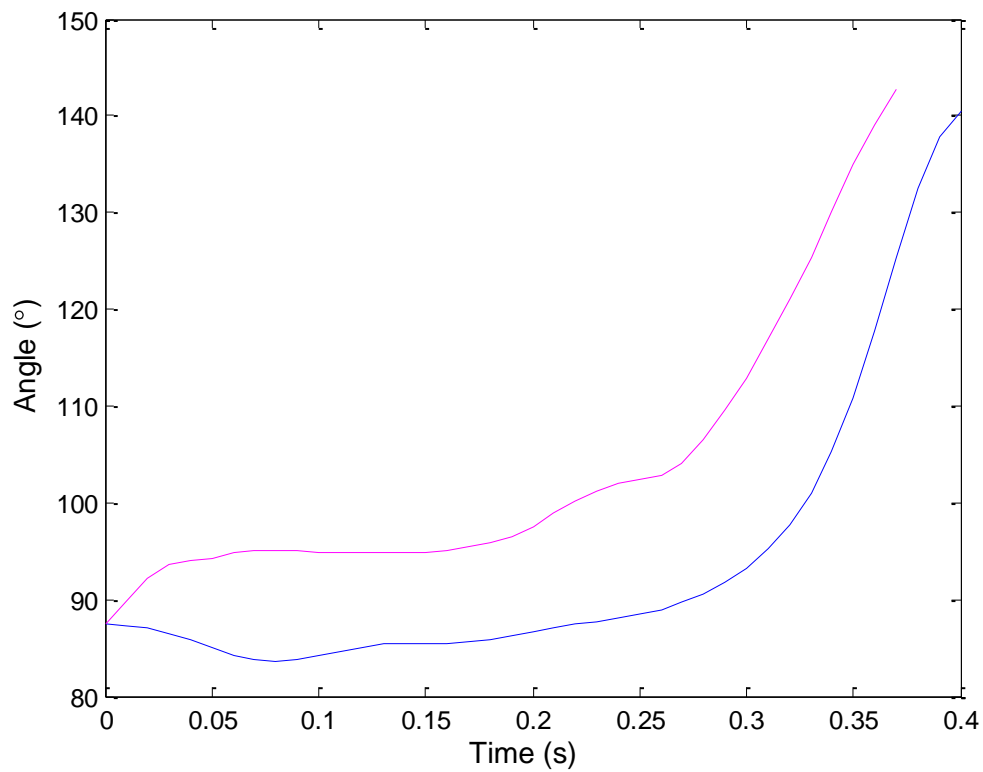
Figure 5.42. Comparison of ankle angle during the measured start and modelled bullet start. Blue = measured start, pink = bullet start. Match = 14.19° RMS error.
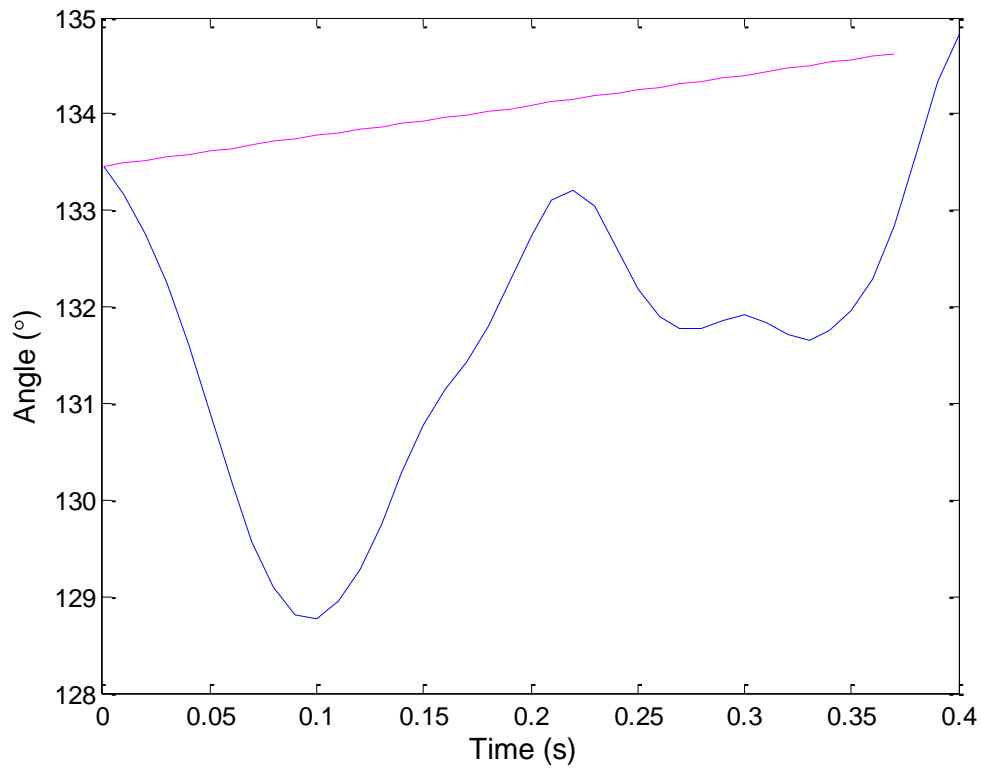
Figure 5.43. Comparison of T10 angle during the measured start and modelled bullet start. Blue = measured start, pink = bullet start. Match = 2.85° RMS error.
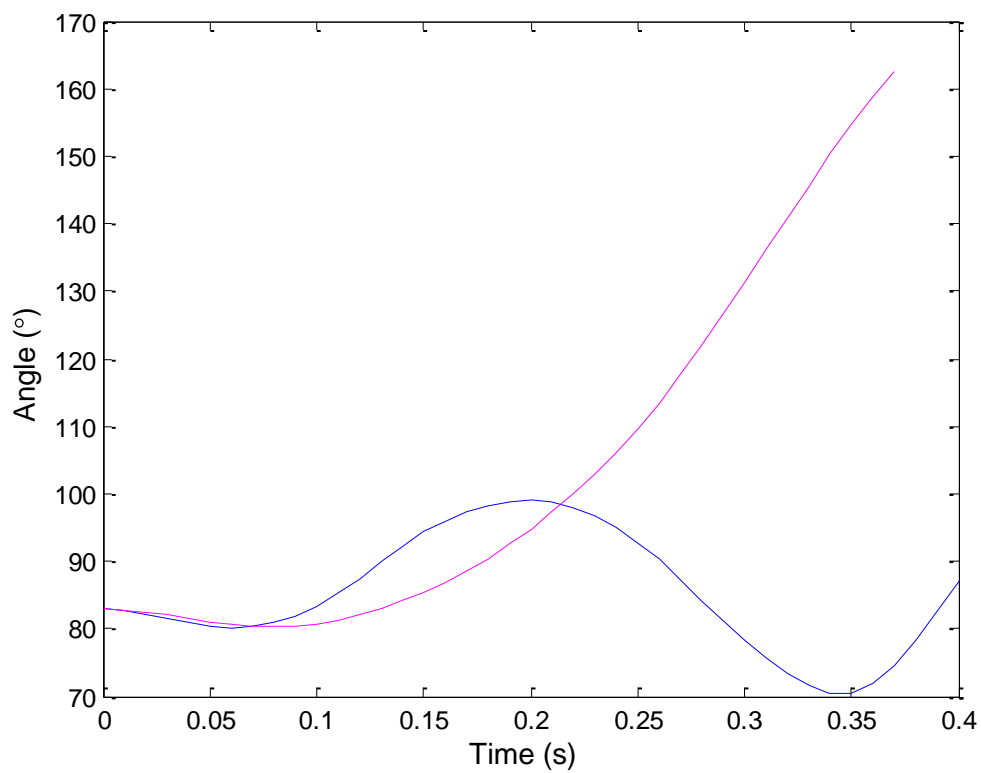
Figure 5.44. Comparison of Left shoulder angle during the measured start and modelled bullet start. Blue = measured start, pink = bullet start. Match = 36.70° RMS error.
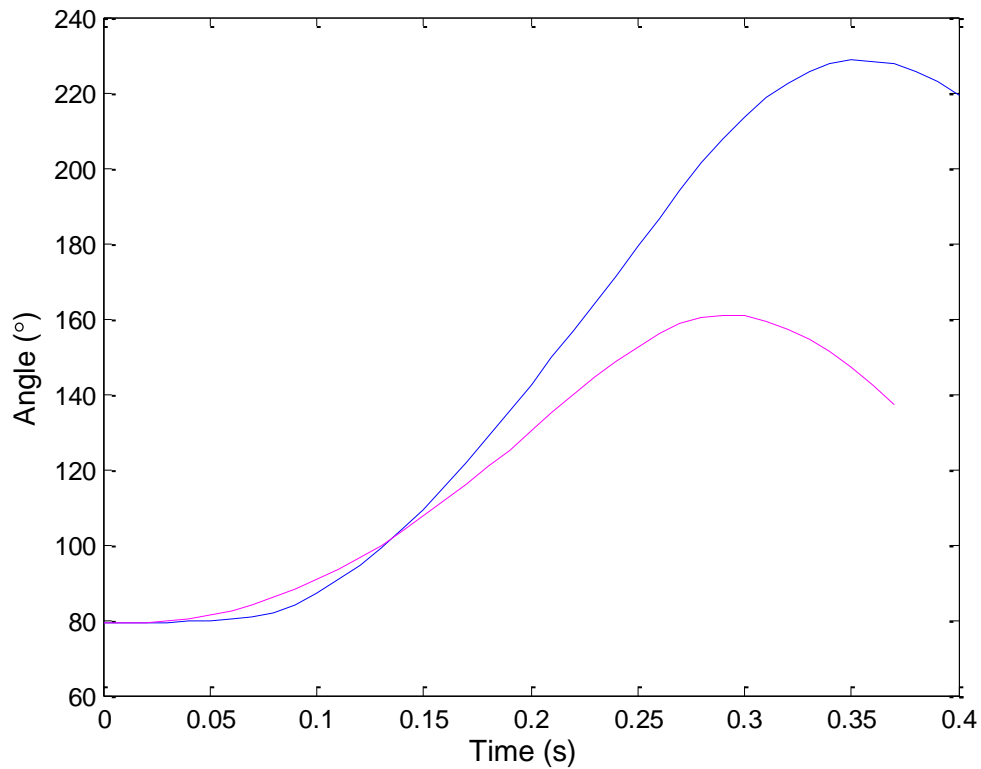
Figure 5.45. Comparison of right shoulder angle during the measured start and modelled bullet start. Blue = measured start, pink = bullet start. Match = 37.11° RMS error.
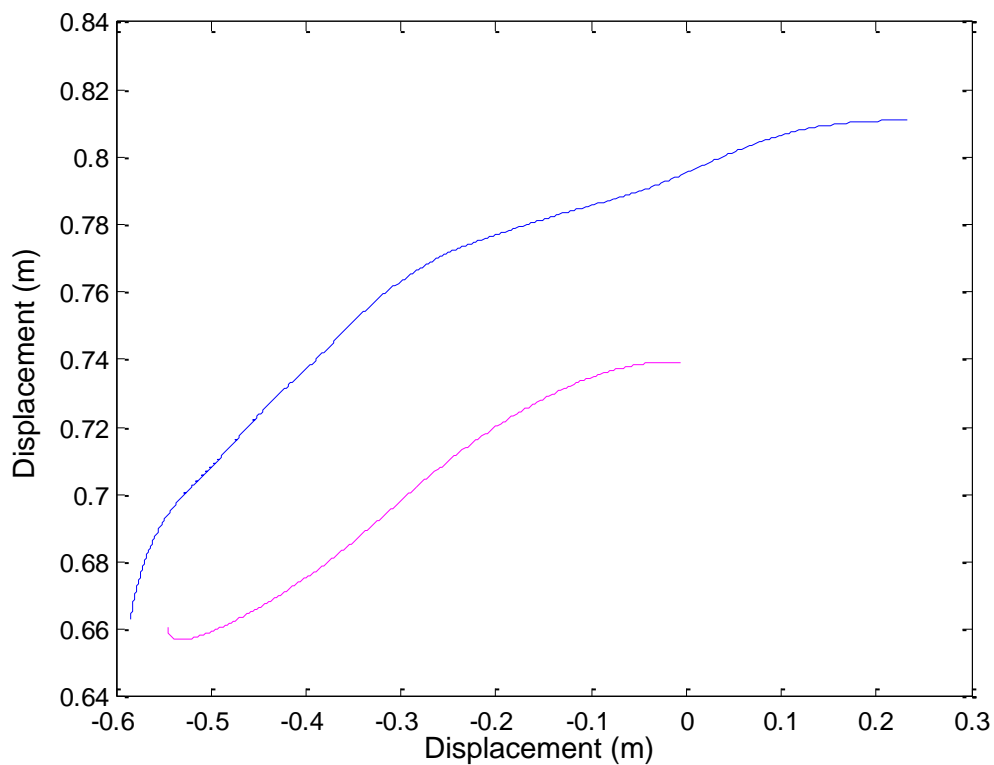
Figure 5.46. Comparison of CoM movement during the measured start and modelled bullet start. Blue = measured start, pink = bullet start. Match = 0.026 m RMS error horizontally and 0.0464 m RMS error vertically.

When examining the activation profiles, Figures 5.47a – e, it can be seen that the hip and knee are 50-60 % maximally activated in extension compared to the ankle which reaches the maximum possible activation extremely quickly (after 0.023 s). The knee also is very slow to develop activation and is only 10 % at 0.141 s. This may help explain why the knee failed to extend as rapidly as in the measured start and further suggest that the solution found was not a global optimum.
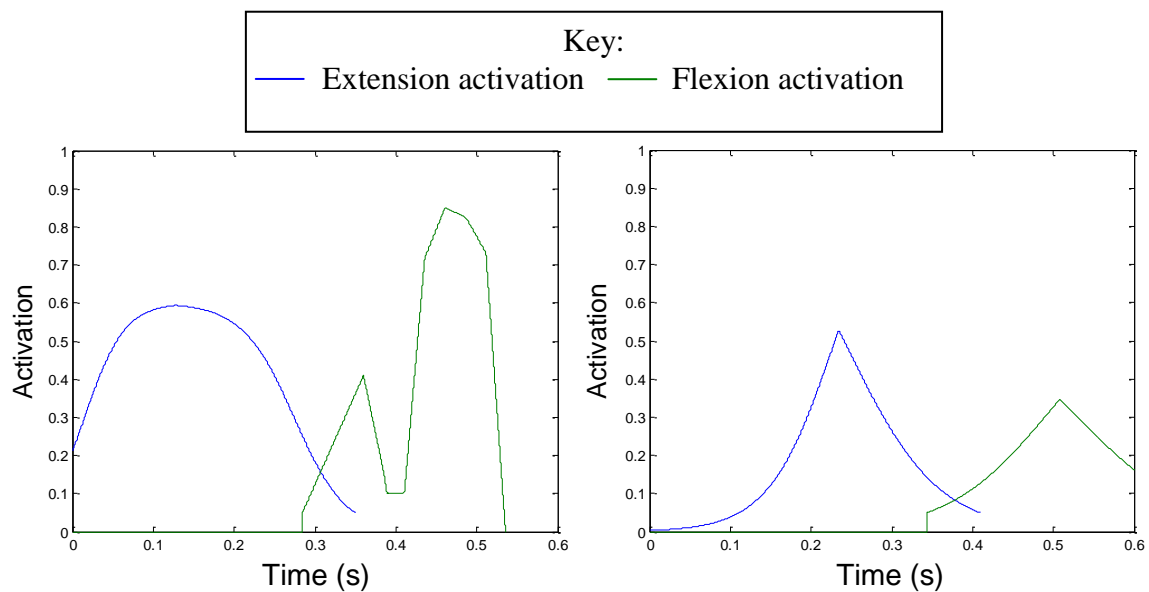
Figure 5.47a. Hip activation during the bullet start.

Figure 5.47b. Knee activation during the bullet start.
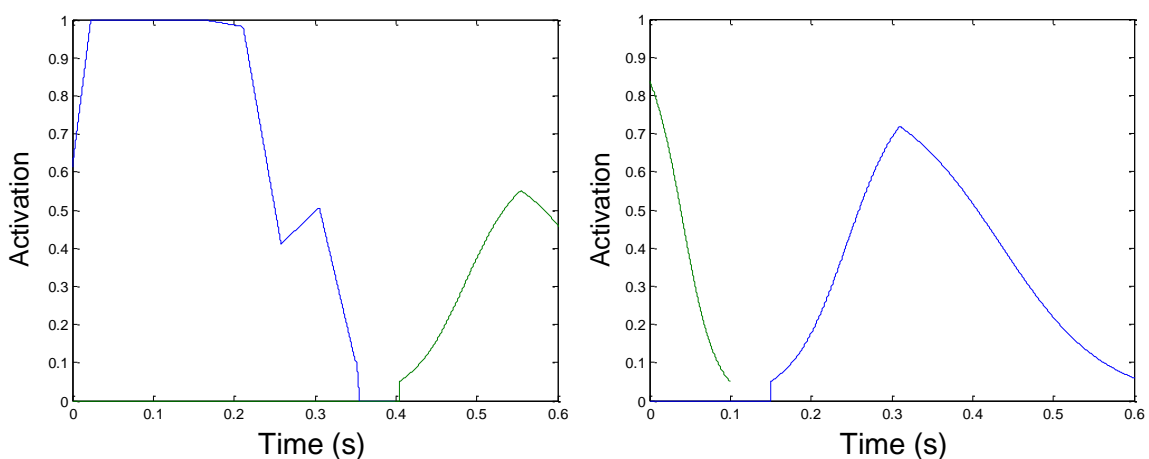
Figure 5.47c. Ankle activation during the bullet start.

Figure 5.47d. Left shoulder activation during the bullet start.
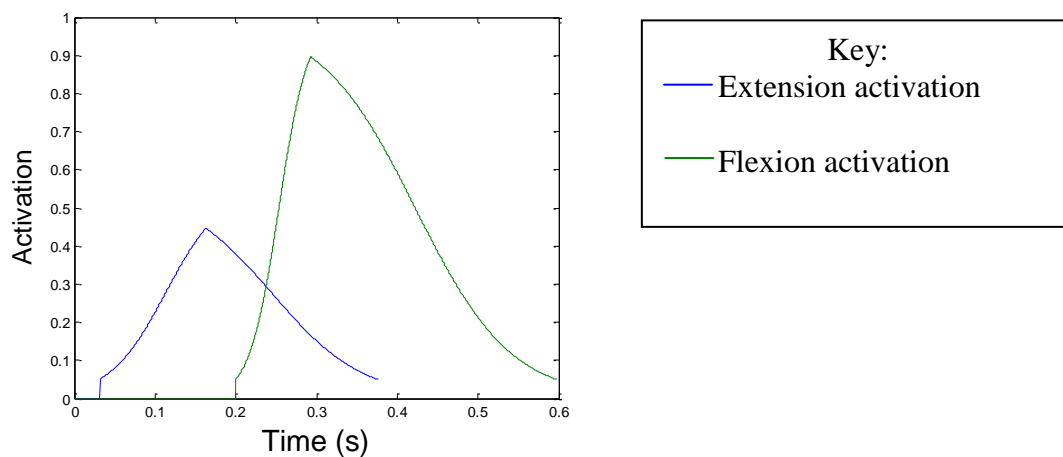
Figure 5.47e. Right shoulder activation during the bullet start.

The data for the bullet start suggests that this method of starting may provide an athlete with an effect method of starting a race based on a similar contact time and velocity when leaving the starting block compared to that found in the matched simulation. What is not clear is how the athlete may progress in the race from the end position found in the optimisation, as the athlete has both a negative vertical velocity and both legs together. A more finely optimised simulation that progresses further into the race is needed to make more definite conclusions about this method of starting.

5.9 Discussion

In this section two computer simulation models of the sprint start were created and evaluated; a fourteen segment angle driven model and a fourteen segment torque driven model. The angle driven model was used to optimise spring parameters for use in the torque driven model where it could be seen that the forces and patterns of force production were within reasonable limits. The torque driven model should perhaps be more correctly termed a twelve segment model due to the fixed angle at each elbow. The models are easily adaptable for use with different athletes and therefore whilst

they are useful for identifying relationships and important features in the sprint start, they will also be useful for improving the starts of individual athletes.

The time and computing power needed for optimisation meant that a full optimised match for the torque driven model was not found however the data produced did provide a constructive insight and showed that the model will be useful tool for future investigations. In the future, simulation time may be improved by compiling the model either within Matlab or another programming language such as C++ (e.g Almási and Padua, 2002). Furthermore, using a different optimisation algorithm such as genetic optimisation combined with parallel processing is likely to improve both simulation and optimisation times without compromising in finding a global minimum solution (e.g. Kwok and Ahmed, 1997; Hou et al, 1994).

The number of variables that were optimised to drive the torque driven model was large (120) which also meant a large number of simulations would be needed to find the global optimum solution. Simulated annealing was selected for the optimisation process as its ability to find global minima has been proven (Goffe at al., 1994). Given the long simulation time and the number of variables, it may have been an advantage to use a faster but perhaps less robust method such as Simplex or Direct. Direct optimisation was not used as, whilst it may have been slightly faster than simulated annealing, it does not use an initial guess, therefore when optimisations crashed, the data gained could only be used to tighten bounds rather than provide a better initial guess. Simplex was also not selected based on initial work with it where it tended to find local minima in problems with far fewer variables. It was therefore decided that an incomplete optimisation using simulated annealing would provide better results than the other options available at the time. As the much of the final solution was manually optimised a debate remains at to the best solution for future work.

When examining the activation profiles used to control the models, it was noticeable that linear activation profiles made little use of their ability to both rise and fall within their period of activation. It is likely that, given more time to optimise, these profiles would become more refined. Furthermore, this method is capable of providing profiles which don't follow a regular pattern such as provided by the sigmoid

function. It may also be considered that this method may be more appropriate for use in muscle driven models rather than torque driven models. For example Spagele et al. (1999) used a linear method for their jumping model but modelled nine muscle groups whereas King et al. (2006) used a sigmoid type function for their torque driven model. Therefore when muscles are represented in groups such as occurs in torque driven models, their relative contributions may become smoothed.

It was interesting that the front knee required little activation in the matching simulation but still extended more rapidly than in the measured start. Given the limitations of this kinetic chain little torque may indeed be needed if the torque at the hip is high. Consider a situation where there is high extension torque at the hip, a knee angle greater than 90° (as was the case here) and an angle at the ankle that is relatively stable, the knee will extend passively and so is not needed to propel the athlete. Conversely, the EMG data collected suggested strong contractions at the knee and this therefore may support the importance of the use of bi-articular muscle action in the sprint start. This also supports data presented in the four segment model where performance dropped when the knee angle approached 90°.

In Chapter 4 it was discussed that representation of bi-articular muscle action in the model may have improved performance. Van Soest et al. (1993) found that in their jumping model that the model jumped 10 mm higher with the use of a bi-articular Gasrocnemius. The difference in horizontal CoM movement between the matched model and one based on the measured performance was 20 mm and so this is a significant portion of the difference. Even if the bi-articular muscles are not active, Riener and Edrich (1999) observed that the elastic properties of the bi-articular muscle alone will contribute to joint torque but that this is also quite dependent on the joint angle at the first joint crossed. Whilst the effect of this was relatively small, it does raise questions for the sprint start as to the influence of joint angles on the effect of the bi-articular muscle action. Bobbert and Van Ingen Schenau (1988) noted that the Gastrocnemius is likely to be particularly important in the last 60 ms of push off in jumping. This is when the angle at the knee is large and increasing and therefore helps to increase the level of torque possible at the ankle.

With the seemingly high importance for obtaining large horizontal impulses in the start it was surprising that the athlete did not approach full extension at rear knee during the data collections. This concurs with Merni et al (1992) who noted rear leg knee angle on takeoff to be 144° which was an extension of just 5° from the 'set' position. To achieve a high velocity movement, many sports use a large RoM, e.g. baseball pitching, javelin throwing, and football punting. Blazevich (2007) described how sprinters attempt to extend the lower limb as far as possible in order to increase the time of force application and so impulse. Conversely, to achieve a movement in the fastest possible time, Jessop and Pain (2004) showed that reducing RoM through reducing the number of segments allowed a reduced time for completion of the movement but at the expense of a high peak velocity. This may therefore explain relatively small extension in the rear leg, i.e. the athlete sacrificed some impulse in favour of completing the movement more quickly.

A large RoM , particularly at the hip and knee, may have been needed in the simulation in order to help achieve a higher velocity which it lacked. With factors such as this in mind it confirms that only simulating until takeoff is quite limiting and much information could be gained from simulating further into the race. Furthermore this is something that has implications for optimum block spacings.

A longer simulation would also be necessary to give appropriate consideration to different starting positions. It seems that a variety of points may need to be considered when examining sprint start performance. Vitally some measure beyond the initial start should be considered. For example, if an athlete finds a start that allows them to perform the first few steps extremely quickly but then they fall over, this would only be shown with measurement taken later on. With this in mind it seems sensible that studies should continue analysing the athlete after the start but also consider that the further the athlete is from the start the greater the amount of time has passed in which intervening events may occur.

The results of the bullet start indicated that this method of starting has some potential but it also seemed likely that it would cause coordination issues for athletes performing it. In Section 4.4 it was discussed that a large amount of training is likely

to be required for a successful alteration of starting position due to muscular limitations but coordination/ neural limitation are also likely to be important. One criticism of previous studies is that insufficient practise has been given for athletes to learn alternative starting positions and hence this is likely to contribute to the finding that many studies observe 'medium' type starts to be preferred. Bobbert and van Soest (1994) suggested that high velocity and short times involved in jumping movements reduce the level of neural feedback which may be used to control the performance. If in turn the movement is not well learned, the likely result is a below optimal control pattern and movement sequence. It is considered that the same will apply to the sprint start. Indeed Ridderikhoff et al. (1999) noted how the "adaptation of net joint moments to the inclination angle of the jump is anticipated" for a standing long jump.

One of the areas where the matched and bullet simulations appeared to lack in similarity to measured data was at the shoulders. A reduced RoM was clear although the left shoulder was headed in the right direction by the end of the simulation. The activations at the shoulders were relatively large although not maximal and therefore this problem may be solved through increased activation. The alternative is that the poor RoM is caused due the fixing of the elbow angle. Figures depicting the model based on measured data shows that the elbows do become quite flexed and therefore obtain a much smaller moment of inertia. This will reduce the torque required and hence allow a greater RoM in a smaller time span. The difficulty of including this into the model would not be large. As mentioned, the joint angle was fixed initially to simplify the model and reduce the number of parameters needed to optimise it. Therefore once an optimal solution is found for the existing model, it would not be a great step further to include torque generators at the elbows.

The removal of the horizontal springs at the hands in the fourteen segment torque driven model allowed the computer model to run more smoothly. From a modelling perspective, the absence of horizontal springs at the hands may encourage an optimum solution which has insufficient vertical velocity of the CoM. This is because, without horizontal springs, the model can travel forwards even if the vertical springs at the hands are exerting large forces (due to a little or negative displacement of the hands). With horizontal springs at the hands, large vertical forces would not be permitted as

the hands would have to rise in order to allow positive horizontal movement of the CoM. The inclusion of horizontal springs at the hands may be particularly important in future versions of the model for investigations into strength and muscle activations in the 'set' position. Guitérrez-Dávila et al. (2006) observed that quick removal of negative forces at the hands is key if attempting to increase positive horizontal forces at the feet. Not representing the horizontal forces at the hands in this model may therefore have allowed higher horizontal velocities than would be seen with the inclusion of such springs.

This section has shown that a number of improvements are required to the model such as faster simulations, horizontal forces at the hands in the set position, simulation further into the race and torque driven elbows for it fulfil its potential. Beyond this, constructing the model in three dimensions would also provide interesting insights into issues such as block widths. This is likely to be complicated by the limitations of obtaining the relevant torque data but a start which simulates adduction/ abduction movements is certainly more feasible. Currently however, the simulation model has shown promising results which can be worked on in the future.

Chapter 6.

Summary and Conclusions

This section will bring together the research that has been presented and previously discussed. It will also be considered how various factors caused limitations for the project. Finally the research questions that were set out in Chapter 1 will be answered and the thesis concluded.

6.1. Summary

This study has presented methods for collecting experimental sprint start data as well as four and fourteen segment computer simulation models of the sprint start. The computer models simulate the athlete in the set position up until takeoff from the starting blocks or touchdown in the first step. The models may be easily customised to individual athletes to reflect their anthropometric and strength characteristics and so are considered a potentially useful tool for sprint start research.

Methods for collection of sprint start data have been presented. Particularly an anatomic model and marker set were designed for collection of kinematic data which included methods for finding marker locations which become occluded when the athlete is in the 'set' position. A method was also presented for calibration of force transducers inserted into starting blocks.

It has been shown that simple models have been able to establish important relationships in activities such at the jumping. The four segment model of the sprint start presented in this project suggested that several important interactions exist when determining the initial starting position for an athlete, particularly at the hip and knee. At the hip the model suggested that using as small an angle as possible is important whilst at the knee an optimum position, which was not far from the existing position used by the subject, was found.

The effects of increased strength and increased muscle activation were examined in the four segment torque driven model. Increasing strength increased horizontal velocity on takeoff for some simulations but not all whilst increased activations did not result in concurrent increases in velocity. This may be due to model control, model complexity or most likely, is the result of local minima when optimising. Both increased activations and strength did however result in increases in horizontal acceleration.

The models were created using Matlab and Simulink and whilst this was regarded as relatively user friendly, long simulation times and large amounts of required computing power resulted in a good match not being found for the fourteen segment torque driven model.

6.2. Limitations

The sprint start has been said to influence the rest of the race, with this in mind, studies conducted on sprint starting should consider how the start affects the whole race and should not be regarded as an isolated event (Menely and Rosemier, 1969). Furthermore block velocity may be a poor indication of performance by as early as 20m (Mendoza and Schölhorn, 1993). With these points in mind, modelling the sprint start further into the race seems an important consideration for future models as well as selection of objective functions for optimisation.

The study has shown that, for each athlete, there is an ideal optimum start based on the athlete's strength profile. Bradshaw et al. (2007) note that sprinters should have a "flexible joint coordination strategy" which would help them cope with small environmental differences such as the surface type and small differences in block positioning. Therefore is should be considered that environmental factors may also influence the athlete as well as their consistency in finding their start position.

With initial testing revealing that it would not be possible to collect data in one session it became infeasible to collect data on an athletics track. Data for the study was all collected in the Loughborough University Biomechanics Laboratory and

therefore the subject was not able to wear sprint shoes/ spikes due to the thin carpet surface and uncovered force platform. Whilst the athlete did not complain of slipping, this was quite a different environment to the beginning of a 100 m race in competition. To help ensure high quality data the subject was motivated by the researcher and others present to try their hardest and high speed video of the starts were provided back to the athlete to view with their coach.

The difficulty of dynamically calibrating the starting blocks does bring in to question the validity of the force data used for matching the simulations and establishing spring parameters. Therefore, whilst the force data appeared to be reasonable, greater time and sophistication of methods used for calibration are likely to bring about improved accuracy in the resulting measurements.

As previously discussed, the marker set and anatomic model developed for data collection allowed useful kinematic data to be collected. The major limitation of this model was the large number of markers that were used. Whilst this help ensure a high quality of kinematic data, it was part of the issues that prevent all the data being collect at one time and hence the EMG data used for the model came from a different trial to that used for the movement data. Whilst an effort was made to ensure that the best possible match was found, this can still be considered something that should be addressed for future developments of the model. Developments and the increasing availability of wireless technology may also permit use of EMG equipment alongside the marker set. This is because the surface EMG electrodes are placed over the belly of muscles whereas the reflective markers used for motion tracking were always placed on bony prominences to avoid unwanted movement. It was noticeable when researching information for the anatomic model that much information was available on the hip and quite a lot on the shoulder. For other joints such as the ankle and wrist, research appeared to be relatively sparse. It is considered that this didn't impinge on the results of the study but further research for these joints may be warranted.

Whilst the number of segments used to model the start appears be sufficient, there are a number of other enhancements that models for other activities have utilised in order to increase their closeness to reality. Models that replicate landings often include non- rigid segments or wobbling masses. For example, Mills et al. (2008) in

gymnastic landings, Wilson et al. (2007) in high jump take offs and Allen et al. 2010 for triple jumping. Gruber et al. (1998) note that very different torques and forces are calculated in a model without wobbling masses particularly during the first 10-30 ms of an impact and Gittoes et al. (2006) noted a 52% improvement in the replication of force profiles. As no impact was modelled in this project, the neglect of wobbling masses doesn't seem problematic however, to model the sprint start further in to the race; this is something that should be considered.

Series and parallel elastic elements are also often modelled in conjunction with a contractile component. These recreate the elastic properties of tissues such at the tendon and aperneuroses which are connected to the muscle tissue and whilst the parallel component may be ignored as their influence in sports movements is small, series elastic components are often included (Yeadon and King, 2008). Muramatsu et al. (2001) note that the series elastic component becomes stretched during muscle contractions and also act as a mechanical buffer (Griffiths, 1990; cited in Muramatsu et al., 2001) and therefore the effects of this are not integrated into the model presented here of the sprint start. This may therefore have had particular influence toward RoM limits and large contractions.

Finally, it has previously been discussed that modelling the sprint start using a muscle model in order to include the effects of bi-articular muscles might have helped to better model the joint movements in the sprint start. Furthermore, the limited amount of the race simulated restricts the conclusions that may be drawn from the model.

6.3. Answers to Research Questions

This section will use the findings of the investigation in order answer the questions set out at in chapter 1.

Q1. Does the optimum start depend upon the methods used to evaluate it?

The question was answered using the four segment torque driven model and optimising 100Sim (the simulation based on measured data) using different objective

functions in the score equation. It was shown that optimising using velocity and impulse will lead to the same result but optimising using time or acceleration will not. This therefore also raises the question of which is most useful?

Q2. How do joint angles in the 'set' position influence the start?.

The four segment models showed that optimum joint angles in the 'set' position exist for individual athletes. Results from the four segment angle driven model suggested that the athlete in this study would benefit from using smaller joint angles in the 'set' position. The four segment torque driven model identified that the athlete will particularly benefit from using an angle smaller (than his current 83°) at the front hip. The variation in the angles chosen was too great to determine if the athlete should alter the angle at the knee. Due to the incomplete optimisation of the fourteen segment model, this question can only be answered based on the results from the four segment model. Furthermore, given the discussion presented on the inclusion of bi-articular muscles in models of the sprint start, it would seem wise to acknowledge and investigate this area further.

Q3. How does increasing muscle tension in the 'set' position affect the start?

Initial activations were increased in the four segment torque driven model in order to reflect increased muscle tension at the start. It was shown that increased activation failed to increase the athlete's horizontal velocity on takeoff but did increase horizontal acceleration. Increasing the number of body segments and model control may help to further investigate this area in the future.

Q4. Does increased strength alter the best starting technique?

Strength was shown to limit sprint start performance in the four segment angle driven model as it limited the RoM that might be used in the 'set' position. In the four

segment torque driven model, an increase in strength was shown to increase horizontal velocity from the starting block by a small amount.

6.4. Future work

The four segment model has provided interesting results for this project and therefore it would be interesting to increase both the RoMs examined at the same time as reducing the increment between angles. This would therefore both allow a better overview of the interactions involved as well as increase the model's ability to find optimum joint angles. It may also be interesting to optimise the block angle as a separate variable.

Whilst the 14 segment model has been shown to work, its ability to accurately represent a sprint start has still not been successfully proven. This was primarily due to the large amount of computing power and time needed to optimise the simulations. Time in the future may be best spent compiling the model using a difference code or software package. This would allow the simulations to run faster and therefore increase it use and value as a research tool.

Given the previous discussions surrounding modelling the effects of bi-articular muscles, it would be interesting to develop a model which includes this. Even if this was only done in the four segment model initially, it would be interesting to examine the effects on resulting simulations.

Once the model runs satisfactorily it will be interesting to examine the effects of changes in the 'set' position, as well as increases in strength and initial activations in order to further investigate the findings from the four segment models. Furthermore, it will be useful to improve the model to simulate the start further into the race. In this way it would be more possible to specify initial conditions and movement patterns and indeed if velocity or acceleration provides the most use criteria when assessing sprint start technique. This data may also be gained experimentally and would therefore provide useful comparison data for the model.

Working with athletes would also be a useful step in using the model for practical situations to find their optimum starts. As previously discussed, it may take long time for athletes to become accustomed to any changes but, after all, the ultimate aim of research such as this is to improve athletes' performances.

6.5. Conclusion

The data needed run a comprehensive model of the sprint start is large. Methods have been presented for collecting subject specific kinetic and kinematic sprint start data. Simple computer simulation of the sprint start using Matlab and Simulink has been shown to be possible and has allowed fundamental issues to be examined. The major practical findings in this study have been based around four segment angle and four segment torque driven models of the sprint start. It has been shown that an optimum 'set' position exists and that this is will be individual to each athlete. Improved RoM (if strong enough), strength and muscle activations are all likely to lead to increases in starting performance.

Increasing model complexity resulted in a concurrent increase in the computing power needed to run and optimise the model. It is therefore considered that future work will focus on methods of running simulations more quickly. Additional evaluation and optimisation of the more complex models in this study, in conjunction with practical work with athletes, will allow refinement of predictions made on 'real life' performances.

REFERENCES

Alexander, R, McN. (1991). Optimum timing of muscle activation for simple models of throwing. *Journal of Theoretical Biology*. **150**, 349-372.

Alexander, R. McN. (1990). Optimum take-off techniques for high and long jump. *Philosophical Transactions of the Royal Society of London, Series B*. **329**, 3-10.

Allen, S. J. (2010). Optimisation of performance in the triple jump using computer simulation. *A Doctoral Thesis*. Loughborough University.

Allen, S. J., King, M. A. and Yeadon, M. R. (2010). Is a single or double arm technique more advantageous in triple jumping. *Journal of Biomechanics*. **43**, pp. 3156 – 3161.

Almási, G. and Padua, D. (2002). Majic: compiling matlab for speed and responsiveness. In: *Procceedings of ACM SIGPLAN Conference on Programing Language Design and Implementation*. June, 294-303.

Anderson, L. L. and Aagaard, P. (2006). Influence of maximal muscle strength and intrinsic muscle contractile properties on contractile rate of force development. *European Journal of Applied Physiology*. **96** (1), 46-52.

Atwater, A. E. (1982). Kinematic analyses of sprinting. *Track and Field Quarterly Review*. **82**, 12-16.

Baker, R. (2003). ISB recommendation on definition of joint coordinate systems for the reporting of human joint motion—part I: ankle, hip and spine**.** *Journal of* Biomechanics. **36** (2), 300-302.

Bartlett, R. M. (1980). The mechanics of sprint starting- frictional considerations. *Athletics Coach*. **14** (4), 20-23.

Baumann, W. (1976). Kinematic and dynamic characteristics of the sprint start. In Komi, P. V. (Ed) *Biomechanics V-B*, University Park Press, Baltimore, 1976.

Beaumont, G. D. (1980). Biomechanical aspects of sprint starting. *Athletics Coach*. **14** (2), 25-28.

Beiser, T. F., Sturnieks, D. L., Alderson, J. A. and Lloyd, D. G. (2003). Repeatability of gait data using a functional hip joint centre and a mean helical knee axis. *Journal of Biomechanics*. **36**, 1159-1168.

Bell, A. L., Brand, R. A. and Pederson, D. R. (1989). Prediction of hip joint centre location from external landmarks. *Human Movement Science*. **8**, 3-16.

Bell, A. L., Pederson, D. R. and Brand, R. A. (1990). A comparison of the accuracy of several hip centre location prediction methods. *Journal of Biomechanics*. **23** (6), 617-621.

Bezodis, N., Trewartha, G. and Salo, A. I. T. (2007). Choice of performance measure affects the evaluation of sprint start performance. In: *Annual Conference of the British Association of Sport and Exercise Sciences 2007*, 11 - 13 September, 2007, University of Wolverhampton, Walsall Campus, UK.

Bezodis, N., Salo, A. I. T. and Trewartha, G. (2010). Choice of sprint start performance measure affects the performance-based ranking within a group of sprinters: which is the most appropriate measure? *Sports Biomechanics*. **9** (4), pp. 258 – 269.

Bhommick, A. K. and Bhattacharyya, A. K. (1988). Kinematic analysis of arm movements in sprint start. *Journal of Sports Medicine*. **28**, 315-323.

Biancani, A. (1975). Wider foot placement for faster starts. *Track Technique*. **62**, 1961.

Blader, B. F. (1968). The analysis of movements and forces in the sprint start. *Biomechanics I*. 1st International Seminar, Zurich (1967), 278-281. Karger, Basel/ New York.

Blazevich, A. J., Cannavanm D., Horne, S., Coleman, D. R. and Aagaard, P. (2009). Changes in muscle force-length properties affect the early rise of force in vivo. *Muscle and Nerve*. **39** (4), 512-520.

Blazevich, A. J. (2007). *Sports Biomechanics: The Basics: Optimising Human Performance*. A & C Black

Borzov, V. (1980). An optimal starting position. *Modern Athlete and Coach*. **18** (1), 4-5.

Bobbert, M. F. and Van Ingen Schenau, G. J. (1988), Coordination in vertical jumping. *Journal of Biomechanics*. **21** (3), 249-262.

Bobbert, M. F. and Soest A. J. van (1994). Effects of muscle strengthening on vertical jump height: a simulation study. *Medicine and Science in Sport and Exercise*. **26** (8), 1012-1020.

Bojsen-Møller, J., Magnusson, S. P., Rasmussen, L. R., Kjaer, M. and Aagaar, P. (2005). Muscle performance during maximal isometric and dynamic contractions is influenced by the stiffness of the tendinous structure. *Journal Applied Physiology*. **99** (3), 986-994.

Brooks, S. P. and Morgan, B. J. T. (1995). Optimisation using simulated annealing. *Statistician*. **44** (2), 241-257.

Cappozzo, A., Catani, F., Della Croce, U. and Leardini, A. (1995). Position and orientation in space of bones in movement: anatomical frame determination and definition. *Clinical Biomechanics*. **10** (4), 171-178.

Cavanagh, P. R. and Komi, P. V. (1979). Electromechanical delay in human skeletal muscle under concentric and eccentric conditions. *European Journal of Applied Physiology and Occupational Physiology*. **42** (3), 159-163.

Chow, J. W., Darling, W. G. and Ehrhadt, J. C. (1999). Determining the force-length-velocity relations of the quadriceps muscles: 1. Anatomical and geometric parameters. *Journal of Applied Biomechanics*. **15,** 182-190.

Chowdhary, A. G. and Challis, J. H. (2001). The biomechanics of an overarm throwing task: a simulation model examination of optimal time of muscle actions. *Journal of Theoretical Biology*. **211**, 39-53.

Christie, L. (1995). *To Be Honest With You*. Michael Joseph: London.

Clarke, D. H. and Clarke, H. (1984). *Research Processes in Physical Education*. Prentice Hall: London.

Čoh, M., Jošt, B., Škof, B., Tomažin, K. and Dolenec, A. (1998). Kinematic and kinetic parameters of the sprint start and start acceleration model of top sprinters. *Gymnica.* **28**, 33-44.

Corana, A., Marchesi, M., Martini, C. and Ridella, S. (1987). Minimising multimodal functions of continuous variables with the 'simulated annealing' algorithm. *ACM Transactions on Mathematical software*. **13** (3), 262-280.

Davis III, R. B. Õunpuu, S., Tyburski, D. and Gage, J. R. (1991). A gait analysis data collection and reduction technique. *Human Movement Science*. **10**, 575-587.

Dempster, W.T. (1955). Space requirements of the seated operator. *Technical Report USAF, WADC TR-55-159 (AD 87 892)*. Wright Air Development Center, Wright-Patterson Air Force Base, Ohio.

Desipres, M. (1978). Kneeling and standing sprint starts. *Track Technique*. **72**, 2302-2303.

Dickenson, A. D. (1934). The effect of foot spacing on the starting time and speed in sprinting and the relation of physical measurements to foot spacing. *Research Quarterly*. **5**, 12-19.

Domire, Z. J. and Challis, J. H. (2007). The influence of squat depth on maximal vertical jump performance. *Journal of Sports Sciences*. **25** (2), 193-200.

Dudley, G. A., Harris, R. T., Duvoisin, M. R., Hather, B. M. and Buchanan, P. (1990), Effect of voluntary vs. artificial activation on the relationship of torque to speed. *Journal of Applied Phyisology*. **69**, 2215-2221.

Faverial, J., Basset, F., Azizah, M. G. and Teesdale, N. (2000). Kinetic and kinematic analysis of the sprint start. *Archives of Physiology and Biochemistry.* **108** (1/2), 135.

Ferdinands, R. E. D., Kersting, U. and Marshall, R. N. (2008). A preliminary forward solution model of cricket bowling. *International Journal of Sports Science and Engineering*. **2** (4), 211-215.

Finkel, D. E. (2003). *DIRECT Optimisation Algorithm User Guide*. Centre for Research in Scientific Computation: North Carolina State University.

Forrester, S. (2006). Joint torque data. [electronic files] (personal communication).

Fujii, Y. and Fujimoto, H. (1999). Proposal of an impulse response evaluation method for force transducers. *Measurement Science and Technology*. **10**, N31 – N33.

Gagnon, M. A. (1978). Kinetic analysis of the kneeling and standing starts in female sprinters of different ability. In: Asmussen, E. and Jorgensen, K. (eds). *Biomechanics VI-B*. Baltimore: University Park Press.

Gander, R. E., McClements, J. D., Sanderson, L. K., Rostad, B. A. Josephson, K. E. and Pratt, A. J. (1994). Sprint Start Instrumentation. *IEEE Transactions on Instrumentation and Measurement*. **43** (4), 637 – 643.

Gittoes, M. J. R., Brewin, M. A. and Kerwin, D. G. (2006). Soft tissue contributions to impact forces simulated using a four-segment wobbling mass model of forefoot-heel landings. *Human Movement Science*. **25**, 775 – 787.

Goffe, W. L., Ferrier, G. D. and Rogers, J. (1994). Global optimisation of statistical functions with simulated annealing. *Journal of Econometrics*. **60**, 65-99.

Griffiths, R. I. (1991). Shortening of muscle fibres during stretch of the active cat medial gastrocnemius muscle: the role of tendon compliance. *Journal of Physiology*. **436**, pp. 219 – 236.

Gruber, K. Ruder, H. and Denoth, J. (1998). A comparative study of impact dynamics: wobbling mass model versus rigid body models. *Journal of Biomechanics*. **31** (5), pp. 439 – 444.

Guissard, N., Duchateau, J. and Hainaut, K. (1992). EMG and mechanical changes during sprint starts at different block obliquities. *Medicine and Science in Sport and Exercise*. **24** (11), 1257-1263.

Guissard, N. and Duchateau, J. (1990). Electromyography of the sprint start. *Journal of Human Movement Studies*. **18**, 97-106.

Gutiérrez-Davilla, M., Dapena, J. and Campos, J. (2006). The effect of muscular pre-tensing on the sprint start. *Journal of Applied Biomechanics*. **22**, 195-201.

Harland, M. J. and Steele, J. R. (1997). Biomechanics of the sprint start. *Sports Medicine*. **23** (1), 11-20.

Hatze, H. (1983). Computerized opimization of sports motions: An overview of possibilities, methods and recent developments. *Journal of Sports Sciences*. **1** (1) 3-12.

Hatze, H. (1981a). A comprehensive model for human motion simulation and its application to the take-off phase in the long jump. *Journal of Biomechanics*. **14**, 135-142.

Hatze, H. (1980b). Estimation of myodynamic parameter values from observation on isometrically contracting muscle groups. *European Journal of Applied Physiology*. **46**, 325-338.

Hatze, H. (1980). A mathematical model for the computational determination of parameter values of anthropomorphic segments. *Journal of Biomechanics*. 13, 833-843.

Hayden, T. C. and Walker, G. A. (1933). A comparison of the starting time of runners using holes in the track and starting block. *The Research Quarterly*. **4**, 117-123.

Hawkins, D. and Smeulders, M. (1999). An investigation of the relationship between hip extension torque, hip extension velocity and muscle activation. *Journal of Applied Biomechanics*. **15**, 253-269.

Helmick, K. (2003). Biomechanical analysis of sprint start positioning. *Track Coach*. **163**, 5209-5214.

Henry, F. M. (1952). Force-time Characteristics of the sprint start. *The Research Quarterly*. **23**, 301-318.

Henson, P., Cooper, J. and Perry, T. (2002). A wider look at the sprint start. *Track and Field Coaches Review*. **75** (4), 19-21.

Hiley, M. J. and Yeadon, M. R. (2003). Optimum technique for generating angular momentum in accelerated backward giant circles prior to dismount. *Journal of Applied Biomechanics*. **19** (2), 119-130.

Hill, A. V. (1938). The heat of shortening and dynamic constants of muscle. *Proceedings of the Royal Society B*. **126**, 136 -195.

Hobara, H., Kimura, K., Omuro, K., Gomi, K., Muraoka, T., Iso, S. and Kanosue, K. (2008). Determinants of difference in leg stiffness between endurance- and power-trained athletes. *Journal of Biomechanics*. **41**, 506-514.

Hof, A. L. (1984). EMG and muscle force: an introduction. *Human Movement Science*. **3**, 119-153.

Hou, E. S. H., Ansári, N. and Ren, H. (1994). A genetic algorithm for multiprocessor scheduling. *IEEE Transactions on Parallel and Distributed Systems*. **5** (2), 113-120.

Hollister, A. M., Jatana, S., Singh, A. K., Sullivan, W. S. and Lupichuk, A. (1993). The axes of rotation of the knee. *Clinical Orthopaedics and Related Research*. **290**, 259 – 268.

Hoster, M. and May, E. (1979). Notes on the biomechanics of the sprint start. *Athletics Coach*. **13** (2), 2-7.

Hubbard, M. (1993). Computer simulation in sort and industry. *Journal of Biomechanics*. **26** (suppl. 1), 53-61.

Huxley, A. F. (1957). Muscle structure and theories of contraction. *Prog Biophys Chem*. **7**, 255 – 318.

IAAF (2009). http://www.iaaf.org/community/athletics/trackfield/newsid=4661.html. [Accessed: 28/7/2009].

IAAF (2010). Competition Rules 2010 -2011. http://www.iaaf.org/mm/Document/AboutIAAF/Publications/05/47/80/20091027085 725_httppostedfile_CompRules-BAT_17164.pdf. [Accessed: 05/08/10].

Ikai, M. (1967). Biomechanics of sprint running with respect to the speed curve. *Biomechanics I, 1st International Seminar, Zurich*. 282-290. Karger: Basel/ New York.

Ingen Schenau, G. J. van ., Bobbert, M. F. and Rozendal, R. H. (1987). The unique action of bi-articuar muscles in complex movements. *Journal of Anatomy*. **155**, 1-5.

Jacobs, R. and Van Ingen Schnau, G. J. (1992). Intermuscular coordination in a sprint push-off. *Journal of Bioemchanics*. **25** (9), 953-965.

Jacobs, R., Bobbert, M. F., Van Ingen Schenau, G. J. (1996). Mechanical output from individual muscles during explosive leg extensions: the role of bi-articular muscles. *Journal of Biomechanics*. **29** (4), 513-523.

Jensen, R. K. (1976). Model for body segment parameters. In *Biomechanics V-B Komi, P. J. (Ed)*. Baltimore: University Park Press. 380-386.

Jessop, D. M. and Pain, M. T. G. (2004). Strategies for Maximum Velocity Movements in Relation to Reaction Time and Performance Outcome. *In Proceedings of the Annual Conference of The British Association of Sport and Exercise Sciences*. Liverpool John Moores University, 7th-9th September 2004. 17-18.

King, M. A. and Yeadon, M. R. (2004). Maximising somersault rotation in tumbling. *Journal of Biomechanics*. **37**, 471-477.

King, M. A. and Yeadon, M. R. (2002). Determining subjects specific torque parameters for use in a troque- driven simulation model of dynamic jumping. *Journal of Applied Biomechanics*. **18**, 207-217.

King, M. A., Yeadon, M. R. and Kerwin, D. G. (1999). A two segment model of long horse vaulting. *Journal of Sports Sciences*. **17**, 313-324.

King, M. A., Wilson, C. and Yeadon, M. R. (2006). Evaluation of a torque-driven model of jumping for height. *Journal of Applied Biomechanics*. **22**, 264-274.

Kistler, J. W. (1934). A study of the distribution of the force exerted upon the blocks in starting the sprint from various starting positions. *Research Quarterly*. **5** (Suppl. 1), 27-32

Komi, P. V. (1984). Biomechanics and neuromuscular performance. *Medicine and Science in Sports and Exercise*. **16**, 26-28.

Kubo, K., Kanehisa, H., Kawakami, Y. and Fukunaga, T. (2000). Elasticity of tendon structures of the lower limbs in sprinters. *Acta Physiologica Scandanavica*. 168, 327-335.

Kulig, K., Andrews, J. G., Hay, J. G. (1985). Human Strength Curves. *Exercise and Sport Sciences Reviews*. **13** (1), 417-466.

Kuo, A. D. (2001). The action of two-joint muscles: the legacy of W. P. Lombard. In: Latash, M and Zatsiorsky, V. (eds), *Classics in Movement Science*. Ch. 10, 289-315.

Kunz, H. and Kaufmann, C. A. (1981). Biomechanical Analysis of Sprinting: Decathletes versus champions. *British Journal of Sports Medicine*. **15** (3), 177-181.

Kwok, Y-K. and Ahmed, I. (1997). Efficient scheduling of arbitrary task graphs to multi-processors using a parallel genetic algorithm. *Journal of Parallel Distributed Computing*. **47** (1). 58-77.

Leva, P. de. (1996). Adjustments to Zatsiorsky-Seluyanov's segment inertia parameters. *Journal of biomechanics*. **29** (9), 1223-1230.

Leva, P. de (1996b). Joint centre longitudinal positions computed from a subset of Chandler's data. *Journal of Biomechanics*. **29** (9), 1231-1233.

London, J. T. (1981). Kinematics of the elbow. *Journal of Bone and Joint Surgery, American Volume*. **63**, 529 – 535.

Luca C. J. de, and Forrest, W. J. (1973). Force analysis of individual muscles acting simultaneously on the shoulder joint during isometric abduction. *Journal of Biomechanics*. **6**, 385 – 393.

Ludwig, D. A. (1978). Increased thrust duration during block starting. *Scholastic Coach*. **47**, 125-127.

Martin, D. E. and Buoncristiani, J. F. (1995). Influence of reaction time on athletic performance. *New Studies in Athletics*. **10** (1), 67-79.

Maughan, R. J., Watson, J. S. and Weir, J. (1983). Strength and cross-sectional area of human skeletal muscle. *Journal of Physiology*. 338, 37-49.

McInnis, A. (1980). In quest of speed- Improving farward body lean in the sprint start and early acceleration phase. *Track and Field Quarterly Review*. **80** (2), 25-31.

Mendoza, L. and Schollhorn, W. (1993). Training of the sprint start technique with biomechanical feedback. *Journal of Sports Sciences*. **11** (1), 25 - 9.

Menely, R. C. and Rosemier, R. A. (1969). Effectiveness of four track positions on acceleration. *The Research Quarterly*. **39** (1), 161-165.

Merni, F., Cicchella, B., Bombardi, F., Cacci, S., Magenti, L., Olmucci, S. and Coppini, L. (1992), Kinematic and dynamic analysis of sprint start. *International Symposium of Biomechanics in Sports (10th: 1992: Milan: Italy)*.

Mero, A. (1988). Force-time characteristics and running velocity of male sprinter during the acceleration phase of sprinting. *Research Quarterly for Exercise and Sport*. **59** (2), 94-98.

Mero, A., Harland, M. J., Kuitunen, S. and Komi, P. V. (1997). In: *Interrelationships between ground reaction forces and velocity during acceleration phase of the sprint start*. In: *XVIth ISB Tokyo Congress, August 25-29, 1997, Hosted by the University of Tokyo. Book of Abstracts, International Society of Biomechanics*. 301.

Mero, A. and Komi, P. V. (1990). Reaction time and electromyographic activity during a sprint start. *European Journal of Applied Physiology and Occupational Physiology*. **61**, 73-80.

Mero, A., Komi, P. V. and Gregor, R. J. (1992). Biomechanics of sprint running: a review. *Sports Medicine*. **13** (6), 376-392.

Mero, A., Luhtanen, P. and Komi, P. V. (1983). A Biomechanical study of the sprint start. *Scandinaian Journal of Sports Sciences*. **5** (1), 20-28.

Mero, A., Kuitunen, S., Harland, M., Kyrolainen, H. and Komi, P. (2006). Effects of muscle-tendon length on joint moment and power during sprint starts. *Journal of Sports Sciences*. **24** (2), 165-173.

Meskers, C. G. M., van der Helm, F. C. T., Rozendaal, L. A. and Rozing, P. M. (1998). In vivo estimation of the glenohumeral joint rotation centre form scapular bony landmarks by linear regression. *Journal of Biomechanics*. **31**, 93-96.

Mills, C., Pain, M. T. G. and Yeadon, M. R. (2008). The influence of simulation model complexity on the estimation of the internal loading in gymnastics landings. *Journal of Biomechanics*. **41** (3), 620-628.

Moore, N. E. (1980). The sprint start. *Track and Field Quarterly Review*. **80** (2), 22-23.

Morin, J. B. and Belli, A. (2002). Mechanical muscular parameters influencing 100m performance in trained athletes. *In Koskolou, M. (ed.), European College of Sport Science, Proceedings of the 7th annual congress of the European College of Sport Science, Athens, Greece, 24-28 July 2002, Athens*, Pashalidis Medical Publisher, 91.

Morrey, B. F. and Chao (1976). Passive motion of the elbow joint. *Journal of Bone and Joint Surgery, American Volume*. **58**, 501-508.

Muramatsu, T., Muraoka, T., Takeshita, D., Kawakami, Y., Hirano, Y. and Funkunaga, T. (2001). Mechanical properties of tendon and aperneurosis of human gastronemius muscle in vivo. *Journal of Applied Physiology*. **90**, pp. 1671 – 1678.

Neptune, R. R., Clake, D. J. and Kautz, S. A. (2009). Modular control of human walking: a simulation study. *Journal of Biomechanics*. **42** (9), 1282-1287.

Nesser, T. W., Latin, R. W., Berg, K. and Prentice, E. (1996). Physiological determinants of 40-metre sprint performance in young male athletes. *Journal of Strength and Conditioning Research*. **10** (4), 263-267.

Nelder, J. A. and Mead, R. (1965). A simplex method for function minimisation. *Computer Journal*. **7**, 308-313.

Nigg, B. M. and Herzog, W. (1999). *Biomechanics of the Musculo-Skeletal System*. Chichester; Wiley.

Oleson, M., Adler, D. and Goldsmith, P. (2005). A comparison of forefoot stiffness in running and running shoe bending stiffness. *Journal of Biomechanics*. **38** (9), 1886-1894.

Oxford Metrics Ltd. (2002a). *Bodybuilder for Biomechanics*. Oxford: Oxford Metrics Ltd.

Pain, M. T. G. and Challis, J. H. (2001). The role of heel pad and shank soft tissue during impacts: a further resolution of a paradox. *Journal of Biomechanics*. **34** (3), 327-333.

Pain, M. T. G. and Hibbs, A. (2007). Sprint starts and the minimum auditory reaction time. *Journal of Sports Sciences*. 25 (1), 79-86.

Palastanga, N., Field, D. and Soames, R. (2002). *Anatomy and Human Movement*. Oxford: Butterworth-Heinemann.

Pandy, M .G. (2003), Simple and complex models for studying muscle function in walking. *Philosophical transactions of the Royal Society of London, Series B*. **358**, 1501-1509.

Pandy, M. G. and Anderson, F. C. (2000). Dynamic simulation of human movement using large-scale models of the body. *Phonetica*. **57**, 219-228.

Pandy, M. G., Zajac, F. E., Sim, E. and Levine, W. S. (1990). An optimal control model for maximum height human jumping. *Journal of Biomechanics*. **23** (12), 1185-1198.

Panjab, M. (1979). Validation of mathematical models. *Journal of Biomechanics*. **12**, 238.

Payne, A. H. and Blader, F. B. (1971). The mechanics of the sprint start. *Medicine and Sport Vol 6: Biomechanics II,* 225-231. Karger, Basel.

Pender, M. (1983). The mechanics of the start. *Track and Field Quarterly Review*. **83** (2), p. 22.

Ridderikhoff, A., Batelaan, J. A. and Bobbert, M. F. (1999). Jumping for distance: control of the external force in squat jumps. *Medicine and Science in Sports and Exercise*. **31** (8), 1196-1204.

Riener, R. and Edrich, T. (1999). Identification of passive elastic joint moments in the lower extremities. *Journal of Biomechanics*. **32**. 539 – 544.

Salo, A. and Bezodis, I. (2004). Which starting style is fastest in sprint running-standing or crouch start? *Sports Biomechanics*. **3** (1), 43-54.

Schmidt, R., Disselhorst-Klug, C., Silny, J. and Rau, G. (1999). A marker-based measurement procedure for unconstrained wrist and elbow motions. *Journal of Biomechanics*. **32**, 615 – 621.

Schot, P. K. and Knutzen, K. M. (1992). A biomechanical analysis of four sprint start positions. *Research Quarterly for Exercise and Sport*. **63** (2), 137-147.

Seeley, R. R., Stephens, T. D., Tate, P. (1992). *Anatomy and Physiology*. St Louis; Mosby Year Book.

Seidel, G. K., Marchinda, D. M., Dijkers, M. and Soutas-Little, R. W. (1995). Hip joint centre locations from palpable bony landmarks – a cadaver study. *Journal of biomechanics*. **28** (8), 995-998.

Selbie, W. S. and Caldwell, G. E. (1996). A simulation study of vertical jumping from different starting postures. *Journal of Biomechanics*. **29** (9), 1137-1146.

Sigurseth, P. O. and Ginaker, V. F. (1962). Effect of foot spacing on velocity in sprints. *Research Quarterly for Sport and Exercise*. **33**, 599-606.

Shea, K. M., Lenhoff, M. W., Otis, M. W. and Backus, S. L. (1997). Validation of a method for location of the hip joint centre. *Gait and Posture*. **5** (2), 157-158.

Soest, J. van, Schwalb, A. L., Bobbert, M. F. and van Ingen Schenau, G. J. (1993). The influence of biarticularity of the gastrocnemius muscle on vertical-jumping achievement. *Journal of Biomechanics*. **26** (1), 1-8.

Spagele, T., Kistner, A. and Gollhofer, A. (1999). Modelling, simulation and optimisation of a human vertical jump. *Journal of Biomechanics*. **32** (5), 521-530.

Spiegelman, J. J. and Woo, S. L. –Y. (1987). A rigid-body method for finding centres of rotation and angular displacements of planar joint motion. *Journal of Biomechanics*. **20** (7), 715-721.

Stefanyshyn, D. J. and Nigg B. M. (2000). Influence of midsole bending stiffness on joint energy and jump height performance. *Medicine and Science in Sports and Exercise*. **32** (2), 471-476.

Stevenson, M. (1997). The sprint start. *Coach and Athletic Director*. **66** (8), 18-21.

Stock, M. (1962). Influence of various track starting positions on speed. *Research Quarterly for Exercise and Sport*. **33**, 607-614.

Stokdijk, M., Meskers, C. G. M., Veeger, H. E. J., de Boer, Y. A. and Rozing, P. M. (1999). Determination of the optimal elbow axis for evaluation of placement of prostheses. *Clinical Biomechanics*. **14**, 177-184.

Stokdijk, M., Nagels, J. and Rozing, P. M. (2000). The glenohumeral joint rotations centre in vivo. *Journal of Biomechanics*. **33**, 1629-1636.

Tellez, T. and Dolittle, D. (1984). Sprinting from start to finish. *Track Technique*. 88, 2802-2805.

Thomas, J. R. and Nelson, J. K. (2001). *Research Methods in Physical Activity*. Human Kinetics: Champaign, Illinois.

Tillin, N. A., Jimenez-Reyes, P., Pain, M. T. G. and Folland, J. P. (2010). Neuromuscular performance of explosive power athletes versus untrained individuals. *Medicine and Science in Sports and Exercise*. **42** (4), 781-790.

Uth, N. (2005). Anthropometric comparison of world-class sprinters and normal populations. *Journal of Sports Science and Medicine*. **4**, 608-616.

Veeger, H. E. J., Yu, B., An, K. –N. and Rozendal, R. H. (1997). Parameters for modelling the upper extremity. *Journal of Biomechanics*. **30** (6), 647-652.

Verdejo, R. and Mills, N. J. (2004). Heel-shoe interactions and the durability of EVA foam running-shoe midsoles. *Journal of Biomechanics*. **37**, 1379-1386.

Vos, E. J., Mullender, M. G. and van Ingen Schenau, G. J. (1990). Electromechanical delay in the vastus lateralis muscle during dynamic isometric contractions. *European Journal of Applied Physiology*. **60**, 467-471.

Watkin, S. (1997). Your starter for ten. *Athletics Weekly*. Jan, 29.

Westing, S. H., Creswell, A. G., and Thorstensson, A. (1991). Muscle activation during maximal voluntary eccentric and concentric knee extension. *European Journal of Applied Physiology and Occupational Physiology*. **62**, 104-108.

Williams, W. L. (1980). Sprinting, *Track and Field Quarterly Review*. **80** (2), 18-22.

Wilson, C., Yeadon, M. R. and King, M. A. (2007). Considerations that affect optimised simulation in a running jump for hight. *Journal of Biomechanics*. **40**, pp. 3155 – 3161.

Winter, E. M. and Brookes, F. B. C. (1991). Electromechanical response times and muscles elasticity in men and women. *European Journal of Applied Physiology*. **63**, 124-128.

Wu, G. and Cavanagh, P. R. (1995). ISB Recommendations for standardization in the reporting of kinematic data. *Journal of Biomechanics*. **28** (10), 1275-1261.

Wu, G., van der Helm, F. C. T., Veeger, H. E. J., Makhsous, M., Van Roy, P., Anglin, C., Nagels, J., Karduna, A. R., McQuade, K., Wang, X., Werner, F. W. and Buchholz, B. (2005). ISB recommendation on definitions of joint coordinate systems of various joints for reporting of human joint motion – part II: shoulder, elbow, wrist and hand. *Journal of Biomechanics*. **38**, 981-992.

Yeadon, M. R., King, M. A. and Wilson, C. (2006). Modelling the maximum voluntary torque/ angular velocity relationship in human movement. *Journal of Biomechanics*. **39**, 476-482.

Yeadon, M. R. (2005), What are the limitations of experimental and theoretical approaches in sports biomechanics? In: McMamee, M. (ed). *Philosophy and the Sciences of Exercise, Health and Sport: Philosophical Perspectives on Research Methods*. London: Routledge. 133-143.

Yeadon, M.R. (1990b). The simulation of aerial movement – II. A mathematical inertia model of the human body. *Journal of Biomechanics*. **23** (1), 67-74.

Yeadon, M. R., Atha, J. and Hales, F. D.(1990). The simulation of aerial movement – IV. A computer simulation model. *Journal of Biomechanics*. **23** (1), 85-89.

Yeadon, M. R. and Challis, J. H. (1994). The future of performance-related sports biomechanics research. *Journal of Sports Sciences*. **12**, 3-32.

Yeadon, M. R. and King, M. A. (2002). Evaluation of a torque-driven simulation model of tumbling. *Journal of Applied Biomechanics*. **18**, 195-206.

Yeadon, M. R., Kong, P. W. and King, M. A. (2006). Parameter determination for a computer simulation model of a diver and a springboard. *Journal of Applied Biomechanics*. **22**, 167-176.

Zatsiorsky, V. M. (1998). *Kinematics of Human Motion*. Champaign Illinois: Human Kinetics.

APPENDIX A

Anatomic Model File for Vicon

{*Model using anatomical landmarks and location from the literature*}

Gorigin = {0,0,0}

Global = [Gorigin,{1,0,0},{0,0,1},xyz]

{*If a point in the hip disapears this will predict it's location based on the other

three*}

{*=====================*}

macro REPLACE4(p1,p2,p3,p4)

{*Replaces any point missing from set of four fixed in a segment*}

s234 = [p3,p2-p3,p3-p4]

p1V = Average(p1/s234)*s234

s341 = [p4,p3-p4,p4-p1]

p2V = Average(p2/s341)*s341

s412 = [p1,p4-p1,p1-p2]

p3V = Average(p3/s412)*s412

s123 = [p2,p1-p2,p2-p3]

p4V = Average(p4/s123)*s123

{* Now only replaces if original is missing 11-99 *}

p1 = p1 ? p1V

p2 = p2 ? p2V

p3 = p3 ? p3V

p4 = p4 ? p4V

endmacro

{*Pelvis and Hip joint centres*}

      Replace4(LSIC,LPSI,RPSI,LASI)

      Replace4(RSIC,RPSI,LPSI,RASI)

      Replace4(LASI,RASI,RPSI,LPSI)

OptionalPoints(LFIN,LLMP,RFIN,RLMP)

OptionalPoints(T10,L1)

OptionalPoints(LSFT,LSBK,RSFT,RSBK)

{*define sacrum*}
SACR = (LPSI+RPSI)/2

{*define pelvis centre to use as origin*}
PELF = (LASI+RASI)/2

{*define pelvis segment - PELF is origin, x is Lasis to Rasis, y is sacrum to PELF, z is vertical*}
Pelvis = [PELF,RASI-LASI,SACR-PELF,xzy]

{*Interasis distance*}
distasis = DIST(LASI,RASI)-$MarkerDiameter

{*Locate joint centre based on percentages from paramter file*}
LHJCX = ((((100-$hjcXpcent)/100)*distasis)*-1)/2
LHJCY = (($hjcYpcent/ 100)*distasis)
LHJCZ = (($hjcZpcent/ 100)*distasis)*-1

RHJCX = (((100-$hjcXpcent)/100)*distasis)/2
RHJCY = (($hjcYpcent/ 100)*distasis)
RHJCZ = (($hjcZpcent/ 100)*distasis)*-1

LHJC = {LHJCX,LHJCY,LHJCZ}*pelvis
RHJC = {RHJCX,RHJCY,RHJCZ}*pelvis
MHIP = (LHJC + RHJC) / 2

{*Thigh and Knee*}
{*Knee origins*}
LKNEO = (LKME+LKNE)/2
RKNEO = (RKME+RKNE)/2

{*define thigh segment- LKMEO is origin, x is from medial epicondyle to lateral (for left, opp on right), z is from mid point in knee to hip centre*}

Lthigh = [LKNEO,LKME-LKNE,LHJC-LKNEO,xyz]

Rthigh = [RKNEO,RKNE-RKME,RHJC-RKNEO,xyz]

{*Knee joint centre*}

LKJC = (LKME+LKNE)/2

RKJC = (RKME+RKNE)/2

{*Shank and Ankle*}

{*Ankle origins*}

LANKO = (LAMM+LANK)/2

RANKO = (RAMM+RANK)/2

{*define shank segment*}

Lshank = [LANKO,LAMM-LANK,LKJC-LANKO,xyz]

Rshank = [RANKO,RANK-RAMM,RKJC-RANKO,xyz]

{*locate joint centres in x,y,z*}

ANKX = 0

ANKY = 0

ANKZ = ($Lateralankjcz+$Medialankjcz)/2

LAJC = {ANKX,ANKZ,ANKY}*Lshank

RAJC = {ANKX,ANKZ,ANKY}*Rshank

{*Foot*}

LFOOTO = (LMT1+LMT5)/2

RFOOTO = (RMT1+RMT5)/2

{*define foot segment axes*}

Lfoot = [LFOOTO,LMT1-LMT5,LHEE-LFOOTO,xyz]

Rfoot = [RFOOTO,RMT1-RMT5,RHEE-RFOOTO,xyz]

228

Ltoes = [LTOE,LMT1-LMT5,LFOOTO-LTOE,xyz]

Rtoes = [RTOE,RMT1-RMT5,RFOOTO-RTOE,xyz]

{*ADJUST FOOT SO THAT WORKS ACCORDING TO BONES AND NOT MARKERS*}

If $Static == 1

{*LMT1 Joint centre*}

NEWY = ((LMT1(3) -$MarkerRadius + $Shoemed)/2)

$%NLMTL = {LMT1(1),LMT1(2),NEWY}/LFOOT

PARAM($%NLMTL)

{*LMT5 Joint centre*}

NEWY5 = ((LMT5(3) -$MarkerRadius + $Shoelat)/2)

$%NLMTL5 = {LMT5(1),LMT5(2),NEWY5}/LFOOT

PARAM($%NLMTL5)

{*LTOE Joint centre*}

NEWYT = ((LTOE(3) -$MarkerRadius)/2)

$%NLMTLT = {LTOE(1),LTOE(2),NEWYT}/Ltoes

PARAM($%NLMTLT)

{*LMT1 Joint centre*}

REWY = ((RMT1(3) -$MarkerRadius + $Shoemed)/2)

$%NRMTL = {RMT1(1),RMT1(2),REWY}/RFOOT

PARAM($%NRMTL)

{*LRMT5 Joint centre*}

REWY5 = ((RMT5(3) -$MarkerRadius + $Shoelat)/2)

$%NRMTL5 = {RMT5(1),RMT5(2),REWY5}/RFOOT

PARAM($%NRMTL5)

{*LRTOE Joint centre*}

REWYT = ((RTOE(3) -$MarkerRadius)/2)

$%NRMTLT = {RTOE(1),RTOE(2),NEWYT}/Rtoes

PARAM($%NRMTLT)

ENDIF

LMPJ1 = $%NLMTL*LFOOT

LMPJ5 = $%NLMTL5*LFOOT

LTOEC = $%NLMTLT*Ltoes

RMPJ1 = $%NRMTL*RFOOT

RMPJ5 = $%NRMTL5*RFOOT

RTOEC = $%NRMTLT*Rtoes

{*CREATE NEW FOOT SEGMENT BASED ON CALCULATED POINTS*}

LFORI = (LMPJ1+LMPJ5)/2

RFORI = (RMPJ1+RMPJ5)/2

{*define foot segment axes*}

LFOOTB = [LFORI,LMPJ1-LMPJ5,LHEE-LFORI,xyz]

RFOOTB = [RFORI,RMPJ1-RMPJ5,RHEE-RFORI,xyz]

LTOEB = [LTOEC,LMPJ1-LMPJ5,LFORI-LTOEC,xyz]

RTOEB = [RTOEC,RMPJ1-RMPJ5,RFORI-RTOEC,xyz]

{*Shoulder and Upperarm*}

{*define Shoulder axes*}

Lshoulder = [LSHO,LSTS-LSHO,LSHO-LSIA,xzy]

Rshoulder = [RSHO,RSHO-RSTS,RSHO-RSIA,xzy]

{*locate shoulder centre in x,y,z*}

SHOX = $sjcx

LSHOX = -$sjcx

SHOY = $sjcy-$MarkerRadius

SHOZ = $sjcz-$MarkerRadius

LSJC = {LSHOX,SHOZ,SHOY}*Lshoulder

RSJC = {SHOX,SHOZ,SHOY}*Rshoulder

{*upper arm origins*}

LARMO = (LELB+LEME)/2

RARMO = (RELB+REME)/2

{*upperarm axes definition*}

Lupper = [LARMO,LEME-LELB,LSJC-LARMO,xyz]

Rupper = [RARMO,RELB-REME,RSJC-RARMO,xyz]

{*shoulder Joint centre location 2 - using front and back of shoulder markers*}

If ExistAtAll(LSFT,LSBK,RSFT,RSBK)

SHOJC2 = 1

LSJC2 = (LSFT+LSBK)/2

RSJC2 = (RSFT+RSBK)/2

NECK = (C7+CLAV)/2

If ExistAtAll (L1)

Lshoulder2 = [LSJC2,NECK-LSJC2,C7-L1,xyz]

Rshoulder2 = [RSJC2,NECK-RSJC2,C7-L1,xyz]

Else

Lshoulder2 = [LSJC2,NECK-LSJC2,C7-SACR,xyz]

Rshoulder2 = [RSJC2,NECK-RSJC2,C7-SACR,xyz]

EndIf

Else

SHOJC2 = 0

Endif

{*trunk*}

If ExistAtAll (L1) Then

Trunk = [C7,L1-C7,RSJC-LSJC,zyx]

Else

Trunk = [C7,SACR-C7,RSJC-LSJC,zyx]

EndIf

{*find STER or CLAV if dissapeared in the set position*}

If $Static == 1

$%STERB = STER/Trunk

$%CLAVB = CLAV/Trunk

PARAM($%STERB)

PARAM($%CLAVB)

Endif

NEWSTER = $%STERB*Trunk

STER = STER ? NEWSTER

NEWCLAV = $%CLAVB*Trunk

CLAV = CLAV ? NEWCLAV

OUTPUT (NEWSTER, NEWCLAV)

{*single segment trunk*}

Body = [C7,PELF-C7,RSJC-LSJC,ZYX]

{*Head*}

Replace4(LFHD,RFHD,LBHD,RBHD)

HEADO = (LFHD+RFHD+LBHD+RBHD)/4

bkhead = (LBHD+RBHD)/2

fthead = (LFHD+RFHD)/2

Head = [HEADO,RBHD-LBHD,fthead-bkhead,1]

{*Elbow and forearm*}

LWJC = (LWRB+LWRA)/2

RWJC = (RWRA+RWRB)/2

{*elbow joint centre location*}

ELBX = 0

ELBY = -$elbowy

ELBZ = $elbowz

LEJC = {ELBX,ELBY,ELBZ}*Lupper

REJC = {ELBX,ELBY,ELBZ}*Rupper

{*Lfore = [LWJC,LWRA-LWRB,LARMO-LWJC,xyz]*}

Lfore = [LWJC,LWRA-LWRB,LARMO-LWJC,yxz]

Rfore = [RWJC,RWRA-RWRB,RARMO-RWJC,yxz]

{*Hand*}

Lhand = [LWJC,LWJC-LFIN,LWRB-LWRA,3]

Rhand = [RWJC,RWJC-RFIN,RWRB-RWRA,3]

If $Static == 1

{*LFinger Joint centre*}

NEWLTIP = LTIP(2) +($MarkerRadius + 4.16)

$%NLTIP = {LTIP(1),NEWLTIP,LTIP(3)}/Lhand

PARAM($%NLTIP)

NEWLFIN = LFIN(2) +($MarkerRadius + 17.83)

$%NLFIN = {LFIN(1),NEWLFIN,LFIN(3)}/Lhand

PARAM($%NLFIN)

NEWLLMP = LLMP(2) +($MarkerRadius + 17.83)

$%NLLMP = {LLMP(1),NEWLLMP,LLMP(3)}/Lhand

PARAM($%NLLMP)

NEWRTIP = RTIP(2) +($MarkerRadius + 4.16)

$%NRTIP = {RTIP(1),NEWRTIP,RTIP(3)}/Rhand

PARAM($%NRTIP)

NEWRFIN = RFIN(2) +($MarkerRadius + 17.83)

$%NRFIN = {RFIN(1),NEWRFIN,RFIN(3)}/Rhand

PARAM($%NRFIN)

NEWRLMP = RLMP(2) +($MarkerRadius + 17.83)

$%NRLMP = {RLMP(1),NEWRLMP,RLMP(3)}/Rhand

PARAM($%NRLMP)

ENDIF

LTIP2 = $%NLTIP*Lhand

LFIN2 = $%NLFIN*Lhand

LLMP2 = $%NLLMP*Lhand

RTIP2 = $%NRTIP*Rhand

RFIN2 = $%NRFIN*Rhand

RLMP2 = $%NRLMP*Rhand

OUTPUT (LTIP2,LFIN2,LLMP2,RTIP2,RFIN2,RLMP2)

{* local and global points

pointI = %pointI*segmentP   converts local %pointI in segmentP to global pointI

%pointI = pointI/segmentP   converts global pointI into local %pointI in segmentP

Note that it is the operators in the expression which define the action, not the %

character in the name of the point object.*}

{*output shoulder joint centre locations in terms of local coords*}

{*llocalsho = lsjc / trunk

llocalshoii = lsjc2 / trunk*}

234

{*Move toe to joint centre*}

    {*If Static = 1

        $LMPJ1X = LMPJ1+{0,-15,0}

    elseLMPJ1 = LMT1{0,-115,0}*Lfoot

*}

{*OUTPUT Calculated points*}

OUTPUT (LHJC,RHJC,LKJC,RKJC,LAJC,RAJC)

OUTPUT (LSJC,RSJC,LEJC,REJC,LWJC,RWJC)

OUTPUT (LHJC,RHJC,LKJC,RKJC,LAJC,RAJC)

OUTPUT (LSJC2,RSJC2)

OUTPUT (LMPJ1,LMPJ5,LTOEC,RMPJ1,RMPJ5,RTOEC)

{*CALCULATE COM POSITION!!!*}

NECK = (C7 + CLAV) / 2

CHST = (T10 + STER) / 2

{*trunkcom   = HEADO + ((PELF - HEADO)* 0.604)*}

headcom	= HEADO
chestcom	= NECK + ((CHST - NECK) * 0.4851)
abscom	= CHST + ((MHIP - cHST) * 0.1321)
pelcom	= CHST + ((MHIP - CHST) * 0.602)
lthighcom	= LHJC + ((LKJC - LHJC)* 0.433)
lshankcom	= LKJC + ((LANKO - LKJC)* 0.433)
lfootcom	= LANKO + ((LFOOTO - LANKO)* 0.429)
rthighcom	= RHJC + ((RKJC - RHJC)* 0.433)
rshankcom	= RKJC + ((RANKO - RKJC)* 0.433)
rfootcom	= RANKO + ((RFOOTO - RANKO)* 0.429)
luppercom	= LSJC + ((LARMO - LSJC)* 0.436)
lforecom	= LARMO + ((LWJC - LARMO)*0.43)
lhandcom	= LWJC + ((LFIN - LWJC)*0.506)
ruppercom	= RSJC + ((RARMO - RSJC)* 0.436)

rforecom   = RARMO + ((RWJC - RARMO)*0.43)

rhandcom   = RWJC + ((RFIN - RWJC)*0.506)

{*trunkmo = trunkcom * $trunkr*}

headmo   = headcom * $headr

chestmo   = chestcom * $chestr

absmo = abscom * $absr

pelmo   = pelcom * $pelr

lthighmo   = lthighcom * $thighr

lshankmo   = lshankcom * $shankr

lfootmo   = lfootcom * $footr

rthighmo   = rthighcom * $thighr

rshankmo   = rshankcom * $shankr

rfootmo   = rfootcom * $footr

luppermo   = luppercom * $upperr

lforemo   = lforecom * $forer

lhandmo   = lhandcom * $handr

ruppermo   = ruppercom * $upperr

rforemo   = rforecom * $forer

rhandmo   = rhandcom * $handr

COM = headmo + chestmo + absmo + pelmo + lthighmo + lshankmo + lfootmo + rthighmo + rshankmo + rfootmo + luppermo + lforemo + lhandmo + ruppermo + rforemo + rhandmo

{*OUTPUT (COM)*}

OUTPUT (COM, headcom, chestcom, abscom, pelcom, lthighcom, lshankcom, lfootcom, rthighcom, rshankcom, rfootcom, luppercom, lforecom, lhandcom, ruppercom, rforecom, rhandcom)

{*Joint Angles*}

{*============*}

{*The first segment in the <> brackets is the child, or moving segment, whose

orientation is to be described relative to the second segment (or global frame of reference). The second segment, if present, is the parent or fixed segment.*}

{*Calculate joint angles*}
{*neck: trunk >> head*}
NeckAngles = -<head,trunk,xyz>

{*Pelvis:trunk*}
TrunkAngles = -<Pelvis,trunk>

{*Hips: Pelvis >> Femora*}
LHipAngles = -<Lthigh,Pelvis,xyz>
RHipAngles = -<Rthigh,Pelvis,xyz>

LHipAngles2 = -<Lthigh,Body,xyz>
RHipAngles2 = -<Rthigh,Body,xyz>

{*Shoulders: shoulders >> Humerus*}
LShoulderAngles = -<Lupper,Lshoulder,xyz>
RShoulderAngles = -<Rupper,Rshoulder,xyz>

LShoulder2Angles = -<lupper,trunk,xyz>
RShoulder2Angles = -<rupper,trunk,xyz>

{*Elbows: Humeri >> Radii*}
LElbowAngles = -<Lfore,Lupper,xyz>
RElbowAngles = -<Rfore,Rupper,xyz>

{*Wrists: Radii >> Hands*}
LWristAngles = -<Lhand,Lfore,xyz>
RWristAngles = -<Rhand,Rfore,xyz>

{*Knees: Femora >> Tibia*}
LKneeAngles = -<Lshank,Lthigh,xyz>

RKneeAngles = -<Rshank,Rthigh,xyz>

{*Ankles: Shank >> Foot*}
LAnkleAngles = -<Lfoot,Lshank,xzy>
RAnkleAngles = -<Rfoot,Rshank,xyz>

{*Ankle: Shank >> Footb - calculated one!*}
LAnkleAngCALC = -<LFOOTB,Lshank,xyz>
RAnkleAngCALC = -<RFOOTB,Lshank,xyz>

{*Toes:foot*}
LtoeAngles = -<Ltoes,Lfoot,xyz>
RtoeAngles = -<Rtoes,Rfoot,xyz>

{*MPJ: Toes >> FOOT - Caclulated one!*}
LMPJAngles = -<LTOEB,LFOOTB>
RMPJAngles = -<RTOEB,RFOOTB>

{*Output angles*}
OUTPUT(NeckAngles,TrunkAngles,LShoulderAngles,RShoulderAngles,LShoulder2
Angles,RShoulder2Angles)
OUTPUT(LElbowAngles,RElbowAngles,LWristAngles,RWristAngles)
OUTPUT(LHipAngles,RHipAngles,LKneeAngles,RKneeAngles,LAnkleAngles,RAn
kleAngles,LtoeAngles,RtoeAngles)
OUTPUT(LHipAngles2,RHipAngles2)
OUTPUT(LAnkleangCALC,RAnkleAngCALC,LMPJAngles,RMPJAngles)

{*OUTPUT segment angles relative to global*}
TrunkGlobal = <trunk,1>
PelvisGlobal = <Pelvis,1>
LthighGlobal = <Lthigh,1>
RthighGlobal = <Rthigh,1>
LupperGlobal = <Lupper,1>
RupperGlobal = <Rupper,1>

LforeGlobal = <Lfore,1>

RforeGlobal = <Rfore,1>

LhandGlobal = <Lhand,1>

RhandGlobal = <Rhand,1>

LshankGlobal = <Lshank,1>

RshankGlobal = <Rshank,1>

LFOOTBGlobal = <LFOOTB,1>

RFOOTBGlobal = <RFOOTB,1>

LTOEBGlobal = <LTOEB,1>

RTOEBGlobal = <RTOEB,1>

OUTPUT(TrunkGlobal,PelvisGlobal,LthighGlobal,RthighGlobal,LshankGlobal,RshankGlobal,LFOOTBGlobal,RFOOTBGlobal,LTOEBGlobal,RTOEBGlobal)

OUTPUT(LupperGlobal,RupperGlobal,LforeGlobal,RforeGlobal,LhandGlobal,RhandGlobal)

MARKER FILE

!MKR#2

[Autolabel]

LFHD Left front head

RFHD Right front head

LBHD Left back head

RBHD Right back head

CLAV Clavicle

STER   Sternum

C7   Cervicle vertebrae 7

T10   Thoracic vertebrae 10

L1   Lumber vretebrae 1

LASI   Left ASIS

LPSI   Left PSIS

RASI   Right ASIS

RPSI   Right PSIS

LSIC   Left suprailiac crest

RSIC   Right suprailiac crest

LHJC Left hip joint centre

RHJC Right hip joint centre

LKME Left knee medial epicondyle

LKNE Left knee lateral epicondyle

RKME Right knee medial epicondyle

RKNE Right knee lateral epicondyle

LKJC Left knee joint centre

RKJC Right knee joint centre

LAMM   Left ankle medial malleoli

LANK   Left ankle lateral malleoli

RAMM   Right ankle medial malleoli

RANK   Right ankle lateral malleoli

LAJC Left ankle joint centre

RAJC Right ankle joint centre

LTOE Left foot 2nd toe

LMT1 Left foot big toe knuckle

LMT5 Left foot little toe knuckle

LHEE Left heel

RTOE Right foot 2nd toe

RMT1 Right foot big toe knuckle

RMT5 Right foot little toe knuckle

RHEE Right heel

LSHO Left shoulder accromion angle

LSTS Left shoulder trigonum spinae

LSIA Left shoulder inferior angle

RSHO Right shoulder accromion angle

RSTS Right shoulder trigonum spinae

RSIA Right shoulder inferior angle

RSFT Right shoulder front

RSBK Right shoulder back

LSFT Left shoulder front

LSBK Left shoulder back

LSJC Left shoulder joint centre

RSJC Right shoulder joint centre

LSJC2 Left shoulder centre calc 2

RSJC2 Right shoulder centre calc 2

LELB Left elbow lateral epicondyle

LEME Left elbow medial epicondlye

RELB Right elbow lateral epicondyle

REME Right elbow medial epicondlye

LEJC Left elbow joint centre

REJC Right elbow joint centre

LWRA Left wirst medial epicondyle

LWRB Left wrist lateral epicondyle

RWRA   Right wirst medial epicondyle

RWRBRight wrist lateral epicondyle

LWJC Left wrist joint centre

RWJC right wrist joint centre

LFIN   Left index finger metacarple phalangial joint

LLMP Left little finger metacarple phalangial joint

LTIP   Left middle finger tip

RFIN   Right index finger metacarple phalangial joint

RLMP Right little finger metacarple phalangial joint

RTIP   Right middle finger tip

COM   Centre of Mass

headcom

chestcom

abscom

pelcom

LMPJ1 Left MPJ1 (corrected)

LMPJ5 Left MPJ5 (corrected)

LTOEC Left TOE (corrected)

RMPJ1 Right MPJ1 (corrected)

RMPJ5 Right MPJ5 (corrected)

RTOEC Right TOE (corrected)

NEWSTER

NEWCLAV

NLTIP2

LTIP2

LFIN2

LLMP2

RTIP2

RFIN2

RLMP2

Head = LFHD,RFHD,LBHD,RBHD
Spine = C7,T10,L1,CLAV,STER
Pelvis = LASI,RASI,LPSI,RPSI,LHJC,RHJC
Lthigh = LHJC,LKNE,LKME,LKJC
Rthigh = RHJC,RKNE,RKME,RKJC
Lshank = LKNE,LKME,LAJC
Rshank = RKNE,RKME,RAJC
Lfoot = lMPJ1,LMPJ5,LHEE,LAJC
Ltoes = LTOEC,LMPJ5,LMPJ1
Rfoot = RMPJ1,RMPJ5,RHEE,RAJC
Rtoes = RTOEC,RMPJ5,RMPJ1
Lsho = LSHO,LSTS,LSIA
Rsho = RSHO,RSTS,RSIA
Larm = LSJC,LEME,LELB,LEJC
Rarm = RSJC,REME,RELB,REJC
Lfore = LELB,LEME,LWJC
Rfore = RELB,REME,RWJC
Lhand = LWJC,LFIN,LLMP
Rhand = RWJC,RFIN,RLMP
Lfingers = LFIN,LLMP,LTIP
Rfingers = RFIN,RLMP,RTIP

[Angles]

LShoulderAngles   Left shoulder rotation
RShoulderAngles   Right shoulder rotation
LElbowAngles   Left elbow rotation
RElbowAngles   Right elbow rotation
LWristAngles Left wrist rotation
RWristAngles Right wrist rotation
LHipAngles   Left hip rotation

RHipAngles	Right hip rotation
LKneeAngles	Left knee rotation
RKneeAngles	Right knee rotation
LAnkleAngles	Left ankle rotation
RankleAngles	Right ankle rotation
LAnkleAngCALC	Left ankle rotation CALCed
RAnkleAngCALC	Right ankle rotation CALCed
LMPJAngles	Left MPJ rotation CALCed
RMPJAngles	Right ankle rotation CALCed
LShoulder2Angles	Method2
RShoulder2Angles	method2
NeckAngles	Neck rotations
TrunkAngles	
LHipAngles2	Hip angle to 1 segment trunk
RHipAngles2	Hip angle to 1 segment trunk
TrunkGlobal	ANGLE OF SEGS TO HORIZ
PelvisGlobal	
LthighGlobal	
RthighGlobal	
LupperGlobal	
RupperGlobal	
LforeGlobal	
RforeGlobal	
LhandGlobal	
RhandGlobal	
LshankGlobal	
RshankGlobal	
LFOOTBGlobal	
RFOOTBGlobal	
LTOEBGlobal	
RTOEBGlobal	

PARAMETER FILE

{* Paramter file *}

{*for use with AnatomicMODEL*}

{*ALL DISTANCE MEASUREMENTS IN millimeters, ALL ANGLES IN degrees*}

{*General Parameters*}
{*=================*}

$static = 0

$MarkerDiameter = 14
$MarkerRadius = 7

$Shoeheel = 37 {*depth of shoe at heel*}
$Shoelat = 24 {*depth of shoe at MT5*}
$Shoemed = 26 {*depth of shoe at MT1*}

{*Body Inertia Paramters*}
{*com is dist of CoM from Proximal joint centre*}

$BodyMass = 65
$Lthighmass = 10.562
$Lthighcom = 166
$Lthighlength = 400
$Lthighmi= {0.142,0.142,0.043}

$trunkmass = 39.871
$headmass = 5.157
$chestmass = 22.3825
$absmass = 2.1585

$Pelmass = 7.0662

$thighmass = 12.2935

$shankmass = 5.038

$footmass = 1.0635

$uppermass = 2.778

$foremass = 1.4865

$handmass = 0.459

totalmass = $headmass + $chestmass + $pelmass+ $absmass + (2* ($thighmass + $shankmass + $footmass + $uppermass + $foremass + $handmass))

{*relative segment weight*}

$headr = $headmass/ totalmass

$trunkr = $trunkmass / totalmass

$chestr = $chestmass / totalmass

$absr = $absmass / totalmass

$pelr = $pelmass / totalmass

$thighr = $thighmass / totalmass

$shankr = $shankmass / totalmass

$footr = $footmass / totalmass

$upperr = $uppermass / totalmass

$forer = $foremass / totalmass

$handr = $handmass / totalmass

{*hip joint centre percentages based on that of Seidel (1995)*}

$hjcXpcent = 14 {*medially*}

$hjcYpcent = -24 {*posteriorly*}

$hjcZpcent = 30 {*distally*}

{*knee joint centre based on Churchill et al. (1998)-midpoint of femeral epicondyles*}

246

{*ankle joint centre based on Inman (1976)*}

$Lateralankjcz = 3 {*Z dist from lateral malleoli to JC)*}

$medialankjcz = 5 {*Z dist from lateral malleoli to JC)*}

{*shoulder joint centre based on Stokdijk et al. (2000)*}

$sjcx = -13.5

$sjcy = 39.4

$sjcz = 48.4

{*elbow joint centre based on Stokdijk et al. (1999) values given from the lateral epicondyle*}

$elbowz = 8.1 {*cranially*}

$elbowy = 18.6 {*ventrally of the epicondylus lateralis at 15.3o to the frontal plane*}

{*wrist - no info found :(*}

$%Hiplfpos = {-136.818,88.9841,167.444}

$%Hiprtpos = {-117.391,-86.8317,168.815}

$%NLMTL = {56.9934,-13.0743,-0.613458}

$%NLMTL5 = {-56.1409,-15.7445,-0.739091}

$%NLMTLT = {1.06761,-33.188,14.2603}

$%NRMTL = {45.608,21.3047,1.06394}

$%NRMTL5 = {-55.4431,4.22033,0.210763}

$%NRMTLT = {-10.7799,27.9645,1.62587}

$%STERB = {7.59132,202.264,226.694}

$%CLAVB = {3.26443,137.072,68.0096}

$%NLTIP = {-39.3888,18.6458,-191.072}

$%NLFIN = {-18.8538,-15.7416,-100.213}

$%NLLMP = {-36.1031,45.5147,-71.3496}

$%NRTIP = {66.8797,23.2888,-179.571}

$%NRFIN = {22.5957,-10.1707,-93.1472}

$%NRLMP = {48.7759,56.9432,-56.094}

APPENDIX B

Subject Informed Consent

Blank page for informed consent

APPENDIX C

Anthropometry

SEGMENTAL INERTIA PARAMETER VALUES

UNITS: MASS IN KG
    DISTANCE IN METRES
    MOMENT OF INERTIA IN KG*M**2

FORMAT AND SEQUENCE OF DATA PRESENTATION
SEGMENT NAME
MASS, DISTANCE OF MASS CENTRE FROM PROXIMAL JOINT,
SEGMENT LENGTH
PRINCIPAL MOMENTS OF INERTIA

HEAD H
  5.1567   0.1193   0.2420
  0.0268   0.0269   0.0177
TRUNK PTC
 31.6072   0.3083   0.5930
  1.0143   1.1754   0.3556
UPPER ARM 1A
  2.7594   0.1325   0.3060
  0.0239   0.0239   0.0040
UPPER ARM 1B
  2.7970   0.1310   0.3070
  0.0242   0.0242   0.0041
FOREARM 2A
  1.5116   0.1220   0.2880
  0.0100   0.0101   0.0012
FOREARM 2B
  1.4612   0.1186   0.2850
  0.0093   0.0094   0.0012
HAND 3A
  0.4576   0.0750   0.1930
  0.0012   0.0011   0.0002
HAND 3B
  0.4596   0.0784   0.2010
  0.0013   0.0011   0.0003
THIGH 1J
 11.8545   0.2025   0.4670
  0.2131   0.2131   0.0476
THIGH 1K
 12.7321   0.2109   0.4860
  0.2468   0.2469   0.0527
CALF 2J
  5.0063   0.2108   0.4830
  0.0856   0.0856   0.0078
CALF 2K
  5.0701   0.2067   0.4760
  0.0859   0.0859   0.0081
FOOT 3J
  1.0568   0.0796   0.2190
  0.0036   0.0035   0.0010
FOOT - BALL
  0.9016   0.0634   0.1450
  0.0019   0.0018   0.0009
FOOT BALL - NAILS
  0.1551   0.0283   0.0740
  0.0001   0.0001   0.0001
FOOT 3K
  1.0699   0.0791   0.2120
  0.0036   0.0035   0.0010
FOOT - BALL
  0.9178   0.0638   0.1450
  0.0020   0.0018   0.0009
FOOT BALL - NAILS
  0.1521   0.0266   0.0670
  0.0001   0.0001   0.0001
TOTAL MASS = 83.00 KG   DENSITY = 1.003

APPENDIX D

Reduced Model and Marker Set Used for Data Collection 2

{* Test model *}

{*Model using anatomical landmarks and location from the literature*}

{*THIS VERSION HAS BEEN ALTERED SO THAT ALL THE MARKER
NAMES
ARE THE SAME AS GOLEM - SOME OF THEM MAY BE IN SLIGHTLY
DIFFERENT
LOCATIONS*}

Gorigin = {0,0,0}
Global = [Gorigin,{1,0,0},{0,0,1},xyz]

{*If a point in the hip disapears this will predict it's location based on the other
three*}
{*=====================*}
macro REPLACE4(p1,p2,p3,p4)
{*Replaces any point missing from set of four fixed in a segment*}
s234 = [p3,p2-p3,p3-p4]
p1V = Average(p1/s234)*s234
s341 = [p4,p3-p4,p4-p1]
p2V = Average(p2/s341)*s341
s412 = [p1,p4-p1,p1-p2]
p3V = Average(p3/s412)*s412
s123 = [p2,p1-p2,p2-p3]
p4V = Average(p4/s123)*s123
{* Now only replaces if original is missing 11-99 *}
p1 = p1 ? p1V
p2 = p2 ? p2V
p3 = p3 ? p3V
p4 = p4 ? p4V
endmacro

OptionalPoints(LFIN,LLMP,RFIN,RLMP)

OptionalPoints(T10,L1)

OptionalPoints(LSFT,LSBK,RSFT,RSBK)

{*define pelvis centre to use as origin*}

PELF = (LASI+RASI)/2

{*Interasis distance*}

distasis = DIST(LASI,RASI)-$MarkerDiameter

LHJC = LASI

RHJC = RASI

MHIP = (LHJC + RHJC) / 2

{*Thigh and Knee*}

{*Knee origins*}

LKNEO = (LKME+LKNE)/2

RKNEO = (RKME+RKNE)/2

{*define thigh segment- LKMEO is origin, x is from medial epicondyle to lateral (for left, opp on right), z is from mid point in knee to hip centre*}

Lthigh = [LKNEO,LKME-LKNE,LHJC-LKNEO,xyz]

Rthigh = [RKNEO,RKNE-RKME,RHJC-RKNEO,xyz]

{*Knee joint centre*}

LKJC = (LKME+LKNE)/2

RKJC = (RKME+RKNE)/2

{*Shank and Ankle*}

{*Ankle origins*}

LANKO = (LAMM+LANK)/2

RANKO = (RAMM+RANK)/2

{*define shank segment*}

Lshank = [LANKO,LAMM-LANK,LKJC-LANKO,xyz]

Rshank = [RANKO,RANK-RAMM,RKJC-RANKO,xyz]

{*locate joint centres in x,y,z*}

ANKX = 0

ANKY = 0

ANKZ = ($Lateralankjcz+$Medialankjcz)/2

LAJC = {ANKX,ANKZ,ANKY}*Lshank

RAJC = {ANKX,ANKZ,ANKY}*Rshank

{*Foot*}

LFOOTO = (LMT1+LMT5)/2

RFOOTO = (RMT1+RMT5)/2

{*define foot segment axes*}

Lfoot = [LFOOTO,LMT1-LMT5,LHEE-LFOOTO,xyz]

Rfoot = [RFOOTO,RMT1-RMT5,RHEE-RFOOTO,xyz]

Ltoes = [LTOE,LMT1-LMT5,LFOOTO-LTOE,xyz]

Rtoes = [RTOE,RMT1-RMT5,RFOOTO-RTOE,xyz]

{*ADJUST FOOT SO THAT WORKS ACCORDING TO BONES AND NOT
MARKERS*}

If $Static == 1

{*LMT1 Joint centre*}

NEWY = ((LMT1(3) -$MarkerRadius + $Shoemed)/2)

$%NLMTL = {LMT1(1),LMT1(2),NEWY}/LFOOT

PARAM($%NLMTL)

{*LMT5 Joint centre*}

NEWY5 = ((LMT5(3) -$MarkerRadius + $Shoelat)/2)

$%NLMTL5 = {LMT5(1),LMT5(2),NEWY5}/LFOOT

PARAM($%NLMTL5)

{*LTOE Joint centre*}

NEWYT = ((LTOE(3) -$MarkerRadius)/2)

$%NLMTLT = {LTOE(1),LTOE(2),NEWYT}/Ltoes

PARAM($%NLMTLT)

{*LMT1 Joint centre*}

REWY = ((RMT1(3) -$MarkerRadius + $Shoemed)/2)

$%NRMTL = {RMT1(1),RMT1(2),REWY}/RFOOT

PARAM($%NRMTL)

{*LRMT5 Joint centre*}

REWY5 = ((RMT5(3) -$MarkerRadius + $Shoelat)/2)

$%NRMTL5 = {RMT5(1),RMT5(2),REWY5}/RFOOT

PARAM($%NRMTL5)

{*LRTOE Joint centre*}

REWYT = ((RTOE(3) -$MarkerRadius)/2)

$%NRMTLT = {RTOE(1),RTOE(2),NEWYT}/Rtoes

PARAM($%NRMTLT)

ENDIF

LMPJ1 = $%NLMTL*LFOOT

LMPJ5 = $%NLMTL5*LFOOT

LTOEC = $%NLMTLT*Ltoes

RMPJ1 = $%NRMTL*RFOOT

RMPJ5 = $%NRMTL5*RFOOT

RTOEC = $%NRMTLT*Rtoes

{*CREATE NEW FOOT SEGMENT BASED ON CALCULATED POINTS*}

LFORI = (LMPJ1+LMPJ5)/2

RFORI = (RMPJ1+RMPJ5)/2

{*define foot segment axes*}

LFOOTB = [LFORI,LMPJ1-LMPJ5,LHEE-LFORI,xyz]

RFOOTB = [RFORI,RMPJ1-RMPJ5,RHEE-RFORI,xyz]

LTOEB = [LTOEC,LMPJ1-LMPJ5,LFORI-LTOEC,xyz]

RTOEB = [RTOEC,RMPJ1-RMPJ5,RFORI-RTOEC,xyz]

{*Shoulder and Upperarm*}

{*define Shoulder axes*}

LSJC = LSHO

RSJC = RSHO

{*upper arm origins*}

LARMO = (LELB+LEME)/2

RARMO = (RELB+REME)/2

{*upperarm axes definition*}

Lupper = [LARMO,LEME-LELB,LSJC-LARMO,xyz]

Rupper = [RARMO,RELB-REME,RSJC-RARMO,xyz]

{*trunk*}

If ExistAtAll (T10) Then

Trunk = [C7,T10-C7,RSJC-LSJC,zyx]

EndIf

{*find STER or CLAV if dissapeared in the set position*}

If $Static == 1

$%STERB = STER/Trunk

$%CLAVB = CLAV/Trunk

PARAM($%STERB)
PARAM($%CLAVB)
Endif

NEWSTER = $%STERB*Trunk
STER = STER ? NEWSTER

NEWCLAV = $%CLAVB*Trunk
CLAV = CLAV ? NEWCLAV

{*single segment trunk*}
        Body = [C7,PELF-C7,RSJC-LSJC,ZYX]

{*Head*}
        Replace4(LFHD,RFHD,LBHD,RBHD)
        HEADO = (LFHD+RFHD+LBHD+RBHD)/4
        bkhead = (LBHD+RBHD)/2
        fthead = (LFHD+RFHD)/2
        Head = [HEADO,RBHD-LBHD,fthead-bkhead,1]

{*Elbow and forearm*}
        LWJC = (LWRB+LWRA)/2
        RWJC = (RWRA+RWRB)/2

        {*elbow joint centre location*}
        ELBX = 0
        ELBY = -$elbowy
        ELBZ = $elbowz

        LEJC = {ELBX,ELBY,ELBZ}*Lupper
        REJC = {ELBX,ELBY,ELBZ}*Rupper

        {*Lfore = [LWJC,LWRA-LWRB,LARMO-LWJC,xyz]*}

Lfore = [LWJC,LWRA-LWRB,LARMO-LWJC,yxz]

Rfore = [RWJC,RWRA-RWRB,RARMO-RWJC,yxz]

{*Hand*}

Lhand = [LWJC,LWJC-LFIN,LWRB-LWRA,3]

Rhand = [RWJC,RWJC-RFIN,RWRB-RWRA,3]

If $Static == 1

{*LFinger Joint centre*}

NEWLTIP = LTIP(2) +($MarkerRadius + 4.16)

$%NLTIP = {LTIP(1),NEWLTIP,LTIP(3)}/Lhand

PARAM($%NLTIP)

NEWLFIN = LFIN(2) +($MarkerRadius + 17.83)

$%NLFIN = {LFIN(1),NEWLFIN,LFIN(3)}/Lhand

PARAM($%NLFIN)

NEWLLMP = LLMP(2) +($MarkerRadius + 17.83)

$%NLLMP = {LLMP(1),NEWLLMP,LLMP(3)}/Lhand

PARAM($%NLLMP)

NEWRTIP = RTIP(2) +($MarkerRadius + 4.16)

$%NRTIP = {RTIP(1),NEWRTIP,RTIP(3)}/Rhand

PARAM($%NRTIP)

NEWRFIN = RFIN(2) +($MarkerRadius + 17.83)

$%NRFIN = {RFIN(1),NEWRFIN,RFIN(3)}/Rhand

PARAM($%NRFIN)

NEWRLMP = RLMP(2) +($MarkerRadius + 17.83)

$%NRLMP = {RLMP(1),NEWRLMP,RLMP(3)}/Rhand

PARAM($%NRLMP)

ENDIF

LTIP2 = $%NLTIP*Lhand

LFIN2 = $%NLFIN*Lhand

LLMP2 = $%NLLMP*Lhand

RTIP2 = $%NRTIP*Rhand

RFIN2 = $%NRFIN*Rhand

RLMP2 = $%NRLMP*Rhand

{* local and global points

pointI = %pointI*segmentP   converts local %pointI in segmentP to global pointI

%pointI = pointI/segmentP   converts global pointI into local %pointI in segmentP

Note that it is the operators in the expression which define the action, not the %

character in the name of the point object.*}

{*output shoulder joint centre locations in terms of local coords*}

{*llocalsho = lsjc / trunk

llocalshoii = lsjc2 / trunk*}

{*Move toe to joint centre*}

     {*If Static = 1

         $LMPJ1X = LMPJ1+{0,-15,0}

    elseLMPJ1 = LMT1{0,-115,0}*Lfoot

*}

{*OUTPUT Calculated points*}

OUTPUT (LHJC,RHJC,LKJC,RKJC,LAJC,RAJC)

OUTPUT (LSJC,RSJC,LEJC,REJC,LWJC,RWJC)

OUTPUT (LHJC,RHJC,LKJC,RKJC,LAJC,RAJC)

OUTPUT (LMPJ1,LMPJ5,LTOEC,RMPJ1,RMPJ5,RTOEC)

{*CALCULATE COM POSITION!!!*}

NECK = (C7 + CLAV) / 2

CHST = (T10 + STER) / 2

{*trunkcom   = HEADO + ((PELF - HEADO)* 0.604)*}

headcom   = HEADO

chestcom   = NECK + ((CHST - NECK) * 0.4851)

abscom   = CHST + ((MHIP - CHST) * 0.1321)

pelcom   = CHST + ((MHIP - CHST) * 0.602)

lthighcom   = LHJC + ((LKJC - LHJC)* 0.433)

lshankcom   = LKJC + ((LANKO - LKJC)* 0.433)

lfootcom   = LANKO + ((LFOOTO - LANKO)* 0.429)

rthighcom   = RHJC + ((RKJC - RHJC)* 0.433)

rshankcom   = RKJC + ((RANKO - RKJC)* 0.433)

rfootcom   = RANKO + ((RFOOTO - RANKO)* 0.429)

luppercom   = LSJC + ((LARMO - LSJC)* 0.436)

lforecom   = LARMO + ((LWJC - LARMO)*0.43)

lhandcom   = LWJC + ((LFIN - LWJC)*0.506)

ruppercom   = RSJC + ((RARMO - RSJC)* 0.436)

rforecom   = RARMO + ((RWJC - RARMO)*0.43)

rhandcom   = RWJC + ((RFIN - RWJC)*0.506)

{*trunkmo   = trunkcom * $trunkr*}

headmo   = headcom * $headr

chestmo   = chestcom * $chestr

absmo = abscom * $absr

pelmo   = pelcom * $pelr

lthighmo   = lthighcom * $thighr

lshankmo   = lshankcom * $shankr

lfootmo   = lfootcom * $footr

rthighmo   = rthighcom * $thighr

rshankmo   = rshankcom * $shankr

rfootmo   = rfootcom * $footr

luppermo   = luppercom * $upperr

lforemo   = lforecom * $forer

lhandmo   = lhandcom * $handr

ruppermo   = ruppercom * $upperr

rforemo   = rforecom * $forer

rhandmo   = rhandcom * $handr

COM = headmo + chestmo + absmo + pelmo + lthighmo + lshankmo + lfootmo + rthighmo + rshankmo + rfootmo + luppermo + lforemo + lhandmo + ruppermo + rforemo + rhandmo

{*OUTPUT (COM)*}
OUTPUT (COM)

{*Joint Angles*}
{*============*}

{*The first segment in the <> brackets is the child, or moving segment, whose orientation is to be described relative to the second segment (or global frame of reference). The second segment, if present, is the parent or fixed segment.*}

{*Calculate joint angles*}
{*neck: trunk >> head*}
NeckAngles = -<head,trunk,xyz>

{*Hips: Pelvis >> Femora*}
LHipAngles = -<Lthigh,trunk,xyz>
RHipAngles = -<Rthigh,trunk,xyz>

{*Shoulders: shoulders >> Humerus*}
LShoulderAngles = -<Lupper,trunk,xyz>
RShoulderAngles = -<Rupper,trunk,xyz>

{*Elbows: Humeri >> Radii*}
LElbowAngles = -<Lfore,Lupper,xyz>
RElbowAngles = -<Rfore,Rupper,xyz>

{*Knees: Femora >> Tibia*}
LKneeAngles = -<Lshank,Lthigh,xyz>
RKneeAngles = -<Rshank,Rthigh,xyz>

{*Ankles: Shank >> Foot*}
LAnkleAngles = -<Lfoot,Lshank,xzy>
RAnkleAngles = -<Rfoot,Rshank,xyz>

{*Ankle: Shank >> Footb - calculated one!*}
LAnkleAngCALC = -<LFOOTB,Lshank,xyz>
RAnkleAngCALC = -<RFOOTB,Lshank,xyz>

{*Toes:foot*}
LtoeAngles = -<Ltoes,Lfoot,xyz>
RtoeAngles = -<Rtoes,Rfoot,xyz>

{*MPJ: Toes >> FOOT - Caclulated one!*}
LMPJAngles = -<LTOEB,LFOOTB>
RMPJAngles = -<RTOEB,RFOOTB>

{*Output angles*}
OUTPUT(LShoulderAngles,RShoulderAngles)
OUTPUT(LElbowAngles,RElbowAngles)
OUTPUT(LHipAngles,RHipAngles,LKneeAngles,RKneeAngles,LAnkleAngles,RAnkleAngles)
OUTPUT(LMPJAngles,RMPJAngles)

{*OUTPUT segment angles relative to global*}
TrunkGlobal = <trunk,1>
LthighGlobal = <Lthigh,1>

RthighGlobal = <Rthigh,1>

LupperGlobal = <Lupper,1>

RupperGlobal = <Rupper,1>

LforeGlobal = <Lfore,1>

RforeGlobal = <Rfore,1>

LhandGlobal = <Lhand,1>

RhandGlobal = <Rhand,1>

LshankGlobal = <Lshank,1>

RshankGlobal = <Rshank,1>

LFOOTBGlobal = <LFOOTB,1>

RFOOTBGlobal = <RFOOTB,1>

LTOEBGlobal = <LTOEB,1>

RTOEBGlobal = <RTOEB,1>

OUTPUT(TrunkGlobal,LthighGlobal,RthighGlobal,LshankGlobal,RshankGlobal,LF
OOTBGlobal,RFOOTBGlobal)

OUTPUT(LupperGlobal,RupperGlobal,LforeGlobal,RforeGlobal)

!MKR#2

[Autolabel]

LFHD Left front head

RFHD Right front head

LBHD Left back head

RBHD Right back head

CLAV Clavicle

STER   Sternum

C7   Cervicle vertebrae 7

T10   Thoracic vertebrae 10

L1   Lumber vretebrae 1

LASI Left ASIS

LPSI Left PSIS

RASI Right ASIS

RPSI Right PSIS

LSIC Left suprailiac crest

RSIC Right suprailiac crest

LHJC Left hip joint centre

RHJC Right hip joint centre

LKME Left knee medial epicondyle

LKNE Left knee lateral epicondyle

RKME Right knee medial epicondyle

RKNE Right knee lateral epicondyle

LKJC Left knee joint centre

RKJC Right knee joint centre

LAMM   Left ankle medial malleoli

LANK   Left ankle lateral malleoli

RAMM   Right ankle medial malleoli

RANK   Right ankle lateral malleoli

LAJC Left ankle joint centre

RAJC Right ankle joint centre

LTOE Left foot 2nd toe

LMT1 Left foot big toe knuckle

LMT5 Left foot little toe knuckle

LHEE Left heel

RTOE Right foot 2nd toe

RMT1 Right foot big toe knuckle

RMT5 Right foot little toe knuckle

RHEE Right heel

LSHO Left shoulder accromion angle

LSTS Left shoulder trigonum spinae

LSIA Left shoulder inferior angle

RSHO Right shoulder accromion angle

RSTS Right shoulder trigonum spinae

RSIA Right shoulder inferior angle

RSFT Right shoulder front

RSBK Right shoulder back

LSFT Left shoulder front

LSBK Left shoulder back

LSJC Left shoulder joint centre

RSJC Right shoulder joint centre

LSJC2 Left shoulder centre calc 2

RSJC2 Right shoulder centre calc 2

LELB Left elbow lateral epicondyle

LEME Left elbow medial epicondlye

RELB Right elbow lateral epicondyle

REME Right elbow medial epicondlye

LEJC Left elbow joint centre

REJC Right elbow joint centre

LWRA Left wirst medial epicondyle

LWRB Left wrist lateral epicondyle

RWRA   Right wirst medial epicondyle

RWRB Right wrist lateral epicondyle

LWJC Left wrist joint centre

RWJC right wrist joint centre

LFIN   Left index finger metacarple phalangial joint

LLMP Left little finger metacarple phalangial joint

LTIP   Left middle finger tip

RFIN   Right index finger metacarple phalangial joint

RLMP Right little finger metacarple phalangial joint

RTIP   Right middle finger tip

LMPJ1   Left MPJ1 (corrected)

LMPJ5   Left MPJ5 (corrected)

LTOEC   Left TOE (corrected)

RMPJ1   Right MPJ1 (corrected)

RMPJ5   Right MPJ5 (corrected)

RTOEC   Right TOE (corrected)

NEWSTER

NEWCLAV

NLTIP2

LTIP2

LFIN2

LLMP2

RTIP2

RFIN2

RLMP2

Head = LFHD,RFHD,LBHD,RBHD

Spine = C7,T10,L1,CLAV,STER

Pelvis = LASI,RASI,LPSI,RPSI,LHJC,RHJC

Lthigh = LHJC,LKNE,LKME,LKJC

Rthigh = RHJC,RKNE,RKME,RKJC

Lshank = LKNE,LKME,LAJC

Rshank = RKNE,RKME,RAJC

Lfoot = lMPJ1,LMPJ5,LHEE,LAJC

Ltoes = LTOEC,LMPJ5,LMPJ1

Rfoot = RMPJ1,RMPJ5,RHEE,RAJC

Rtoes = RTOEC,RMPJ5,RMPJ1

Lsho = LSHO,LSTS,LSIA

Rsho = RSHO,RSTS,RSIA

Larm = LSJC,LEME,LELB,LEJC

Rarm = RSJC,REME,RELB,REJC

Lfore = LELB,LEME,LWJC

Rfore = RELB,REME,RWJC

Lhand = LWJC,LFIN,LLMP

Rhand = RWJC,RFIN,RLMP

Lfingers = LFIN,LLMP,LTIP

Rfingers = RFIN,RLMP,RTIP

[Angles]

LShoulderAngles   Left shoulder rotation

RShoulderAngles   Right shoulder rotation

LElbowAngles   Left elbow rotation

RElbowAngles	Right elbow rotation
LWristAngles	Left wrist rotation
RWristAngles	Right wrist rotation
LHipAngles	Left hip rotation
RHipAngles	Right hip rotation
LKneeAngles	Left knee rotation
RKneeAngles	Right knee rotation
LAnkleAngles	Left ankle rotation
RankleAngles	Right ankle rotation
LAnkleAngCALC	Left ankle rotation CALCed
RAnkleAngCALC	Right ankle rotation CALCed
LMPJAngles	Left MPJ rotation CALCed
RMPJAngles	Right ankle rotation CALCed
LShoulder2Angles	Method2
RShoulder2Angles	method2
NeckAngles	Neck rotations
TrunkAngles	
LHipAngles2	Hip angle to 1 segment trunk
RHipAngles2	Hip angle to 1 segment trunk
TrunkGlobal	ANGLE OF SEGS TO HORIZ
PelvisGlobal	
LthighGlobal	
RthighGlobal	
LupperGlobal	
RupperGlobal	
LforeGlobal	
RforeGlobal	
LhandGlobal	
RhandGlobal	
LshankGlobal	
RshankGlobal	
LFOOTBGlobal	
RFOOTBGlobal	
LTOEBGlobal	

277

RTOEBGlobal

{* Paramter file *}

{*for use with AnatomicMODEL*}

{*ALL DISTANCE MEASUREMENTS IN millimeters, ALL ANGLES IN degrees*}

{*General Parameters*}
{*==================*}
    $static = 0

    $MarkerDiameter = 14
    $MarkerRadius = 7

    $Shoeheel = 37 {*depth of shoe at heel*}
    $Shoelat = 24 {*depth of shoe at MT5*}
    $Shoemed = 26 {*depth of shoe at MT1*}

{*Body Inertia Paramters*}
{*com is dist of CoM from Proximal joint centre*}

    $BodyMass = 65
    $Lthighmass = 10.562
    $Lthighcom = 166
    $Lthighlength = 400
    $Lthighmi= {0.142,0.142,0.043}

    $trunkmass = 39.871
    $headmass   = 5.157
    $chestmass = 22.3825
    $absmass   = 2.1585
    $Pelmass   = 7.0662

```
$thighmass   = 12.2935
$shankmass   = 5.038
$footmass    = 1.0635
$uppermass   = 2.778
$foremass    = 1.4865
$handmass    = 0.459


totalmass   = $headmass + $chestmass + $pelmass+ $absmass + (2*
($thighmass + $shankmass + $footmass + $uppermass + $foremass + $handmass))


{*relative segment weight*}
$headr   = $headmass/ totalmass
$trunkr  = $trunkmass / totalmass
$chestr  = $chestmass / totalmass
$absr    = $absmass / totalmass
$pelr    = $pelmass / totalmass
$thighr  = $thighmass / totalmass
$shankr  = $shankmass / totalmass
$footr   = $footmass / totalmass
$upperr  = $uppermass / totalmass
$forer   = $foremass / totalmass
$handr   = $handmass / totalmass


{*hip joint centre percentages based on that of Seidel (1995)*}
$hjcXpcent = 14 {*medially*}
$hjcYpcent = -24 {*posteriorly*}
$hjcZpcent = 30 {*distally*}



{*knee joint centre based on Churchill et al. (1998)-midpoint of femeral
epicondyles*}


{*ankle joint centre based on Inman (1976)*}
$Lateralankjcz = 3 {*Z dist from lateral malleoli to JC)*}
```

$medialankjcz = 5 {*Z dist from lateral malleoli to JC)*}

{*shoulder joint centre based on Stokdijk et al. (2000)*}
$sjcx = -13.5
$sjcy = 39.4
$sjcz = 48.4

{*elbow joint centre based on Stokdijk et al. (1999) values given from the lateral epicondyle*}
$elbowz = 8.1 {*cranially*}
$elbowy = 18.6 {*ventrally of the epicondylus lateralis at 15.3o to the frontal plane*}

{*wrist - no info found :(*}

$%Hiplfpos = {-136.818,88.9841,167.444}
$%Hiprtpos = {-117.391,-86.8317,168.815}

$%NLMTL = {56.9934,-13.0743,-0.613458}
$%NLMTL5 = {-56.1409,-15.7445,-0.739091}
$%NLMTLT = {1.06761,-33.188,14.2603}
$%NRMTL = {45.608,21.3047,1.06394}
$%NRMTL5 = {-55.4431,4.22033,0.210763}
$%NRMTLT = {-10.7799,27.9645,1.62587}
$%STERB = {7.59132,202.264,226.694}
$%CLAVB = {3.26443,137.072,68.0096}
$%NLTIP = {-39.3888,18.6458,-191.072}
$%NLFIN = {-18.8538,-15.7416,-100.213}
$%NLLMP = {-36.1031,45.5147,-71.3496}

$%NRTIP = {66.8797,23.2888,-179.571}
$%NRFIN = {22.5957,-10.1707,-93.1472}
$%NRLMP = {48.7759,56.9432,-56.094}

APPENDIX E

Spring Subsystems in Simulink

Figure E1. Spring Top Level

Figure E2. Vertical Spring 'If' Subsystem

MA = (-k*pos^2)-(r*vel(pos));

if { }

Action Port
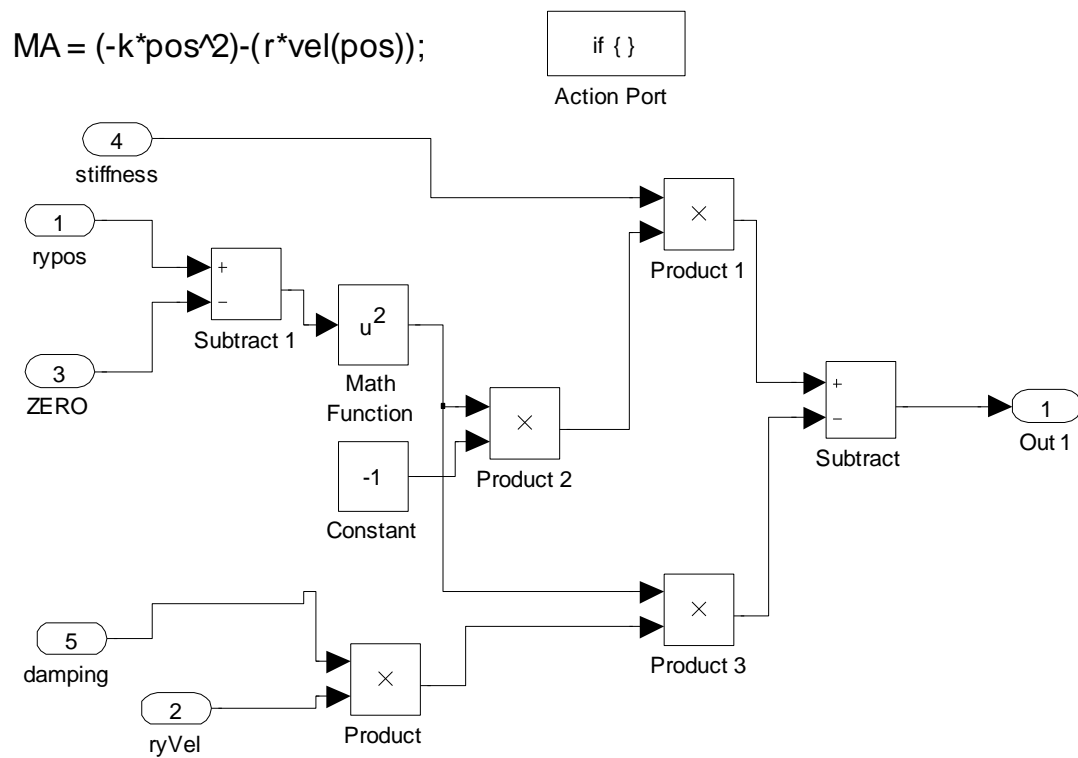
Figure E3. Vertical Spring in Ground Contact
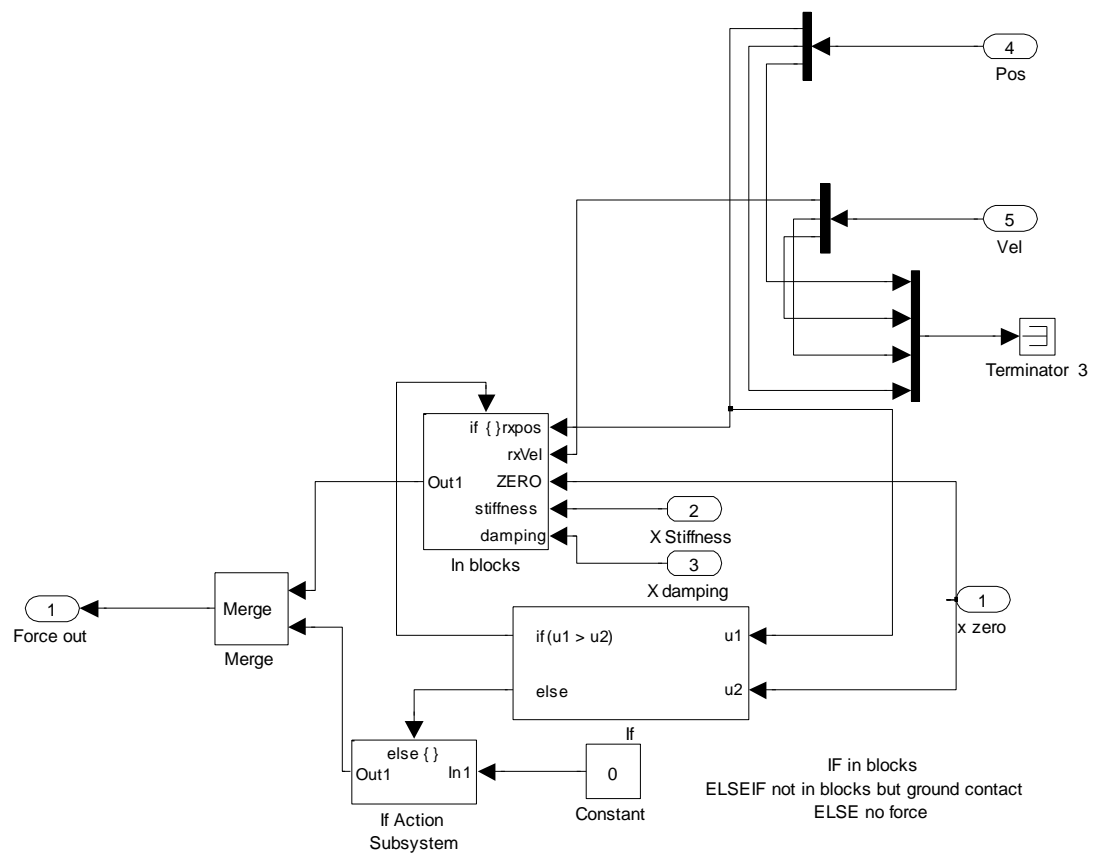
Figure E4. Horizontal Spring 'If' System

283
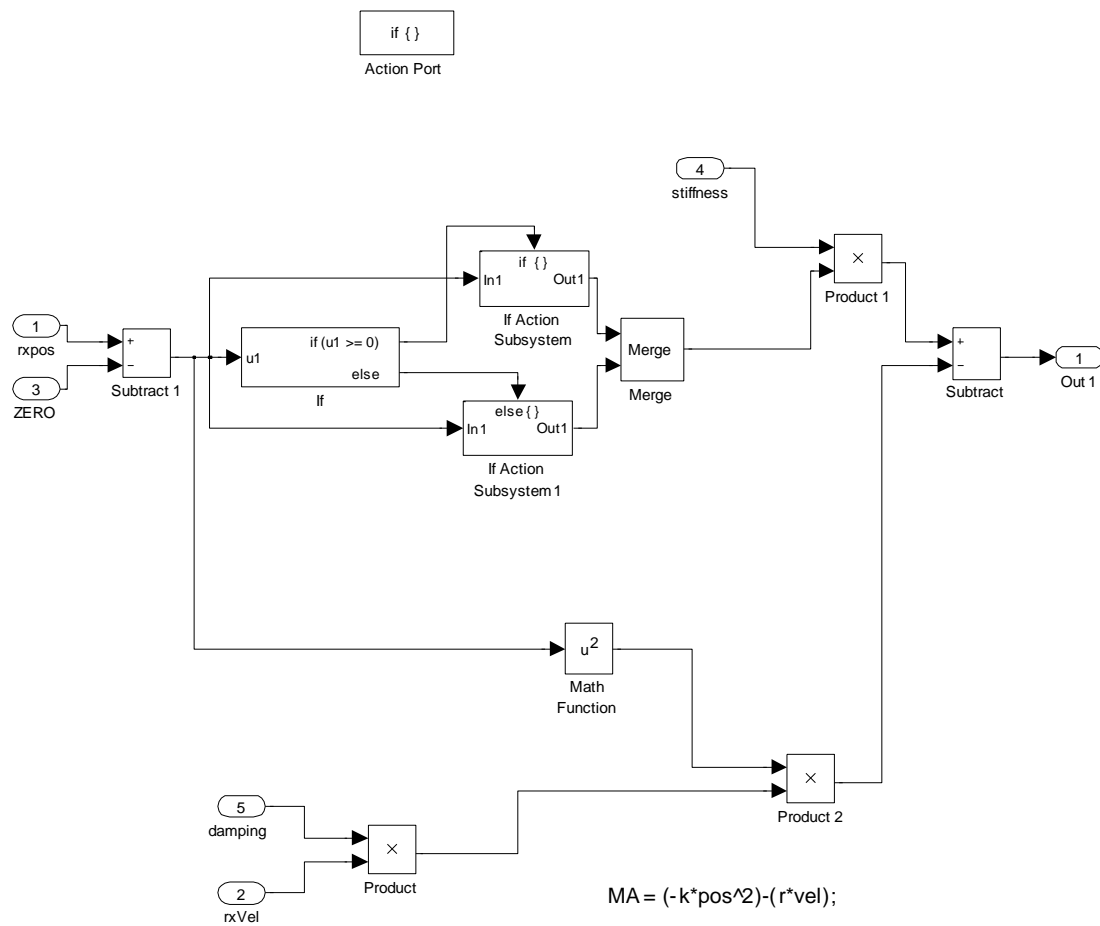
Figure E5. Horizontal Spring

APPENDIX F

Four Segment Model Spring Score

```matlab
function [score, x] = springsSCORE (x)

%limit peak force?
%knee angle/vel on leaving?

global ystiff
global xstiff
global ydamp
global xdamp
global toemove
global simno
global Xforce
global Yforce
global timeout
global saveparam

ystiff = x(1);
ydamp = x(2);
xstiff = x(3);
xdamp = x(4);
% ystiff = 12925015456.19589;
% ydamp =  16529970.45464;
% xstiff = 26211940020.22325;
% xdamp = 3359170940.616130;


sim ('foursegmodel')

toex = toemove(:,1);
toey = toemove(:,2);

toescore = (min(toex)+0.025) + (min(toey)+ 0.025);

%Try to stop vibrations
findxf = find (Xforce (3:length(Xforce)) ==0);
if sum(Xforce(findxf:length(Xforce)))>50
    xforcepen = 10;
else
    xforcepen = 0;
end

findyf = find (Yforce (3:length(Yforce)) ==0);
if sum(Yforce(findyf:length(Yforce)))>50
    yforcepen = 10;
else
    yforcepen = 0;
end
forcepens = xforcepen+yforcepen;

%Try to make sure its moving
if toex (length(toex))<0.3
    toepen = 50;
else
    toepen = 0;
end
%
%
%
%
%
```

```matlab
%Second lot of penalties (above alone gave spring params springs =
[8333750.00000000;5348823.06220258;556027.777777778;5000200;];
%
%
%
%dropping to zero before leaving
leavex = find(Xforce == 0);
if leavex > 0 %if has left the block at all!
leavetimex = timeout(leavex(1)); %time on zero x force
findxos = find(Xforce(3:leavex(1))<10);
xospen = 0.3*length(findxos);
else
    xospen = 20;
    leavetimex = timeout(length(timeout));
end


leavey = find(Yforce == 0);
if leavey > 0 %if has left the block at all!
leavetimey = timeout(leavey(1)); %time on zero y force
findyos = find(Yforce(3:leavey(1))<10);
yospen = 0.3*length(findyos);
else
    yospen = 20;
    leavetimey = timeout(length(timeout));
end


%try to limit forces to be realistic
maxx = max(Xforce);
if maxx > 1200
    maxxpen = (maxx-1200)/100;
else
    maxxpen = 0;
end


maxy = max(Yforce);
if maxy > 1200
    maxypen = (maxy-1200)/100;
else
    maxypen = 0;
end
%above pens gave:
% springs =
[1805911.60000000;3306819.20000000;6851182.60000000;9844269.10000000;
9.20185270000000;];


%added 13/3/09
%ensure that middle force is big
forcexfinishtime = (find (Xforce==0));
if forcexfinishtime > 1
forcexfinishtimefind = forcexfinishtime(2);
else
    forcexfinishtimefind = length(Xforce);
end
forceXrange = Xforce(1:forcexfinishtimefind);
forcexmidlocate = round((length(forceXrange))/2);
middlexforce = forceXrange(forcexmidlocate);
meanforcex = mean(forceXrange);
if middlexforce < meanforcex
    xmiddlepeakpen = 0.1*(meanforcex-middlexforce);
else
```

287

```matlab
    xmiddlepeakpen = 0;
end


%ensure that middle force is big
forceyfinishtime = (find (Yforce==0));
if forceyfinishtime > 1
forceyfinishtimefind = forceyfinishtime(2);
else
    forceyfinishtimefind = length(Yforce);
end
forceYrange = Yforce(1:forceyfinishtimefind);
forceymidlocate = round((length(forceYrange))/2);
middleyforce = forceYrange(forceymidlocate);
meanforcey = mean(forceYrange);
if middleyforce < meanforcey
    ymiddlepeakpen = 0.1*(meanforcey-middleyforce);
else
    ymiddlepeakpen = 0;
end



%similar release times
releasepen = sqrt((leavetimex-leavetimey)^2);

%Score sum
scorein =
sqrt((toescore)^2)+toepen+forcepens+xospen+yospen+releasepen+maxxpen+
maxypen+xmiddlepeakpen+ymiddlepeakpen;


saveparams = [ystiff;ydamp;xstiff;xdamp;scorein];
saveparam (:,simno) = saveparams;
save testingparams saveparam -ascii


simno = simno+1;


global toeswitch
toeswitch = 0;
score = scorein
```

APPENDIX G

Simulink Block Models and Subsystems
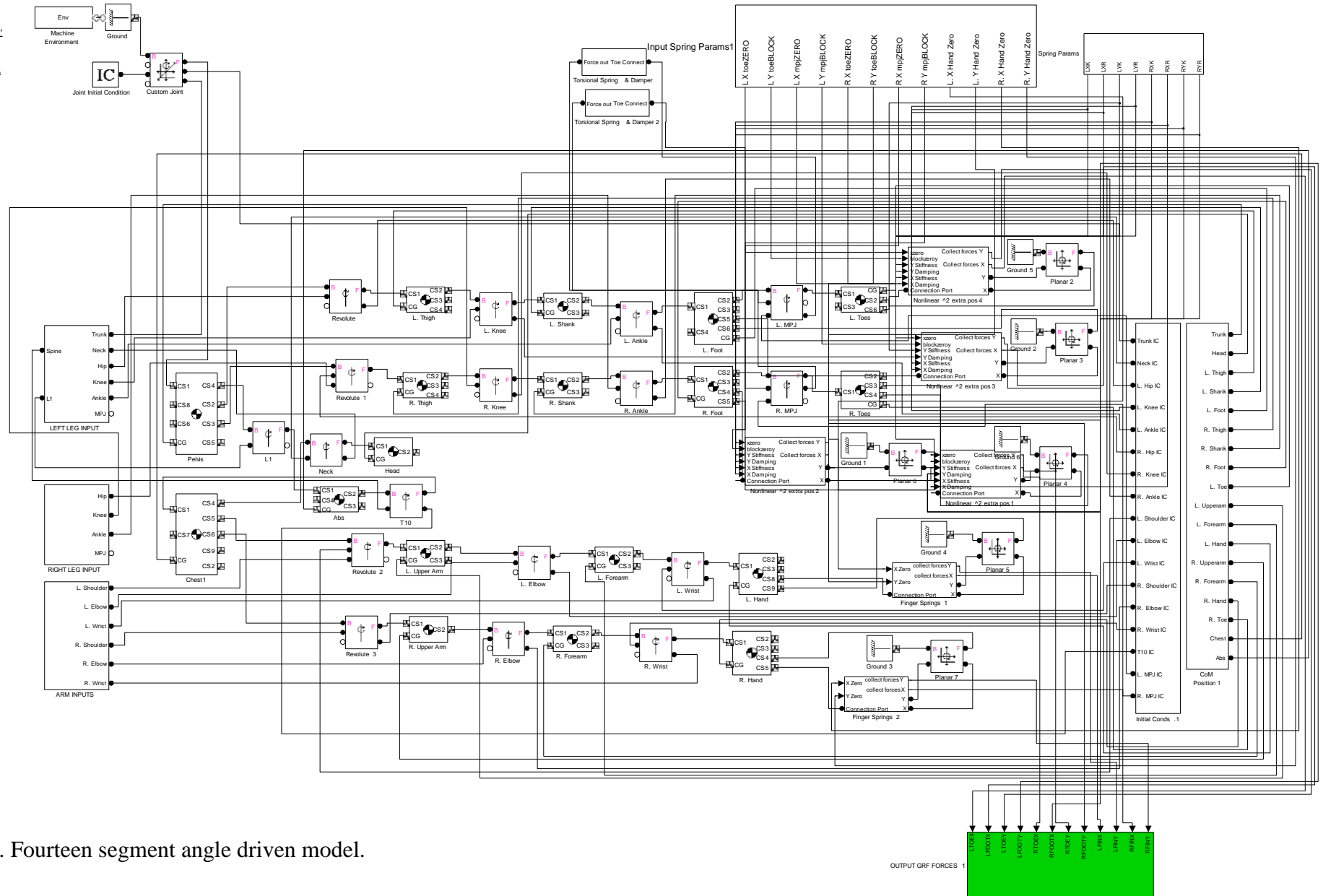
Figure G1. Fourteen segment angle driven model.
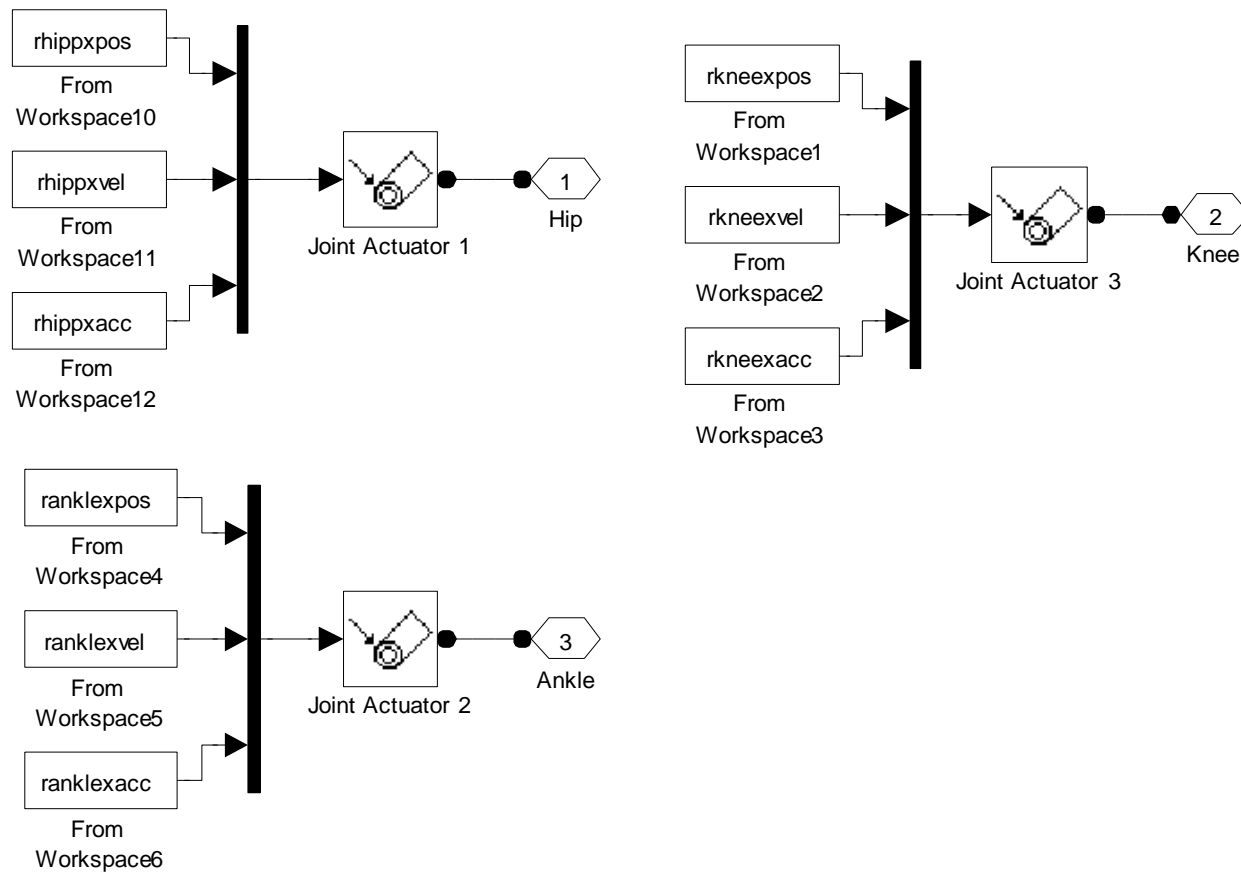
Figure G2. Example subsystem for angle inputs (right leg).
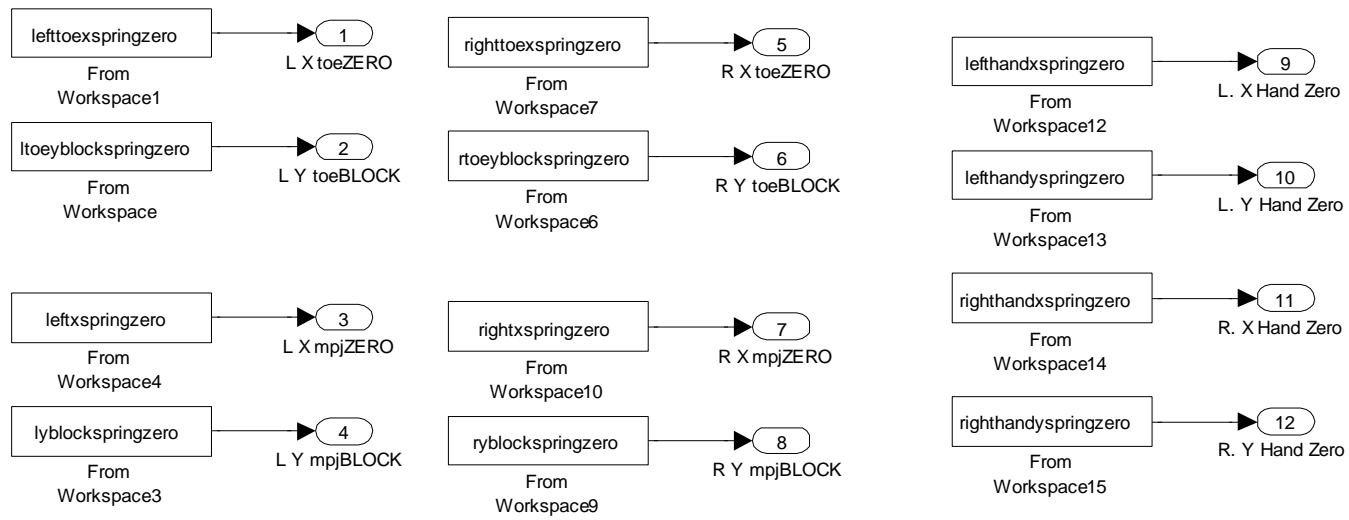
**Figure G3**. Subsystem for inputting for constant values (spring parameters).

**Figure G4**. Fourteen segment torque driven model in Simulink

293
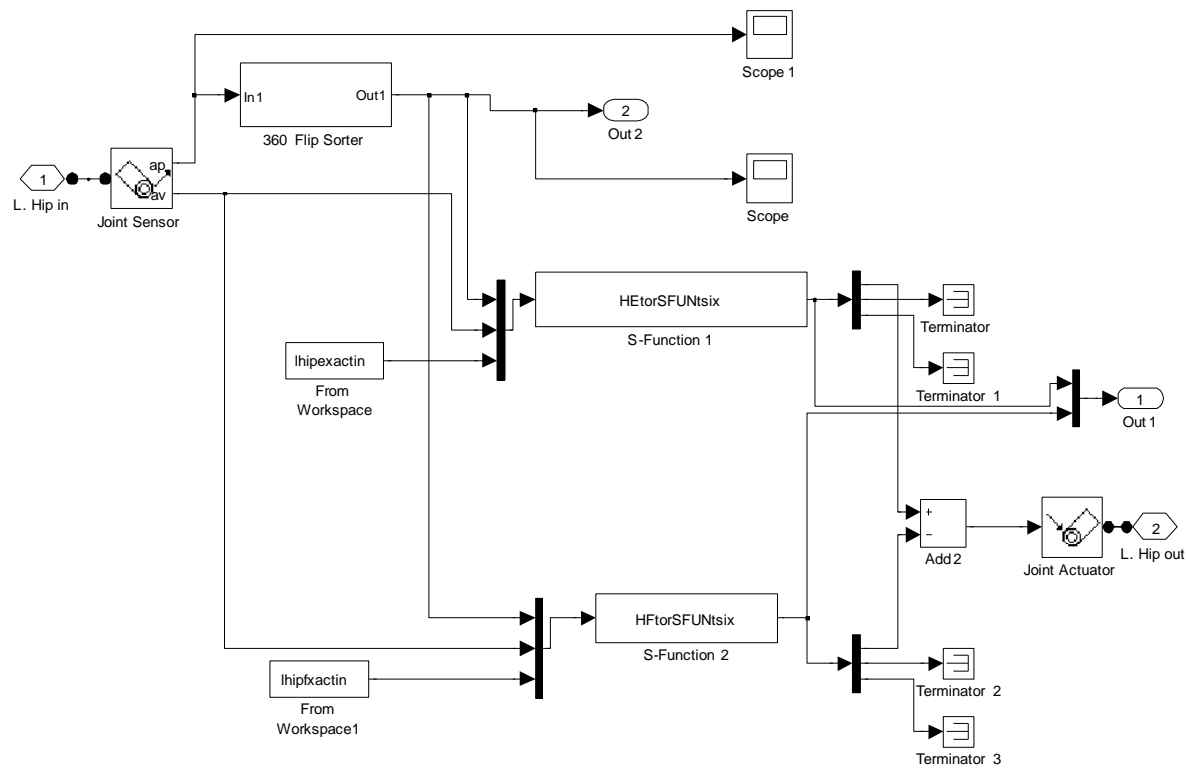
Figure G5. Torque input subsystem (left hip).

APPENDIX H

Joint Angle Comparison and EMG Plots
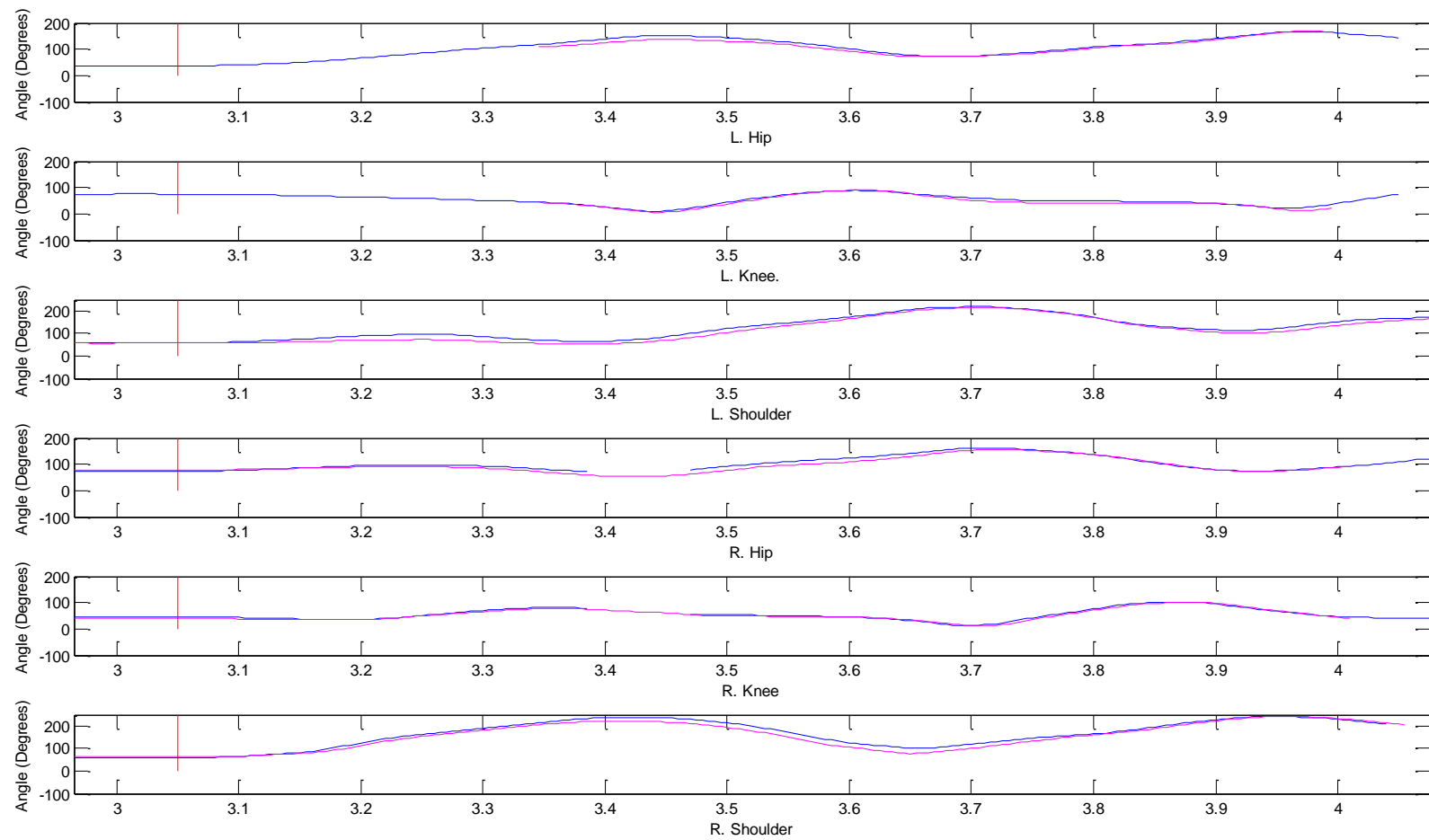
Figure H1. Comparison of joint angles for selected trials in data collections 1 and 2. Note, the blue line = data collection 1, pink line = data collection 2.
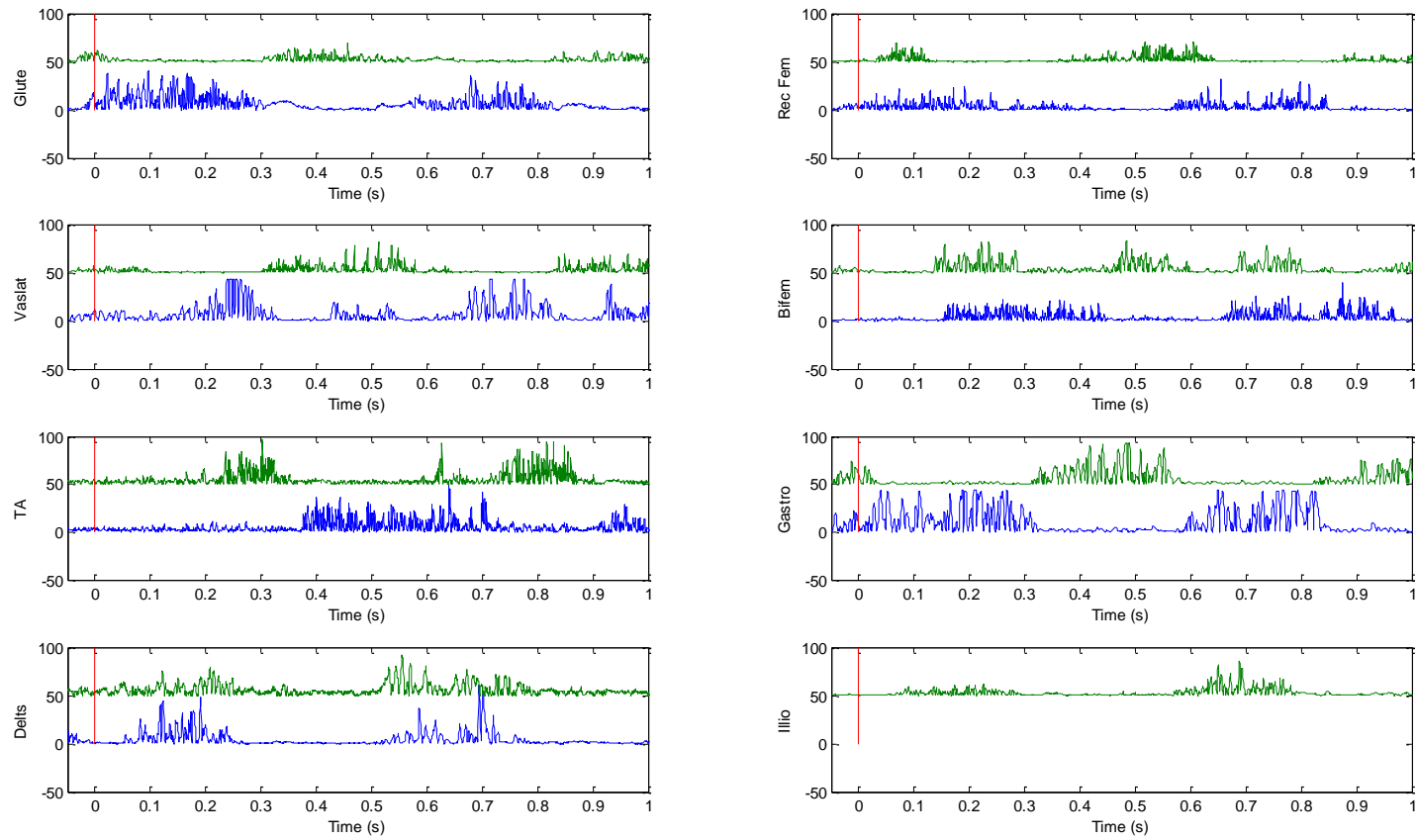
Figure H2. rEMG for the selected start. Red line indicates start of simulation, green lines are right side and blue are left. Note, all figures have been enlarged for clear viewing and for the right to be plotted above the left.

APPENDIX I

**Joint Activation Profiles and EMG Plots**
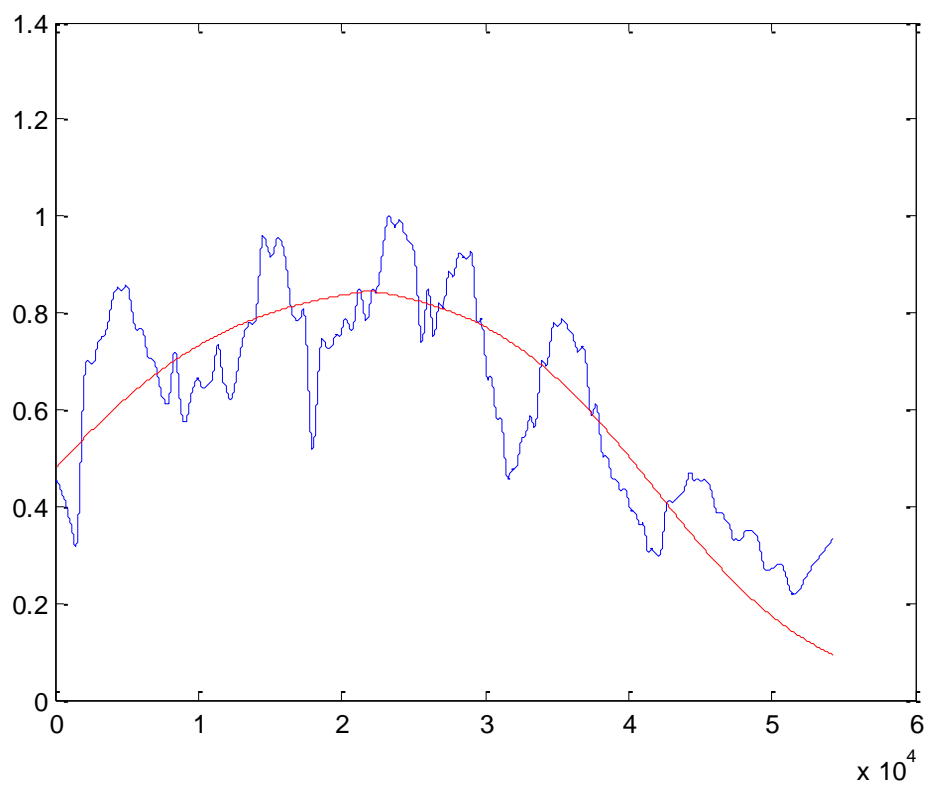
**Figure I1.** Left hip extension
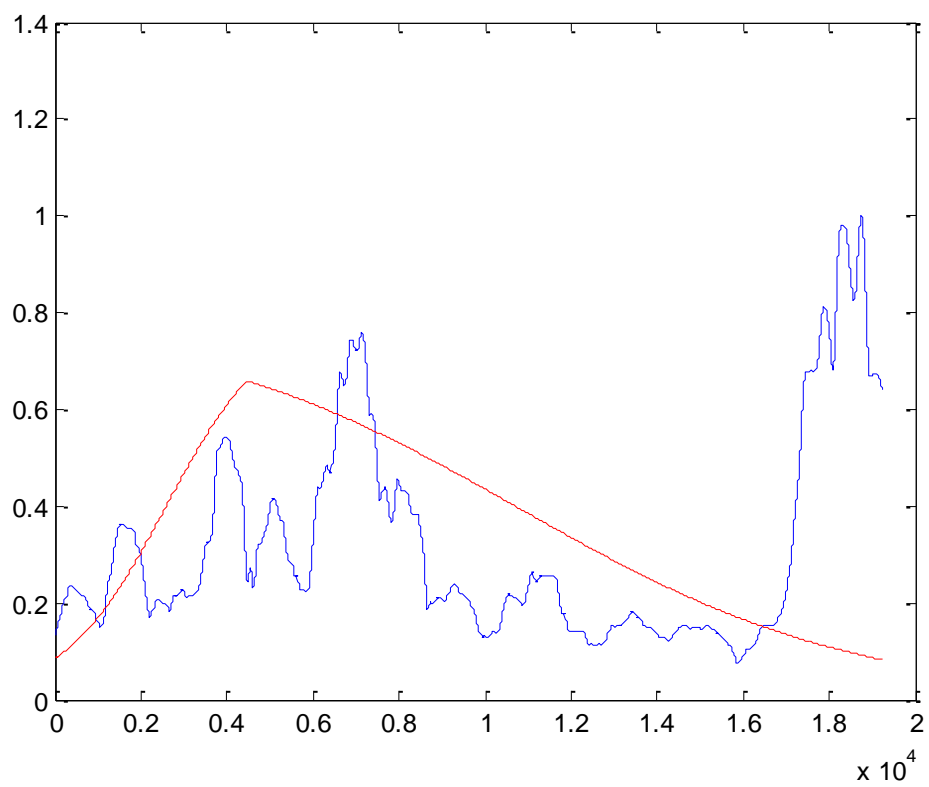
Figure I2. Right shoulder extension
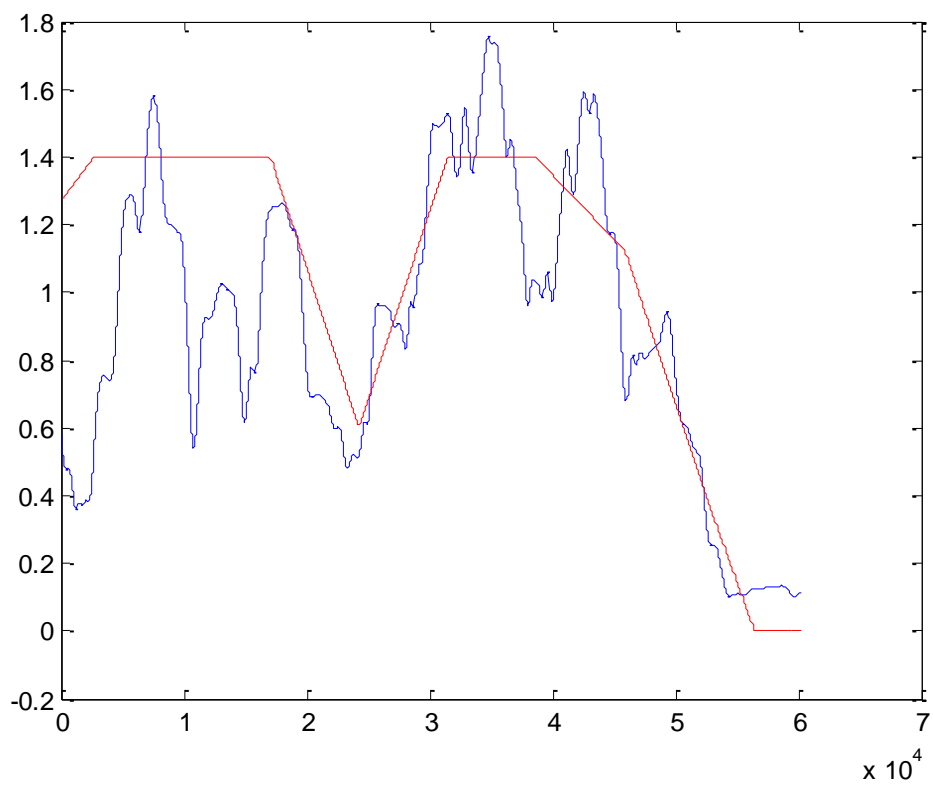
**Figure I3.** Left ankle plantarflexion
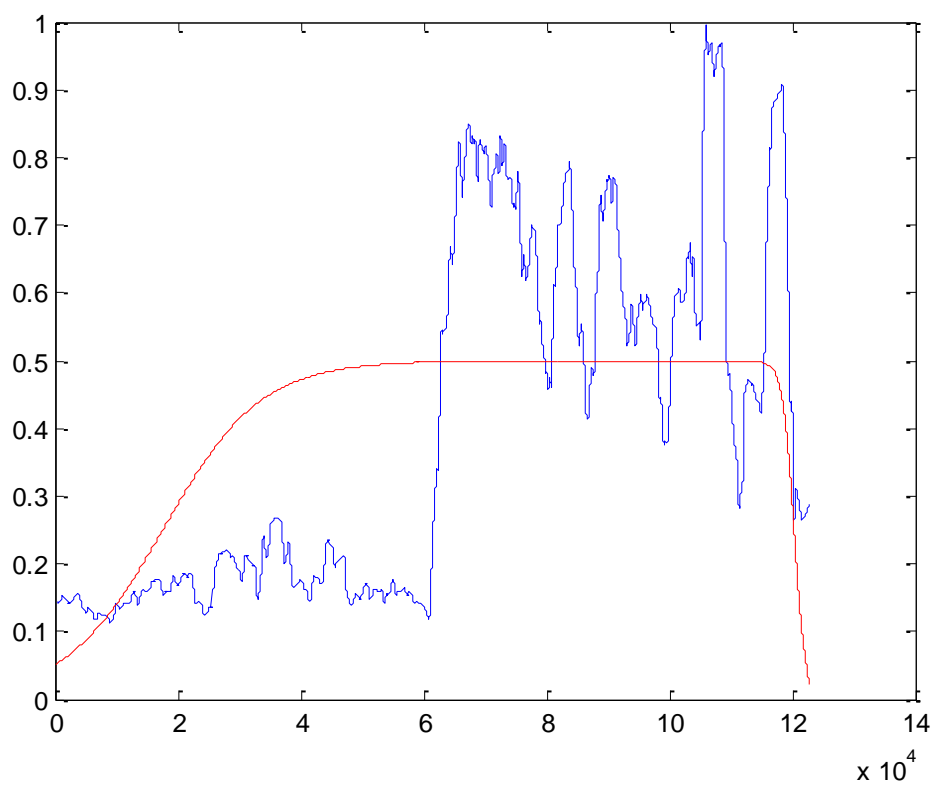

**Figure I4.** Left ankle dorsiflexion
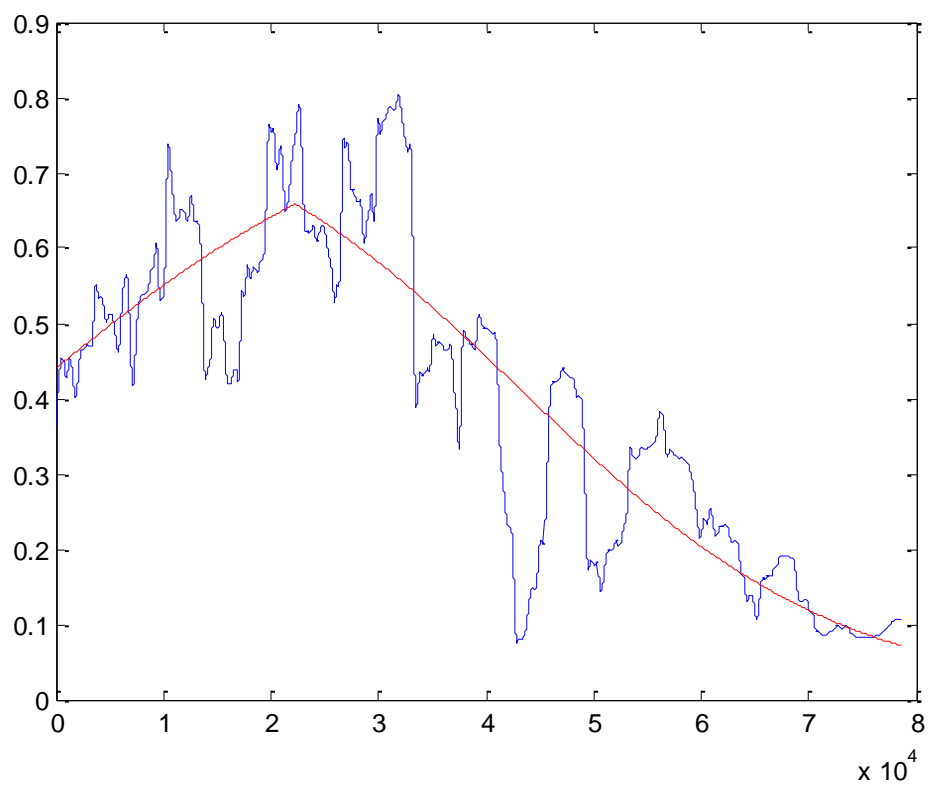
**Figure I5.** Left knee extension.
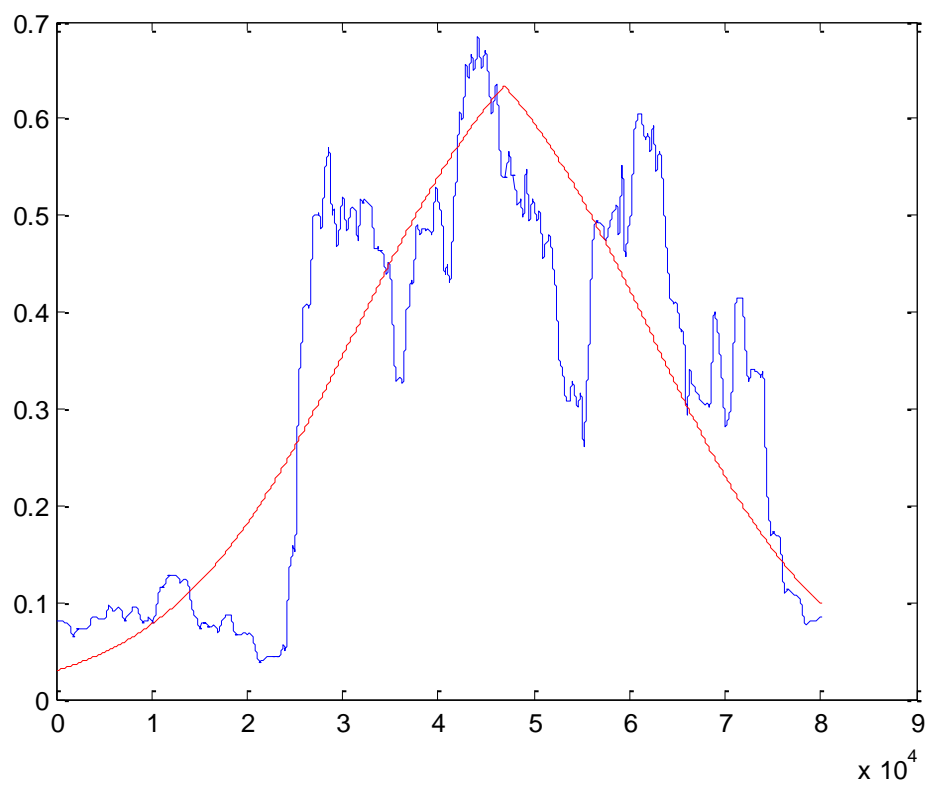
Figure I6. Left knee flexion
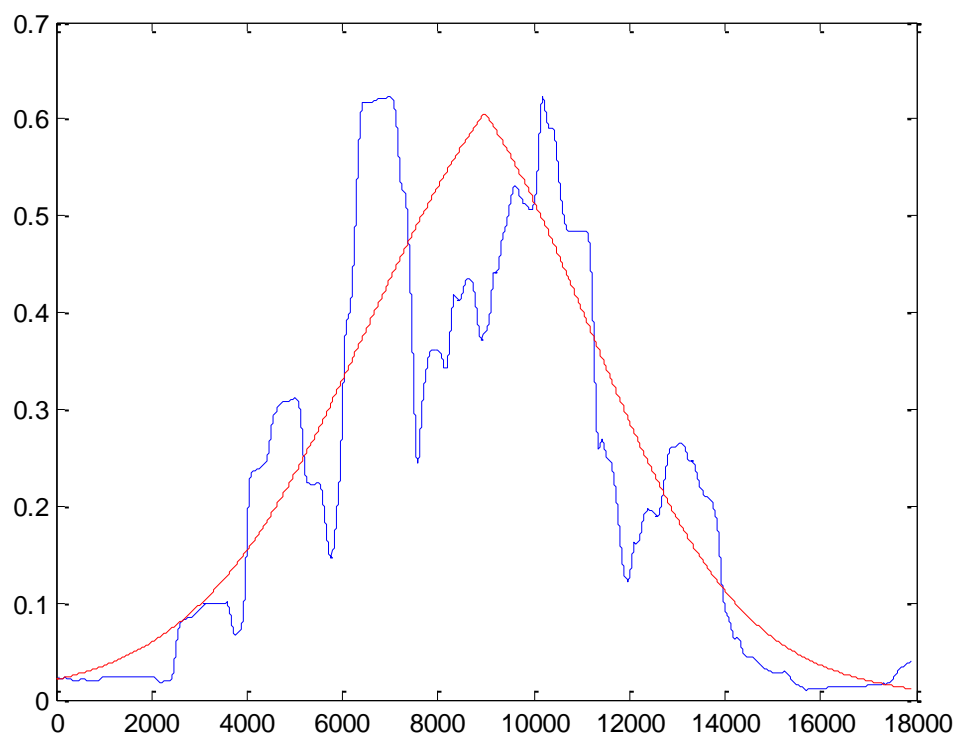
Figure I7. Left shoulder flexion
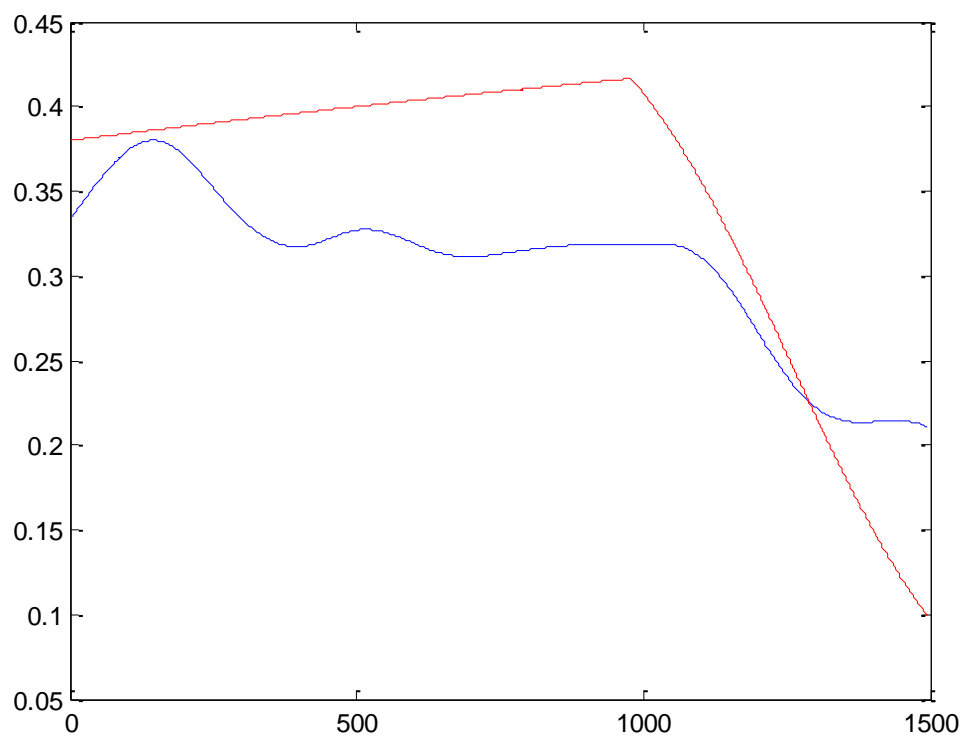

**Figure I8.** Right ankle plantar flexion
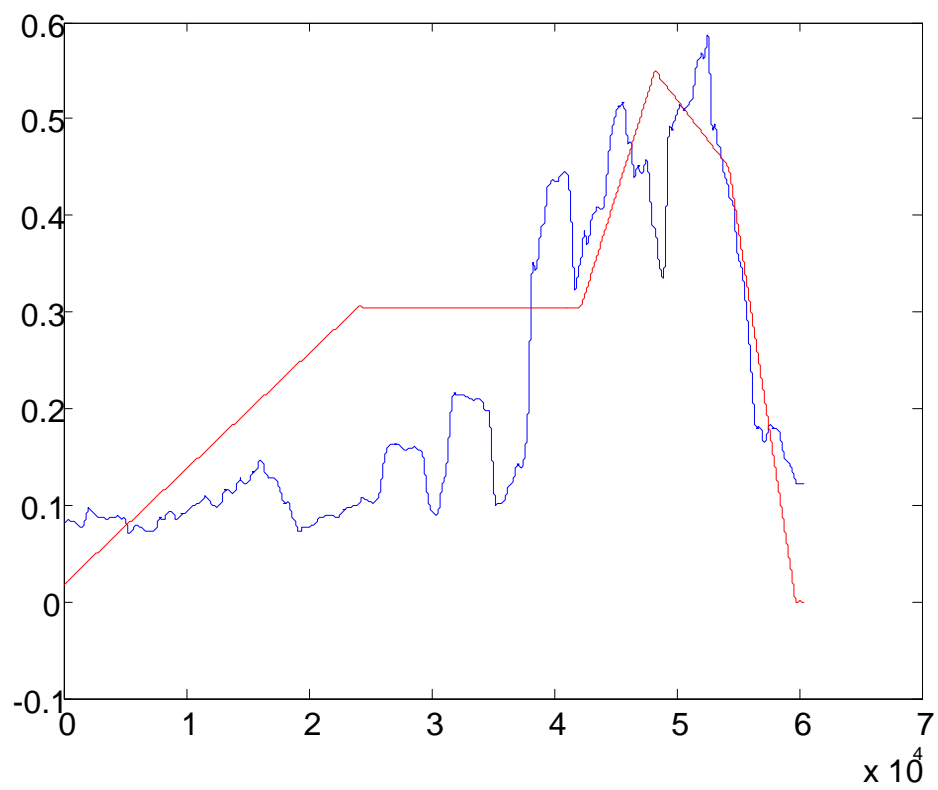
Figure I9. Right ankle dorsi flexion
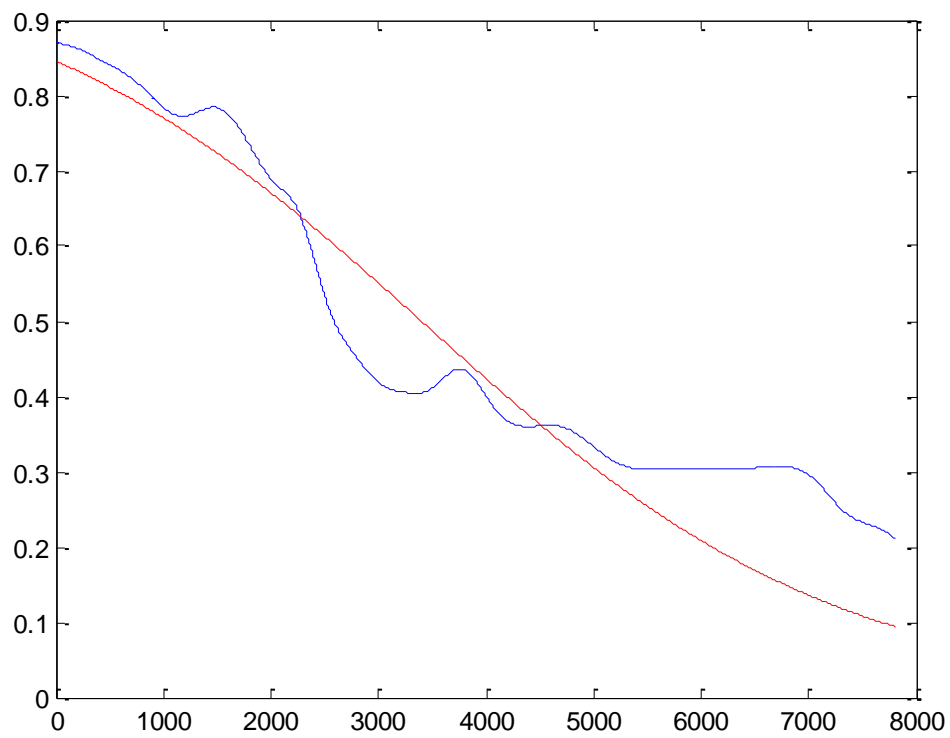

**Figure I10**. Right hip extension
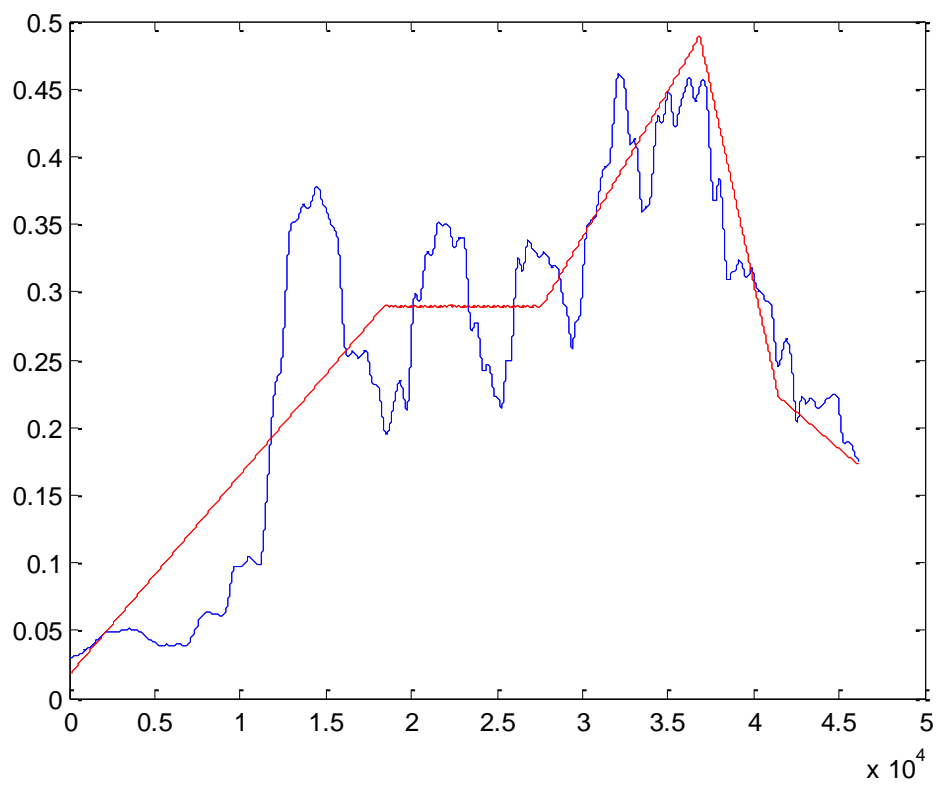
**Figure I11.** Right hip flexion
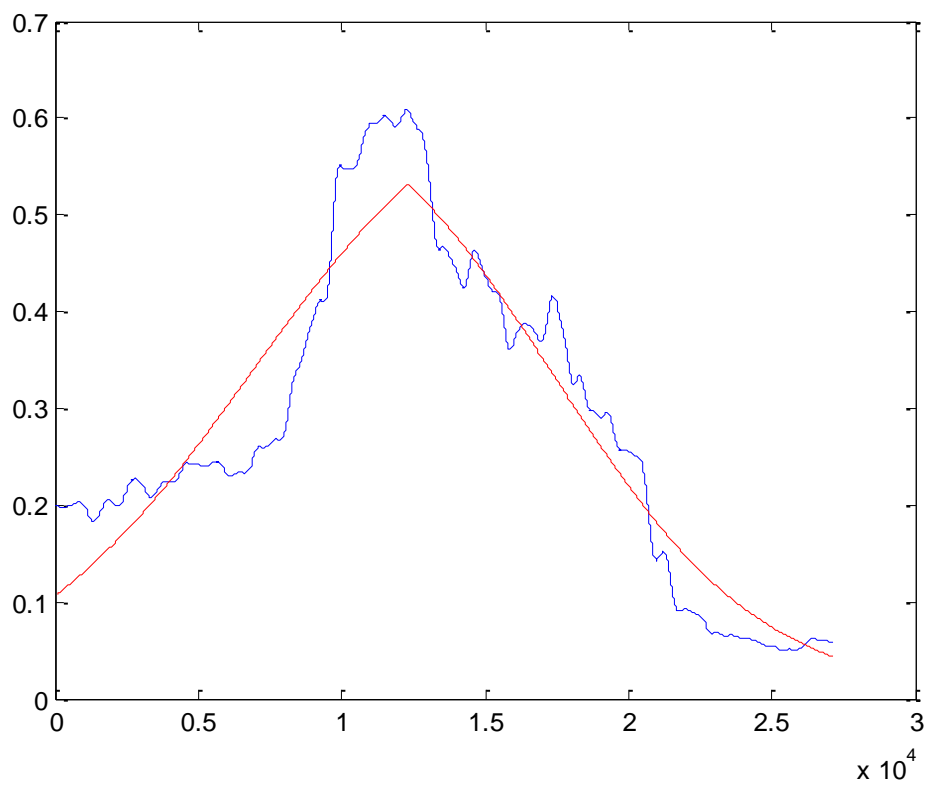
Figure I12. Right knee extension
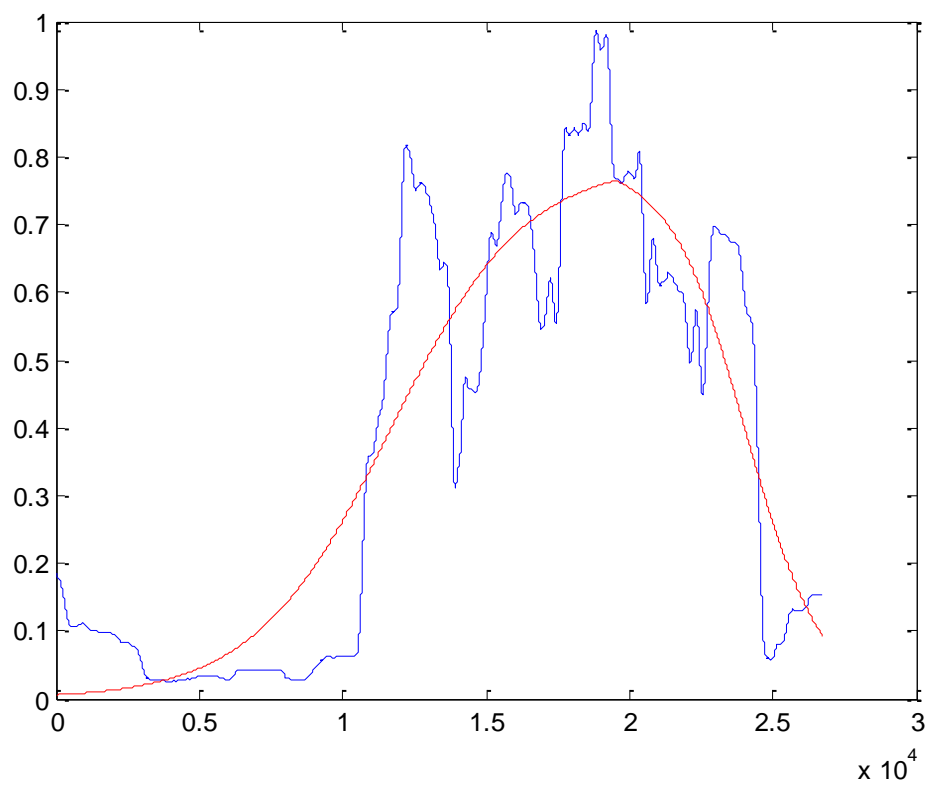
Figure I13. Right knee flexion

APPENDIX J

Joint Activation Input to Model

```matlab
%as SCOREC but allows for shortened activation profiles for when
%activations start before zero

%as SCOREB however inputs into model are given as one variable so
less for
%model to deal with
%each activation prfile is set in here instead of having to give the
sim on
%off and activations

%score prog to calc activation profiles for torques
function score = activationSCOREE(x)


%%%%%%%%%%%%%%%%%%%%%%%%%%%%%%%%%%%%%%%%%%%%%%%%%%%%%%%%%%
%%%%%%%%%%%%%%%%%%%%%%%%%%%%%%%%%%%%%%%%%%%%%%%%%%%%%%%%%%

%THINGS TO CHECK BEFORE ANY TIME THIS RUNS!

%Do you want to match the force?
%1 = match everything, 2 = match only the force, 3 = match only the
angles
matchforces = 3; %yes=1 no=0

%%%%% PENALTY FOR TOO MUCH FORCE IN TOE %%%%%%
%Include? Yes = 1 no = 0
toeforcelimit = 0;

%Compare joint angles?
%1 = yes, 0 = no
compangs = 1;

%how many sims should be saved
savelast = 2;

%%%%%%%%%%%%%%%%%%%%%%%%%%%%%%%%%%%%%%%%%%%%%%%%%%%%%%%%%%
%%%%%%%%%%%%%%%%%%%%%%%%%%%%%%%%%%%%%%%%%%%%%%%%%%%%%%%%%

%if using linear method, 'linear' else 'sig'
lapf = 'lin';
ladf = 'sig';
lke = 'sig'; %Left knee extension
lkf = 'sig'; %Left knee flexion
lhe = 'sig';
lhf = 'lin';

rapf = 'sig';
radf = 'lin';
rke = 'sig'; %Left knee extension
rkf = 'sig'; %Left knee flexion
rhe = 'sig';
rhf = 'lin';

%SHOULDERS
lse = 'sig';
lsf = 'sig';
rse = 'sig';
rsf = 'sig';
```

```matlab
%Two part activations
rheb = 'sig';
rkeb = 'sig';
radfb = 'sig';
rapfb = 'sig';


%
%tend = 0.438; %time of trial
%
% %ON OFF TIMES
% lhexton =0.0000000001;
% lhextof =0.2995;
% lhfxton =0.0745;
% lhfxtof=0.282;
%
% lkexton =0.0000000001;
% lkextof=0.3275;
% lkfxton =0.1485;
% lkfxtof=0.4425;
%
% laexton =0.2215
% laextof=0.349
% lafxton =0.00000001
% lafxtof=0.3215
%
% rhexton =0;
% rhextof=0.038;
% rhfxton =0.0745;
% rhfxtof=0.282;
%
% rkexton =0;
% rkextof=0.0975;
% rkfxton =0.129;
% rkfxtof=0.282;
%
% raexton =0.3675;
% raextof=tend;
% rafxton =0;
% rafxtof=0.025;
%
% lsexton =0.0000000001;
% lsextof=0.3275;
% lsfxton =0.1485;
% lsfxtof=0.4425;
%
% rsexton =8;%%%%%%%%%%%%%%%%0.0000000001;
% rsextof=9;%%%%%%%%%%%%%%0.3275;
% rsfxton =0.000000001;%%%%%%%%%%%%%%%%0.1485;
% rsfxtof=0.5;%%%%%%%%%%%%%%%%0.4425;
%
% %two part activations
% rhebxton = 0.299;
% rhebxtof=tend;
%
% rkebxton = 0.2965;
% rkebxtof= tend;
%
% rafbxton = 0.306;
% rafbxtof= tend;
```

```
global toeswitch
toeswitch = 0;

%global simpostwod9TSS
global simposfortor
%global simpos0438
global simpos
%global ltoexyz
%global rtoexyz

%FORCE FROM MODEL
%global ltoexforce
%global lmpjxforce
global lfootxforce

%global rtoexforce
%global rmpjxforce
global rfootxforce

%global ltoeyforce
%global lmpjyforce
global lfootyforce

%global rtoeyforce
%global rmpjyforce
global rfootyforce

global lfootresforce
global rfootresforce

%global lhandxforce
%global lhandyforce
%global lhandresforce

%global rhandxforce
%global rhandyforce
%global rhandresforce

%%%%%%%%%LOADED IN FROM ANGLEDRIVERGLOBAL%%%%%%%%%%%
global startfield %startfield of simulation
global endfield

%FORCE PLATE DATA
%global forcex
%global forcey
%global forcez
global highspeedsynch

%STARTING BLOCK DATA
global stlblockx
global stlblocky
global stlblockz
%global stlblockres

global strblockx
global strblocky
global strblockz
%global strblockres
```

309

```matlab
%WHEN LEFT BLOCKS?
global abcompend
global cdcompend
global hssblock

%This allows the spring on each step to be changes each trial
global ltoei
global lmpji
global rtoei
global rmpji

%global oddeven
global simno
global savno
global bestscore

global finishtime
global cputime
global startcputime
global clockstart
global simstop
global currentparamandscore
global currentparamsonly

global grouptorsim
%global grouptorn
global outtime
global timeout
global stopreason
global realjointangles

global leftmpjpos
global lefttoepos
global rightmpjpos
global righttoepos
% global lkexton
% global lkextof

global lhipangssav
global lhipangssim

%Things that I will set
global    lhipextmeas
global    rhipextmeas
global    lkneextmeas
global    rkneextmeas
global    lankextmeas
global    rankextmeas

laexton =  lankextmeas(1);
lkexton = lkneextmeas(1);
lhexton = lhipextmeas(1);
raexton = rankextmeas(1);
rkexton = rkneextmeas(1);
rhexton = rhipextmeas(1);
initialact = 0.05;
endact = 0.05;

%changes from doing the RMSEMG
```

```
laeinitialact = 0.8;
lkeinitialact = 0.1;
raeinitialact = 0.3;
rheinitialact = 0.1;


%things to opt
laextof      = x (    1   );
laemaxact    = x (    2   );
laesa   = x (    3   );
laesb   = x (    4   );
laesc   = x (    5   );
laese   = x (    6   );
laesf   = x (    7   );
laesg   = x (    8   );
laesh   = x (    9   );
laesi   = x (   10   );
laesj   = x (   11   );
lafxton      = x (   12   );
lafxtof      = x (   13   );
lafmaxact    = x (   14   );
lafsteepratio   = x (   15   );
lafs    = x (   16   );
lkextof      = x (   17   );
lkemaxact    = x (   18   );
lkesteepratio   = x (   19   );
lkes    = x (   20   );
lkfxton      = x (   21   );
lkfxtof      = x (   22   );
lkfmaxact    = x (   23   );
lkfsteepratio   = x (   24   );
lkfs    = x (   25   );
lhextof      = x (   26   );
lhemaxact    = x (   27   );
lhesteepratio   = x (   28   );
lhes    = x (   29   );
lhfxton      = x (   30   );
lhfxtof      = x (   31   );
lhfmaxact    = x (   32   );
lhfsa   = x (   33   );
lhfsb   = x (   34   );
lhfsc   = x (   35   );
lhfsd   = x (   36   );
lhfse   = x (   37   );
lhfsf   = x (   38   );
lhfsg   = x (   39   );
lhfsh   = x (   40   );
lhfsi   = x (   41   );
lhfsj   = x (   42   );
raextof      = x (   43   );
raemaxact    = x (   44   );
raesteepratio   = x (   45   );
raes    = x (   46   );
rafxton      = x (   47   );
rafxtof      = x (   48   );
rafmaxact    = x (   49   );
rafsa   = x (   50   );
rafsc   = x (   51   );
rafsd   = x (   52   );
rafse   = x (   53   );
rafsg   = x (   54   );
rafsh   = x (   55   );
```

311

```
rafsi   = x (    56  );
rafsj   = x (    57  );
rkextof    = x (    58  );
rkemaxact   = x (    59  );
rkesteepratio   = x (    60  );
rkes   = x (    61  );
rkfxton    = x (    62  );
rkfxtof    = x (    63  );
rkfmaxact   = x (    64  );
rkfsteepratio   = x (    65  );
rkfs   = x (    66  );
rhextof    = x (    67  );
rhemaxact   = x (    68  );
rhesteepratio   = x (    69  );
rhes   = x (    70  );
rhfxton    = x (    71  );
rhfxtof    = x (    72  );
rhfsa   = x (    73  );
rhfsb   = x (    74  );
rhfsc   = x (    75  );
rhfse   = x (    76  );
rhfsg   = x (    77  );
rhfsi   = x (    78  );
rhfsj   = x (    79  );
rhfmaxact   = x (    80  );
lsexton    = x (    81  );
lsextof    = x (    82  );
lsemaxact   = x (    83  );
lsesteepratio   = x (    84  );
lses   = x (    85  );
lsfxton    = x (    86  );
lsfxtof    = x (    87  );
lsfmaxact   = x (    88  );
lsfsteepratio   = x (    89  );
lsfs   = x (    90  );
rsexton    = x (    91  );
rsextof    = x (    92  );
rsemaxact   = x (    93  );
rsesteepratio   = x (    94  );
rses   = x (    95  );
rsfxton    = x (    96  );
rsfxtof    = x (    97  );
rsfmaxact   = x (    98  );
rsfsteepratio   = x (    99  );
rsfs   = x (    100 );
rhebxton   = x (    101 );
rhebxtof   = x (    102 );
rhebmaxact   = x (    103 );
rhebsteepratio  = x (    104 );
rhebs   = x (    105 );
rkebxton   = x (    106 );
rkebxtof   = x (    107 );
rkebmaxact   = x (    108 );
rkebsteepratio  = x (    109 );
rkebs   = x (    110 );
rafbxton   = x (    111 );
rafbxtof   = x (    112 );
rafbmaxact   = x (    113 );
rafbsteepratio  = x (    114 );
rafbs   = x (    115 );
raebxton    = x (    116 );
```

312

```
raebxtof    = x (   117 );
raebmaxact  = x (   118 );
raebsteepratio = x (   119 );
raebs   = x (   120 );



laesd = laesc;
rafsf = rafse;
rafsb = rafsa;
rhfsd = rhfsc;
rhfsf = rhfsd;
rhfsh = rhfsg;


currentparams = [laextof    laemaxact    laesa    laesb    laesc    laesd
laese    laesf    laesg    laesh    laesi  laesj lafxton      lafxtof
lafmaxact    lafsteepratio    lafs    lkextof      lkemaxact
lkesteepratio    lkes    lkfxton      lkfxtof      lkfmaxact
lkfsteepratio    lkfs    lhextof      lhemaxact    lhesteepratio    lhes
lhfxton      lhfxtof    lhfmaxact    lhfsa  lhfsb    lhfsc    lhfsd
lhfse    lhfsf    lhfsg    lhfsh    lhfsi    lhfsj    raextof      raemaxact
raesteepratio    raes    rafxton      rafxtof      rafmaxact    rafsa
rafsb    rafsc    rafsd    rafse    rafsf    rafsg    rafsh    rafsi    rafsj
rkextof      rkemaxact    rkesteepratio    rkes    rkfxton      rkfxtof
rkfmaxact    rkfsteepratio    rkfs    rhextof      rhemaxact
rhesteepratio    rhes    rhfxton      rhfxtof      rhfsa    rhfsb    rhfsc
rhfsd    rhfse    rhfsf    rhfsg    rhfsh    rhfsi    rhfsj    rhfmaxact
lsexton    lsextof    lsemaxact    lsesteepratio    lses    lsfxton
lsfxtof    lsfmaxact    lsfsteepratio    lsfs    rsexton      rsextof
rsemaxact    rsesteepratio    rses    rsfxton      rsfxtof      rsfmaxact
rsfsteepratio    rsfs    rhebxton    rhebxtof    rhebmaxact
rhebsteepratio    rhebs    rkebxton    rkebxtof    rkebmaxact
rkebsteepratio    rkebs    rafbxton    rafbxtof    rafbmaxact
rafbsteepratio    rafbs    raebxton    raebxtof    raebmaxact
raebsteepratio    raebs ]';


save currentparamsE currentparams -ascii

%find muscle activation profile for given params
%order:
(on,off,ramplimit,initialact,maxact,sa,sb,sc,sd,se,sf,sg,sh,si,sj)

%LEFT HIP EXTENSION
if lhe == 'lin'
    [lhetimepro,lheactpro] =
muscleactivationFUNd(lhexton,lhextof,initialact,lhemaxact,lhesa,lhesb
,lhesc,lhesd,lhese,lhesf,lhesg,lhesh,lhesi,lhesj);
lhipexact = [lhetimepro,lheactpro];
elseif lhe == 'sig'
    [lhetime,lheactout] =
muscleactivationsigFUNb(lhexton,lhextof,initialact,endact,lhemaxact,l
hesteepratio,lhes);
lhipexact = [lhetime,lheactout];
end
%'LHE'
%LEFT HIP FLEXION
if lhf == 'lin'
    [lhftimepro,lhfactpro] =
muscleactivationFUNd(lhfxton,lhfxtof,initialact,lhfmaxact,lhfsa,lhfsb
,lhfsc,lhfsd,lhfse,lhfsf,lhfsg,lhfsh,lhfsi,lhfsj);
lhipfxact = [lhftimepro,lhfactpro];
```

313

```matlab
elseif lhf == 'sig'
    [lhftimeb,lhfactout] =
muscleactivationsigFUNb(lhfxton,lhfxtof,initialact,endact,lhfmaxact,l
hfsteepratio,lhfs);
lhipfxact = [lhftimeb,lhfactout];
end
%'LHF'

%LEFT KNEE EXTENSION
if lke == 'lin'
    [lketimepro,lkeactpro] =
muscleactivationFUNd(lkexton,lkextof,lkeinitialact,lkemaxact,lkesa,lk
esb,lkesc,lkesd,lkese,lkesf,lkesg,lkesh,lkesi,lkesj);
lkneexact = [lketimepro,lkeactpro];
elseif lke == 'sig'
    [lketime,lkeactout] =
muscleactivationsigFUNb(lkexton,lkextof,lkeinitialact,endact,lkemaxac
t,lkesteepratio,lkes);
lkneexact = [lketime,lkeactout];
end
%'LKE'
%LEFT KNEE FLEXION
if lkf == 'lin'
    [lkftimepro,lkfactpro] =
muscleactivationFUNd(lkfxton,lkfxtof,initialact,lkfmaxact,lkfsa,lkfsb
,lkfsc,lkfsd,lkfse,lkfsf,lkfsg,lkfsh,lkfsi,lkfsj);
lknefxact = [lkftimepro,lkfactpro];
elseif lkf == 'sig'
    [lkftimeb,lkfactout] =
muscleactivationsigFUNb(lkfxton,lkfxtof,initialact,endact,lkfmaxact,l
kfsteepratio,lkfs);
lknefxact = [lkftimeb,lkfactout];
end
%'LKF'


%LEFT ANKLE EXTENSION
if lapf == 'lin'
    [lapftimepro,lapfactpro] =
muscleactivationFUNd(laexton,laextof,laeinitialact,laemaxact,laesa,la
esb,laesc,laesd,laese,laesf,laesg,laesh,laesi,laesj);
lankexact = [lapftimepro,lapfactpro];
elseif lapf == 'sig'
    [lapftime,lapfactout] =
muscleactivationsigFUNb(laexton,laextof,laeinitialact,endact,laemaxac
t,laesteepratio,laes);
lankexact = [lapftime,lapfactout];
end
%'LAE'
%LEFT ANKLE FLEXION
if ladf == 'lin'
    [ladftimepro,ladfactpro] =
muscleactivationFUNd(lafxton,lafxtof,initialact,lafmaxact,lafsa,lafsb
,lafsc,lafsd,lafse,lafsf,lafsg,lafsh,lafsi,lafsj);
lankfxact = [ladftimepro,ladfactpro];
elseif ladf == 'sig'
    [ladftimeb,ladfactout] =
muscleactivationsigFUNb(lafxton,lafxtof,initialact,endact,lafmaxact,l
afsteepratio,lafs);
lankfxact = [ladftimeb,ladfactout];
end
```

```matlab
%'LAF'


%RIGHT HIP EXTENSION
if rhe == 'lin'
    [rhetimepro,rheactpro] =
muscleactivationFUNd(rhexton,rhextof,rheinitialact,rhemaxact,rhesa,rh
esb,rhesc,rhesd,rhese,rhesf,rhesg,rhesh,rhesi,rhesj);
rhipexact = [rhetimepro,rheactpro];
elseif rhe == 'sig'
    [rhetime,rheactout] =
muscleactivationsigFUNb(rhexton,rhextof,rheinitialact,endact,rhemaxac
t,rhesteepratio,rhes);
rhipexact = [rhetime,rheactout];
end
%'RHE'
%RIGHT HIP FLEXION
if rhf == 'lin'
    [rhftimepro,rhfactpro] =
muscleactivationFUNd(rhfxton,rhfxtof,initialact,rhfmaxact,rhfsa,rhfsb
,rhfsc,rhfsd,rhfse,rhfsf,rhfsg,rhfsh,rhfsi,rhfsj);
rhipfxact = [rhftimepro,rhfactpro];
elseif rhf == 'sig'
    [rhftimeb,rhfactout] =
muscleactivationsigFUNb(rhfxton,rhfxtof,initialact,endact,rhfmaxact,r
hfsteepratio,rhfs);
rhipfxact = [rhftimeb,rhfactout];
end
%'RHF'



%RIGHT KNEE EXTENSION
if rke == 'lin'
    [rketimepro,rkeactpro] =
muscleactivationFUNd(rkexton,rkextof,initialact,rkemaxact,rkesa,rkesb
,rkesc,rkesd,rkese,rkesf,rkesg,rkesh,rkesi,rkesj);
rkneexact = [rketimepro,rkeactpro];
elseif rke == 'sig'
    [rketime,rkeactout] =
muscleactivationsigFUNb(rkexton,rkextof,initialact,endact,rkemaxact,r
kesteepratio,rkes);
rkneexact = [rketime,rkeactout];
end
%'RKE'
%RIGHT KNEE FLEXION
if rkf == 'lin'
    [rkftimepro,rkfactpro] =
muscleactivationFUNd(rkfxton,rkfxtof,initialact,rkfmaxact,rkfsa,rkfsb
,rkfsc,rkfsd,rkfse,rkfsf,rkfsg,rkfsh,rkfsi,rkfsj);
rknefxact = [rkftimepro,rkfactpro];
elseif rkf == 'sig'
    [rkftimeb,rkfactout] =
muscleactivationsigFUNb(rkfxton,rkfxtof,initialact,endact,rkfmaxact,r
kfsteepratio,rkfs);
rknefxact = [rkftimeb,rkfactout];
end
%'RKF'



%RIGHT ANKLE EXTENSION
```

```matlab
if rapf == 'lin'
    [rapftimepro,rapfactpro] =
muscleactivationFUNd(raexton,raextof,raeinitialact,raemaxact,raesa,ra
esb,raesc,raesd,raese,raesf,raesg,raesh,raesi,raesj);
rankexact = [rapftimepro,rapfactpro];
elseif rapf == 'sig'
    [rapftime,rapfactout] =
muscleactivationsigFUNb(raexton,raextof,raeinitialact,endact,raemaxac
t,raesteepratio,raes);
rankexact = [rapftime,rapfactout];
end
%'RAE'
%RIGHT ANKLE FLEXION
if radf == 'lin'
    [radftimepro,radfactpro] =
muscleactivationFUNd(rafxton,rafxtof,initialact,rafmaxact,rafsa,rafsb
,rafsc,rafsd,rafse,rafsf,rafsg,rafsh,rafsi,rafsj);
rankfxact = [radftimepro,radfactpro];
elseif radf == 'sig'
    [radftimeb,radfactout] =
muscleactivationsigFUNb(rafxton,rafxtof,initialact,endact,rafmaxact,r
afsteepratio,rafs);
rankfxact = [radftimeb,radfactout];
end
%'RAF'


%LEFT SHOULDER EXTENSION
if lse == 'lin'
    [lsetimepro,lseactpro] =
muscleactivationFUNd(lsexton,lsextof,initialact,lsemaxact,lsesa,lsesb
,lsesc,lsesd,lsese,lsesf,lsesg,lsesh,lsesi,lsesj);
lshoexact = [lsetimepro,lseactpro];
elseif lse == 'sig'
    [lsetime,lseactout] =
muscleactivationsigFUNb(lsexton,lsextof,initialact,endact,lsemaxact,l
sesteepratio,lses);
lshoexact = [lsetime,lseactout];
end
%'LSE'
%LEFT SHOULDER FLEXION
if lsf == 'lin'
    [lsftimepro,lsfactpro] =
muscleactivationFUNd(lsfxton,lsfxtof,initialact,lsfmaxact,lsfsa,lsfsb
,lsfsc,lsfsd,lsfse,lsfsf,lsfsg,lsfsh,lsfsi,lsfsj);
lshofxact = [lsftimepro,lsfactpro];
elseif lsf == 'sig'
    [lsftimeb,lsfactout] =
muscleactivationsigFUNb(lsfxton,lsfxtof,initialact,endact,lsfmaxact,l
sfsteepratio,lsfs);
lshofxact = [lsftimeb,lsfactout];
end
%'LSF'


%RIGHT SHOULDER EXTENSION
if rse == 'lin'
    [rsetimepro,rseactpro] =
muscleactivationFUNd(rsexton,rsextof,initialact,rsemaxact,rsesa,rsesb
,rsesc,rsesd,rsese,rsesf,rsesg,rsesh,rsesi,rsesj);
```

```matlab
rshoexact = [rsetimepro,rseactpro];
elseif rse == 'sig'
    [rsetime,rseactout] =
muscleactivationsigFUNb(rsexton,rsextof,initialact,endact,rsemaxact,r
sesteepratio,rses);
rshoexact = [rsetime,rseactout];
end
%'RSE'
%RIGHT SHOULDER FLEXION
if rsf == 'lin'
    [rsftimepro,rsfactpro] =
muscleactivationFUNd(rsfxton,rsfxtof,initialact,rsfmaxact,rsfsa,rsfsb
,rsfsc,rsfsd,rsfse,rsfsf,rsfsg,rsfsh,rsfsi,rsfsj);
rshofxact = [rsftimepro,rsfactpro];
elseif rsf == 'sig'
    [rsftimeb,rsfactout] =
muscleactivationsigFUNb(rsfxton,rsfxtof,initialact,endact,rsfmaxact,r
sfsteepratio,rsfs);
rshofxact = [rsftimeb,rsfactout];
end
%'RSF'



%%%%%%%%%%%%%%%%%%%%%%%%%%%%%%%
%%%% TWO PART ACTIVATIONS %%%%%
%%%%%%%%%%%%%%%%%%%%%%%%%%%%%%%

%this bit provides the input for the second activation

%RIGHT KNEE EXTENSION Part B
if rkeb == 'lin'
    [rkebtimepro,rkebactpro] =
muscleactivationFUNd(rkebxton,rkebxtof,initialact,rkemaxact,rkebsa,rk
ebsb,rkebsc,rkebsd,rkebse,rkebsf,rkebsg,rkebsh,rkebsi,rkebsj);
rknebexact = [rkebtimepro,rkebactpro];
elseif rkeb == 'sig'
    [rkebtime,rkebactout] =
muscleactivationsigFUNb(rkebxton,rkebxtof,initialact,endact,rkebmaxac
t,rkebsteepratio,rkebs);
rknebexact = [rkebtime,rkebactout];
end



%RIGHT HIP EXTENSION Part B
if rhe == 'lin'
    [rhetimepro,rheactpro] =
muscleactivationFUNd(rhebxton,rhebxtof,initialact,rhemaxact,rhebsa,rh
ebsb,rhebsc,rhebsd,rhebse,rhebsf,rhebsg,rhebsh,rhebsi,rhebsj);
rhipbexact = [rhetimepro,rheactpro];
elseif rheb == 'sig'
    [rhebtime,rhebactout] =
muscleactivationsigFUNb(rhebxton,rhebxtof,initialact,endact,rhebmaxac
t,rhebsteepratio,rhebs);
rhipbexact = [rhebtime,rhebactout];
end



%RIGHT ANKLE FLEXION
if radfb == 'lin'
```

```matlab
    [radfbtimepro,radfbactpro] =
muscleactivationFUNd(rafbxton,rafbxtof,initialact,rafbmaxact,rafbsa,r
afbsb,rafbsc,rafbsd,rafbse,rafbsf,rafbsg,rafbsh,rafbsi,rafbsj);
rankbfxact = [radfbtimepro,radfbactpro];
elseif radfb == 'sig'
    [radfbtimeb,radfbactout] =
muscleactivationsigFUNb(rafbxton,rafbxtof,initialact,endact,rafbmaxac
t,rafbsteepratio,rafbs);
rankbfxact = [radfbtimeb,radfbactout];
end

%RIGHT ANKLE EXTENSION
if rapfb == 'lin'
    [rapfbtimepro,rapfbactpro] =
muscleactivationFUNd(raebxton,raebxtof,initialact,raebmaxact,raebsa,r
aebsb,raebsc,raebsd,raebse,raebsf,raebsg,raebsh,raebsi,raebsj);
rankbexact = [rapfbtimepro,rapfbactpro];
elseif radfb == 'sig'
    [rapfbtimeb,rapfbactout] =
muscleactivationsigFUNb(raebxton,raebxtof,initialact,endact,raebmaxac
t,raebsteepratio,raebs);
rankbexact = [rapfbtimeb,rapfbactout];
end

%for some reason lhfxtof will not go into model so is changed to this
%before running sim
global lhfxtofa
lhfxtofa = lhfxtof;
global rankbfxactb
rankbfxactb = rankbfxact;

global lankexactin
global lankfxactin
global lhipexactin
global lhipfxactin
global lkneexactin
global lknefxactin
global lshoexactin
global lshofxactin
global rankexactin
global rankfxactin
global rhipexactin
global rhipfxactin
global rkneexactin
global rknefxactin
global rshoexactin
global rshofxactin

%for some reason lhfxtof will not go into model so is changed to this
before running sim
% global lhfxtofa
% global rankbfxactb

%Set whole profile so can be put into sim
%left hip
if lhexton > 0
lhextontimcol = [(0:(lhexton/100):lhexton-(lhexton/100))';(lhexton-
(lhexton/1000))]; %time col for before activation starts
lhextonzoscol = zeros(length(lhextontimcol),1); %zero activation for
before activation start
```

```matlab
lhextstos = [lhextontimcol,lhextonzoscol]; %time and zero activation
before real activation
lhipexactin = [lhextstos;lhipexact]; %activation profile for whole
trial - NOTE tick set to zero once finished in simulink from
workspace block
else
    lhipexactin = lhipexact;
end


if lhfxton > 0
lhfxtontimcol = [(0:(lhfxton/100):lhfxton-(lhfxton/100))';(lhfxton-
(lhfxton/1000))]; %time col for before activation starts made to sit
as close as poss to the act start
lhfxtonzoscol = zeros(length(lhfxtontimcol),1); %zero activation for
before activation start
lhfxtstos = [lhfxtontimcol,lhfxtonzoscol]; %time and zero activation
before real activation
lhipfxactin = [lhfxtstos;lhipfxact]; %activation profile for whole
trial - NOTE tick set to zero once finished in simulink from
workspace block
else
    lhipfxactin = lhipfxact;
end


%left knee
if lkexton > 0
lkextontimcol = [(0:(lkexton/100):lkexton-(lkexton/100))';(lkexton-
(lkexton/1000))]; %time col for before activation starts
lkextonzoscol = zeros(length(lkextontimcol),1); %zero activation for
before activation start
lkextstos = [lkextontimcol,lkextonzoscol]; %time and zero activation
before real activation
lkneexactin = [lkextstos;lkneexact]; %activation profile for whole
trial - NOTE tick set to zero once finished in simulink from
workspace block
else
    lkneexactin = lkneexact;
end


if lkfxton > 0
lkfxtontimcol = [(0:(lkfxton/100):lkfxton-(lkfxton/100))';(lkfxton-
(lkfxton/1000))]; %time col for before activation starts
lkfxtonzoscol = zeros(length(lkfxtontimcol),1); %zero activation for
before activation start
lkfxtstos = [lkfxtontimcol,lkfxtonzoscol]; %time and zero activation
before real activation
lknefxactin = [lkfxtstos;lknefxact]; %activation profile for whole
trial - NOTE tick set to zero once finished in simulink from
workspace block
else
    lknefxactin = lknefxact;
end


%left ankle
if laexton > 0
laextontimcol = [(0:(laexton/100):laexton-(laexton/100))';(laexton-
(laexton/1000))]; %time col for before activation starts
laextonzoscol = zeros(length(laextontimcol),1); %zero activation for
before activation start
```

```matlab
laextstos = [laextontimcol,laextonzoscol]; %time and zero activation
before real activation
lankexactin = [laextstos;lankexact]; %activation profile for whole
trial - NOTE tick set to zero once finished in simulink from
workspace block
else
    lankexactin = lankexact;
end


if lafxton > 0
lafxtontimcol = [(0:(lafxton/100):lafxton-(lafxton/100))';(lafxton-
(lafxton/1000))]; %time col for before activation starts
lafxtonzoscol = zeros(length(lafxtontimcol),1); %zero activation for
before activation start
lafxtstos = [lafxtontimcol,lafxtonzoscol]; %time and zero activation
before real activation
lankfxactin = [lafxtstos;lankfxact]; %activation profile for whole
trial - NOTE tick set to zero once finished in simulink from
workspace block
else
    lankfxactin = lankfxact;
end


%right hip (two part act for ext)
% if rhexton > 0
% rhextontimcol = [(0:(rhexton/100):rhexton-(rhexton/100))';(rhexton-
(rhexton/1000))]; %time col for before activation starts
% rhextonzoscol = zeros(length(rhextontimcol),1); %zero activation
for before activation start
% rhextstos = [rhextontimcol,rhextonzoscol]; %time and zero
activation before real activation
rhipgaptimcol = [(rhextof:(rhebxton-rhextof)/100:rhebxton-((rhebxton-
rhextof)/100))';(rhebxton-(rhebxton/5000))]; %time for gap when there
is no activation during 2 part acts
rhipgapzoscol = zeros(length(rhipgaptimcol),1);
rhextgpos = [rhipgaptimcol,rhipgapzoscol];
rhipexactin = [rhipexact;rhextgpos;rhipbexact]; %activation profile
for whole trial - NOTE tick set to zero once finished in simulink
from workspace block
% end


if rhfxton > 0
rhfxtontimcol = [(0:(rhfxton/100):rhfxton-(rhfxton/100))';(rhfxton-
(rhfxton/1000))]; %time col for before activation starts
rhfxtonzoscol = zeros(length(rhfxtontimcol),1); %zero activation for
before activation start
rhfxtstos = [rhfxtontimcol,rhfxtonzoscol]; %time and zero activation
before real activation
rhipfxactin = [rhfxtstos;rhipfxact]; %activation profile for whole
trial - NOTE tick set to zero once finished in simulink from
workspace block
else
    rhipfxactin = rhipfxact;
end


%old
%rhipexact =
[rhipexact;[(rhipexact(length(rhipexact),1)+0.001:0.001)':
rhipbexact(1,1)-0.001]; rhipbexact]; rhexton
```

```matlab
%right knee
% if rkexton > 0
% rkextontimcol = [(0:(rkexton/100):rkexton-(rkexton/100))';(rkexton-
(rkexton/1000))]; %time col for before activation starts
% rkextonzoscol = zeros(length(rkextontimcol),1); %zero activation
for before activation start
% rkextstos = [rkextontimcol,rkextonzoscol]; %time and zero
activation before real activation
rknegaptimcol = [(rkextof:(rkebxton-rkextof)/100:rkebxton-((rkebxton-
rkextof)/100))';(rkebxton-(rkebxton/5000))]; %time for gap when there
is no activation during 2 part acts
rknegapzoscol = zeros(length(rknegaptimcol),1);
rkextgpos = [rknegaptimcol,rknegapzoscol];
rkneexactin = [rkneexact;rkextgpos;rknebexact]; %activation profile
for whole trial - NOTE tick set to zero once finished in simulink
from workspace block
% end

if rkfxton > 0
rkfxtontimcol = [(0:(rkfxton/100):rkfxton-(rkfxton/100))';(rkfxton-
(rkfxton/1000))]; %time col for before activation starts
rkfxtonzoscol = zeros(length(rkfxtontimcol),1); %zero activation for
before activation start
rkfxtstos = [rkfxtontimcol,rkfxtonzoscol]; %time and zero activation
before real activation
rknefxactin = [rkfxtstos;rknefxact]; %activation profile for whole
trial - NOTE tick set to zero once finished in simulink from
workspace block
else
    rknefxactin = rknefxact;
end

%right ankle
rafxtontimcol = [(0:(rafxton/100):rafxton-(rafxton/100))';(rafxton-
(rafxton/1000))]; %time col for before activation starts
rafxtonzoscol = zeros(length(rafxtontimcol),1); %zero activation for
before activation start
rafxtstos = [rafxtontimcol,rafxtonzoscol]; %time and zero activation
before real activation
rankgaptimcol = [(rafxtof:(rafbxton-rafxtof)/100:rafbxton-((rafbxton-
rafxtof)/100))';(rafbxton-(rafbxton/5000))]; %time for gap when there
is no activation during 2 part acts
rankgapzoscol = zeros(length(rankgaptimcol),1);
rafxtgpos = [rankgaptimcol,rankgapzoscol];
rankfxactin = [rafxtstos;rankfxact;rafxtgpos;rankbfxact]; %activation
profile for whole trial - NOTE tick set to zero once finished in
simulink from workspace block


% if raexton > 0
% raextontimcol = [(0:(raexton/100):raexton-(raexton/100))';(raexton-
(raexton/1000))]; %time col for before activation starts
% raextonzoscol = zeros(length(raextontimcol),1); %zero activation
for before activation start
% raextstos = [raextontimcol,raextonzoscol]; %time and zero
activation before real activation
rankegaptimcol = [(raextof:(raebxton-raextof)/100:raebxton-
((raebxton-raextof)/100))';(raebxton-(raebxton/5000))]; %time for gap
when there is no activation during 2 part acts
rankegapzoscol = zeros(length(rankegaptimcol),1);
```

```matlab
raextgpos = [rankegaptimcol,rankegapzoscol];
rankexactin = [rankexact;raextgpos;rankbexact]; %activation profile
for whole trial - NOTE tick set to zero once finished in simulink
from workspace block
% end

%left shoulder
if lsexton > 0
lsextontimcol = [(0:(lsexton/100):lsexton-(lsexton/100))';(lsexton-
(lsexton/1000))]; %time col for before activation starts
lsextonzoscol = zeros(length(lsextontimcol),1); %zero activation for
before activation start
lsextstos = [lsextontimcol,lsextonzoscol]; %time and zero activation
before real activation
lshoexactin = [lsextstos;lshoexact]; %activation profile for whole
trial - NOTE tick set to zero once finished in simulink from
workspace block
else
    lshoexactin = lshoexact;
end

if lsfxton > 0
lsfxtontimcol = [(0:(lsfxton/100):lsfxton-(lsfxton/100))';(lsfxton-
(lsfxton/1000))]; %time col for before activation starts
lsfxtonzoscol = zeros(length(lsfxtontimcol),1); %zero activation for
before activation start
lsfxtstos = [lsfxtontimcol,lsfxtonzoscol]; %time and zero activation
before real activation
lshofxactin = [lsfxtstos;lshofxact]; %activation profile for whole
trial - NOTE tick set to zero once finished in simulink from
workspace block
else
    lshofxactin = lshofxact;
end

%right shoulder
if rsexton > 0
rsextontimcol = [(0:(rsexton/100):rsexton-(rsexton/100))';(rsexton-
(rsexton/1000))]; %time col for before activation starts
rsextonzoscol = zeros(length(rsextontimcol),1); %zero activation for
before activation start
rsextstos = [rsextontimcol,rsextonzoscol]; %time and zero activation
before real activation
rshoexactin = [rsextstos;rshoexact]; %activation profile for whole
trial - NOTE tick set to zero once finished in simulink from
workspace block
else
    rshoexactin = rshoexact;
end

if rsfxton > 0
rsfxtontimcol = [(0:(rsfxton/100):rsfxton-(rsfxton/100))';(rsfxton-
(rsfxton/1000))]; %time col for before activation starts
rsfxtonzoscol = zeros(length(rsfxtontimcol),1); %zero activation for
before activation start
rsfxtstos = [rsfxtontimcol,rsfxtonzoscol]; %time and zero activation
before real activation
rshofxactin = [rsfxtstos;rshofxact]; %activation profile for whole
trial - NOTE tick set to zero once finished in simulink from
workspace block
```

```matlab
else
    rshofxactin = rshofxact;
end


%run simulation
tic
clockstart = clock;
sim ('TORQUEMODSIMmpjspringsESIM');
toc

%Reset spring zeros for steps after sim has run
ltoei = 0;
lmpji = 0;
rtoei = 0;
rmpji = 0;

%%%%%%%%%%%%%%%% Score function %%%%%%%%%%%%%%%%%%%%%%%%
%scoreout =
SCOREFUNiii(simpos,simposfortor,matchforces,finishtime,compangs);
%scoreout = SCOREFUNoptimpulse(finishtime);
%scoreout = SCOREFUNoptvel(outtime,simpos);
scoreout = SCOREFUNvstronger(outtime,simpos);
%%%%%%%%%%%%%%%%%%%%%%%%%%%%%%%%%%%%%%%%%%%%%%%%%%%%%%%%

%runs out of memory saves everything everytime so just save last
10000 sims
if savno == savelast;
    savno =1;
%      tic
%      pack %saves all variables and clears the memory
%      display 'packtime'
%      toc
end
currentparamandscore(:,savno) = [currentparams;scoreout;simno];
save savedtorparamsE currentparamandscore -ascii%%%%%%%%%%%%%

%%%%%%%%%%%%%%%%%%%%%%%%%%%%%%%
savno = savno + 1;
simno = simno + 1;
display (simno)
%%%%%%%%%%%%%%%%%%%%%%%%%%%%%%%

%save best trial so far
if scoreout < bestscore
    savstuff = [currentparams;scoreout;simno];
    save bestparams savstuff -ascii
    save xsaver x -ascii
    bestscore = scoreout;
end


global counter
global counterS
global rrr
global qqq
global mmm
global nnn
```

```matlab
rrr = 0;
qqq = 0;
mmm = 0;
nnn = 0;
counter = 1;
counterS = 1;


%Set up for individual angle calcs
%need to due to rrr and qqq needing to be set to zero and without one
joint
%will ruin calc for another by raising from zero to early.
%MINUS
global lankcounter
global lankrrr
global lankqqq

global rshocounter
global rshorrr
global rshoqqq

global rknecounter
global rknerrr
global rkneqqq

global lshocounter
global lshorrr
global lshoqqq

%PLUS
global lknecounter
global lknerrr
global lkneqqq

global rankcounter
global rankrrr
global rankqqq

global lelbcounter
global lelbrrr
global lelbqqq

global spinecounter
global spinerrr
global spineqqq

global t10counter
global t10rrr
global t10qqq

%NORM
global lhipcounter
global lhiprrr
global lhipqqq

global rhipcounter
global rhiprrr
global rhipqqq
```

```
%MINUS
lankcounter = 1;
lankrrr = 0;
lankqqq = 0;

rshocounter = 1;
rshorrr = 0;
rshoqqq = 0;
global rsposmone
rsposmone = 0;

rknecounter = 1;
rknerrr = 0;
rkneqqq = 0;

lshocounter = 1;
lshorrr = 0;
lshoqqq = 0;
global lsposmone
lsposmone = 0;

%PLUS
lknecounter = 1;
lknerrr = 0;
lkneqqq = 0;

rankcounter = 1;
rankrrr = 0;
rankqqq = 0;

lelbcounter = 1;
lelbrrr = 0;
lelbqqq = 0;

spinecounter = 1;
spinerrr = 0;
spineqqq = 0;

t10counter = 1;
t10rrr = 0;
t10qqq = 0;

%NORM
lhipcounter = 1;
lhiprrr = 0;
lhipqqq = 0;
global lhposmone
lhposmone = 0;

rhipcounter = 1;
rhiprrr = 0;
rhipqqq = 0;
global rhposmone
rhposmone = 0;

clear   laexton
clear   laextof
clear   laeinitialact
clear   laemaxact
```

```
clear    laeendact
clear    laesteepratio
clear    laes
clear    lafxton
clear    lafxtof
clear    lafinitialact
clear    lafsa
clear    lafsb
clear    lafsc
clear    lafsd
clear    lafse
clear    lafsf
clear    lafsg
clear    lafsh
clear    lafsi
clear    lafsj
clear    lafmaxact
clear    lkexton
clear    lkextof
clear    lkeinitialact
clear    lkemaxact
clear    lkeendact
clear    lkesteepratio
clear    lkes
clear    lkfxton
clear    lkfxtof
clear    lkfinitialact
clear    lkfmaxact
clear    lkfendact
clear    lkfsteepratio
clear    lkfs
clear    lhexton
clear    lhextof
clear    lheinitialact
clear    lhesa
clear    lhesb
clear    lhesc
clear    lhesd
clear    lhese
clear    lhesf
clear    lhesg
clear    lhesh
clear    lhesi
clear    lhesj
clear    lhemaxact
clear    lhfxton
clear    lhfinitialact
clear    lhfsa
clear    lhfsb
clear    lhfsc
clear    lhfsd
clear    lhfse
clear    lhfsf
clear    lhfsg
clear    lhfsh
clear    lhfsi
clear    lhfsj
clear    lhfmaxact
clear    raexton
clear    raextof
clear    raeinitialact
```

```
clear    raesa
clear    raesb
clear    raesc
clear    raesd
clear    raese
clear    raesf
clear    raesg
clear    raesh
clear    raesi
clear    raesj
clear    raemaxact
clear    rafxton
clear    rafxtof
clear    rafinitialact
clear    rafmaxact
clear    rafendact
clear    rafsteepratio
clear    rafs
clear    rkexton
clear    rkextof
clear    rkeinitialact
clear    rkesa
clear    rkesb
clear    rkesc
clear    rkesd
clear    rkese
clear    rkesf
clear    rkesg
clear    rkesh
clear    rkesi
clear    rkesj
clear    rkemaxact
clear    rkfxton
clear    rkfxtof
clear    rkfinitialact
clear    rkfmaxact
clear    rkfendact
clear    rkfsteepratio
clear    rkfs
clear    rhexton
clear    rhextof
clear    rheinitialact
clear    rhemaxact
clear    rheendact
clear    rhesteepratio
clear    rhes
clear    rhfxton
clear    rhfxtof
clear    rhfinitialact
clear    rhfsa
clear    rhfsb
clear    rhfsc
clear    rhfsd
clear    rhfse
clear    rhfsf
clear    rhfsg
clear    rhfsh
clear    rhfsi
clear    rhfsj
clear    rhfmaxact
clear    lsexton
```

```
clear   lsextof
clear   lseinitialact
clear   lsemaxact
clear   lseendact
clear   lsesteepratio
clear   lses
clear   lsfxton
clear   lsfxtof
clear   lsfinitialact
clear   lsfmaxact
clear   lsfendact
clear   lsfsteepratio
clear   lsfs
clear   rsexton
clear   rsextof
clear   rseinitialact
clear   rsemaxact
clear   rseendact
clear   rsesteepratio
clear   rses
clear   rsfxton
clear   rsfxtof
clear   rsfinitialact
clear   rsfmaxact
clear   rsfendact
clear   rsfsteepratio
clear   rsfs
clear   rhebxton
clear   rhebxtof
clear   rhebinitialact
clear   rhebmaxact
clear   rhebendact
clear   rhebsteepratio
clear   rhebs
clear   rkebxton
clear   rkebxtof
clear   rkebinitialact
clear   rkebmaxact
clear   rkebendact
clear   rkebsteepratio
clear   rkebs
clear   rafbxton
clear   rafbxtof
clear   rafbinitialact
clear   rafbmaxact
clear   rafbendact
clear   rafbsteepratio
clear   rafbs
clear   toeswitch

finishtime = [];

score = scoreout
```

APPENDIX K

Joint Torque Profiles
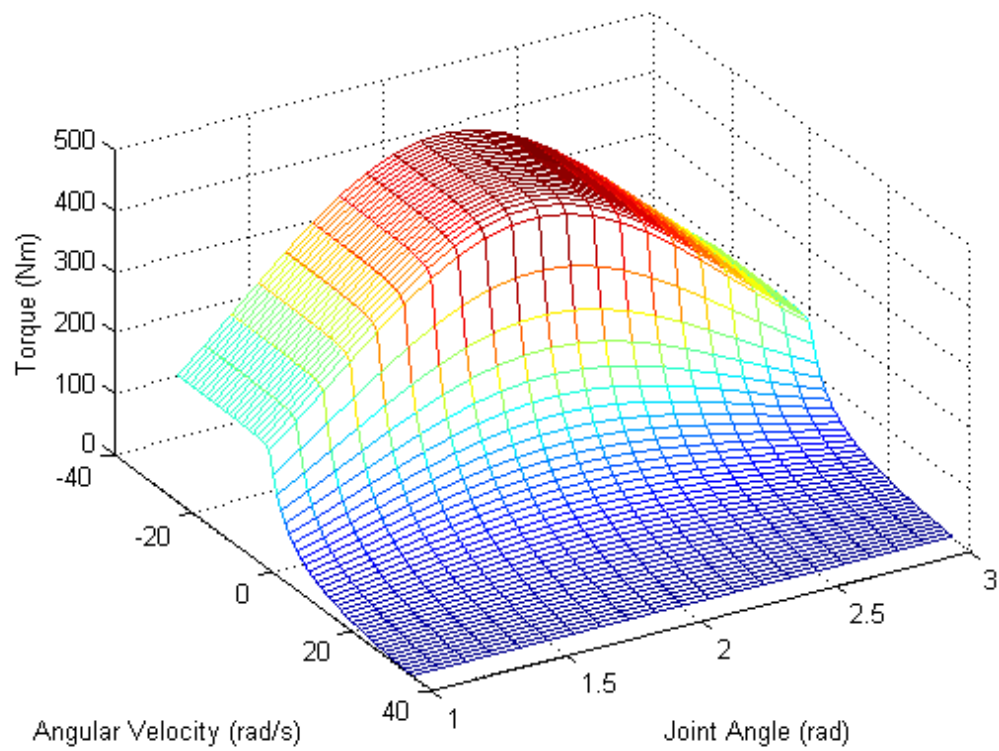
Figure K1. Hip Extension joint torque/ angle/ angular velocity profile
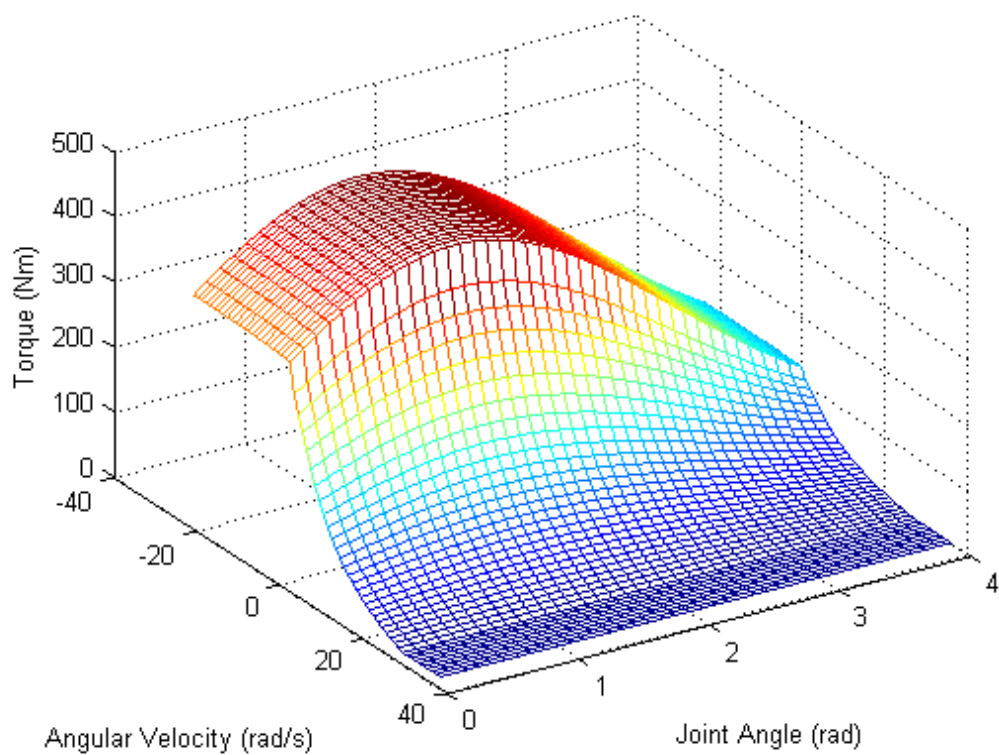
Figure K2. Hip Flexion joint torque/ angle/ angular velocity profile
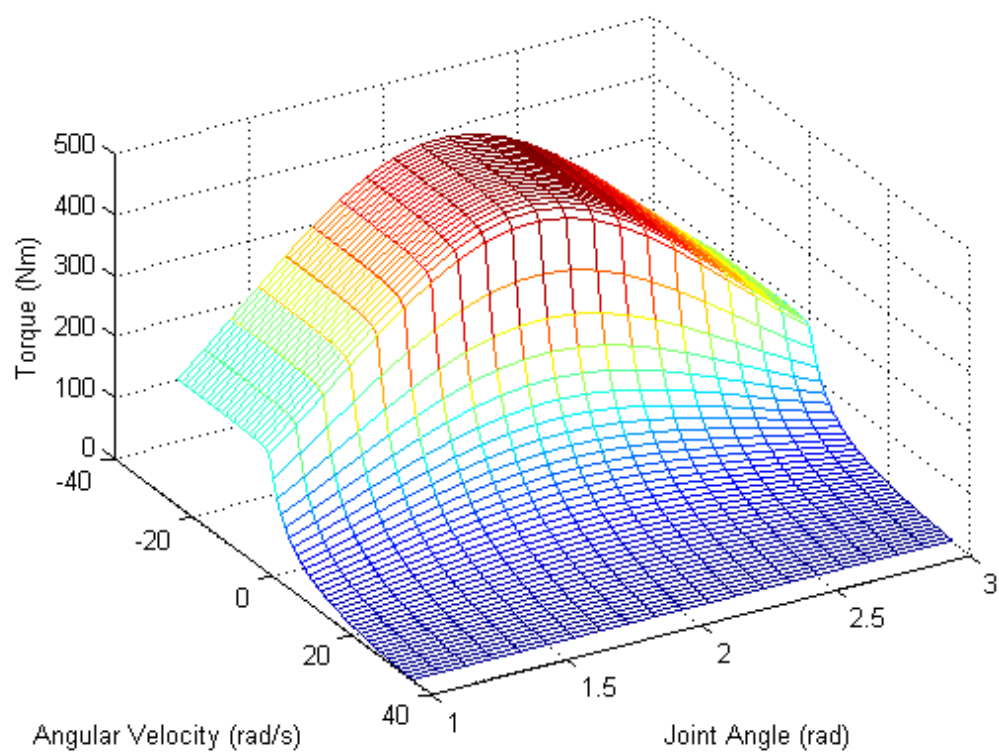
Figure K3. Knee Extension joint torque/ angle/ angular velocity profile
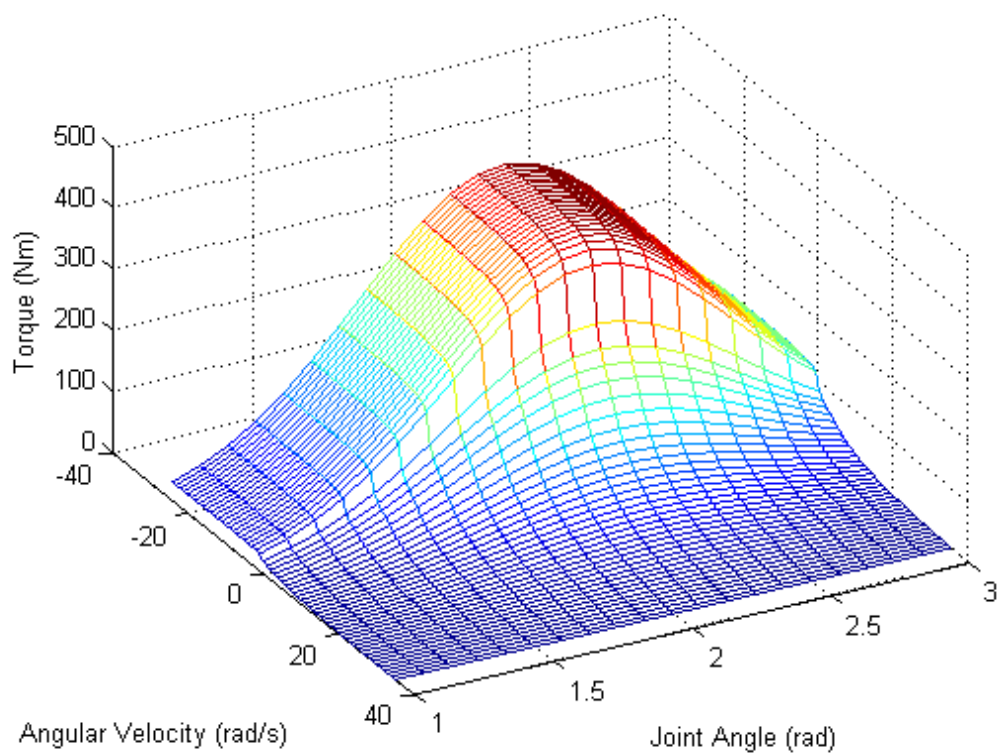
Figure K4. Knee flexion joint torque/ angle/ angular velocity profile

331
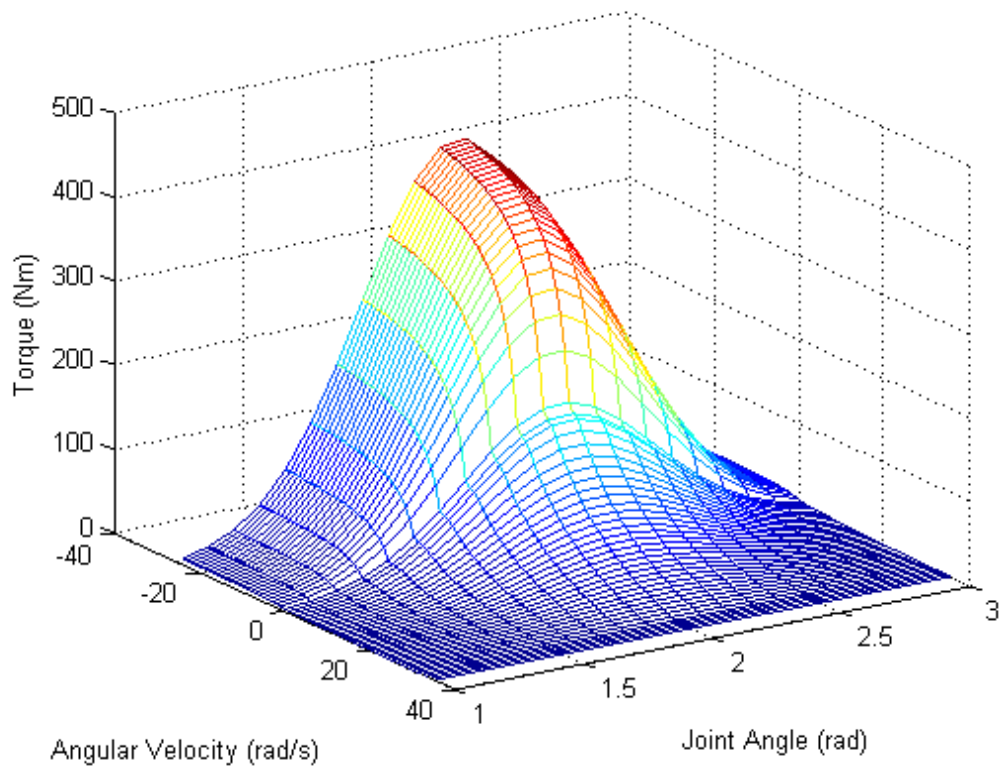
Figure K5. Ankle plantar flexion joint torque/ angle/ angular velocity profile
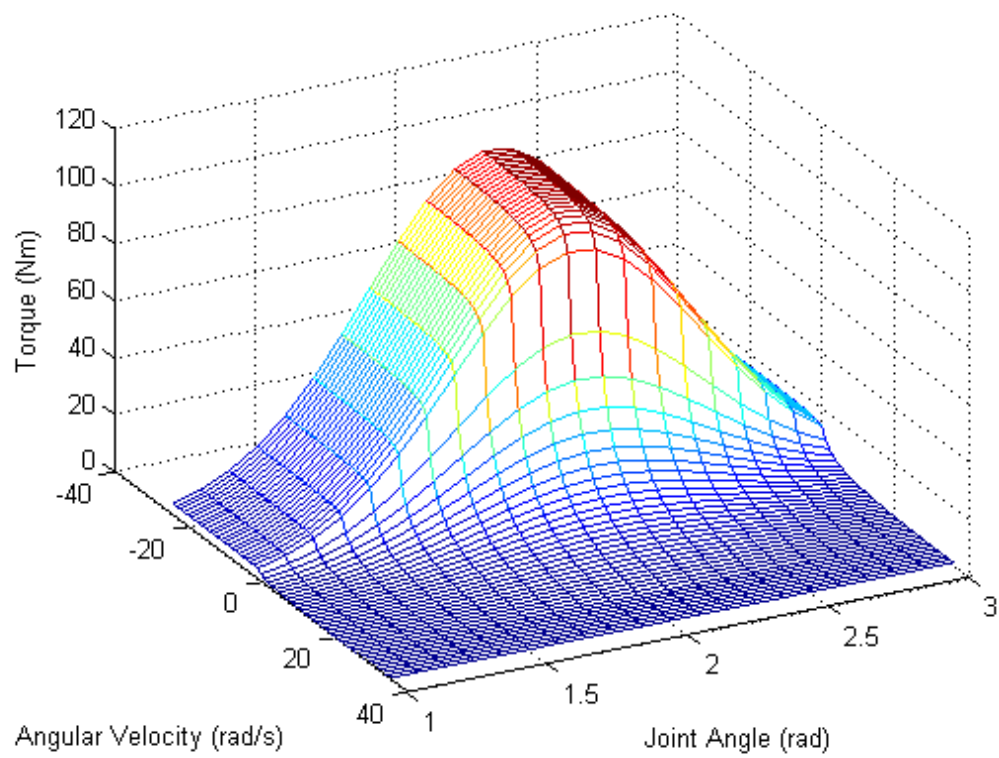
Figure K6. Ankle dorsi-flexion joint torque/ angle/ angular velocity profile

APPENDIX L

Matlab Code for Calculation of Joint Torque.
Based on code donated by Dr. Steph Forrester (2006)

```matlab
%Torque driver S-function
%9 Parameter function based on stephs version

function [result,x0,str,ts] = APFtorSFUNtsix(t,x,u,flag)
%Above line function [name of output, x0, str, ts] = name of this
file
%(t,x,u,flag)

% Dispatch the flag. The switch function controls the calls to
% S-function routines at each simulation stage of the S-function.
%
switch flag,
  %%%%%%%%%%%%%%%%%%
  % Initialization %
  %%%%%%%%%%%%%%%%%%
  % Initialize the states, sample times, and state ordering strings.
  case 0
    [result,x0,str,ts]=mdlInitializeSizes;

  %%%%%%%%%%
  % Outputs %
  %%%%%%%%%%
  % Return the outputs of the S-function block.
  case 3
    result=mdlOutputs(t,x,u);

  %%%%%%%%%%%%%%%%%%%
  % Unhandled flags %
  %%%%%%%%%%%%%%%%%%%
  % There are no termination tasks (flag=9) to be handled.
  % Also, there no continuous or discrete states,
  % so flags 1,2, and 4 are not used, so return an emptyu
  % matrix
  case { 1, 2, 4, 9 }
    result=[];

  %%%%%%%%%%%%%%%%%%%%%%%%%%%%%%%%%%%%%
  % Unexpected flags (error handling)%
  %%%%%%%%%%%%%%%%%%%%%%%%%%%%%%%%%%%%%
  % Return an error message for unhandled flag values.
  otherwise
    error(['Unhandled flag = ',num2str(flag)]);

end

% end timestwo

%
%=======================================================================
=========
% mdlInitializeSizes
% Return the sizes, initial conditions, and sample times for the S-
function.
%=======================================================================
=========
%
function [result,x0,str,ts] = mdlInitializeSizes()
```

```matlab
sizes = simsizes;
sizes.NumContStates  = 0;
sizes.NumDiscStates  = 0;
sizes.NumOutputs     = 3;  % dynamically sized
sizes.NumInputs      = 3;  % dynamically sized
sizes.DirFeedthrough = 1;   % has direct feedthrough
sizes.NumSampleTimes = 1;

result = simsizes(sizes);
str = [];
x0  = [];
ts  = [-1 0];   % inherited sample time

% end mdlInitializeSizes


%
%=========================================================================
=========
% mdlOutputs
% Return the output vector for the S-function
%=========================================================================
=========
%
function result = mdlOutputs(t,x,u)

jtcc = 1;
% current surface fit solution (select which No. is which varible)
% ================================================================
%tmax = x(1); %max eccentric torque
%Ankle Plantar Flexion
params = [550 380 30.8 15.38 0.88 0.40 1.38 0.37 (2*pi)-4.22];
tmax = params(1);
to = params(2);
wmax = params(3);
wc = params(4);
amin = params (5);
wramp = params(6);
w1 = params(7);
width = params (8);
lopt = params(9);

% CALCULATE THE FITTED SURFACE USING THE CURRENT PARAMETER GUESS
% ================================================================


             w = u(2);%Vmeas; %velocity
           len = u(1); %Lmeas; %length
           l = (len/360)*(2*pi);
%           activ = u(3);
%            if activ > 0
%                act = 1;
%            else
%                act = 0;
%             end

           %lopt = (2*pi)-lopt; %reorientate for opt angle

           % DIFFERENTIAL ACTIVATION
```

```matlab
            % from function difact
amax = 1; % assume maximum activation plateau is 1.0
dactFIT = amin+((amax-amin)/(1+exp(-(w-w1)/wramp)));

            % TETANIC FORCE - VELOCITY
            k=4.3;


if (w < 0) % eccentrics
    we=(tmax-to)*(wmax*wc)/(k*to*(wmax+wc));
    E=-(tmax-to)*we;
    tqtet=(E/(we-w))+tmax;


else % concentrics
    Tc=to*wc/wmax;
    C=Tc*(wmax+wc);
    tqtet=(C/(wc+w))-Tc;
end;
if w > wmax
    tqtet = 0;
end

            FVtetfit = tqtet;
            FVmvcfit=FVtetfit*dactFIT;

            % TORQUE - ANGLE
            % velocity specific optimal length
if (jtcc==1); loptv=lopt; end % joint no velocity effects
%if (jtcc==2); loptv=lopt-((tqtetv-to)/kstiff); end % cc velocity
effects
if (jtcc==2); loptv=lopt; end % cc velocity effects

tqlen=exp(-((l-loptv)^2)/(2*width*width));

%FLVtetfit=FVtetfit*tqlen;
FLVmvcfit=FVmvcfit*tqlen;

result(1) = FLVmvcfit*u(3);
result(2) = u(3);
result(3) = l;
```

APPENDIX M

Clock S-Function in Matlab

```matlab
function [result,x0,str,ts] = findtimeSFUN(t,x,u,flag)
%Above line function [name of output, x0, str, ts] = name of this
file
%(t,x,u,flag)

% Dispatch the flag. The switch function controls the calls to
% S-function routines at each simulation stage of the S-function.
%
switch flag,
  %%%%%%%%%%%%%%%%%
  % Initialization %
  %%%%%%%%%%%%%%%%%%%
  % Initialize the states, sample times, and state ordering strings.
  case 0
    [result,x0,str,ts]=mdlInitializeSizes;

  %%%%%%%%%%%
  % Outputs %
  %%%%%%%%%%%
  % Return the outputs of the S-function block.
  case 3
    result=mdlOutputs(t,x,u);

  %%%%%%%%%%%%%%%%%%%
  % Unhandled flags %
  %%%%%%%%%%%%%%%%%%%%
  % There are no termination tasks (flag=9) to be handled.
  % Also, there are no continuous or discrete states,
  % so flags 1,2, and 4 are not used, so return an emptyu
  % matrix
  case { 1, 2, 4, 9 }
    result=[];

  %%%%%%%%%%%%%%%%%%%%%%%%%%%%%%%%%%%%%
  % Unexpected flags (error handling)%
  %%%%%%%%%%%%%%%%%%%%%%%%%%%%%%%%%%%%%
  % Return an error message for unhandled flag values.
  otherwise
    error(['Unhandled flag = ',num2str(flag)]);

end

% end timestwo

%
%=====================================================================
=========
% mdlInitializeSizes
% Return the sizes, initial conditions, and sample times for the S-
function.
%=====================================================================
=========
%
function [result,x0,str,ts] = mdlInitializeSizes()

sizes = simsizes;
sizes.NumContStates  = 0;
sizes.NumDiscStates  = 0;
sizes.NumOutputs     = 2;  % dynamically sized
sizes.NumInputs      = 1;  % dynamically sized
```

```matlab
sizes.DirFeedthrough = 1;    % has direct feedthrough
sizes.NumSampleTimes = 1;


result = simsizes(sizes);
str = [];
x0  = [];
ts  = [-1 0];    % inherited sample time


% end mdlInitializeSizes


%
%=======================================================================
=========
% mdlOutputs
% Return the output vector for the S-function
%=======================================================================
=========
%
function result = mdlOutputs(t,x,u)


%must state u(1) as this is the input No.
inputin      = u(1); %time simstarted in seconds
clocknow = clock;


         %months made large as vary in time || Seconds per day ||
Seconds per hour || Seconds per min || Seconds
currentcputime = (clocknow(2)*1000000000) + (clocknow(3)*86400) +
(clocknow(4)*3600) + (clocknow(5)*60)+clocknow(6); %real time
maxsimtime = 500; %max time allowed for 1 simulation in seconds
currentsimtime = currentcputime - inputin;
if currentsimtime > maxsimtime
    timerout = 2;
else
    timerout = 1;
end


%output
result(1) = timerout;
result(2) = currentcputime;
```

APPENDIX N

Example Score Code in Matlab

```matlab
function score =
SCOREFUNvi(simupos,measupos,matchforces,finishtime,compangs)
%SCOREFUN designed for use with torque model
%Same as scorefuniv but extra penalties for joints not extending

%%%%%%%%LOADED IN FROM ANGLEDRIVERGLOBAL%%%%%%%%%%%
global startfield %startfield of simulation
% global endfield

%FORCE PLATE DATA
% global forcex
% global forcey
% global forcez
global highspeedsynch

%STARTING BLOCK DATA
% global stlblockx
global stlblocky
global stlblockz
% global stlblockres

% global strblockx
global strblocky
global strblockz
% global strblockres

%WHEN LEFT BLOCKS?
global abcompend
global cdcompend
global hssblock

%FORCE FROM MODEL
% global ltoexforce
% global lmpjxforce
global lfootxforce

% global rtoexforce
% global rmpjxforce
% global rfootxforce

% global ltoeyforce
% global lmpjyforce
global lfootyforce

% global rtoeyforce
% global rmpjyforce
% global rfootyforce

global lfootresforce
global rfootresforce

% global lhandxforce
% global lhandyforce
% global lhandresforce
%
% global rhandxforce
% global rhandyforce
% global rhandresforce
%
```

341

```matlab
% global ltoeresforce
% global lmpjresforce
% global rtoeresforce
% global rmpjresforce

global simstop
% global scoreprog
%
% global oddeven
% global simno
% global bestscore
global realjointangles
load grouptorn
%global grouptorn %this is jointang and joint tor output from angle
model
global grouptorsim %joint angs and tors from sim
global stopreason
if isempty (stopreason)
else
display (stopreason)
end

global simxpos
global lhipangssav
global lhipangssim
%select areas of each relavent to simulated portion
stsammhz = startfield * 5; %sim start sample for 1000hz data in vicon
% endsammhz = endfield * 5; %sim start sample for 1000hz data in
vicon

synchblockfp = hssblock - highspeedsynch;
blockstartsim = synchblockfp+stsammhz; %when the simulation starts in
the block data
% blockendsim = synchblockfp+endsammhz; %when the simulation ends in
the block data
%


if finishtime(length(finishtime))<simstop
    shortsim = size(grouptorsim,1);
    %shortori = size(grouptorn,1);
    simcomsize = size(simupos,1);
    mescomsize = size(measupos,1);
        if simcomsize < mescomsize
        grouptorn = grouptorn(1:shortsim,:);
        measupos = measupos(1:size(simupos,1),:);
        %find takeoff
        %use the last moment of force production
        %x
        findlastxforcehi = find(lfootxforce > 0);
        findlastxforcelo = find(lfootxforce < 0);
        if isempty (findlastxforcelo) %if contact is never lost
            findlastxforcelo = 1;
        end
        if isempty (findlastxforcehi) %if force is never applied -
from the start the foot is being pulled from the block
            findlastxforcehi = 1;
        end
```

```matlab
        findxforce =
max([findlastxforcehi(length(findlastxforcehi)),findlastxforcelo(leng
th(findlastxforcelo))]);
        %y
        findlastyforcehi = find(lfootyforce > 0);
        findlastyforcelo = find(lfootyforce < 0);
        if isempty (findlastyforcelo)
            findlastyforcelo = 1;
        end
         if isempty (findlastyforcehi) %if force is never applied -
from the start the foot is being pulled from the block
            findlastyforcehi = 1;
        end
        findyforce =
max([findlastyforcehi(length(findlastyforcehi)),findlastyforcelo(leng
th(findlastyforcelo))]);
        %max
        findcontact = max([findxforce,findyforce]);

        %Calculate 2-D resultants
        stlblockiidres = sqrt(stlblocky.^2 + stlblockz.^2);
        strblockiidres = sqrt(strblocky.^2 + strblockz.^2);

        %Starting block data used in simulation (contact period)
%        lblocksinblocksx =
stlblockx(blockstartsim:blockstartsim+findcontact);
%        lblocksinblocksy =
stlblocky(blockstartsim:blockstartsim+findcontact);
%        lblocksinblocksz =
stlblockz(blockstartsim:blockstartsim+findcontact);
        lblocksinblocksiidres = stlblockiidres
(blockstartsim:blockstartsim+(findcontact-1));
%        rblocksinblocksx =
strblockx(blockstartsim:blockstartsim+findcontact);
%        rblocksinblocksy =
strblocky(blockstartsim:blockstartsim+findcontact);
%        rblocksinblocksz =
strblockz(blockstartsim:blockstartsim+findcontact);
        rblocksinblocksiidres = strblockiidres
(blockstartsim:blockstartsim+(findcontact-1));

        %simforce data in blocks
%        lsiminblocksx = lfootxforce(1:findcontact);
%        lsiminblocksy = lfootyforce(1:findcontact);
        %lsiminblocksz = lfootyforce(1:findcontact);
        lsiminblocksres = lfootresforce(1:findcontact);
%        rsiminblocksx = rfootxforce(1:findcontact);
%        rsiminblocksy = rfootyforce(1:findcontact);
        %rsiminblocksz = rfootyforce(1:findcontact);
        rsiminblocksres = rfootresforce(1:findcontact);

        else
        end
end

%Penalties for sim stopping too soon.
if isempty(stopreason)
    earlystoppen = 0;
    elseif stopreason < 2 %landed on the correct foot - all ok
        earlystoppen = 0;
```

343

```matlab
        elseif stopreason == 2 %goes off/ completely wrong
            earlystoppen = 88888;
        elseif stopreason == 3 %head or shoulder touch ground first
            earlystoppen = 1200;
        elseif stopreason == 4 %hip touches ground first
            earlystoppen = 1000;
        elseif stopreason == 5 %left or right knee touch ground first
            earlystoppen = 900;
        elseif stopreason == 6 %left or right ankle touch ground first
            earlystoppen = 300;
end


%%%%%%%%%%%%%%%%%%%%%%%%%%%%%%%%%%%%%%%%%%%%%%%%%%%%%%%%%%%%%%%%%%%%%%%%%%
%%
%%%%%%%%%%%%%%%%%%%%%%%%%%%%%%%%%%%%%%%%%%%%%%%%%%%%%%%%%%%%%%%%%%%%%%%%%%
%%
%%%%%%%%%%%%%%%%%%%%% JOINT ANGLE MATCHES
%%%%%%%%%%%%%%%%%%%%%%%%%%%%%%%%
%%%%%%%%%%%%%%%%%%%%%%%%%%%%%%%%%%%%%%%%%%%%%%%%%%%%%%%%%%%%%%%%%%%%%%%%%%
%%
%%%%%%%%%%%%%%%%%%%%%%%%%%%%%%%%%%%%%%%%%%%%%%%%%%%%%%%%%%%%%%%%%%%%%%%%%%
%%
%PENALTIES FOR EXCEEDING ROM
lhiprealang = realjointangles(:,1);
lknerealang = realjointangles(:,2);
lankrealang = realjointangles(:,3);
rhiprealang = realjointangles(:,4);
rknerealang = realjointangles(:,5);
rankrealang = realjointangles(:,6);
% lshorealang = realjointangles(:,7);
% rshorealang = realjointangles(:,8);


maxhipang = 220;
minhipang = 15;
maxkneang = 180;
minkneang = 30;
maxankang = 180;
minankang = 70;


if max(lhiprealang) > maxhipang
    lhippenhi = 5000 + (max(lhiprealang) - maxhipang)^2;
else lhippenhi = 0;
end
if min(lhiprealang) < minhipang
    lhippenlo = 5000 + (minhipang - min(lhiprealang))^2;
else lhippenlo = 0;
end
if max(lknerealang) > maxkneang
    lknepenhi = 5000 + (max(lknerealang) - maxkneang)^2;
else lknepenhi = 0;
end
if min(lknerealang) < minkneang
    lknepenlo = 5000 + (minkneang - min(lknerealang))^2;
else lknepenlo = 0;
end
if max(lankrealang) > maxankang
    lankpenhi = 5000 + (max(lankrealang) - maxankang)^2;
else lankpenhi = 0;
end
if min(lankrealang) < minankang
    lankpenlo = 5000 + (minankang - min(lankrealang))^2;
```

```matlab
else lankpenlo = 0;
end
if max(rhiprealang) > maxhipang
    rhippenhi = 5000 + (max(rhiprealang) - maxhipang)^2;
else rhippenhi = 0;
end
if min(rhiprealang) < minhipang
    rhippenlo = 5000 + (minhipang - min(rhiprealang))^2;
else rhippenlo = 0;
end
if max(rknerealang) > maxkneang
    rknepenhi = 5000 + (max(rknerealang) - maxkneang)^2;
else rknepenhi = 0;
end
if min(rknerealang) < minkneang
    rknepenlo = 5000 + (minkneang - min(rknerealang))^2;
else rknepenlo = 0;
end
if max(rankrealang) > maxankang
    rankpenhi = 5000 + (max(rankrealang) - maxankang)^2;
else rankpenhi = 0;
end
if min(rankrealang) < minankang
    rankpenlo = 5000 + (minankang - min(rankrealang))^2;
else rankpenlo = 0;
end
rompens =
lhippenhi+lhippenlo+lknepenhi+lknepenlo+lankpenhi+lankpenlo+rhippenhi
+rhippenlo+rknepenhi+rknepenlo+rankpenhi+rankpenlo;


%extra penalties if joints arn't extending
hkext = 165;
anext = 140;

if max(lhiprealang) < hkext
    lhippenext = 1000 + (hkext - max(lhiprealang))^2;
else lhippenext = 0;
end
if max(lknerealang) < 150
    lknepenext = 1000 + (hkext - max(lknerealang))^2;
else lknepenext = 0;
end
if max(lankrealang) < anext
    lankpenext = 1000 + (hkext - max(lankrealang))^2;
else lankpenext = 0;
end
% if max(rhiprealang) < hkext %not needed
%     rhippenext = 1000 + (hkext - max(rhiprealang))^2;
% else rhippenext = 0;
% end
% if max(rknerealang) < hkext
%     rknepenext = 1000 + (hkext - max(rknerealang))^2;
% else rknepenext = 0;
% end
if max(rankrealang) < anext
    rankpenext = 1000 + (hkext - max(rankrealang))^2;
else rankpenext = 0;
end
```

```matlab
notextenoughpen = lhippenext + lknepenext + lankpenext + rankpenext;

%Add more penalties for joints which start spining round
lhipflips = flipcheckerrecorderFUNii(lhiprealang);
lkneflips = flipcheckerrecorderFUNii(lknerealang);
lankflips = flipcheckerrecorderFUNii(lankrealang);
rhipflips = flipcheckerrecorderFUNii(rhiprealang);
rkneflips = flipcheckerrecorderFUNii(rknerealang);
rankflips = flipcheckerrecorderFUNii(rankrealang);
flippens = (lhipflips + lkneflips + lankflips + rhipflips + rkneflips
+ rankflips) * 100;




if compangs == 1;

%      if length(grouptorsim) < length (grouptor)
%          grouptor = grouptor(1:length(grouptorsim),:);
%      end

%%%%%%%%%%%%%%%%%%%%%%%%%%%%%%%%%%%%%%%%%%
%%%%%%%%%%%%%%%%%%%%%%%%%%%%%%%%%%%%%%%%%%
ttenangssav=      grouptorn  (:,  1   );
%pelangssav=       grouptorn  (:,  3   );
lhipangssav=      grouptorn  (:,  5   );
lkneangssav=      grouptorn  (:,  7   );
lankangssav=      grouptorn  (:,  9   );
%lmpjangssav=      grouptorn  (:,  11  );
lshoangssav=      grouptorn  (:,  13  );
%lelbangssav=      grouptorn  (:,  15  );
%lwriangssav=      grouptorn  (:,  17  );
rhipangssav=      grouptorn  (:,  19  );
rkneangssav=      grouptorn  (:,  21  );
rankangssav=      grouptorn  (:,  23  );
%rmpjangssav=      grouptorn  (:,  25  );
rshoangssav=      grouptorn  (:,  27  );
%relbangssav=      grouptorn  (:,  29  );
%rwriangssav=      grouptorn  (:,  31  );
%timangtor=        grouptorn  (:,  33  );


%ttentorssav=      grouptorn  (:,  2   );
%peltorssav=       grouptorn  (:,  4   );
%lhiptorssav=      grouptorn  (:,  6   );
% lknetorssav=     grouptorn  (:,  8   );
% lanktorssav=     grouptorn  (:,  10  );
% lmpjtorssav=     grouptorn  (:,  12  );
% lshotorssav=     grouptorn  (:,  14  );
% lelbtorssav=     grouptorn  (:,  16  );
% lwritorssav=     grouptorn  (:,  18  );
% rhiptorssav=     grouptorn  (:,  20  );
% rknetorssav=     grouptorn  (:,  22  );
% ranktorssav=     grouptorn  (:,  24  );
% rmpjtorssav=     grouptorn  (:,  26  );
% rshotorssav=     grouptorn  (:,  28  );
% relbtorssav=     grouptorn  (:,  30  );
% rwritorssav=     grouptorn  (:,  32  );


ttenangssim=      grouptorsim     (:,  1   );
% pelangssim=     grouptorsim (:,  3   );
lhipangssim=      grouptorsim (:,  5   );
```

```matlab
lkneangssim=    grouptorsim (:, 7   );
lankangssim=    grouptorsim (:, 9   );
% lmpjangssim=  grouptorsim (:, 11  );
lshoangssim=    grouptorsim (:, 13  );
% lelbangssim=  grouptorsim (:, 15  );
% lwriangssim=  grouptorsim (:, 17  );
rhipangssim=    grouptorsim (:, 19  );
rkneangssim=    grouptorsim (:, 21  );
rankangssim=    grouptorsim (:, 23  );
% rmpjangssim=  grouptorsim (:, 25  );
rshoangssim=    grouptorsim (:, 27  );
% relbangssim=  grouptorsim (:, 29  );
% rwriangssim=  grouptorsim (:, 31  );
% timangtorsim= grouptorsim (:, 33  );

% ttentorssim=  grouptorsim (:, 2   );
% peltorssim=      grouptorsim   (:, 4   );
% lhiptorssim=  grouptorsim (:, 6   );
% lknetorssim=  grouptorsim (:, 8   );
% lanktorssim=  grouptorsim (:, 10  );
% lmpjtorssim=  grouptorsim (:, 12  );
% lshotorssim=  grouptorsim (:, 14  );
% lelbtorssim=  grouptorsim (:, 16  );
% lwritorssim=  grouptorsim (:, 18  );
% rhiptorssim=  grouptorsim (:, 20  );
% rknetorssim=  grouptorsim (:, 22  );
% ranktorssim=  grouptorsim (:, 24  );
% rmpjtorssim=  grouptorsim (:, 26  );
% rshotorssim=  grouptorsim (:, 28  );
% relbtorssim=  grouptorsim (:, 30  );
% rwritorssim=  grouptorsim (:, 32  );


%%%%%%%%%%%%%%%%%%%%%%%%%%%%%%%%%%%%%%%%%%%%%%%%%
%%%%%%%%%%%%%%%%%%%%%%%%%%%%%%%%%%%%%%%%%%%%%%%%%
lhipangscore = RMSD(lhipangssav,lhipangssim);
rhipangscore = RMSD(rhipangssav,rhipangssim);
lkneangscore = RMSD(lkneangssav,lkneangssim);
rkneangscore = RMSD(rkneangssav,rkneangssim);
lankangscore = RMSD(lankangssav,lankangssim);
rankangscore = RMSD(rankangssav,rankangssim);
lshoangscore = RMSD(lshoangssav,lshoangssim);
rshoangscore = RMSD(rshoangssav,rshoangssim);
spineangscore = RMSD(ttenangssav,ttenangssim);

bodyangscore = lhipangscore + rhipangscore + lkneangscore +
rkneangscore + lankangscore + rankangscore + lshoangscore +
rshoangscore + spineangscore;

else
    bodyangscore = 0;
end


%load results of simulation for comparison
simxpos = simupos(:,1);
simypos = simupos(:,2);

%Actual
comx = measupos(:,1);
```

```matlab
comy = measupos(:,2);

%compare
xdiff = comx - simxpos;
ydiff = comy - simypos;
% actualdiffsq = sqrt(xdiff.^2 + ydiff.^2);
% actdiffpcenttot = (100./(sqrt(comx.^2+comy.^2))).*actualdiffsq;
% actdiffpcent = mean (actdiffpcenttot);
disttravelled = sqrt((comx(1)-
comx(length(comx)))^2+(comy(length(comy))-comy(1))^2);
actdiffpcent = (100/disttravelled)* mean((sqrt(xdiff.^2))
+(sqrt(ydiff.^2)));

if matchforces == 1

if finishtime(length(finishtime))>= simstop
%Calculate 2-D resultants
stlblockiidres = sqrt(stlblocky.^2 + stlblockz.^2);
strblockiidres = sqrt(strblocky.^2 + strblockz.^2);

%Starting block data used in simulation (contact period)
% lblocksinblocksx = stlblockx(blockstartsim:abcompend-1);
% lblocksinblocksy = stlblocky(blockstartsim:abcompend-1);
% lblocksinblocksz = stlblockz(blockstartsim:abcompend-1);
lblocksinblocksiidres = stlblockiidres (blockstartsim:abcompend-1);
% rblocksinblocksx = strblockx(blockstartsim:cdcompend-1);
% rblocksinblocksy = strblocky(blockstartsim:cdcompend-1);
% rblocksinblocksz = strblockz(blockstartsim:cdcompend-1);
rblocksinblocksiidres = strblockiidres (blockstartsim:cdcompend-1);

%simforce data in blocks
% lsiminblocksx = lfootxforce(1:abcompend-blockstartsim);
% lsiminblocksy = lfootyforce(1:abcompend-blockstartsim);
%lsiminblocksz = lfootyforce(1:abcompend-blockstartsim);
lsiminblocksres = lfootresforce(1:abcompend-blockstartsim);
% rsiminblocksx = rfootxforce(1:cdcompend-blockstartsim);
% rsiminblocksy = rfootyforce(1:cdcompend-blockstartsim);
%rsiminblocksz = rfootyforce(1:cdcompend-blockstartsim);
rsiminblocksres = rfootresforce(1:cdcompend-blockstartsim);
end

%Force score in blocks - as percentage
lforcediff= lblocksinblocksiidres - lsiminblocksres;
lforcediffsqsqrt = sqrt(lforcediff.^2);
%lactualdiff = mean (lforcediffsqsqrt);
lforcepcenttot = (100./lblocksinblocksiidres).*lforcediffsqsqrt;
%lforcenorm = sqrt((lforcepcenttot - 100).^2);
lforcepcent = mean (lforcepcenttot);%(lforcenorm);
% ALLOW FORCE TO BE GREATER DUE TO TOUCHING FLOOR!!!
%if lforcepcent < 10
%    lforcepcent = 0;
%else
%    lforcepcent = lforcepcent;
%end

rforcediff= rblocksinblocksiidres - rsiminblocksres;
rforcediffsqsqrt = sqrt(rforcediff.^2);
%ractualdiff = mean (rforcediffsqsqrt);
rforcepcenttot = (100./rblocksinblocksiidres).*rforcediffsqsqrt;
%rforcenorm = sqrt((rforcepcenttot - 100).^2);
```

```matlab
rforcepcent = mean (rforcepcenttot);%(rforcenorm);
%if rforcepcent < 10
%    rforcepcent = 0;
%else
%    rforcepcent = rforcepcent;
%end


scoreno = actdiffpcent*5 + lforcepcent + rforcepcent+ bodyangscore +
earlystoppen + flippens + rompens;


elseif matchforces == 2


%select areas of each relavent to simulated portion
stsammhz = startfield * 5; %sim start sample for 1000hz data in vicon
% endsammhz = endfield * 5; %sim start sample for 1000hz data in
vicon


synchblockfp = hssblock - highspeedsynch;
blockstartsim = synchblockfp+stsammhz; %when the simulation starts in
the block data
% blockendsim = synchblockfp+endsammhz; %when the simulation ends in
the block data


if finishtime(length(finishtime))>= simstop
%Calculate 2-D resultants
stlblockiidres = sqrt(stlblocky.^2 + stlblockz.^2);
strblockiidres = sqrt(strblocky.^2 + strblockz.^2);


%Starting block data used in simulation (contact period)
% lblocksinblocksx = stlblockx(blockstartsim:abcompend-1);
% lblocksinblocksy = stlblocky(blockstartsim:abcompend-1);
% lblocksinblocksz = stlblockz(blockstartsim:abcompend-1);
lblocksinblocksiidres = stlblockiidres (blockstartsim:abcompend-1);
% rblocksinblocksx = strblockx(blockstartsim:cdcompend-1);
% rblocksinblocksy = strblocky(blockstartsim:cdcompend-1);
% rblocksinblocksz = strblockz(blockstartsim:cdcompend-1);
rblocksinblocksiidres = strblockiidres (blockstartsim:cdcompend-1);


%simforce data in blocks
% lsiminblocksx = lfootxforce(1:abcompend-blockstartsim);
% lsiminblocksy = lfootyforce(1:abcompend-blockstartsim);
%lsiminblocksz = lfootyforce(1:abcompend-blockstartsim);
lsiminblocksres = lfootresforce(1:abcompend-blockstartsim);
% rsiminblocksx = rfootxforce(1:cdcompend-blockstartsim);
% rsiminblocksy = rfootyforce(1:cdcompend-blockstartsim);
%rsiminblocksz = rfootyforce(1:cdcompend-blockstartsim);
rsiminblocksres = rfootresforce(1:cdcompend-blockstartsim);
end


%Force score in blocks - as percentage
lforcediff= lblocksinblocksiidres - lsiminblocksres;
lforcediffsqsqrt = sqrt(lforcediff.^2);
%lactualdiff = mean (lforcediffsqsqrt);
lforcepcenttot = (100./lblocksinblocksiidres).*lforcediffsqsqrt;
%lforcenorm = sqrt((lforcepcenttot - 100).^2);
lforcepcent = mean (lforcepcenttot);%(lforcenorm);
% ALLOW FORCE TO BE GREATER DUE TO TOUCHING FLOOR!!!
%if lforcepcent < 10
%    lforcepcent = 0;
%else
```

```matlab
%     lforcepcent = lforcepcent;
%end

rforcediff= rblocksinblocksiidres - rsiminblocksres;
rforcediffsqsqrt = sqrt(rforcediff.^2);
%ractualdiff = mean (rforcediffsqsqrt);
rforcepcenttot = (100./rblocksinblocksiidres).*rforcediffsqsqrt;
%rforcenorm = sqrt((rforcepcenttot - 100).^2);
rforcepcent = mean (rforcepcenttot);%(rforcenorm);
%if rforcepcent < 10
%     rforcepcent = 0;
%else
%     rforcepcent = rforcepcent;
%end

scoreno = lforcepcent + rforcepcent+bodyangscore + earlystoppen +
flippens + rompens;

% %Plot the useful force graphs
% figure (1)
% plot (lblocksinblocksiidres)
% hold on
% plot (lsiminblocksres,'m')
% title ('Left block resultant force')
% legend ('Real','Sim')
%
% figure (2)
% plot (rblocksinblocksiidres)
% hold on
% plot (rsiminblocksres,'m')
% title ('Right block resultant force')
% legend ('Real','Sim')
%
% figure (3)
% plot (lblocksinblocksz)
% hold on
% plot (lsiminblocksy,'--')
% hold on
% plot (lblocksinblocksy,'r')
% hold on
% plot (lsiminblocksx*-1,'r--')
% title ('Left block horizontal and vertical forces')
% legend ('real vertical','sim vertical','real horiz','sim horiz')
%
% figure (4)
% plot (rblocksinblocksz)
% hold on
% plot (rsiminblocksy,'--')
% hold on
% plot (rblocksinblocksy,'r')
% hold on
% plot (rsiminblocksx*-1,'r--')
% title ('Right block horizontal and vertical forces')
% legend ('real vertical','sim vertical','real horiz','sim horiz')
%
% figure (15)
% plot (comx,comy,'k',simxpos,simypos,'k--')
% legend ('Real, Sim')
%
% global lefttoepos
% global righttoepos
```

350

```matlab
% global timeouter
%
% global lefttoexspringzero
% global ltoeyblockspringzero
% global righttoexspringzero
% global rtoeyblockspringzero
%
% ltoeonex = lefttoepos(:,1)-lefttoexspringzero(2);
% ltoeoney = lefttoepos(:,2)-ltoeyblockspringzero(2);
% rtoeonex = righttoepos(:,1)-righttoexspringzero(2);
% rtoeoney = righttoepos(:,2)-rtoeyblockspringzero(2);
%
% ltoeoneres = sqrt(ltoeonex.^2+ltoeoney.^2);
% rtoeoneres = sqrt(rtoeonex.^2+rtoeoney.^2);
%
% figure (6)
% plot (timeouter,ltoeoneres,timeouter,rtoeoneres)
% title ('Resultant spring length with time')
%
% figure (7)
% plot
(timeouter,ltoeonex,timeouter,ltoeoney,timeouter,rtoeonex,timeouter,r
toeoney)
% title ('Spring length with time')
% legend ('LX','LY','RX','RY')
%
% global yposa
% figure (8)
% plot (timeouter,yposa(:,2))
% title ('CoM Y pos')
else

scoreno = actdiffpcent+bodyangscore + earlystoppen + flippens +
rompens + notextenoughpen ;% + penalties;

figure (1)
plot (lhipangssav)
hold on
plot (lhipangssim,'m')
title ('L Hip Angle')

figure (2)
plot (rhipangssav)
hold on
plot (rhipangssim,'m')
title ('R Hip Angle')

figure (3)
plot (lkneangssav)
hold on
plot (lkneangssim,'m')
title ('L Knee Angle')
figure (4)
plot (rkneangssav)
hold on
plot (rkneangssim,'m')
title ('R Knee Angle')
figure (5)
plot (lankangssav)
hold on
```

```matlab
plot (lankangssim,'m')
title ('L Ankle Angle')
figure (6)
plot (rankangssav)
hold on
plot (rankangssim,'m')
title ('R Ankle Angle')
figure (7)
plot (lshoangssav)
hold on
plot (lshoangssim,'m')
title ('L Shoulder Angle')
figure (8)
plot (rshoangssav)
hold on
plot (rshoangssim,'m')
title ('R Shoulder Angle')
figure (9)
plot (ttenangssav)
hold on
plot (ttenangssim,'m')
title ('Tten Angle')
figure (10)
plot (comx,comy)
hold on
plot (simxpos,simypos,'m')
title ('CoM Movement')

end

% figure (15)
% plot (comx,comy,'k',simxpos,simypos,'k--')
% legend ('Real, Sim')

clear lsimxrow; clear lsimyrow; clear rsimxrow; clear rsimyrow;
clear lsimxpen; clear lsimypen; clear rsimxpen; clear rsimypen;
clear finishtime
clear measupos
clear comx
clear comy
clear simupos
clear grouptorsim
clear grouptorn
clear shortsim
clear shortori
clear findlastxforcehi
clear lfootxforce
clear findlastxforcelo
clear lfootxforce
clear stopreason
clear lhipangssim
clear rhipangssim
clear lkneangssim
clear rkneangssim
clear lankangssim
clear rankangssim
clear lshoangssim
clear rshoangssim
clear ttenangssim
clear lhippenext
clear lknepenext
```

```matlab
clear lankpenext
%clear rhippenext
%clear rknepenext
clear rankpenext

score = scoreno;
% end
end
```